

MIT Open Access Articles

Colored line ensembles for stochastic vertex models

The MIT Faculty has made this article openly available. **Please share** how this access benefits you. Your story matters.

Citation: Aggarwal, A., Borodin, A. Colored line ensembles for stochastic vertex models. Sel. Math. New Ser. 30, 105 (2024).

As Published: <https://doi.org/10.1007/s00029-024-00989-5>

Publisher: Springer International Publishing

Persistent URL: <https://hdl.handle.net/1721.1/159421>

Version: Author's final manuscript: final author's manuscript post peer review, without publisher's formatting or copy editing

Terms of use: Creative Commons Attribution-Noncommercial-ShareAlike



Amol Aggarwal

Department of Mathematics
Columbia University
2990 Broadway, New York, NY 10027, USA

and

Clay Mathematics Institute
1624 Market Street, Suite 226 #17261, Denver, CO 80202, USA

E-mail: amolagga@gmail.com
amolaggarwal@math.columbia.edu

Alexei Borodin

Department of Mathematics
Massachusetts Institute of Technology
77 Massachusetts Avenue, Cambridge, MA 02139, USA
E-mail: borodin@math.mit.edu

COLORED LINE ENSEMBLES FOR STOCHASTIC VERTEX MODELS

AMOL AGGARWAL AND ALEXEI BORODIN

ABSTRACT. In this paper we assign a family of n coupled line ensembles to any $U_q(\widehat{\mathfrak{sl}}_{n+1})$ colored stochastic fused vertex model, which satisfies two properties. First, the joint law of their top curves coincides with that of the colored height functions for the vertex model. Second, the n line ensembles satisfy an explicit Gibbs property prescribing their laws if all but a few of their curves are conditioned upon. We further describe several examples of such families of line ensembles, including the ones for the colored stochastic six-vertex and q -boson models. The appendices (which may be of independent interest) include an explanation of how the $U_q(\widehat{\mathfrak{sl}}_{n+1})$ colored stochastic fused vertex model degenerates to the log-gamma polymer, and an effective rate of convergence of the colored stochastic six-vertex model to the colored ASEP.

CONTENTS

1. Introduction	1
2. Yang–Baxter Equation and Partition Functions	10
3. Probability Measures and Matchings	18
4. Colored Line Ensembles for Colored Six-Vertex Models	26
5. Examples	33
6. Fusion	37
7. Colored Line Ensembles for Fused Vertex Models	49
8. Line Ensembles for Discrete Time q -Boson Models	53
Appendix A. Degeneration to the Log-Gamma Polymer	57
Appendix B. Effective Convergence of the Six-Vertex Model to ASEP	79
References	86

1. INTRODUCTION

1.1. **Preface.** Over the past twenty-five years, a striking interplay has materialized between equilibrium random surface models and out-of-equilibrium stochastic growth systems. One of the first such correspondences is due to Jockusch–Propp–Shor [57] in 1998, who showed an equality in law between the facet edge for a uniformly random domino tiling of the Aztec diamond, and the height function of a certain discrete-time totally asymmetric simple exclusion process (TASEP). Using ideas of Rost [79], they proved a hydrodynamical limit theorem for the latter TASEP, which together with their matching result implied that the limiting trajectory for the domino tiling facet boundary is a circle.

Such correspondences have also been fruitful in reverse (namely, to study stochastic growth models through random surfaces), starting with the work of Prähofer–Spohn [77]. They analyzed the polynuclear growth (PNG) model by introducing an associated *line ensemble*, which is a sequence

of random curves (that may be viewed as level lines of a surface model), whose top curve coincides in law with the PNG height function. Using the solvability of this line ensemble through the framework of determinantal point processes, they (and also subsequently Johansson [58]) showed that its fluctuations converge to a scaling limit called the Airy line ensemble (which they introduced in [77] as a determinantal point process with the extended Airy correlation kernel), now known to be a universal object in the Kardar–Parisi–Zhang (KPZ) universality class [60]. From this, they deduced that the PNG height fluctuations converge to its top curve, the Airy_2 process.

The combinatorial underpinnings behind the two matchings described above were originally quite different. The first was based on the shuffling algorithm introduced by Elkies–Kuperberg–Larsen–Propp [42], to sample random domino tilings of the Aztec diamond. The second was based on the Robinson–Schensted–Knuth (RSK) correspondence, which was also used by Baryshnikov [12], O’Connell–Yor [75, 72], and Warren [82] to produce line ensembles associated with various models of last passage percolation. Borodin–Petrov [21] later explained that both can be viewed as special cases of a natural family of $(2 + 1)$ -dimensional Markov chains (whose first forms date back to Borodin–Ferrari [19]) on the Schur processes of Okounkov–Reshetikhin [76].

Line ensembles have also been introduced for certain random polymers at positive temperature, based on a geometric lift of the RSK correspondence due to Kirillov [61] and Noumi–Yamada [71] (which, due to work of Matveev–Petrov [68], can also be thought of as a special case of certain $(2 + 1)$ -dimensional Markov chains on the q -Whittaker process of Borodin–Corwin [16]). These include for the O’Connell–Yor polymer and KPZ equation through works of O’Connell–Warren [73, 74], Corwin–Hammond [36], and Nica [70], as well as for the log-gamma polymer through works of Corwin–O’Connell–Seppäläinen–Zygouras [38], Johnston–O’Connell [59], and Wu [85]. For the (single-species) asymmetric simple exclusion process (ASEP) and stochastic six-vertex model, line ensembles were produced in a different way (which will be closer to the direction of this paper) by Borodin–Bufetov–Wheeler [15], Corwin–Dimitrov [33], and Bufetov–Petrov [28]. They first used the Yang–Baxter equation to match the height functions of these systems with specific marginals of the Hall–Littlewood measure, and then interpreted the latter measure as a line ensemble.

All of the above line ensembles admit explicit *Gibbs properties* describing their laws if all but a few of their curves are conditioned upon. Starting with the paper [35] of Corwin–Hammond, such *Gibbsian line ensembles* have emerged as fundamental instruments for probabilistically analyzing the associated stochastic growth models. For example, work of Hammond [51, 48, 49, 50] used them to study the on-scale polymer geometry of Brownian last passage percolation in detail. Later, Matetski–Quastel–Remenik [67] and Dauvergne–Ortmann–Virág [41] provided the full space-time scaling limit for TASEPs and last passage percolation models under arbitrary initial data, and the latter [41] showed that this limit can be described entirely through the Airy line ensemble.

Gibbsian line ensembles have also been used to understand the fine probabilistic structure of non-determinantal models in the KPZ universality class, such as the KPZ equation, (single-species) ASEP and stochastic six-vertex model, and log-gamma polymer. Results in this direction include proofs of tightness and correlation bounds by Corwin–Hammond–Ghosal [36, 34], Wu [85], and Barraquand–Corwin–Dimitrov [33, 11], as well as polymer path properties (possibly under large deviation events) by Das–Zhu [32], Wu [83, 84], and Ganguly–Hegde–Zhang [44, 43]. More recent work of Aggarwal–Huang [7] established that the Airy line ensemble is the unique line ensemble satisfying the Gibbs property for non-intersecting Brownian bridges, whose top curve is approximately parabolic. This (together with the above-mentioned tightness frameworks) could potentially lead to a systematic way of proving that discrete stochastic growth models converge to their scaling limit, whenever such models can be associated with a Gibbsian line ensemble.

This activity leads to the (closely related) questions of, (a) in what generality can Gibbsian line ensembles be associated with a stochastic growth model, and (b) what is the mechanism that enables their appearance? The purpose of this paper is to work towards these questions.

We consider the colored stochastic fused vertex models, associated with the affine quantum group $U_q(\widehat{\mathfrak{sl}}_{n+1})$, introduced by Kuniba–Mangazeev–Maruyama–Okado [63] and studied in detail by Borodin–Wheeler [25]. Our main result is that any such model can be associated with a family of line ensembles satisfying two properties. The first is that their top curves coincide in law with the colored height functions of the stochastic vertex model (Theorem 4.7 and Theorem 7.7); the second is that they satisfy an explicit Gibbs property (Theorem 4.8 and Theorem 7.8). Our arguments generalize those in [15, 33, 28], by using the Yang–Baxter equation underlying these vertex models to match their colored height functions to marginals of certain measures on compositions (Proposition 3.7 and Proposition 6.23); by their definitions, the latter can be interpreted as families of line ensembles with explicit Gibbs properties (Definition 4.1 and Definition 7.1). In a sense, this pinpoints the Yang–Baxter equation as the algebraic source for Gibbsian line ensembles associated with the integrable stochastic vertex models studied here.¹

We have several reasons for operating at the level of the $U_q(\widehat{\mathfrak{sl}}_{n+1})$ stochastic fused vertex models. The first is their scope; they are fairly general objects that degenerate to most systems proven to be in the KPZ universality class (though not all of them, such as the non-nearest neighbor exclusion processes considered by Quastel–Sarkar [78]). See Figure 1 for a (not entirely complete) list of degenerations to known models;² all of them should be associated with Gibbsian line ensembles, obtained by taking the appropriate specializations or limits of our most general ones for the stochastic fused vertex model. While we will not describe these line ensembles in detail for all of the models depicted in Figure 1, we will do so for a few examples (such as the colored stochastic six-vertex and discrete-time q -boson models) in Section 5 and Section 8 below.

The second is that for $n > 1$ these models enable us to access *colored*, also called *multi-species*, systems (in which some particles may have a higher priority than others). Prior to this work, we were unaware of Gibbsian line ensembles associated with any example of a multispecies model. A new effect arises here; when the model comprises $n > 1$ species, we associate not one but a family of n coupled line ensembles, called a *colored line ensemble*, with the multi-species system. The top curve in the c -th ensemble, jointly over all $c \in [1, n]$, of the family coincides in law with the height function tracking particles in the model of color at least c . The full colored line ensemble further satisfies an explicit Gibbs property that prescribes the joint law of all n ensembles in the family, upon conditioning on all but a few of their curves. This provides a potential way of asymptotically analyzing colored systems. We refrain from pursuing such probabilistic studies in this paper and instead point to the forthcoming work of Aggarwal–Corwin–Hegde [6] that will use the colored line ensembles introduced here to analyze the scaling limit of the multi-species ASEP and stochastic six-vertex model.

¹There also exist stochastic systems satisfying the Yang–Baxter equation, which are not special cases of our $U_q(\widehat{\mathfrak{sl}}_{n+1})$ stochastic fused vertex model. These include ones considered by Cantini [31] and Chen–de Gier–Hiki–Sasamoto–Usui [32], as well as ones with boundary conditions, studied for example by Barraquand–Borodin–Corwin–Wheeler [9], He [54, 55], and Yang [86]. It would be interesting to investigate whether Gibbsian line ensembles can be associated with these models, too. For the half-space log-gamma polymer, this has been done by Barraquand–Corwin–Das [10] (using the geometric RSK correspondence).

²Many of these degenerations were previously discussed by Borodin–Gorin–Wheeler [20, Figure 2], but that work does not explain how to degenerate the colored vertex model to the log-gamma polymer. We address this point in Appendix A below.

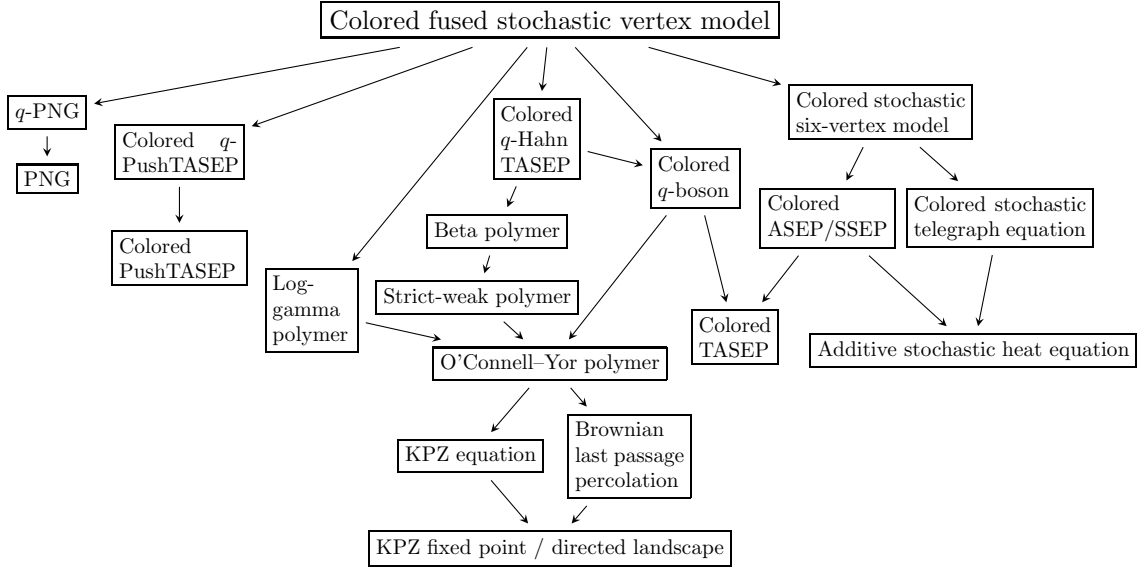


FIGURE 1. Depicted above are various degenerations of the $U_q(\widehat{\mathfrak{sl}}_{n+1})$ colored fused stochastic vertex model.

Before continuing, let us briefly comment on $(2 + 1)$ -dimensional Markov chains. As mentioned previously, they have been prevalent in many prior studies on line ensembles but at first may not seem to make a direct presence here. However, such dynamics do implicitly underly the proofs behind our matching statements (Proposition 3.7 and Proposition 6.23), which involve several sequences of applications of the Yang–Baxter equation to move every vertex of an $M \times N$ rectangle across a lattice. Starting from a frozen (or “empty”) configuration, this lattice gets randomly transformed every time a vertex is moved through it. The process of moving one vertex at time induces a $(2 + 1)$ -dimensional Markovian evolution on the lattice, which in the uncolored ($n = 1$) case was studied in works of Bufetov–Mucciconi–Petrov [28, 27, 69] under the name *Yang–Baxter bijectivization*. The resulting dynamics are quite general and encapsulate the RSK correspondence as a special case [69, Section 5]. An interesting question is to introduce colors ($n > 1$) in these bijectivization dynamics, and to investigate whether different (possibly nonsymmetric³) RSK-type correspondences arise.

We now proceed to give a more detailed sense of our results. To keep the notation as light as possible in this introductory section, we will not state them in fullest generality here. Instead, we only describe a fairly special case of our results that is still new, namely, for the $q = 0$ colored stochastic six-vertex model. For the most general versions of our results, we refer to Theorem 4.7 and Theorem 4.8 (for the colored stochastic six-vertex model), and to Theorem 7.7 and Theorem 7.8 (for the colored stochastic fused vertex model). For further examples and degenerations, we refer to Section 5 (for other special cases of the stochastic six-vertex model) and Section 8 (for the colored discrete time q -boson model).

Throughout this work, for any real numbers $a, b \in \mathbb{R}$ with $a \leq b$, we write $\llbracket a, b \rrbracket = [a, b] \cap \mathbb{Z}$.

³One nonsymmetric RSK algorithm was introduced by Mason [66] and studied by Haglund–Mason–Remmel [47].

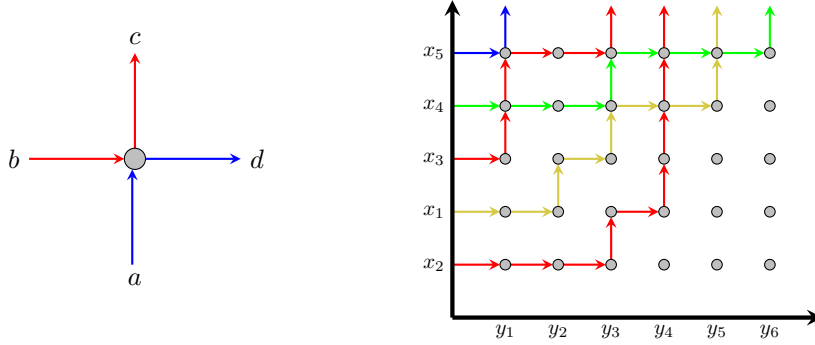


FIGURE 2. Shown to the left is a vertex with arrow configuration $(a, b; c, d) = (2, 1; 1, 2)$, where red and blue are colors 1 and 2, respectively. Shown to the right is a colored model on the quadrant.

1.2. Colored Stochastic Six-Vortex Model. The colored stochastic six-vertex model is a certain probability measure on colored six-vertex ensembles on $\mathbb{Z}_{>0}^2$; we begin by defining the latter. To that end, a *colored six-vertex arrow configuration* is a quadruple $(a, b; c, d) \in \mathbb{Z}_{\geq 0}^4$ of nonnegative integers, which we view as an assignment of directed up-right arrows to a vertex $v \in \mathbb{Z}_{>0}^2$, as follows. We assume that each of the four edges incident to v accomodates one arrow, and that each arrow is labeled by a nonnegative integer, called a *color*; edges occupied by an arrow of color 0 are typically viewed as unoccupied (so arrows of color 0 are ignored). We then interpret the integers a, b, c , and d of the arrow configuration as the colors of the arrows vertically entering v , horizontally entering v , vertically exiting v , and horizontally exiting v , respectively; see the left side of Figure 2 for an example. We will typically impose that $\{a, b\} = \{c, d\}$ as multi-sets, a restriction known as *arrow conservation*; it indicates that an arrow of any color entering v must also exit v .

A *domain* is a subset $\mathcal{D} \subseteq \mathbb{Z}^2$, and a *colored six-vertex ensemble* on a domain $\mathcal{D} \subset \mathbb{Z}^2$ is an assignment of an arrow configuration to each vertex of \mathcal{D} in such a way that neighboring arrow configurations are *consistent*; this means that, if $v_1, v_2 \in \mathcal{D}$ are two adjacent vertices, then there is an arrow of color $c \in \mathbb{Z}_{\geq 0}$ to v_2 in the configuration at v_1 if and only if there is an arrow of color c from v_1 in the configuration at v_2 . Observe in particular that the arrows in a colored six-vertex ensemble form colored up-right directed paths connecting vertices of \mathcal{D} .

Boundary data for a colored six-vertex ensemble is prescribed by dictating which points on the boundary of a domain are entrance (or exit) sites for a path of a given color. If the domain \mathcal{D} is a rectangle or quadrant, we will typically restrict to the case when paths only enter horizontally through the west boundary of \mathcal{D} ; see the right side of Figure 2 for a depiction. Given a function $\sigma : \llbracket 1, N \rrbracket \rightarrow \mathbb{Z}_{\geq 0}$, we say that a colored six-vertex ensemble on the rectangle domain $\mathcal{D}_{M;N} = \llbracket 1, M \rrbracket \times \llbracket 1, N \rrbracket$ has σ -*entrance data* if the following holds. For each $j \in \llbracket 1, N \rrbracket$, one path of color $\sigma(j)$ horizontally enters $\mathcal{D}_{M;N}$ from the site $(0, j)$ on the y -axis, and no path vertically enters $\mathcal{D}_{M;N}$ from any site on the x -axis.

Associated with any six-vertex ensemble \mathcal{E} on a domain $\mathcal{D} \subseteq \mathbb{Z}^2$ are *height functions* $\mathfrak{h}_{>c}^{\leftarrow} : \mathbb{Z}^2 \rightarrow \mathbb{Z}$, which for any integer $c \geq 1$ are defined as follows. For any vertex $v = (i, j) \in \mathbb{Z}^2$, let $\mathfrak{h}_{>c}^{\leftarrow}(v)$ denote the number of paths of color at least c in \mathcal{E} that do not pass below v , namely, that do not intersect the vertical ray (pointing south) connecting $(i + 1/2, j + 1/2)$ to $(i + 1/2, -\infty)$.

$i \geq 0$	$j > i \geq 0$			
$(i, i; i, i)$	$(j, i; j, i)$	$(i, j; i, j)$	$(j, i; i, j)$	$(i, j; j, i)$
1	$\frac{q(1-z)}{1-qz}$	$\frac{1-z}{1-qz}$	$\frac{1-q}{1-qz}$	$\frac{z(1-q)}{1-qz}$

FIGURE 3. The R_z weights are depicted above.

The *colored stochastic six-vertex model* is a probability measure on colored six-vertex ensembles on $\mathbb{Z}_{>0}^2$ that depends on two infinite sequences of real parameters $\mathbf{x} = (x_1, x_2, \dots)$ and $\mathbf{y} = (y_1, y_2, \dots)$. We view x_j as associated with the j -th row and y_i as associated with the i -th column, so \mathbf{x} and \mathbf{y} are called *row rapidities* and *column rapidities*, respectively. The specific forms of these probability measures are expressed through weights $R_{y_i/x_j}(a, b, c, d)$ associated with each vertex $v = (i, j) \in \mathbb{Z}_{>0}^2$. In addition to depending on the arrow configuration (a, b, c, d) at v , this vertex weight will also be governed by several parameters. The first is the *quantization parameter* q , which is fixed throughout the model. The second is the *spectral variable* $z = z_{i,j} = x_j^{-1}y_i$, which is given by the ratio of the column and row rapidities at the vertex $v = (i, j)$. Given this notation, we define the following vertex weights originally introduced in [13, 56].

Definition 1.1. For any complex number $z \in \mathbb{C}$ and integers $a, b, c, d \geq 0$, define the vertex weight $R_z(a, b, c, d)$ as follows. For $i < j$, set (see Figure 3)

$$(1.1) \quad \begin{aligned} R_z(i, i; i, i) &= 1; & R_z(j, i; j, i) &= \frac{q(1-z)}{1-qz}; & R_z(i, j; i, j) &= \frac{1-z}{1-qz}; \\ R_z(j, i; i, j) &= \frac{1-q}{1-qz}; & R_z(i, j; j, i) &= \frac{z(1-q)}{1-qz}. \end{aligned}$$

If (a, b, c, d) is not of the above form for some $0 \leq i < j$, then set $R_z(a, b, c, d) = 0$.

Remark 1.2. These R_z weights are *stochastic* in that the sum of all weights with a fixed pair of incoming arrows is equal to 1, namely, $\sum_{c,d \geq 0} R_z(a, b, c, d) = 1$ for each $z \in \mathbb{C}$ and $a, b \geq 0$.

Now let us describe how to sample a random colored six-vertex ensemble on $\mathbb{Z}_{>0}^2$, using the R_z weights from (1.1). We will first define probability measures \mathbb{P}_n on the set of colored six-vertex ensembles whose vertices are all contained in triangles of the form $\mathbb{T}_n = \{(x, y) \in \mathbb{Z}_{>0}^2 : x + y \leq n\}$, and then we will take a limit as n tends to infinity to obtain the vertex models in infinite volume. The first measure \mathbb{P}_0 is supported by the empty ensemble (that has no paths).

For each integer $n \geq 1$, we will define \mathbb{P}_{n+1} from \mathbb{P}_n through the following Markovian update rules. Use \mathbb{P}_n to sample a colored six-vertex ensemble \mathcal{E}_n on \mathbb{T}_n . This yields arrow configurations for all vertices in the triangle \mathbb{T}_{n-1} . To extend this to a colored six-vertex ensemble on \mathbb{T}_{n+1} , we must prescribe arrow configurations to all vertices (x, y) on the complement $\mathbb{T}_n \setminus \mathbb{T}_{n-1}$, which is the diagonal $\mathbb{D}_n = \{(x, y) \in \mathbb{Z}_{>0}^2 : x + y = n\}$. Since any incoming arrow to \mathbb{D}_n is an outgoing arrow from \mathbb{D}_{n-1} , \mathcal{E}_n and the initial data prescribe the first two coordinates (a, b) of the arrow

configuration to each vertex in \mathbb{D}_n . Thus, it remains to explain how to assign the second two coordinates (c, d) of the arrow configuration at any vertex $(i, j) \in \mathbb{D}_n$, given its first two coordinates (a, b) . This is done by producing (c, d) from (a, b) according to the transition probability

$$(1.2) \quad \mathbb{P}_n[(c, d)|(a, b)] = R_{y_i/x_j}(a, b; c, d).$$

We assume that the parameters $(\mathbf{x}; \mathbf{y}; q)$ are chosen so that the probabilities (1.2) are all nonnegative; the stochasticity of the R_z weights (Remark 1.2) then ensures that (1.2) indeed defines a probability measure.

Choosing (c, d) according to the above transition probabilities yields a random colored six-vertex ensemble \mathcal{E}_{n+1} , now defined on \mathbb{T}_{n+1} ; the probability distribution of \mathcal{E}_{n+1} is then denoted by \mathbb{P}_{n+1} . Taking the limit as n tends to ∞ yields a probability measure on colored six-vertex ensembles \mathcal{E} on the quadrant. We refer to it as the *colored stochastic six-vertex model*; observe that it may also be sampled on any rectangle $\mathcal{D} \subset \mathbb{Z}^2$ in the same way as it was above on the quadrant.

1.3. Colored Line Ensembles. In this section we introduce terminology for colored families of line ensembles. We first define the notion of a line ensemble. Those that we consider here will be discrete, and their paths will be non-increasing, which is related to the fact that the associated stochastic models we analyze are discrete. By taking certain limit degenerations, one can obtain continuous line ensembles associated with non-discrete stochastic systems, but we will not pursue that in this work.

Definition 1.3. Fix an interval $I \subseteq \mathbb{Z}$. A (discrete, down-right) *line ensemble* (on I) is an infinite sequence $(\mathbf{L}_1, \mathbf{L}_2, \dots)$ of functions $\mathbf{L}_k : I \rightarrow \mathbb{Z}$ such that

$$(1.3) \quad \mathbf{L}_k(i) \geq \mathbf{L}_{k+1}(i); \quad \mathbf{L}_k(i) \geq \mathbf{L}_k(i+1),$$

for each $(k, i) \in \mathbb{Z}_{>0} \times I$ (where we must have $i+1 \in I$ in the second inequality of (1.3)). We call this line ensemble *simple* if $\mathbf{L}_k(i) - \mathbf{L}_k(i+1) \in \{0, 1\}$ for all $(k, i) \in \mathbb{Z}_{>0} \times I$ with $i+1 \in I$.

We next define colored families of line ensembles, which are sequences of line ensembles whose differences are also line ensembles.

Definition 1.4. Fix an integer $n \geq 1$ and an interval $I \subseteq \mathbb{Z}$. A *colored family of line ensembles*, which we often abbreviate to a *colored line ensemble*, on I is a sequence $\mathbf{L} = (\mathbf{L}^{(1)}, \mathbf{L}^{(2)}, \dots, \mathbf{L}^{(n)})$ of line ensembles $\mathbf{L}^{(c)} = (\mathbf{L}_1^{(c)}, \mathbf{L}_2^{(c)}, \dots)$, such that $\mathbf{\Lambda}^{(c)} = (\mathbf{\Lambda}_1^{(c)}, \mathbf{\Lambda}_2^{(c)}, \dots)$ is a line ensemble for each $c \in \llbracket 1, n \rrbracket$, where

$$\mathbf{\Lambda}_k^{(c)}(i) = \mathbf{L}_k^{(c)}(i) - \mathbf{L}_k^{(c+1)}(i), \quad \text{for each } (k, i) \in \mathbb{Z}_{>0} \times I.$$

Here, we have for convenience defined the constant function $\mathbf{L}_k^{(n+1)} : I \rightarrow \mathbb{Z}$ by setting $\mathbf{L}_k^{(n+1)}(i) = 0$ for any $(k, i) \in \mathbb{Z}_{>0} \times I$. We further call \mathbf{L} *simple* if $\mathbf{L}^{(c)}$ is simple for each $c \in \llbracket 1, n \rrbracket$.

See Figure 4 for examples. Before proceeding, we require the notion of compatibility for colored line ensembles.

Definition 1.5. Fix colored line ensembles $\mathbf{L} = (\mathbf{L}^{(1)}, \mathbf{L}^{(2)}, \dots, \mathbf{L}^{(n)})$ and $\mathbf{l} = (\mathbf{l}^{(1)}, \mathbf{l}^{(2)}, \dots, \mathbf{l}^{(n)})$ on an interval $I \subseteq \mathbb{Z}$, and integers $j \geq i \geq 1$ and $u, v \in I$ with $u \leq v$. We say that \mathbf{l} is $\llbracket i, j \rrbracket \times \llbracket u, v \rrbracket$ -compatible with \mathbf{L} if $\mathbf{l}_k^{(c)}(m) = \mathbf{L}_k^{(c)}(m)$ for each $c \in \llbracket 1, n \rrbracket$ and $(k, m) \in (\mathbb{Z}_{>0} \times I) \setminus (\llbracket i, j \rrbracket \times \llbracket u, v \rrbracket)$.

Observe under the notation of Definition 1.5 that there are only finitely many colored line ensembles that are $\llbracket i, j \rrbracket \times \llbracket u, v \rrbracket$ -compatible with a given one.

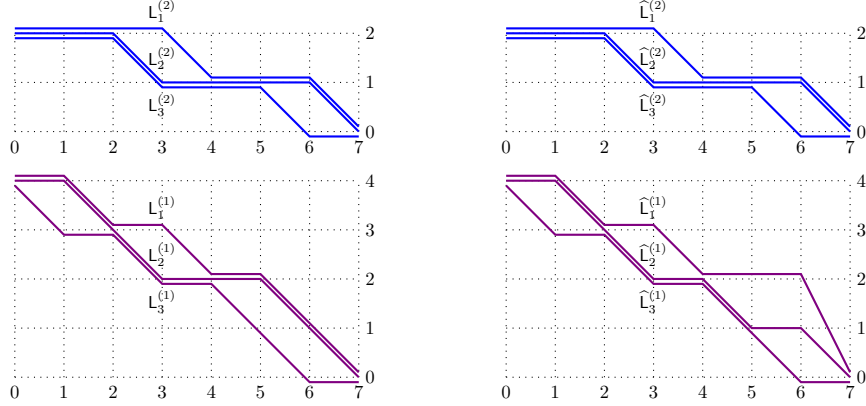


FIGURE 4. Shown above are two colored line ensembles. To the left, \mathbf{L} is simple; to the right, $\widehat{\mathbf{L}}$ is not simple and is $\llbracket 1, 2 \rrbracket \times \llbracket 5, 6 \rrbracket$ -compatible with \mathbf{L} .

1.4. Colored Line Ensembles for the $q = 0$ Stochastic Six-Vortex Model. In this section we state a special case of our main results (see Section 4 and Section 7 below for the more general ones), by associating a colored family of line ensembles to the colored stochastic six-vertex model at $q = 0$. This is provided by the following theorem, which is proven in Section 5.2. Its first part indicates that the top curves of the line ensembles in the colored family have the same joint law as the colored height functions for the stochastic six-vertex model. Its third part provides a Gibbs property (which is well posed by its second part) for the colored line ensemble. In what follows, we fix integers $M, N, n \geq 1$; real numbers $x, y \in (0, 1)$ with $y < x$; and a function $\sigma : \llbracket 1, N \rrbracket \rightarrow \llbracket 1, n \rrbracket$. We also define the rectangle $\mathcal{D}_{M;N} = \llbracket 1, M \rrbracket \times \llbracket 1, N \rrbracket \subset \mathbb{Z}^2$.

Theorem 1.6. *Sample a colored six-vertex ensemble \mathcal{E} on $\mathcal{D}_{M;N}$ according to the stochastic six-vertex model with $q = 0$; all parameters of \mathbf{x} equal to x and of \mathbf{y} equal to y ; and σ -entrance data. For each $c \in \llbracket 1, n \rrbracket$ define $H_c : \llbracket 0, M + N \rrbracket \rightarrow \mathbb{Z}$ by setting*

$$H_c(k) = \mathfrak{h}_{\geq c}^{\leftarrow}(M, k), \quad \text{if } k \in \llbracket 0, N \rrbracket; \quad H_c(k) = \mathfrak{h}_{\geq c}^{\leftarrow}(M + N - k, N), \quad \text{if } k \in \llbracket N, M + N \rrbracket,$$

where $\mathfrak{h}_{\geq c}^{\leftarrow}$ is the colored height function with respect to \mathcal{E} . There exists a random simple colored line ensemble $\mathbf{L} = (\mathbf{L}^{(1)}, \mathbf{L}^{(2)}, \dots, \mathbf{L}^{(n)})$ on $\llbracket 0, M + N \rrbracket$ satisfying the following properties.

- (1) The joint law of the functions $(\mathbf{L}_1^{(1)}, \mathbf{L}_1^{(2)}, \dots, \mathbf{L}_1^{(n)})$ is the same as that of (H_1, H_2, \dots, H_n) .
- (2) For any integers $c \in \llbracket 1, n \rrbracket$; $k \geq 1$; and $m \in \llbracket 1, M + N \rrbracket$ such that $\mathbf{L}_k^{(c+1)}(m) > \mathbf{L}_{k+1}^{(c+1)}(m)$, we almost surely have

$$(1.4) \quad \mathbf{L}_k^{(c)}(m-1) - \mathbf{L}_k^{(c)}(m) = \mathbf{L}_k^{(c+1)}(m-1) - \mathbf{L}_k^{(c+1)}(m).$$

- (3) Fix integers $j \geq i \geq 0$ and $u, v \in \llbracket 0, M + N \rrbracket$ such that $v \geq u$ and $N \notin \llbracket u, v \rrbracket$. Condition on the curves $\mathbf{L}_k^{(c)}(m)$ for all $c \in \llbracket 1, n \rrbracket$ and $(k, m) \notin \llbracket i, j \rrbracket \times \llbracket u, v \rrbracket$. Then the law of \mathbf{L} is uniform over all simple colored line ensembles \mathbf{l} that are $\llbracket i, j \rrbracket \times \llbracket u, v \rrbracket$ -compatible with \mathbf{L} such that the following holds. For any integers $c \in \llbracket 1, n \rrbracket$; $k \geq 1$; and $m \in \llbracket 1, M + N \rrbracket$ such that $\mathbf{l}_k^{(c+1)}(m) > \mathbf{l}_{k+1}^{(c+1)}(m)$, we have

$$\mathbf{l}_k^{(c)}(m-1) - \mathbf{l}_k^{(c)}(m) = \mathbf{l}_k^{(c+1)}(m-1) - \mathbf{l}_k^{(c+1)}(m).$$

Let us make several comments on this theorem. First, the Gibbs property for the line ensemble \mathbf{L} (Item 3 of Theorem 1.6) does not depend on the initial data σ for the stochastic six-vertex model; σ instead will eventually appear as a sort of boundary condition for \mathbf{L} . One cannot directly use this fact to obtain line ensembles for the single-color ($n = 1$ case of the) stochastic six-vertex model under general initial data. Indeed, since 0 is not in the range of σ , each site on the west boundary $\partial_{\text{we}}\mathcal{D}_{M;N} = \{0\} \times \llbracket 1, N \rrbracket$ of $\mathcal{D}_{M;N}$ is an entrance site for a path of some positive color. Thus, σ necessarily gives rise to step (wedge) initial data if $n = 1$. However, one can instead pass to a $n = 2$ color stochastic six-vertex model; use σ to prescribe an arbitrary boundary condition for where the color 2 arrows enter along $\partial_{\text{we}}\mathcal{D}_{M;N}$ (having the color 1 arrows enter at all other sites of $\partial_{\text{we}}\mathcal{D}_{M;N}$); and then project to the color 2 arrows⁴ to yield a single-color stochastic six-vertex model with general boundary conditions along $\partial_{\text{we}}\mathcal{D}_{M;N}$.

Second, if $n = 1$, the constraint that (1.4) holds whenever $\mathbf{L}_k^{(c+1)}(m) > \mathbf{L}_{k+1}^{(c+1)}(m)$ is irrelevant, since $\mathbf{L}_k^{(2)}(m) = 0$ for all $k \geq 1$ and $m \in \llbracket 0, M + N \rrbracket$. The Gibbs property for \mathbf{L} then becomes that of non-intersecting, down-right, discrete random paths conditioned to remain ordered. For $n \geq 2$ colors, this constraint is present and must be taken into account. Similar constraints have implicitly (in the language of vertex models) appeared previously in the context of stationary measures for colored interacting particle systems (see the $q = 0$ case of [8, Section 4.2]). Their presence in our colored line ensembles therefore suggests that the latter may be useful in proving convergence to local stationarity [8] or the stationary horizon [30, 29] for colored stochastic vertex models. An alternative explanation for the constraint (1.4) (by examining the law of the line ensembles $(\mathbf{L}^{(2)}, \mathbf{L}^{(3)}, \dots, \mathbf{L}^{(c)})$ upon conditioning on the first one $\mathbf{L}^{(1)}$) is found in forthcoming work [6], where it will be used to prove scaling limit results for the multi-species asymmetric simple exclusion process and colored stochastic six-vertex model.

1.5. Outline. The remainder of this work is organized as follows. In Section 2 we recall the Yang–Baxter equation and certain families of (non)symmetric functions similar to those in [25]. We use them in Section 3 to produce probability measures related to the colored stochastic six-vertex model. In Section 4 we reinterpret these results to associate colored line ensembles with the stochastic six-vertex model, special cases of which are analyzed in Section 5. We then generalize this framework to the fused setting in Section 6, producing the associated colored line ensembles for stochastic fused vertex models in Section 7. Finally, we explain these colored line ensembles in the example of the multi-species discrete time q -boson model in Section 8. The appendices are not directly related to line ensembles and instead include results about degenerating colored vertex models to other systems (along the lines of Figure 1). Specifically, in Appendix A we explain how to degenerate the colored stochastic fused vertex model to the log-gamma polymer. In Appendix B we provide an effective rate of convergence to the colored stochastic six-vertex model to the colored ASEP.

1.6. Notation. For any integers $n \geq 1$ and $i \in \llbracket 1, n \rrbracket$, we let $\mathbf{e}_i = \mathbf{e}_i^{(n)} \in \mathbb{R}^n$ denote the coordinate vector whose i -th entry is equal to 1 and whose remaining entries are 0; we also let $\mathbf{e}_0 = \mathbf{e}_0^{(n)} \in \mathbb{R}^n$ denote the vector with all entries equal to 0. We denote the entries of any vector $\mathbf{X} \in \mathbb{R}^n$ by $\mathbf{X} = (X_1, X_2, \dots, X_n)$, and we set $|\mathbf{X}| = \sum_{k=1}^n X_k$. For any integers $1 \leq i \leq j \leq n$, we also denote $X_{[i,j]} = \sum_{k=i}^j X_k$. We further write $\mathbf{X} \geq \mathbf{Y}$ for any $\mathbf{X}, \mathbf{Y} \in \mathbb{R}^n$ if $X_i \geq Y_i$ for each

⁴We emphasize, however, that the Gibbs property for \mathbf{L} does not seem to persist under this projection, that is, $\mathbf{L}^{(2)}$ alone does not satisfy a Gibbs property (though $\mathbf{L}^{(1)}$ does; see Proposition 4.11 and Proposition 7.9 below). From this perspective, to treat general initial data (even only for stochastic vertex models with a single color), one must pass to a $n \geq 2$ colored line ensemble.

$i \in \llbracket 1, n \rrbracket$. For any k -tuple $\mathbf{w} = (w_1, w_2, \dots, w_k)$, let $\overleftarrow{\mathbf{w}} = (w_k, w_{k-1}, \dots, w_1)$ denote the order reversal of \mathbf{w} . Throughout this work, we fix a real number $q \in \mathbb{R}$. For any complex number $a \in \mathbb{C}$, we also denote the q -Pochhammer symbol $(a; q)_k = \prod_{j=0}^{k-1} (1 - aq^j)$ for each integer $k \geq 0$ and $(a; q)_k = \prod_{j=1}^{-k} (1 - aq^{-j})$ for each integer $k < 0$.

A *signature* is a sequence $\lambda = (\lambda_1, \lambda_2, \dots, \lambda_\ell)$ of integers such that $\lambda_1 \geq \lambda_2 \geq \dots \geq \lambda_\ell \geq 0$. A *composition* $\mu = (\mu_1, \mu_2, \dots, \mu_\ell) \in \mathbb{Z}_{\geq 0}^\ell$ of some integer $K \geq 0$ is an ℓ -tuple of nonnegative integers such that $\sum_{j=1}^\ell \mu_j = K$ (in particular, any signature is a composition). The integer $\ell = \ell(\mu)$ is called the *length* of μ , and $K = |\mu|$ is its *size*. Given a composition μ , we let $\mathbf{m}_k(\mu) = \#\{j \in \llbracket 1, \ell \rrbracket : \mu_j = k\}$ denote the multiplicity of k in μ , for any integer $k \geq 0$; we also let $\mathbf{m}_{\leq k}(\mu) = \sum_{j=0}^k \mathbf{m}_j(\mu)$ denote the number of entries in μ that are at most equal to k .

Acknowledgements. The authors thank Ivan Corwin, Milind Hegde, Shirshendu Ganguly, and Mikhail Tikhonov for very valuable comments and conversations. The authors also are grateful to the referee for a detailed reading with helpful suggestions. Amol Aggarwal was partially supported by a Packard Fellowship for Science and Engineering, a Clay Research Fellowship, NSF grant DMS-1926686, and the IAS School of Mathematics. Alexei Borodin was partially supported by the NSF grants DMS-1664619, DMS-1853981, and the Simons Investigator program.

2. YANG–BAXTER EQUATION AND PARTITION FUNCTIONS

In this section we collect (largely from [25]) several results on the Yang–Baxter equation and certain families of (non)symmetric functions. In Section 2.1 we recall a certain family of weights and the Yang–Baxter equation they satisfy. In Section 2.2 we provide notation for partition functions and height functions. This will be used to define certain (non)symmetric functions f and G in Section 2.3, whose properties we recall in Section 2.4. Throughout this section, we fix an integer $n \geq 1$.

2.1. Yang–Baxter Equation. In this section we introduce further classes of weights (in addition to the R_z ones given by Definition 1.1), denoted by $L_{z;s}$ and $\widehat{L}_{z;s}$, and state the Yang–Baxter equation that they satisfy.

Associated with an L -weight is a *colored higher spin arrow configuration*, which is a quadruple $(\mathbf{A}, b; \mathbf{C}, d)$ with $b, d \in \llbracket 0, n \rrbracket$ and $\mathbf{A}, \mathbf{C} \in \mathbb{Z}_{\geq 0}^n$. We view this as an assignment of directed up-right colored arrows to a vertex $v \in \mathbb{Z}^2$; the horizontal edges incident to v again accommodate one arrow,⁵ but now the vertical edges incident to v can accommodate arbitrarily many arrows. In particular, b and d denote the colors of the arrows horizontally entering and exiting v , respectively, and A_k and C_k denote the number of arrows of color k vertically entering and exiting v , respectively, for each $k \in \llbracket 1, n \rrbracket$. In what follows, for any $i, j \in \llbracket 1, n \rrbracket$ and $\mathbf{X} \in \mathbb{R}^n$, we set

$$\mathbf{X}_i^+ = \mathbf{X} + \mathbf{e}_i; \quad \mathbf{X}_j^- = \mathbf{X} - \mathbf{e}_j; \quad \mathbf{X}_{ij}^{+-} = \mathbf{X} + \mathbf{e}_i - \mathbf{e}_j.$$

⁵We will remove this restriction in Section 6.1 below, through fusion.

$1 \leq i \leq n$			$1 \leq i < j \leq n$		
$(\mathbf{A}, 0; \mathbf{A}, 0)$	$(\mathbf{A}, 0; \mathbf{A}_i^-, i)$	$(\mathbf{A}, i; \mathbf{A}_i^+, 0)$	$(\mathbf{A}, i; \mathbf{A}_{ij}^{+-}, j)$	$(\mathbf{A}, j; \mathbf{A}_{ji}^{+-}, i)$	$(\mathbf{A}, i; \mathbf{A}, i)$
$\frac{1 - sq^{A_{[1,n]}}}{1 - sx}$	$\frac{x(1 - q^{A_i})q^{A_{[i+1,n]}}}{1 - sx}$	$\frac{1 - s^2q^{A_{[1,n]}}}{1 - sx}$	$\frac{x(1 - q^{A_j})q^{A_{[j+1,n]}}}{1 - sx}$	$\frac{s(1 - q^{A_i})q^{A_{[i+1,n]}}}{1 - sx}$	$\frac{(x - sq^{A_i})q^{A_{[i+1,n]}}}{1 - sx}$

 FIGURE 5. Depicted above are the $L_{x;s}$ weights.

Definition 2.1. Fix complex numbers $x, s \in \mathbb{C}$; define the $L_{x;s} = L_{x;s}^{(n)}$ vertex weight as follows. For any $i \in \llbracket 1, n \rrbracket$ and $\mathbf{A} \in \mathbb{Z}_{\geq 0}^n$, set

$$(2.1) \quad \begin{aligned} L_{x;s}(\mathbf{A}, 0; \mathbf{A}, 0) &= \frac{1 - sq^{A_{[1,n]}}}{1 - sx}; & L_{x;s}(\mathbf{A}, 0; \mathbf{A}_i^-, i) &= \frac{x(1 - q^{A_i})q^{A_{[i+1,n]}}}{1 - sx}; \\ L_{x;s}(\mathbf{A}, i; \mathbf{A}_i^+, 0) &= \frac{1 - s^2q^{A_{[1,n]}}}{1 - sx}; & L_{x;s}(\mathbf{A}, i; \mathbf{A}, i) &= \frac{(x - sq^{A_i})q^{A_{[i+1,n]}}}{1 - sx}. \end{aligned}$$

Moreover, for any $1 \leq i < j \leq n$, set

$$(2.2) \quad L_{x;s}(\mathbf{A}, i; \mathbf{A}_{ij}^{+-}, j) = \frac{x(1 - q^{A_j})q^{A_{[j+1,n]}}}{1 - sx}; \quad L_{x;s}(\mathbf{A}, j; \mathbf{A}_{ji}^{+-}, i) = \frac{s(1 - q^{A_i})q^{A_{[i+1,n]}}}{1 - sx}.$$

We also set $L_{x;s}(\mathbf{A}, b; \mathbf{C}, d) = 0$ if $(\mathbf{A}, b; \mathbf{C}, d)$ is not of the above form (with $\mathbf{A}, \mathbf{C} \in \mathbb{Z}_{\geq 0}^n$); see Figure 5 for a depiction. Also define a normalization $\widehat{L}_{x;s} = \widehat{L}_{x;s}^{(n)}$ of the $L_{x;s}$ weights, by setting

$$(2.3) \quad \widehat{L}_{x;s}(\mathbf{A}, b; \mathbf{C}, d) = \frac{1 - sx}{x - s} \cdot L_{x;s}(\mathbf{A}, b; \mathbf{C}, d),$$

for any $b, d \in \llbracket 0, n \rrbracket$ and $\mathbf{A}, \mathbf{C} \in \mathbb{Z}_{\geq 0}^n$. In particular, we have $\widehat{L}_x(\mathbf{e}_0, i; \mathbf{e}_0, i) = 1$, for any $i \in \llbracket 1, n \rrbracket$.

The following proposition indicates that the R -weights and L -weights from Definition 1.1 and Definition 2.1 satisfy the Yang–Baxter equation.⁶ It was originally due to [56, 13, 62] (though we adopt the notation of [25]), but it can also be verified directly from the explicit forms of these weights.

Lemma 2.2 ([25, Proposition 2.3.1]). *Fix any complex numbers $s, x, y, z \in \mathbb{C}$ with $x, y \neq 0$, and indices $i_1, j_1, k_1, i_3, j_3, k_3 \in \llbracket 0, n \rrbracket$. We have*

$$(2.4) \quad \begin{aligned} & \sum_{0 \leq i_2, j_2, k_2 \leq n} R_{y/x}(i_1, j_1; i_2, j_2) R_{z/x}(k_1, j_2; k_2, j_3) R_{z/y}(k_2, i_2; k_3, i_3) \\ &= \sum_{0 \leq i_2, j_2, k_2 \leq n} R_{z/y}(k_1, i_1; k_2, i_2) R_{z/x}(k_2, j_1; k_3, j_2) R_{y/x}(i_2, j_2; i_3, j_3). \end{aligned}$$

⁶The L -weights can equivalently be described as obtained by applying the fusion procedure [62] to the R -weights. This, given the Yang–Baxter equation for the R -weights (2.4), can be seen to directly imply the Yang–Baxter equations between the L and R weights, provided by (2.5) and (2.6) below; see [25, Appendix B] for further details.

Further fixing integer sequences $\mathbf{K}_1, \mathbf{K}_3 \in \mathbb{Z}_{\geq 0}^n$, we have

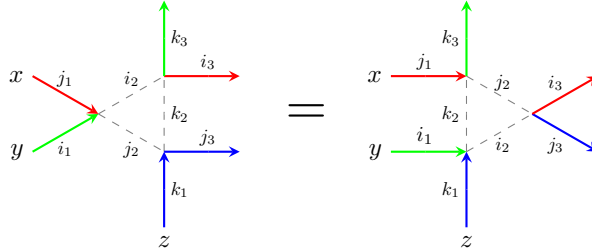
$$(2.5) \quad \begin{aligned} & \sum_{i_2, j_2, \mathbf{K}_2} R_{y/x}(i_1, j_1; i_2, j_2) L_{x;s}(\mathbf{K}_1, j_2; \mathbf{K}_2, j_3) L_{y;s}(\mathbf{K}_2, i_2; \mathbf{K}_3, i_3) \\ &= \sum_{i_2, j_2, \mathbf{K}_2} L_{y;s}(\mathbf{K}_1, i_1; \mathbf{K}_2, i_2) L_{x;s}(\mathbf{K}_2, j_1; \mathbf{K}_3, j_2) R_{y/x}(i_2, j_2; i_3, j_3), \end{aligned}$$

and

$$(2.6) \quad \begin{aligned} & \sum_{i_2, j_2, \mathbf{K}_2} R_{y/x}(i_1, j_1; i_2, j_2) \widehat{L}_{x;s}(\mathbf{K}_1, j_2; \mathbf{K}_2, j_3) L_{y;s}(\mathbf{K}_2, i_2; \mathbf{K}_3, i_3) \\ &= \sum_{i_2, j_2, \mathbf{K}_2} L_{y;s}(\mathbf{K}_1, i_1; \mathbf{K}_2, i_2) \widehat{L}_{x;s}(\mathbf{K}_2, j_1; \mathbf{K}_3, j_2) R_{y/x}(i_2, j_2; i_3, j_3), \end{aligned}$$

where in both equations i_2, j_2 are ranged over $\llbracket 0, n \rrbracket$, and \mathbf{K}_2 is ranged over $\mathbb{Z}_{\geq 0}^n$.

It will often be useful to interpret such equations diagrammatically. The diagrammatic interpretation of (2.4) is given by



where on each side of the equation is a family of vertices, and we view the weight of each family as the product of the weights of its constituent vertices. A rapidity parameter (x , y , or z in the above) is assigned at the beginning of each line, and it remains fixed along this line. Along the solid edges the colors are fixed, and along the dashed ones they are summed over. The equations (2.5) and (2.6) similarly have diagrammatic interpretations (which we do not depict here).

2.2. Height Functions and Partition Functions. In this section we introduce several partition functions (that is, sums of weights of colored path ensembles), which will be of use to us. Similarly to the notion of a colored six-vertex ensemble from Section 1.2, a *colored higher spin path ensemble* on a domain $\mathcal{D} \subseteq \mathbb{Z}^2$ is a consistent assignment of a colored higher spin arrow configuration $(\mathbf{A}(v), b(v); \mathbf{C}(v), d(v))$ to each vertex $v \in \mathcal{D}$.

Associated with a colored higher spin path ensemble are *height functions*, which count how many paths of specified colors are to the right of (equivalently, below) or to the left of (equivalently, above) a given location. More specifically, given a colored higher spin path ensemble \mathcal{E} on a domain $\mathcal{D} \subseteq \mathbb{Z}^2$, for any integer $c \geq 0$, define $\mathfrak{h}_c^{\rightarrow} : \mathbb{Z}^2 \rightarrow \mathbb{Z}$ and $\mathfrak{h}_c^{\leftarrow} : \mathbb{Z}^2 \rightarrow \mathbb{Z}$ as follows. For any $(i, j) \in \mathbb{Z}^2$, set $\mathfrak{h}_c^{\rightarrow}(i, j)$ to be the number of arrows of color c in \mathcal{E} that intersect the vertical ray from $(i + 1/2, j + 1/2)$ to $(i + 1/2, -\infty)$; similarly set $\mathfrak{h}_c^{\leftarrow}(i, j)$ to be the number of arrows of color c in \mathcal{E} that do not intersect the vertical ray from $(i + 1/2, j + 1/2)$ to $(i + 1/2, -\infty)$. Further define $\mathfrak{h}_{\geq c}^{\rightarrow} : \mathbb{Z}^2 \rightarrow \mathbb{Z}_{\geq 0}$ and $\mathfrak{h}_{\geq c}^{\leftarrow} : \mathbb{Z}^2 \rightarrow \mathbb{Z}_{\geq 0}$ by setting $\mathfrak{h}_{\geq c}^{\rightarrow}(i, j) = \sum_{k=c}^{\infty} \mathfrak{h}_k^{\rightarrow}(i, j)$ and $\mathfrak{h}_{\geq c}^{\leftarrow}(i, j) = \sum_{k=c}^{\infty} \mathfrak{h}_k^{\leftarrow}(i, j)$, for each $(i, j) \in \mathbb{Z}^2$. Since the colored stochastic six-vertex model gives rise to a random colored six-vertex ensemble on \mathcal{D} , it also gives rise to a family of random height functions.

We next introduce notation for weights of path ensembles on negative half-strips of the form $\mathbb{Z}_{\leq 0} \times \llbracket 1, N \rrbracket$ (which will frequently be the domain for our models). Observe in what follows that, in the “bulk” $\mathbb{Z}_{< 0} \times \llbracket 1, N \rrbracket$ of the half-strip, we take the spin s to be generic and use the weights $L_{x;s}$ (or $\widehat{L}_{x;s}$). However, on the y -axis boundary of the half-strip, we take $s = 0$ and use the weights $L_{x;0}$. This will later be relevant for producing stochastic matchings, such as Proposition 3.7 below.

Definition 2.3. Fix an integer $N \geq 1$; a complex number $s \in \mathbb{C}$; a sequence of complex numbers $\mathbf{x} = (x_1, x_2, \dots, x_N)$; and a colored higher spin path ensemble \mathcal{E} on $\mathcal{D}_N = \mathbb{Z}_{\leq 0} \times \llbracket 1, N \rrbracket$, whose arrow configuration at any vertex $v \in \mathcal{D}_N$ is denoted by $(\mathbf{A}(v), b(v); \mathbf{C}(v), d(v))$. Set

$$(2.7) \quad \begin{aligned} L_{\mathbf{x};s}(\mathcal{E}) &= \prod_{k=1}^{\infty} \prod_{j=1}^N L_{x_j;s}(\mathbf{A}(-k, j), b(-k, j); \mathbf{C}(-k, j), d(-k, j)) \\ &\quad \times \prod_{j=1}^N L_{x_j;0}(\mathbf{A}(0, j), b(0, j); \mathbf{C}(0, j), d(0, j)); \\ \widehat{L}_{\mathbf{x};s}(\mathcal{E}) &= \prod_{k=1}^{\infty} \prod_{j=1}^N \widehat{L}_{x_j;s}(\mathbf{A}(-k, j), b(-k, j); \mathbf{C}(-k, j), d(-k, j)) \\ &\quad \times \prod_{j=1}^N L_{x_j;0}(\mathbf{A}(0, j), b(0, j); \mathbf{C}(0, j), d(0, j)). \end{aligned}$$

The above notation implicitly assumes that, in each infinite product, all but finitely many factors are equal to 1; this will always be the case below.

We next have the following definition for certain types of compositions; below, we recall from Section 1.6 the notation $\mathbf{m}_k(\mu) = \#\{j \in \llbracket 1, \ell(\mu) \rrbracket : \mu_j = k\}$ and $X_{[i,j]} = \sum_{k=i}^j X_k$ for any $\mathbf{X} \in \mathbb{R}^n$.

Definition 2.4. Let $N \geq 0$ be an integer and $\ell = (\ell_1, \ell_2, \dots, \ell_n) \in \mathbb{Z}_{\geq 0}^n$ be a composition of N . A composition $\mu = (\mu_1, \mu_2, \dots, \mu_N)$ is called ℓ -colored if $\mu_i \geq \mu_j$ whenever $\ell_{[1,c-1]} + 1 \leq i \leq j \leq \ell_{[1,c]}$, for each $c \in \llbracket 1, n \rrbracket$; we then denote the signature $\mu^{(c)} = (\mu_{\ell_{[1,c-1]}+1}, \mu_{\ell_{[1,c-1]}+2}, \dots, \mu_{\ell_{[1,c]}})$.

If μ is ℓ -colored for some $\ell \in \mathbb{Z}_{\geq 0}^n$, then we call μ an n -composition, and we write $\mu = (\mu^{(1)} \mid \mu^{(2)} \mid \dots \mid \mu^{(n)})$. Let Comp_n denote the set of n -compositions, and let $\text{Comp}_n(N) \subseteq \text{Comp}_n$ denote the set of n -compositions of length N . For any n -composition $\mu \in \text{Comp}_n$, and integers $k \geq 0$ and $c \in \llbracket 1, n \rrbracket$, define the (sums of) multiplicities $\mathbf{m}_k^{\geq c}(\mu) = \sum_{i=c}^n \mathbf{m}_k(\mu^{(i)})$ and $\mathbf{m}_{\leq k}^{\geq c}(\mu) = \sum_{i=c}^n \mathbf{m}_{\leq k}(\mu^{(i)})$.

Remark 2.5. Any n -composition $\mu \in \text{Comp}_n(N)$ indexes a family of N colored arrows vertically exiting the row $\mathbb{Z}_{\leq 0}$, in which $\mathbf{m}_k(\mu^{(c)})$ arrows of color c exit through site $-k$, for all integers $c \in \llbracket 1, n \rrbracket$ and $k \geq 0$.

2.3. Nonsymmetric Functions. In this section we define a family of nonsymmetric functions f , and of symmetric ones G , as partition functions for the vertex model with weights given by Definition 2.1. They are similar to those from [25, Definition 3.5.1] and [25, Definition 4.4.1], respectively.

Definition 2.6. Fix an integer $N \geq 0$; two n -compositions $\mu = (\mu^{(1)} \mid \mu^{(2)} \mid \dots \mid \mu^{(n)})$ and $\nu = (\nu^{(1)} \mid \nu^{(2)} \mid \dots \mid \nu^{(n)})$; and a function $\sigma : \llbracket 1, N \rrbracket \rightarrow \llbracket 1, n \rrbracket$.

If $\ell(\mu) = \ell(\nu) + N$, then let $\mathfrak{P}_f(\mu/\nu; \sigma)$ denote the set of colored higher spin path ensembles on $\mathcal{D}_N = \mathbb{Z}_{\leq 0} \times \llbracket 1, N \rrbracket$ with the following boundary data.

- (1) For each $j \in \llbracket 1, N \rrbracket$, an arrow of color $\sigma(j)$ horizontally enters \mathcal{D}_N through⁷ $(-\infty, j)$.
- (2) For each $k \geq 0$ and $c \in \llbracket 1, n \rrbracket$, $\mathbf{m}_k(\nu^{(c)})$ arrows of color c vertically enter \mathcal{D}_N through $(-k, 1)$.
- (3) For each $k \geq 0$ and $c \in \llbracket 1, n \rrbracket$, $\mathbf{m}_k(\mu^{(c)})$ arrows of color c vertically exit \mathcal{D}_N through $(-k, N)$.

See the left side of Figure 6 for a depiction when $\mu = (7, 5 \mid 5, 4, 1 \mid 3, 2, 2)$; $\nu = (\emptyset \mid 6 \mid 6, 5)$; and $(\sigma(1), \sigma(2), \sigma(3), \sigma(4), \sigma(5)) = (1, 3, 2, 1, 2)$. There, red, green, and blue are colors 1, 2, and 3, respectively.

Similarly, if $\ell(\mu) = \ell(\nu)$, then let $\mathfrak{P}_G(\mu/\nu)$ denote the set of colored higher spin path ensembles on $\mathcal{D}_N = \mathbb{Z}_{\leq 0} \times \llbracket 1, N \rrbracket$, with the following boundary data.

- (1) For each integer $j \in \llbracket 1, N \rrbracket$, no arrow horizontally enters or exits \mathcal{D}_N through the j -th row.
- (2) For each $k \geq 0$ and $c \in \llbracket 1, n \rrbracket$, $\mathbf{m}_k(\mu^{(c)})$ arrows of color c vertically enter \mathcal{D}_N through $(-k, 1)$.
- (3) For each $k \geq 0$ and $c \in \llbracket 1, n \rrbracket$, $\mathbf{m}_k(\nu^{(c)})$ arrows of color c vertically exit \mathcal{D}_N through $(-k, N)$.

See the right side of Figure 6 for a depiction when $\mu = (7, 5 \mid 7, 6 \mid 6, 4)$ and $\nu = (5, 2 \mid 5, 1 \mid 3, 2)$.

For any complex number $s \in \mathbb{C}$ and sequence of complex numbers $\mathbf{x} = (x_1, x_2, \dots, x_N)$, let

$$(2.8) \quad f_{\mu/\nu;s}^{\sigma}(\mathbf{x}) = \sum_{\mathfrak{P}_f(\mu/\nu;\sigma)} \widehat{L}_{\mathbf{x};s}(\mathcal{E}); \quad G_{\mu/\nu;s}(\mathbf{x}) = \sum_{\mathfrak{P}_G(\mu/\nu)} L_{\mathbf{x};s}(\mathcal{E}).$$

If $\nu = \emptyset$ is empty, we write $f_{\mu;s}^{\sigma}(\mathbf{x}) = f_{\mu/\emptyset;s}^{\sigma}(\mathbf{x})$ and $G_{\mu;s}(\mathbf{x}) = G_{\mu/0^N;s}(\mathbf{x})$. If $N = 1$, we may write $f_{\mu/\nu;s}^{\sigma(1)}$ in place of $f_{\mu/\nu;s}^{\sigma}$.

Observe that the quantity $\widehat{L}_{\mathbf{x};s}(\mathcal{E})$ appearing as the summand in (2.8) defining $f_{\mu/\nu;s}^{\sigma}$ is bounded, since all but finitely many of the vertices in any ensemble $\mathcal{E} \in \mathfrak{P}_f(\mu/\nu;\sigma)$ have arrow configurations of the form $(\mathbf{e}_0, i; \mathbf{e}_0, i)$ for some integer $i \in \llbracket 1, n \rrbracket$, and we have $\widehat{L}_{x_j}(\mathbf{e}_0, i; \mathbf{e}_0, i) = 1$ by (2.3) and (2.1). Similarly, $L_{\mathbf{x};s}(\mathcal{E})$ appearing as the summand in (2.8) defining $G_{\mu/\nu;s}$ is bounded, since all but finitely many vertices in any $\mathcal{E} \in \mathfrak{P}_G(\mu/\nu)$ have arrow configurations of the form $(\mathbf{e}_0, 0; \mathbf{e}_0, 0)$, and we have $L_x(\mathbf{e}_0, 0; \mathbf{e}_0, 0) = 1$ by (2.1).

2.4. Properties of f and G . In this section we provide properties (that are minor variants of those in [25]) of the f and G functions from Definition 2.6. The first is the symmetry of G in its arguments; we omit its proof, which follows quickly from the Yang–Baxter equation (2.5) (see also [25, Definition 4.4.1] or [22, Proposition 4.7]).

Lemma 2.7. *Adopt the notation of Definition 2.6, and let $\varsigma : \llbracket 1, M \rrbracket \rightarrow \llbracket 1, M \rrbracket$ denote a permutation. We have $G_{\mu/\nu;s}(\mathbf{y}) = G_{\mu/\nu;s}(\varsigma(\mathbf{y}))$, where $\varsigma(\mathbf{y}) = (y_{\varsigma(1)}, y_{\varsigma(2)}, \dots, y_{\varsigma(M)})$.*

The second is a *branching identity*; we omit its proof, which is very similar to that of [25, Proposition 4.2.1] (and quickly follows from “cutting” the vertex models shown in Figure 6 at the line $\{y = k\}$).

⁷This means that, for sufficiently large i , each edge between $(-i-1, j)$ and $(-i, j)$ contains an arrow of color $\sigma(j)$.

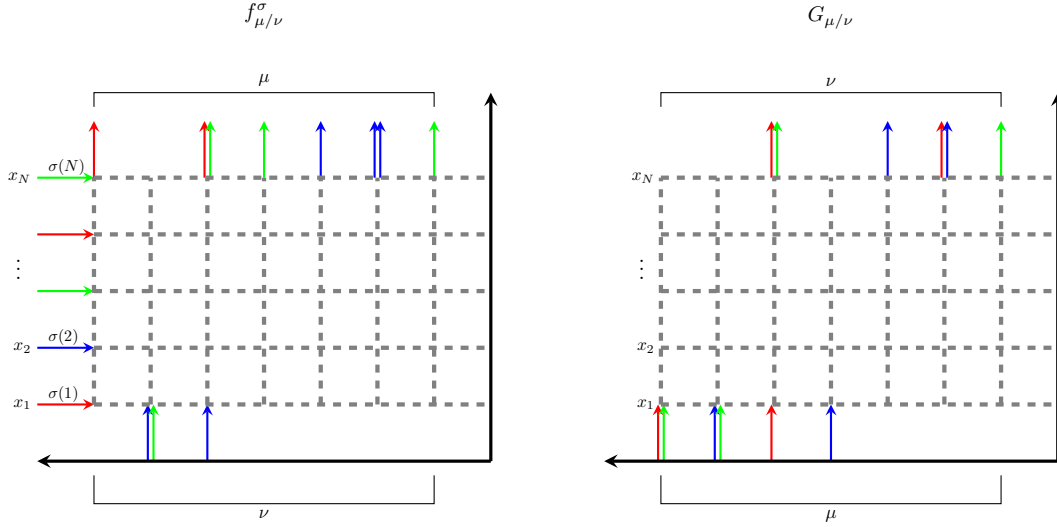


FIGURE 6. Depicted to the left and right are vertex models for $f_{\mu/\nu;s}^\sigma$ and $G_{\mu/\nu;s}$, respectively.

Lemma 2.8. *Adopt the notation of Definition 2.6; let $\ell = \ell(\nu)$; and fix $k \in \llbracket 1, N \rrbracket$. We have*

$$f_{\mu/\nu;s}^\sigma(\mathbf{x}) = \sum_{\kappa \in \text{Comp}_n(\ell+k)} f_{\kappa/\nu;s}^{\sigma|_{\llbracket 1, k \rrbracket}}(\mathbf{x}_{[1, k]}) f_{\mu/\kappa;s}^{\sigma|_{\llbracket k+1, N \rrbracket}}(\mathbf{x}_{[k+1, N]});$$

$$G_{\mu/\nu;s}(\mathbf{x}) = \sum_{\kappa \in \text{Comp}_n(\ell)} G_{\mu/\kappa;s}(\mathbf{x}_{[1, k]}) G_{\kappa/\nu;s}(\mathbf{x}_{[k+1, N]}).$$

Here, we have defined the variable sets $\mathbf{x}_{[1, k]} = (x_1, x_2, \dots, x_k)$ and $\mathbf{x}_{[k+1, N]} = (x_{k+1}, x_{k+2}, \dots, x_N)$. For any interval $I = \llbracket i_0+1, i_0+|I| \rrbracket \subset \llbracket 1, N \rrbracket$, we have also defined the function $\sigma|_I : \llbracket 1, |I| \rrbracket \rightarrow \llbracket 1, n \rrbracket$ by setting $\sigma|_I(i) = \sigma(i + i_0)$ for each $i \in \llbracket 1, |I| \rrbracket$.

The third is a *Cauchy identity*. Its proof is similar to [25, Proposition 4.5.1], following as a consequence of the Yang–Baxter equation (2.6), though we include it here (since some results below, such as Proposition 3.7, will amount to mild modifications of it).

Lemma 2.9. *Fix integers $n, M, N \geq 1$; a complex number $s \in \mathbb{C}$; sequences of complex numbers $\mathbf{x} = (x_1, x_2, \dots, x_N)$ and $\mathbf{y} = (y_1, y_2, \dots, y_M)$; and a function $\sigma : \llbracket 1, N \rrbracket \rightarrow \llbracket 1, n \rrbracket$. If*

$$(2.9) \quad \max_{\substack{1 \leq i \leq M \\ 1 \leq j \leq N}} \left| \frac{1 - sx_j}{x_j - s} \right| \cdot \left| \frac{y_i - s}{1 - sy_i} \right| < 1,$$

then

$$\sum_{\mu \in \text{Comp}_n(N)} f_{\mu;s}^\sigma(\mathbf{x}) G_{\mu;s}(\mathbf{y}) = \prod_{i=1}^M \prod_{j=1}^N \frac{x_j - qy_i}{x_j - y_i}.$$

Proof. For each integer $i \in \llbracket 1, n \rrbracket$, let $\ell_i = \#\{\sigma^{-1}(i)\}$ denote the number of preimages of i under σ , and set $\mathbf{e}_\ell = (\ell_1, \ell_2, \dots, \ell_n)$. We begin by considering the partition function \mathcal{Z} for the vertex model shown in Figure 7.

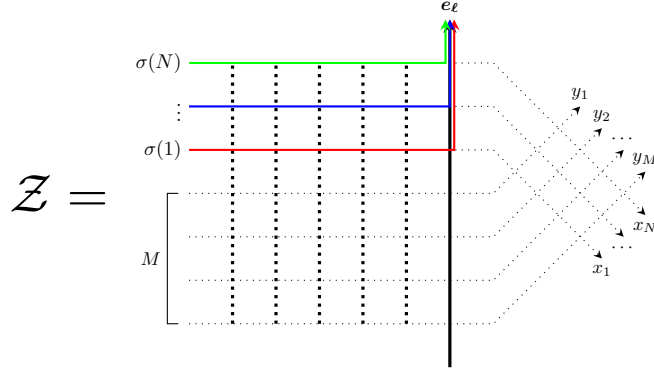


FIGURE 7. Shown above is a vertex model used in the proof of Lemma 2.9.

This model consists of three regions that we denote by \mathcal{R}_1 , \mathcal{R}_2 , and \mathcal{R}_3 . The first region $\mathcal{R}_1 = \mathbb{Z}_{\leq 0} \times \llbracket 1, M \rrbracket$ constitutes the bottom M rows (weakly) to the left of the y -axis. The second region $\mathcal{R}_2 = \mathbb{Z}_{\leq 0} \times \llbracket M + 1, M + N \rrbracket$ constitutes the remaining N rows (weakly) to the left of the y -axis. The third region \mathcal{R}_3 is the $M \times N$ “cross” to the right of the y -axis. Different vertex weights (recall Definition 1.1 and Definition 2.1) are used in these regions. In \mathcal{R}_1 , for each $i \in \llbracket 1, M \rrbracket$, we use the weight $L_{y_i;s}$ at $(-k, i)$ if $k \geq 1$ and $L_{y_i;0}$ at $(0, i)$; in \mathcal{R}_2 , for each $j \in \llbracket 1, N \rrbracket$, we use the weight $\widehat{L}_{x_j;s}$ at $(-k, M + j)$ if $k \geq 1$ and $L_{x_j;0}$ at $(0, M + j)$; and in \mathcal{R}_3 we use the weight R_{y_i/x_j} at the intersection of i -th column (from the left) and j -th row (from the bottom) of the cross.

The boundary conditions for the model in Figure 7 are prescribed as follows. The entrance data is defined by having no arrows vertically enter any column of the model; having no arrow horizontally enter through the bottom M rows of the model; and having an arrow of color $\sigma(j)$ enter through the $(M + j)$ -th row of the model, for each $j \in \llbracket 1, N \rrbracket$. The exit data is defined by having ℓ_i arrows of color i exit the y -axis, for each index $i \in \llbracket 1, n \rrbracket$; having no arrows exit through any other column to the left of the y -axis; and having no arrows exit the cross to the right of the y -axis.

Observe that this vertex model is *frozen*, that is, there is only one colored higher spin path ensemble with this boundary data with nonzero weight. It is the one in which, for each $j \in \llbracket 1, N \rrbracket$, the path of color $\sigma(j)$ in the $(M + j)$ -th row travels horizontally until it reaches the y -axis, and then proceeds vertically until it exits y -axis. Recalling from (1.1), (2.1), and (2.3) that

$$\begin{aligned} L_{y_i;s}(\mathbf{e}_0, 0; \mathbf{e}_0, 0) &= 1; & \widehat{L}_{x_j;s}(\mathbf{e}_0, \sigma(j); \mathbf{e}_0, \sigma(j)) &= 1; \\ L_{x_j;0} \left(\sum_{k=1}^{j-1} \mathbf{e}_{\sigma(k)}, \sigma(j); \sum_{k=1}^j \mathbf{e}_{\sigma(k)}, 0 \right) &= 1; & R_{y_i/x_j}(0, 0; 0, 0) &= 1, \end{aligned}$$

it follows that the partition function for the vertex model from Figure 7 is given by

$$(2.10) \quad \mathcal{Z} = 1.$$

Next, by MN sequences of applications of the Yang–Baxter equation (2.6), the partition function \mathcal{Z} of this vertex model is unchanged if the cross originally in region \mathcal{R}_3 is moved to the left of

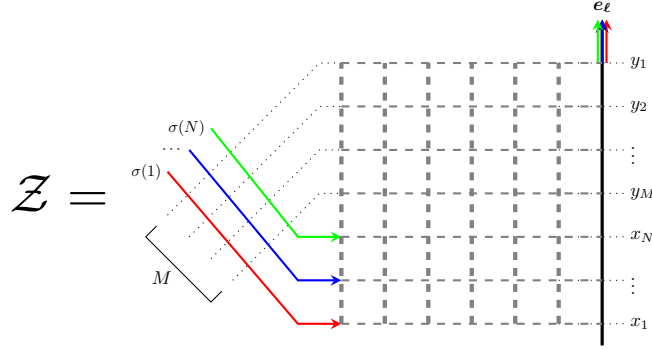


FIGURE 8. Shown above is the vertex model from Figure 7 after using the Yang–Baxter equation to move the cross to the left of $\mathbb{Z}_{\leq 0} \times \llbracket 1, M + N \rrbracket$.

$\mathcal{R}_1 \cup \mathcal{R}_2 = \mathbb{Z}_{\leq 0} \times \llbracket 1, M + N \rrbracket$. In particular, \mathcal{Z} is also the partition function of the vertex model in Figure 8.

This model also consists of three regions \mathcal{R}'_1 , \mathcal{R}'_2 , and \mathcal{R}'_3 . The third \mathcal{R}'_3 is an $M \times N$ cross, that is now to the left of $\mathbb{Z}_{\leq 0} \times \llbracket 1, M + N \rrbracket$. The second $\mathcal{R}'_2 = \mathbb{Z}_{\leq 0} \times \llbracket 1, N \rrbracket$ consists of the bottom N rows to the right of the cross. The first \mathcal{R}'_1 consists of the remaining M rows to the right of the cross. Again different vertex weights are used in these regions. In \mathcal{R}'_1 , for each $i \in \llbracket 1, M \rrbracket$, we use the weight $L_{y_i;s}$ at $(-k, i + N)$ for $k \geq 1$ and $L_{y_i;0}$ at $(0, i + N)$. In \mathcal{R}'_2 , for $j \in \llbracket 1, N \rrbracket$, we use the weight $\widehat{L}_{x_j;s}$ at $(-k, j)$ if $k \geq 1$ and $L_{x_j;0}$ at $(0, j)$. In \mathcal{R}'_3 , we use the weight R_{y_i/x_j} at the intersection of the i -th column and j -th row of the cross.

The boundary data for the model in Figure 8 is prescribed as follows (it must match that of Figure 7). The entrance data is defined by having no arrows vertically enter any column in the model, either in or to the right of the cross, and having an arrow of color $\sigma(j)$ enter through the j -th row (from the bottom) of the cross, for each $j \in \llbracket 1, N \rrbracket$. The exit data is defined by having no arrows horizontally exit through any row of the model; having ℓ_i arrows of color i exit through the y -axis, for each $i \in \llbracket 1, n \rrbracket$; and having no arrows exit through any other column to the left of the y -axis.

Let us now analyze this vertex model. Using the fact from (2.9) (and (2.1) and (2.3)) that, for any $k \in \llbracket 1, n \rrbracket$,

$$\max_{\substack{1 \leq i \leq M \\ 1 \leq j \leq N}} \left| \frac{\widehat{L}_{x_j;s}(\mathbf{e}_0, 0; \mathbf{e}_0, 0) \cdot L_{y_i;s}(\mathbf{e}_0, k; \mathbf{e}_0, k)}{\widehat{L}_{x_j;s}(\mathbf{e}_0, k; \mathbf{e}_0, k) \cdot L_{y_i;s}(\mathbf{e}_0, 0; \mathbf{e}_0, 0)} \right| = \max_{\substack{1 \leq i \leq M \\ 1 \leq j \leq N}} \left| \frac{1 - sx_j}{x_j - s} \cdot \frac{y_i - s}{1 - sy_i} \right| < 1,$$

it is quickly verified (see the proof of [25, Theorem 3.2.3]) that a colored higher spin path ensemble on $\mathbb{Z}_{\leq 0} \times \llbracket 1, M + N \rrbracket$ has nonzero weight only if all but finitely many vertices in \mathcal{R}'_1 have arrow configurations of the form $(\mathbf{e}_0, 0; \mathbf{e}_0, 0)$, and all but finitely many vertices in \mathcal{R}'_2 have arrow configurations of the form $(\mathbf{e}_0, k; \mathbf{e}_0, k)$ for some $k \in \llbracket 1, n \rrbracket$ (which may depend on the vertex). This means that an arrow must horizontally enter \mathcal{R}'_2 through $(-\infty, j)$ for each $j \in \llbracket 1, N \rrbracket$, and no arrow can horizontally enter \mathcal{R}'_1 . Since each edge of the cross \mathcal{R}'_3 can accommodate at most one arrow, it follows that this cross is frozen; the vertex in its i -th column and j -th row must have arrow

configuration $(0, \sigma(j); 0, \sigma(j))$. The weight of \mathcal{R}'_3 is therefore

$$(2.11) \quad \prod_{i=1}^M \prod_{j=1}^N R_{y_i/x_j}(0, \sigma(j); 0, \sigma(j)) = \prod_{i=1}^M \prod_{j=1}^N \frac{x_j - y_i}{x_j - qy_i},$$

where in the last equality we used (1.1).

The colored higher spin path ensembles in \mathcal{R}'_1 and \mathcal{R}'_2 can be arbitrary elements of $\mathfrak{P}_G(\mu/0^N)$ and $\mathfrak{P}_f(\mu/\emptyset; \sigma)$ for any $\mu \in \text{Comp}_n(N)$ that is shared between \mathcal{R}'_1 and \mathcal{R}'_2 (this n -composition μ prescribes the x -coordinates where paths in the ensemble vertically exit \mathcal{R}'_2 and enter \mathcal{R}'_1). Hence, the weight of $\mathcal{R}'_1 \cup \mathcal{R}'_2$ is

$$\sum_{\mu \in \text{Comp}_n(N)} f_{\mu; s}^\sigma(\mathbf{x}) G_{\mu; s}(\overleftarrow{\mathbf{y}}),$$

where we recall the notation $\overleftarrow{\mathbf{y}} = (y_M, y_{M-1}, \dots, y_1)$ from Section 1.6. Together with the weight (2.11) of \mathcal{R}'_3 (and the symmetry of G from Lemma 2.7), it follows that the weight of the vertex model in Figure 8 is

$$(2.12) \quad \mathcal{Z} = \prod_{i=1}^M \prod_{j=1}^N \frac{x_j - y_i}{x_j - qy_i} \cdot \sum_{\mu \in \text{Comp}_n(N)} f_{\mu; s}^\sigma(\mathbf{x}) G_{\mu; s}(\mathbf{y}).$$

The lemma then follows from (2.10) and (2.12). \square

3. PROBABILITY MEASURES AND MATCHINGS

In this section we use the functions f and G from Definition 2.6 to produce probability measures on sequences of compositions, and explain how such measures are related to the stochastic six-vertex model. The former is done in Section 3.1, and the latter is done in Section 3.2 and Section 3.3. Throughout this section, we fix integers $n, M, N \geq 1$; a composition $\ell = (\ell_1, \ell_2, \dots, \ell_n)$ of N ; a function $\sigma : \llbracket 1, N \rrbracket \rightarrow \llbracket 1, n \rrbracket$, such that for each $i \in \llbracket 1, n \rrbracket$ we have $\ell_i = \#\{\sigma^{-1}(i)\}$; a complex number $s \in \mathbb{C}$; and sequences of complex numbers $\mathbf{x} = (x_1, x_2, \dots, x_N)$ and $\mathbf{y} = (y_1, y_2, \dots, y_M)$, such that (2.9) holds.

3.1. Ascending fG Measures. In this section we introduce probability measures that arise from the branching and Cauchy identities (Lemma 2.8 and Lemma 2.9), which are similar to those appearing in [25, Equation (10.3.1)]. We begin with the following definition for certain families of compositions.

Definition 3.1. A sequence $\boldsymbol{\mu} = (\mu(0), \mu(1), \dots, \mu(M+N))$ of n -compositions is called $(M; \sigma)$ -*ascending* if the following hold, using the notation $\mu(i) = (\mu^{(1)}(i) \mid \dots \mid \mu^{(n)}(i))$ below.

- (1) We have $\mu(0) = (\emptyset \mid \dots \mid \emptyset)$ and $\mu(M+N) = (0^{\ell_1} \mid \dots \mid 0^{\ell_n})$.
- (2) (a) For all $j \in \llbracket 0, N \rrbracket$ and $c \in \llbracket 1, n \rrbracket$, we have $\ell(\mu^{(c)}(j)) = \sum_{k=1}^j \mathbb{1}_{\sigma(k)=c}$. Thus, $\ell(\mu(j)) = j$.
- (b) For all $i \in \llbracket N, M+N \rrbracket$ and $c \in \llbracket 1, n \rrbracket$, we have $\ell(\mu^{(c)}(i)) = \ell_c$. Thus, $\ell(\mu(i)) = N$.
- (3) For any $i \in \llbracket 1, M+N \rrbracket$ and $k \in \mathbb{Z}_{\geq 0}$, there is at most one index $\mathbf{q} = \mathbf{q}_\mu(k, i) \in \llbracket 1, n \rrbracket$ so that

$$(3.1) \quad \mathbf{m}_{\leq k-1}(\mu^{(\mathbf{q})}(i)) = \mathbf{m}_{\leq k-1}(\mu^{(\mathbf{q})}(i-1)) + 1.$$

We set $\mathbf{q}_\mu(k, i) = 0$ if no index in $\mathbf{q} \in \llbracket 1, n \rrbracket$ satisfying (3.1) exists. Moreover, for all $c \in \llbracket 1, n \rrbracket$ with $c \neq \mathbf{q}_\mu(k, i)$, we have $\mathbf{m}_{\leq k-1}(\mu^{(c)}(i)) = \mathbf{m}_{\leq k-1}(\mu^{(c)}(i-1))$.

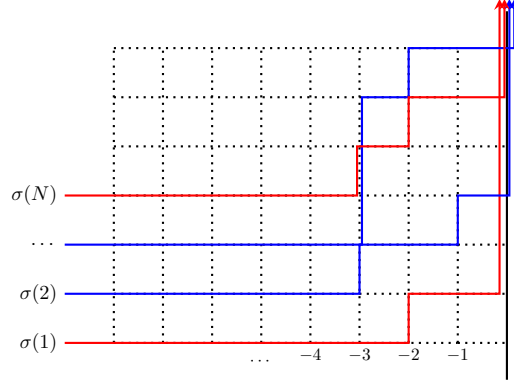


FIGURE 9. Depicted above is the colored higher spin path ensemble associated with the sequence $\boldsymbol{\mu}$ in the example at the end of Remark 3.2. Here, red and blue are colors 1 and 2, respectively.

Let us also define the $(M + N)$ -tuple $\mathbf{q}(\boldsymbol{\mu}) = (\mathbf{q}_{\boldsymbol{\mu}}(1, 1), \mathbf{q}_{\boldsymbol{\mu}}(1, 2), \dots, \mathbf{q}_{\boldsymbol{\mu}}(1, M + N))$.

Remark 3.2. Given an $(M; \sigma)$ -ascending sequence of compositions $\boldsymbol{\mu}$ as in Definition 3.1, we will often view the n -composition $\mu(i)$ as indexing the positions (in the sense of Remark 2.5) of the colored arrows exiting the row $\{y = i\}$, in a vertex model on $\mathbb{Z}_{\leq 0} \times \llbracket 1, M + N \rrbracket$ (of the form arising in the dashed part of Figure 8; see also Figure 9). This gives rise to a colored higher spin path ensemble on $\mathbb{Z}_{\leq 0} \times \llbracket 1, M + N \rrbracket$, that we will denote by $\mathcal{E}_{\boldsymbol{\mu}}$. In this way, $\mathbf{q}_{\boldsymbol{\mu}}(k, i)$ denotes the color of the arrow in $\mathcal{E}_{\boldsymbol{\mu}}$ along the edge connecting $(-k, i)$ to $(1 - k, i)$. Therefore, the $(M + N)$ -tuple $\mathbf{q}(\boldsymbol{\mu})$ records the colors of the arrows (from bottom to top) along the horizontal edges in $\mathcal{E}_{\boldsymbol{\mu}}$ joining the (-1) -st column to the 0-th one.

The boundary data for this ensemble is described as follows. For each $j \in \llbracket 1, N \rrbracket$, it has an arrow of color $\sigma(j)$ horizontally entering the row $\{y = j\}$, and it has no other arrows horizontally entering or exiting any other row of the model. For each $c \in \llbracket 1, n \rrbracket$, it has ℓ_c arrows of color c vertically exiting the y -axis $\{x = 0\}$, and it has no other arrows horizontally entering or exiting any other column of the model. We denote by $\mathfrak{P}_{\text{fG}}(M; \sigma)$ the set of colored higher spin path ensembles on $\mathbb{Z}_{\leq 0} \times \llbracket 1, M + N \rrbracket$ with these boundary conditions, as any $\mathcal{E}_{\boldsymbol{\mu}} \in \mathfrak{P}_{\text{fG}}(M; \sigma)$ can be thought of an ensemble from $\mathfrak{P}_G(\boldsymbol{\mu}/\emptyset)$ that is juxtaposed above one from $\mathfrak{P}_f(\boldsymbol{\mu}/\emptyset; \sigma)$ (recall Definition 2.6), for some n -composition $\boldsymbol{\mu} \in \text{Comp}_n(N)$. It is quickly verified that the above procedure is a bijection between $\mathfrak{P}_{\text{fG}}(M; \sigma)$ and $(M; \sigma)$ -ascending sequences $\boldsymbol{\mu}$ of n -compositions.

See Figure 9 for a depiction, where $(n, M, N) = (2, 3, 4)$ and

$$\begin{aligned} \sigma(1) = 1, \quad \sigma(2) = 2, \quad \sigma(3) = 2, \quad \sigma(4) = 1; \quad & \mu(1) = (2 \mid \emptyset), \quad \mu(2) = (0 \mid 3), \\ \mu(3) = (0 \mid 3, 1), \quad \mu(4) = (3, 0 \mid 3, 0), \quad \mu(5) = (2, 0 \mid 3, 0), \quad \mu(6) = (0, 0 \mid 2, 0). \end{aligned}$$

Next we define the following probability measure on sequences of ascending compositions.

Definition 3.3. Define the probability measure $\mathbb{P}_{\text{fG}}^{\sigma} = \mathbb{P}_{\text{fG}; n; s; \mathbf{x}; \mathbf{y}}^{\sigma}$ on $(M; \sigma)$ -ascending sequences of n -compositions, by setting

$$(3.2) \quad \mathbb{P}_{\text{fG}}^{\sigma}[\boldsymbol{\mu}] = \mathcal{Z}_{\mathbf{x}; \mathbf{y}}^{-1} \cdot \prod_{j=1}^N f_{\mu(j)/\mu(j-1); s}^{\sigma(j)}(x_j) \prod_{i=N+1}^{M+N} G_{\mu(i-1)/\mu(i); s}(y_{i-N}),$$

for each $(M; \sigma)$ -ascending sequence $\boldsymbol{\mu} = (\mu(0), \mu(1), \dots, \mu(M+N))$, where

$$(3.3) \quad \mathcal{Z}_{\mathbf{x}; \mathbf{y}} = \prod_{i=1}^M \prod_{j=1}^N \frac{x_j - qy_i}{x_j - y_i}.$$

Here, we implicitly assume that s , \mathbf{x} , and \mathbf{y} are such that the right side of (3.2) is nonnegative (as is guaranteed by for example setting $q \in [0, 1]$, setting s sufficiently close to 0, and setting $0 < y_i < x_j < 1$ for each $(i, j) \in \llbracket 1, M \rrbracket \times \llbracket 1, N \rrbracket$). The fact that these probabilities sum to one follows from the following lemma.

Lemma 3.4. *Under the notation and assumptions of Definition 3.3, we have*

$$\sum_{\boldsymbol{\mu}} \prod_{j=1}^N f_{\mu(j)/\mu(j-1); s}^{\sigma(j)}(x_j) \cdot \prod_{i=N+1}^{M+N} G_{\mu(i-1)/\mu(i); s}(y_{i-N}) = \mathcal{Z}_{\mathbf{x}; \mathbf{y}},$$

where the sum on the left side is over all $(M; \sigma)$ -ascending sequences of n -compositions $\boldsymbol{\mu} = (\mu(0), \mu(1), \dots, \mu(M+N))$.

Proof. By the branching identity Lemma 2.8, we have for any $\mu^{(N)} \in \text{Comp}_n(N)$ that

$$\sum_{\boldsymbol{\mu}^{[0, N-1]}} \prod_{j=1}^N f_{\mu(j)/\mu(j-1); s}^{\sigma(j)}(x_j) = f_{\mu^{(N)}; s}^{\sigma}(\mathbf{x}); \quad \sum_{\boldsymbol{\mu}^{[N+1, M+N]}} \prod_{i=N+1}^{M+N} G_{\mu(i-1)/\mu(i); s}(y_{i-N}) = G_{\mu^{(N)}; s}(\mathbf{y}).$$

Here, the sums are over all sequences of n -compositions $\boldsymbol{\mu}^{[0, N-1]} = (\mu(0), \mu(1), \dots, \mu(N-1))$ and $\boldsymbol{\mu}^{[N+1, M+N]} = (\mu(N+1), \mu(N+2), \dots, \mu(M+N))$ satisfying the constraints of Definition 3.1. Hence,

$$\sum_{\boldsymbol{\mu}} \prod_{j=1}^N f_{\mu(j)/\mu(j-1); s}^{\sigma(j)}(x_j) \cdot \prod_{i=N+1}^{M+N} G_{\mu(i-1)/\mu(i); s}(y_{i-N}) = \sum_{\mu^{(N)} \in \text{Comp}_n(N)} f_{\mu^{(N)}; s}^{\sigma}(\mathbf{x}) G_{\mu^{(N)}; s}(\mathbf{y}).$$

This, together with the Cauchy identity Lemma 2.9, yields the lemma. \square

3.2. Matching Between Colored Stochastic Six-Vertex Models and $\mathbb{P}_{\text{fG}}^{\sigma}$. In this section we establish a matching between the law of the $(M+N)$ -tuple $\mathbf{q}(\boldsymbol{\mu})$ (recall Definition 3.1) associated with a sequence of compositions sampled from $\mathbb{P}_{\text{fG}}^{\sigma}$ (from Definition 3.3), with a certain random variable associated with the stochastic six-vertex model (from Section 1.2). We begin by defining the latter.

Definition 3.5. Let \mathcal{E} denote a six-vertex ensemble on the rectangular domain $\mathcal{D}_{M;N} = \llbracket 1, M \rrbracket \times \llbracket 1, N \rrbracket$. For each integer $i \in \llbracket 1, M \rrbracket$, let $c_i = c_i(\mathcal{E}) \in \llbracket 0, n \rrbracket$ denote the color of the path in \mathcal{E} vertically exiting $\mathcal{D}_{M;N}$ through (i, N) ; for each integer $j \in \llbracket 1, N \rrbracket$, let $d_j = d_j(\mathcal{E}) \in \llbracket 0, n \rrbracket$ denote the color of the path in \mathcal{E} horizontally exiting $\mathcal{D}_{M;N}$ through (M, j) . Then set $\mathfrak{C}(\mathcal{E}) = (c_1, c_2, \dots, c_M) \in \llbracket 1, n \rrbracket^M$ and $\mathfrak{D}(\mathcal{E}) = (d_1, d_2, \dots, d_N) \in \llbracket 1, n \rrbracket^N$.

We next require notation for the colored stochastic six-vertex model (defined at the end of Section 1.2) with σ -entrance data introduced in Section 1.2.

Definition 3.6. Let $\mathbb{P}_{\text{SV}}^{\sigma} = \mathbb{P}_{\text{SV}; \mathbf{x}; \mathbf{y}}^{\sigma}$ denote the measure on colored six-vertex ensembles on $\mathcal{D}_{M;N}$ obtained by running the colored stochastic six-vertex model on $\mathcal{D}_{M;N}$ under σ -entrance data, with weight R_{y_i/x_j} (recall Definition 1.1) at any vertex $(i, j) \in \mathcal{D}_{M;N}$.

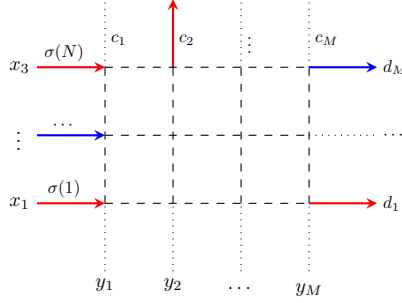


FIGURE 10. Shown above is the entrance and exit data for a colored six-vertex ensemble on $\mathcal{D}_{4;3} = \llbracket 1, 4 \rrbracket \times \llbracket 1, 3 \rrbracket$, under σ -entrance data for $(\sigma(1), \sigma(2), \sigma(3)) = (1, 2, 1)$ (with red being color 1 and blue being color 2).

We refer to Figure 10 for depictions of Definition 3.5 and Definition 3.6. The following proposition now provides a matching between the $(M+N)$ -tuple $\mathbf{q}(\boldsymbol{\mu})$ sampled under $\mathbb{P}_{\text{fG}}^\sigma$ of Definition 3.3 and the $(M+N)$ -tuple $\mathfrak{D}(\mathcal{E}) \cup \overleftarrow{\mathfrak{C}}(\mathcal{E})$ sampled under $\mathbb{P}_{\text{SV}}^\sigma$ of Definition 3.6.⁸ It is a colored generalization of [15, Theorem 5.5], though its proof is similar. We establish it in Section 3.3 below.

Proposition 3.7. *Fix an index sequence $\mathbf{q} = (q_1, q_2, \dots, q_{M+N}) \in \llbracket 0, n \rrbracket^{M+N}$; and define the M -tuple $\mathfrak{C} = (q_{M+N}, q_{M+N-1}, \dots, q_{N+1})$ and N -tuple $\mathfrak{D} = (q_1, q_2, \dots, q_N)$. Then,*

$$(3.4) \quad \mathbb{P}_{\text{SV}}^\sigma \left[\{ \mathfrak{C}(\mathcal{E}) = \mathfrak{C} \} \cap \{ \mathfrak{D}(\mathcal{E}) = \mathfrak{D} \} \right] = \mathbb{P}_{\text{fG}}^\sigma \left[\mathbf{q}(\boldsymbol{\mu}) = \mathbf{q} \right].$$

Here, on the left side of (3.4), the colored six-vertex ensemble \mathcal{E} is sampled under the colored stochastic six-vertex measure $\mathbb{P}_{\text{SV}; \mathbf{x}; \mathbf{y}}^\sigma$. On the right side of (3.4), the $(M; \sigma)$ -ascending sequence $\boldsymbol{\mu}$ of colored compositions is sampled under the measure $\mathbb{P}_{\text{fG}; n; s; \mathbf{x}; \mathbf{y}}^\sigma$.

Before establishing Proposition 3.7, we deduce the following corollary. It equates the joint law of the height functions (recall Section 2.2) evaluated along the exit sites of an $M \times N$ rectangle, sampled under the colored stochastic six-vertex model, with the joint law of the number of zero entries in a family $\boldsymbol{\mu}$ of n -compositions, sampled under the $\mathbb{P}_{\text{fG}}^\sigma$ measure.

Corollary 3.8. *The joint law of all the height functions*

$$(3.5) \quad \bigcup_{c=1}^n (\mathfrak{h}_{\geq c}^{\rightarrow}(M, 1), \mathfrak{h}_{\geq c}^{\rightarrow}(M, 2), \dots, \mathfrak{h}_{\geq c}^{\rightarrow}(M, N), \mathfrak{h}_{\geq c}^{\rightarrow}(M-1, N), \dots, \mathfrak{h}_{\geq c}^{\rightarrow}(0, N)),$$

is equal to the joint law of all zero-entry counts

$$(3.6) \quad \bigcup_{c=1}^n (\mathfrak{m}_0^{\geq c}(\mu(1)), \mathfrak{m}_0^{\geq c}(\mu(2)), \dots, \mathfrak{m}_0^{\geq c}(\mu(N)), \mathfrak{m}_0^{\geq c}(\mu(N+1)), \dots, \mathfrak{m}_0^{\geq c}(\mu(M+N))).$$

⁸Observe that the left side of (3.4) is independent of s , while the right side seems to involve s ; such a phenomenon had already been observed in the uncolored case in [27, Proposition 7.14], and in the different setting of colored stationary measures [8, Remark 4.6]. In our context, this fact will later enable us to freely choose s as we see fit, which will be useful in producing the simplest looking line ensembles.

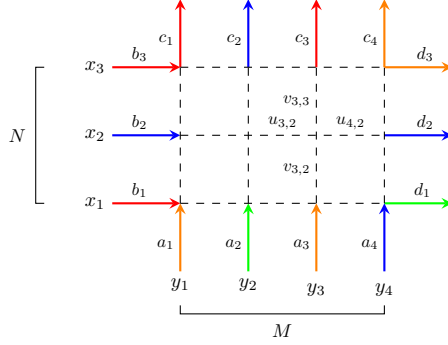


FIGURE 11. Shown above is a diagrammatic interpretation for $R_{\mathbf{x};\mathbf{y}}(\mathfrak{A}, \mathfrak{B}; \mathfrak{C}, \mathfrak{D})$.

Here, the height functions in (3.5) are associated with a colored six-vertex ensemble sampled under $\mathbb{P}_{\text{SV};\mathbf{x};\mathbf{y}}^\sigma$, and the zero-entry counts in (3.6) are associated with a $(M; \sigma)$ -ascending sequence of n -compositions $\boldsymbol{\mu} = (\mu(0), \mu(1), \dots, \mu(M+N))$ sampled under $\mathbb{P}_{\text{IG};n;s;\mathbf{x};\mathbf{y}}^\sigma$.

Proof. Adopt the notation of Proposition 3.7, and denote the M -tuple $\mathfrak{C}(\mathcal{E}) = (c_1, c_2, \dots, c_M)$ and N -tuple $\mathfrak{D}(\mathcal{E}) = (d_1, d_2, \dots, d_N)$. Then for each $c \in \llbracket 1, n \rrbracket$, $i \in \llbracket 1, M-1 \rrbracket$, and $j \in \llbracket 1, N \rrbracket$, we have (from the definition of the height function) that

$$(3.7) \quad \mathfrak{h}_{\geq c}^{\rightarrow}(M, j) = \sum_{a=1}^j \mathbb{1}_{\mathfrak{d}_a \geq c}; \quad \mathfrak{h}_{\geq c}^{\rightarrow}(M-i, N) = \sum_{a=1}^N \mathbb{1}_{\mathfrak{d}_a \geq c} + \sum_{b=1}^i \mathbb{1}_{c_{M-b+1} \geq c}.$$

Furthermore, we have

$$(3.8) \quad \mathfrak{m}_0^{\geq c}(\mu(j)) = \sum_{a=1}^j \mathbb{1}_{\mathfrak{q}_a \geq c}; \quad \mathfrak{m}_0^{\geq c}(\mu(N+i)) = \sum_{a=1}^{N+i} \mathbb{1}_{\mathfrak{q}_a \geq c} = \sum_{a=1}^N \mathbb{1}_{\mathfrak{q}_a \geq c} + \sum_{b=1}^i \mathbb{1}_{\mathfrak{q}_{N+b} \geq c}.$$

Since Proposition 3.7 implies that the $(M+N)$ -tuple $(\mathfrak{d}_1, \mathfrak{d}_2, \dots, \mathfrak{d}_N; c_M, c_{M-1}, \dots, c_1)$ has the same law as $(\mathfrak{q}_1, \mathfrak{q}_2, \dots, \mathfrak{q}_N; \mathfrak{q}_{N+1}, \mathfrak{q}_{N+2}, \dots, \mathfrak{q}_{M+N})$, the lemma follows from (3.7) and (3.8). \square

3.3. Proof of the Matching. In this section we establish Proposition 3.7. Before proceeding, it will be useful to set some notation. For any sequences $\mathfrak{A} = (a_1, a_2, \dots, a_M)$, $\mathfrak{B} = (b_1, b_2, \dots, b_N)$, $\mathfrak{C} = (c_1, c_2, \dots, c_M)$, and $\mathfrak{D} = (d_1, d_2, \dots, d_N)$ of indices in $\llbracket 0, n \rrbracket$, define

$$R_{\mathbf{x};\mathbf{y}}(\mathfrak{A}, \mathfrak{B}; \mathfrak{C}, \mathfrak{D}) = \sum \prod_{i=1}^M \prod_{j=1}^N R_{y_i/x_j}(v_{i,j}, u_{i,j}; v_{i+1,j}, u_{i,j+1}),$$

where the sum is over all sequences $(u_{i,j})$ and $(v_{i,j})$ of indices in $\llbracket 0, n \rrbracket$, with $(v_{k,1}, v_{k,N+1}) = (a_k, c_k)$ for each $k \in \llbracket 1, M \rrbracket$ and $(u_{1,k}, u_{M+1,k}) = (b_k, d_k)$ for each $k \in \llbracket 1, N \rrbracket$. See Figure 11 for a depiction.

Setting $\mathfrak{S}(\sigma) = (\sigma(1), \sigma(2), \dots, \sigma(N))$ and $\mathbf{0}_M = (0, 0, \dots, 0) \in \mathbb{Z}_{\geq 0}^M$, and recalling the notation of Definition 3.5 and Definition 3.6, observe for any $\mathfrak{C} \in \llbracket 0, n \rrbracket^M$ and $\mathfrak{D} \in \llbracket 0, n \rrbracket^N$ that

$$(3.9) \quad \mathbb{P}_{\text{SV};\mathbf{x};\mathbf{y}}^\sigma \left[\{ \mathfrak{C}(\mathcal{E}) = \mathfrak{C} \} \cap \{ \mathfrak{D}(\mathcal{E}) = \mathfrak{D} \} \right] = R_{\mathbf{x};\mathbf{y}}(\mathbf{0}_M, \mathfrak{S}(\sigma); \mathfrak{C}, \mathfrak{D}).$$

Now we can establish Proposition 3.7.

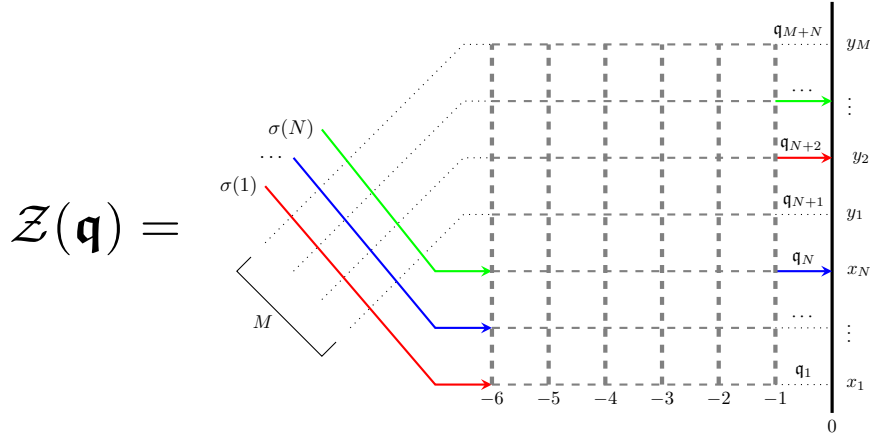


FIGURE 12. Shown above is the vertex model used in the proof of Proposition 3.7.

Proof of Proposition 3.7. The proof of this proposition will be close to that of Lemma 2.9. We begin by considering the partition function $\mathcal{Z}(\mathbf{q})$ for the vertex model depicted in Figure 12.

This model consists of three regions, denoted by \mathcal{R}_1 , \mathcal{R}_2 , and \mathcal{R}_3 . The first region \mathcal{R}_1 is the $M \times N$ “cross” to the left of $\mathbb{Z}_{<0} \times \llbracket 1, M+N \rrbracket$. The second $\mathcal{R}_2 = \mathbb{Z}_{<0} \times \llbracket 1, N \rrbracket$ constitutes the bottom N rows to the right of the cross. The third $\mathcal{R}_3 = \mathbb{Z}_{<0} \times \llbracket N+1, M+N \rrbracket$ constitutes the remaining M rows to the right of the cross. Different vertex weights (recall Definition 1.1 and Definition 2.1) are used in these regions. In \mathcal{R}_1 , we use R_{y_i/x_j} at the intersection of the i -th column (from the left) and j -th row (from the bottom) of the cross; in \mathcal{R}_2 , for each $j \in \llbracket 1, N \rrbracket$, we use $\hat{L}_{x_j;s}$ at each $(-k, j)$; and in \mathcal{R}_3 , for each $i \in \llbracket 1, M \rrbracket$, we use $L_{y_i;s}$ at each $(-k, i+M)$.

The boundary conditions for the model in Figure 12 are prescribed as follows. The entrance data is defined in the same way as for Figure 8 in the proof of Lemma 2.9. Specifically, we have no arrows vertically enter any column of the model, either in or to the right of the cross, and we have an arrow of color $\sigma(j)$ enter through the j -th row (from the bottom) of the cross, for each $j \in \llbracket 1, N \rrbracket$. The exit data is defined differently, by having an arrow of color \mathbf{q}_i horizontally exit through $(-1, i)$ (the i -th row of the model) for each $i \in \llbracket 1, M+N \rrbracket$, and having no arrow vertically exit through any column of the model.

Let us now analyze the partition function for this vertex model. Under the constraint (2.9), it is quickly verified (as in the proof of Lemma 2.9) that a colored higher spin path ensemble in $\mathbb{Z}_{<0} \times \llbracket 1, M+N \rrbracket$ has nonzero weight only if all but finitely many vertices in \mathcal{R}_2 have arrow configurations of the form $(\mathbf{e}_0, i; \mathbf{e}_0, i)$ for some integer $i \in \llbracket 1, n \rrbracket$, and all but finitely many vertices in \mathcal{R}_3 have arrow configurations of the form $(\mathbf{e}_0, 0; \mathbf{e}_0, 0)$. This forces the cross \mathcal{R}_1 to freeze, with the arrow configuration $(0, \sigma(j); 0, \sigma(j))$ at the intersection of its i -th column and j -th row, for each $(i, j) \in \llbracket 1, M \rrbracket \times \llbracket 1, N \rrbracket$. By (1.1), this means that the weight of \mathcal{R}_1 is

$$(3.10) \quad \prod_{i=1}^M \prod_{j=1}^N R_{y_i/x_j}(0, \sigma(j); 0, \sigma(j)) = \prod_{i=1}^M \prod_{j=1}^N \frac{x_j - y_i}{x_j - qy_i}.$$

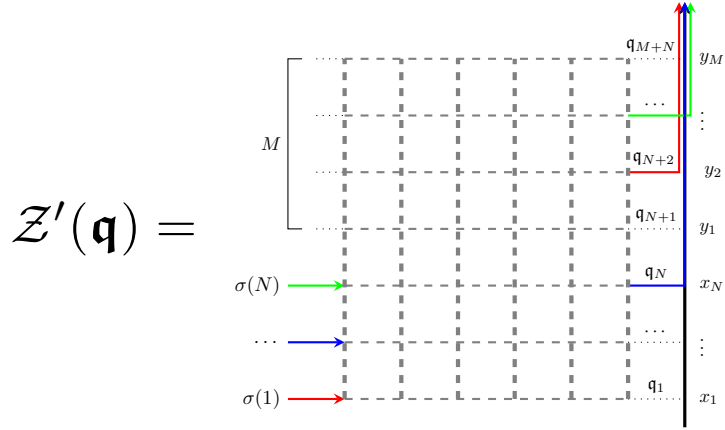


FIGURE 13. Shown above is a modification of the $\mathcal{R}_2 \cup \mathcal{R}_3$ region of the vertex model from Figure 12, in which all paths exit through the y -axis.

We next evaluate the partition function $\check{\mathcal{Z}}(\mathbf{q})$ of $\mathcal{R}_2 \cup \mathcal{R}_3$. To that end, we modify this part of the vertex model shown in Figure 12, by having all of the colored paths exit vertically through the y -axis; see Figure 13 for a depiction. Here, the weights used for the y -axis are $L_{x_j;0}$ at $(0, j)$ for $j \in \llbracket 1, N \rrbracket$ and $L_{y_i;0}$ at $(0, i+N)$ for $i \in \llbracket 1, M \rrbracket$. Since by Definition 2.1 we have for each $i \in \llbracket 1, M \rrbracket$, $j \in \llbracket 1, N \rrbracket$, and $\mathbf{A} \in \mathbb{Z}_{\geq 0}^n$ that

$$(3.11) \quad L_{y_i;0}(\mathbf{A}, \mathbf{q}_{i+N}; \mathbf{A}_{\mathbf{q}_{i+N}}^+, 0) = 1; \quad L_{x_j;0}(\mathbf{A}, \mathbf{q}_j; \mathbf{A}_{\mathbf{q}_j}^+, 0) = 1,$$

the weight of the y -axis in Figure 13 is 1. Hence, denoting the partition function of the vertex model depicted in Figure 13 by $\mathcal{Z}'(\mathbf{q})$, we have $\check{\mathcal{Z}}(\mathbf{q}) = \mathcal{Z}'(\mathbf{q})$. Together with (3.10), this yields

$$(3.12) \quad \mathcal{Z}(\mathbf{q}) = \check{\mathcal{Z}}(\mathbf{q}) \cdot \prod_{i=1}^M \prod_{j=1}^N \frac{x_j - y_i}{x_j - qy_i} = \mathcal{Z}'(\mathbf{q}) \cdot \prod_{i=1}^M \prod_{j=1}^N \frac{x_j - y_i}{x_j - qy_i}.$$

To evaluate $\mathcal{Z}'(\mathbf{q})$, observe that any colored higher spin path ensemble with boundary data as depicted in Figure 13 is determined by a sequence $\boldsymbol{\mu} = (\mu(0), \mu(1), \dots, \mu(M+N))$ of n -compositions, where $\mu(i)$ indexes the locations of the colored arrows exiting the i -th row $\{y = i\}$ of the model, for each $i \in \llbracket 0, M+N \rrbracket$ (in the sense of Remark 2.5). It is quickly verified that any such sequence $\boldsymbol{\mu}$ is $(M; \sigma)$ -ascending (as in Definition 3.1) and satisfies $\mathbf{q}(\boldsymbol{\mu}) = \mathbf{q}$. Moreover Definition 2.6 implies that, for any $j \in \llbracket 1, N \rrbracket$, the j -th row of the model in Figure 13 has weight $f_{\mu^{(j)}/\mu^{(j-1);s}}^{\sigma(j)}(x_j)$. Similarly, for any $i \in \llbracket N+1, M+N \rrbracket$, its i -th row has weight $G_{\mu^{(i-1)}/\mu^{(i);s}}(y_{i-N})$. Thus,

$$\mathcal{Z}'(\mathbf{q}) = \sum_{\boldsymbol{\mu}} \mathbb{1}_{\mathbf{q}(\boldsymbol{\mu})=\mathbf{q}} \cdot \prod_{j=1}^N f_{\mu^{(j)}/\mu^{(j-1);s}}^{\sigma(j)}(x_j) \prod_{i=N+1}^{M+N} G_{\mu^{(i-1)}/\mu^{(i);s}}(y_{i-N}),$$

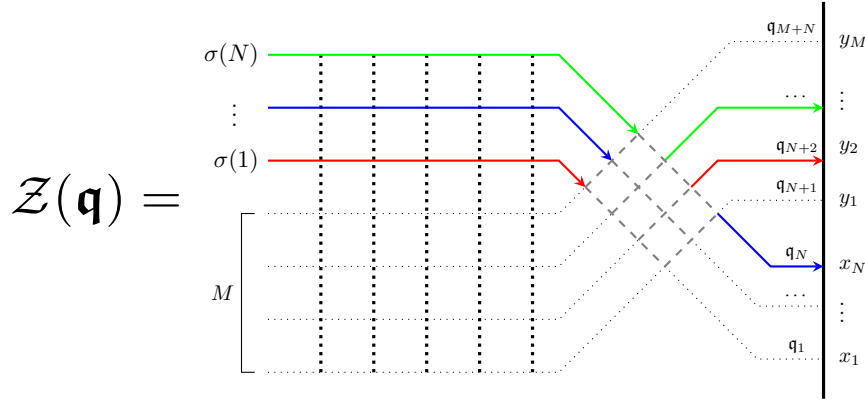


FIGURE 14. Shown above is the vertex model from Figure 12 after using the Yang–Baxter equation to move the cross to the right of $\mathbb{Z}_{<0} \times \llbracket 1, M + N \rrbracket$.

where the sum is over all $(M; \sigma)$ -ascending sequences $\boldsymbol{\mu}$ of n -compositions. Together with (3.12) and Definition 3.3, this gives

$$(3.13) \quad \begin{aligned} \mathcal{Z}(\mathbf{q}) &= \prod_{i=1}^M \prod_{j=1}^N \frac{x_j - y_i}{x_j - qy_i} \cdot \sum_{\boldsymbol{\mu}} \mathbb{1}_{\mathbf{q}(\boldsymbol{\mu}) = \mathbf{q}} \cdot \prod_{j=1}^N f_{\mu^{(j)}/\mu^{(j-1)}; s}^{\sigma(j)}(x_j) \prod_{i=N+1}^{M+N} G_{\mu^{(i-1)}/\mu^{(i)}; s}(y_{i-N}) \\ &= \mathbb{P}_{\text{fG}}^{\sigma}[\mathbf{q}(\boldsymbol{\mu}) = \mathbf{q}]. \end{aligned}$$

Next, by MN sequences of applications of the Yang–Baxter equation (2.6), the partition function $\mathcal{Z}(\mathbf{q})$ of the model from Figure 12 is unchanged if the cross originally in region \mathcal{R}_1 is moved to the right of $\mathcal{R}_2 \cup \mathcal{R}_3 = \mathbb{Z}_{<0} \times \llbracket 1, M + N \rrbracket$. In particular, $\mathcal{Z}(\mathbf{q})$ is also the partition function of the vertex model in Figure 14.

This model also consists of three regions \mathcal{R}'_1 , \mathcal{R}'_2 , and \mathcal{R}'_3 . The first \mathcal{R}'_1 is an $M \times N$ cross, that is now to the right of $\mathbb{Z}_{<0} \times \llbracket 1, M + N \rrbracket$. The third $\mathcal{R}'_3 = \mathbb{Z}_{\leq 0} \times \llbracket 1, M \rrbracket$ consists of the bottom M rows to the left of the cross. The second \mathcal{R}'_2 consists of the remaining N rows to the left of the cross. Again different vertex weights are used in these regions. In \mathcal{R}'_1 , we use the weight R_{y_i/x_j} at the intersection of the i -th column and j -th row of the cross, for each $(i, j) \in \llbracket 1, M \rrbracket \times \llbracket 1, N \rrbracket$; in \mathcal{R}'_2 , for each $j \in \llbracket 1, N \rrbracket$, we use the weight $\widehat{L}_{x_j; s}$ at every $(-k, M + j)$; and in \mathcal{R}'_3 , for each $i \in \llbracket 1, M \rrbracket$, we use the weight $L_{y_i; s}$ at every $(-k, i)$.

The boundary data for the model in Figure 14 is prescribed as follows (it must match that of Figure 12). The entrance data is defined by having no arrows vertically enter any column of the model; no arrow horizontally enter through the bottom M rows of the model; and having an arrow of color $\sigma(j)$ enter through the $(M + j)$ -th row of the model, for each $j \in \llbracket 1, N \rrbracket$. The exit data is defined by having no arrows horizontally exit through any column of the model; having an arrow of color \mathbf{q}_j exit through the j -th row of the cross, for each $j \in \llbracket 1, N \rrbracket$; and having an arrow of color \mathbf{q}_{i+N} exit through the $(M - i + 1)$ -th column of the cross, for each $j \in \llbracket 1, M \rrbracket$.

Observe that the $\mathcal{R}'_2 \cup \mathcal{R}'_3 = \mathbb{Z}_{<0} \times \llbracket 1, M + N \rrbracket$ part of this vertex model is frozen. The one colored higher spin path ensemble there (with that boundary data) that has nonzero weight is the one in which, for each $j \in \llbracket 1, N \rrbracket$, the path of color $\sigma(j)$ in the $(M + j)$ -th row travels horizontally

until it reaches the cross. Recalling from (1.1), (2.1), and (2.3) that

$$L_{y_i;s}(\mathbf{e}_0, 0; \mathbf{e}_0, 0) = 1, \quad \widehat{L}_{x_j;s}(\mathbf{e}_0, \sigma(j); \mathbf{e}_0, \sigma(j)) = 1,$$

it follows that the weight of $\mathcal{R}'_2 \cup \mathcal{R}'_3$ in Figure 14 is equal to 1. The partition function of \mathcal{R}'_1 is given by $R_{\mathbf{x};\mathbf{y}}(\mathbf{0}_M, \mathfrak{S}(\sigma); \mathfrak{C}, \mathfrak{D})$. Together with (3.9), this gives

$$\mathcal{Z}(\mathbf{q}) = \mathbb{P}_{\text{SV}}^\sigma \left[\{ \mathfrak{C}(\mathcal{E}) = \mathfrak{C} \} \cap \{ \mathfrak{D}(\mathcal{E}) = \mathfrak{D} \} \right],$$

which together with (3.13) yields the proposition. \square

Remark 3.9. Observe that the proof of Proposition 3.7 used (3.9), which required that the R -weights from Definition 1.1 were stochastic. It is also possible to formulate a version of Proposition 3.7 for non-stochastic R -weights, in which the stochastic weights of the vertex model describing the left side of (3.4) (equivalently, the stochastic weights of the cross in the proof of Proposition 3.7) would be determined by the R -weights through the stochasticization procedure of [4].

Remark 3.10. Our reason for using the domain $\mathbb{Z}_{<0} \times \llbracket 1, M+N \rrbracket$ above is to avoid having to “reflect” the stochastic cross (to direct its paths up-left instead of up-right) in the proof of Proposition 3.7, which would have been necessary had we instead used the more standard domain $\mathbb{Z}_{>0} \times \llbracket 1, M+N \rrbracket$ from previous works [22, 15, 25, 27].

Remark 3.11. It is possible to formulate a generalization of Proposition 3.7 when its domain $\mathcal{D}_{M;N}$ is not necessarily rectangular but instead “jagged,” that is, bounded by an up-left directed path \mathcal{P} . In this case, the associated measures \mathbb{P}_{fG} would no longer necessarily be ascending, but would rather have ascents and descents (depending on whether a corresponding step of \mathcal{P} is directed north or west); see [15, Theorem 5.6] for such a statement in the colorless ($n = 1$) case.

4. COLORED LINE ENSEMBLES FOR COLORED SIX-VERTEX MODELS

In this section we explain how the results of Section 3 can be reformulated in terms of colored line ensembles. We first associate colored line ensembles with ascending sequences of compositions in Section 4.1 and then discuss properties of random colored line ensembles (associated with random ascending sequences of compositions sampled according to $\mathbb{P}_{\text{fG}}^\sigma$) in Section 4.2. We then describe color merging properties for these random colored line ensembles in Section 4.3. Throughout this section, we fix integers $n, M, N \geq 1$; a composition $\ell = (\ell_1, \ell_2, \dots, \ell_n)$ of N ; a function $\sigma : \llbracket 1, N \rrbracket \rightarrow \llbracket 1, n \rrbracket$, such that for each $i \in \llbracket 1, n \rrbracket$ we have $\ell_i = \#\{\sigma^{-1}(i)\}$; a complex number $s \in \mathbb{C}$; and sequences of complex numbers $\mathbf{x} = (x_1, x_2, \dots, x_N)$ and $\mathbf{y} = (y_1, y_2, \dots, y_M)$, such that (2.9) holds.

4.1. Colored Line Ensembles and Ascending Sequences. In this section we associate a colored line ensemble (see Definition 1.4) with a given $(M; \sigma)$ -ascending sequence $\boldsymbol{\mu}$ of n -compositions. This is done through the following definition.

Definition 4.1. Let $\boldsymbol{\mu} = (\mu(0), \mu(1), \dots, \mu(M+N))$ denote an $(M; \sigma)$ -ascending sequence of n -compositions. The associated simple colored line ensemble $\mathbf{L} = \mathbf{L}_{\boldsymbol{\mu}} = (\mathbf{L}^{(1)}, \mathbf{L}^{(2)}, \dots, \mathbf{L}^{(n)})$ on $\llbracket 0, M+N \rrbracket$ is defined as follows. For each $c \in \llbracket 1, n \rrbracket$ let $\mathbf{L}^{(c)} = \mathbf{L}_{\boldsymbol{\mu}}^{(c)} = (\mathbf{L}_1^{(c)}, \mathbf{L}_2^{(c)}, \dots)$, where for each $k \geq 1$ the function $\mathbf{L}_k^{(c)} = \mathbf{L}_{k;\boldsymbol{\mu}}^{(c)} : \llbracket 0, M+N \rrbracket \rightarrow \mathbb{Z}$ is prescribed by setting

$$(4.1) \quad \mathbf{L}_k^{(c)}(i) = \ell_{[c,n]} - \mathbf{m}_{\leq k-1}^{\geq c}(\mu(i)), \quad \text{for each } i \in \llbracket 0, M+N \rrbracket.$$

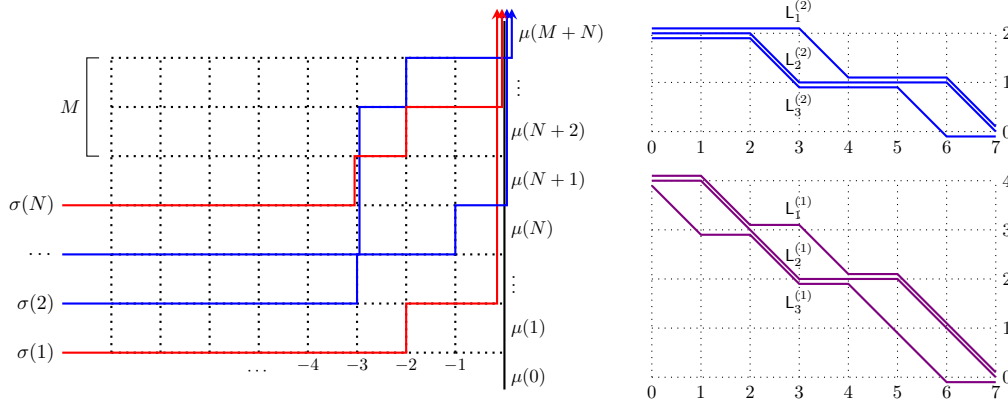


FIGURE 15. Shown to the left is a depiction for an ascending sequence $\boldsymbol{\mu}$ of 2-compositions through a colored higher spin path ensemble (where color 1 is red and color 2 is blue). Shown to the right are the two associated simple line ensembles $\mathbf{L}^{(1)}$ (in purple, as it counts both red and blue paths) and $\mathbf{L}^{(2)}$ (in blue).

The fact that this defines a simple colored line ensemble follows from Lemma 4.3 below. We moreover set the differences $\boldsymbol{\Lambda}^{(c)} = (\Lambda_1^{(c)}, \Lambda_2^{(c)}, \dots)$ of \mathbf{L} by

$$\Lambda_k^{(c)}(i) = \mathbf{L}_k^{(c)}(i) - \mathbf{L}_k^{(c+1)}(i), \quad \text{for each } (k, i) \in \mathbb{Z}_{>0} \times \llbracket 0, M+N \rrbracket,$$

where $\mathbf{L}_k^{(n+1)} : \llbracket 0, M+N \rrbracket \rightarrow \mathbb{Z}$ is defined by setting $\mathbf{L}_k^{(n+1)}(i) = 0$ for each $(k, i) \in \mathbb{Z}_{>0} \times \llbracket 0, M+N \rrbracket$.

Remark 4.2. As in Remark 3.2, we may interpret $\boldsymbol{\mu}$ as associated with a colored higher spin path ensemble $\mathcal{E}_{\boldsymbol{\mu}} \in \mathfrak{P}_{\text{fG}}(M; \sigma)$ on $\mathbb{Z}_{\leq 0} \times \llbracket 1, M+N \rrbracket$. Then $\mathbf{L}_k^{(c)}(i) = \mathfrak{h}_{\geq c}^{\leftarrow}(-k, i)$, where the height function $\mathfrak{h}_{\geq c}^{\leftarrow}$ is with respect to $\mathcal{E}_{\boldsymbol{\mu}}$; stated alternatively, $\mathbf{L}_k^{(c)}(i)$ denotes the number of arrows with color at least c that horizontally exit the column $\{x = -k\}$ strictly above the vertex $(-k, i)$. See Figure 15 for a depiction when $(n, M, N) = (2, 3, 4)$.

Lemma 4.3. *Adopting the notation and assumptions of Definition 4.1, \mathbf{L} is a simple colored line ensemble (recall Definition 1.4), which satisfies the following three properties for any $c \in \llbracket 1, n \rrbracket$, $k \in \mathbb{Z}_{>0}$, and $i \in \llbracket 0, M+N \rrbracket$.*

- (1) *We have $\mathbf{L}_1^{(c)}(i) \geq \mathbf{L}_2^{(c)}(i) \geq \dots$ and $\mathbf{L}_k^{(1)}(i) \geq \mathbf{L}_k^{(2)}(i) \geq \dots$.*
- (2) *We have $\Lambda_k^{(c)}(i) - \Lambda_{k+1}^{(c)}(i) = (\mathbf{L}_k^{(c)}(i) - \mathbf{L}_k^{(c+1)}(i)) - (\mathbf{L}_{k+1}^{(c)}(i) - \mathbf{L}_{k+1}^{(c+1)}(i)) = \mathbf{m}_k(\boldsymbol{\mu}^{(c)}(i))$.*
- (3) *If $i \geq 1$, we have $\mathbf{L}_k^{(c)}(i-1) - \mathbf{L}_k^{(c)}(i) = \mathbb{1}_{\mathfrak{q}_{\boldsymbol{\mu}}(k, i) \geq c}$.*

Proof. Let us first confirm that the three properties in the lemma hold for \mathbf{L} . The first follows from the facts that

(4.2)

$$\mathbf{L}_k^{(c)}(i) - \mathbf{L}_{k+1}^{(c)}(i) = \mathbf{m}_{\leq k}^{\geq c}(\boldsymbol{\mu}(i)) - \mathbf{m}_{\leq k-1}^{\geq c}(\boldsymbol{\mu}(i)) = \mathbf{m}_k^{\geq c}(\boldsymbol{\mu}(i)) = \sum_{c'=c}^n \mathbf{m}_k(\boldsymbol{\mu}^{(c')}(i)) \geq 0;$$

$$\mathbf{L}_k^{(c)}(i) - \mathbf{L}_k^{(c+1)}(i) = \ell_{[c, n]} - \ell_{[c+1, n]} + \mathbf{m}_{\leq k-1}^{\geq c+1}(\boldsymbol{\mu}(i)) - \mathbf{m}_{\leq k-1}^{\geq c}(\boldsymbol{\mu}(i)) = \ell_c - \mathbf{m}_{\leq k-1}(\boldsymbol{\mu}^{(c)}(i)) \geq 0,$$

where in the last bound we used the inequality $\ell_c \geq \ell(\mu^{(c)}(i)) \geq \mathbf{m}_{\leq k-1}(\mu^{(c)}(i))$ (by the second property in Definition 3.1). The second property follows from the fact that

$$\begin{aligned} \Lambda_k^{(c)}(i) - \Lambda_{k+1}^{(c)}(i) &= (\mathbf{L}_k^{(c)}(i) - \mathbf{L}_k^{(c+1)}(i)) - (\mathbf{L}_{k+1}^{(c)}(i) - \mathbf{L}_{k+1}^{(c+1)}(i)) \\ &= \left(\ell_c - \mathbf{m}_{\leq k-1}(\mu^{(c)}(i)) \right) - \left(\ell_c - \mathbf{m}_{\leq k}(\mu^{(c)}(i)) \right) = \mathbf{m}_k(\mu^{(c)}(i)) \geq 0, \end{aligned}$$

where in the second equality we used the second statement in (4.2). The third holds by the equality

$$(4.3) \quad \mathbf{L}_k^{(c)}(i-1) - \mathbf{L}_k^{(c)}(i) = \mathbf{m}_{\leq k-1}^{\geq c}(\mu(i)) - \mathbf{m}_{\leq k-1}^{\geq c}(\mu(i-1)),$$

and the fact that (by arrow conservation) the right side of (4.3) counts the number of arrows with color at least c in \mathcal{E}_μ that horizontally enter the vertex $(k-1, i)$, or equivalently that horizontally exit the vertex (k, i) ; this is $\mathbb{1}_{\mathfrak{q}_\mu(k, i) \geq c}$, by Remark 3.2.

The first and third properties of the lemma verify that each $\mathbf{L}^{(c)}$ is a simple line ensemble. Moreover, each $\Lambda^{(c)}$ is also a line ensemble, since $\Lambda_k^{(c)} \geq \Lambda_{k+1}^{(c)}$ by the second property in the lemma, and

$$\begin{aligned} \Lambda_k^{(c)}(i-1) - \Lambda_k^{(c)}(i) &= \mathbf{L}_k^{(c)}(i-1) - \mathbf{L}_k^{(c)}(i) - (\mathbf{L}_k^{(c+1)}(i-1) - \mathbf{L}_k^{(c+1)}(i)) \\ &= \mathbb{1}_{\mathfrak{q}_\mu(k, i) \geq c-1} - \mathbb{1}_{\mathfrak{q}_\mu(k, i) \geq c} \geq 0, \end{aligned}$$

by the third. This means that \mathbf{L} is a simple colored line ensemble. \square

By Lemma 4.3, Definition 4.1 associates a simple colored line ensemble to a given $(M; \sigma)$ -ascending sequence of n -compositions. Since the latter are in bijection with colored higher spin path ensembles in $\mathfrak{P}_{\text{FG}}(M; \sigma)$ by Remark 3.2, this associates a simple colored line ensemble with any element of $\mathfrak{P}_{\text{FG}}(M; \sigma)$. The following definition is towards the reverse direction; it associates a colored higher spin path ensemble with a simple colored line ensemble \mathbf{L} .

Definition 4.4. Adopt the notation from Definition 1.4 and assume that \mathbf{L} is simple. For any $v = (-k, i) \in \mathbb{Z}_{\leq 0} \times \llbracket 1, M+N \rrbracket$, define the arrow configuration $(\mathbf{A}^{\mathbf{L}}(v), b^{\mathbf{L}}(v); \mathbf{C}^{\mathbf{L}}(v), d^{\mathbf{L}}(v))$ as follows. The n -tuples $\mathbf{A}^{\mathbf{L}}(v) = (A_1^{\mathbf{L}}(v), A_2^{\mathbf{L}}(v), \dots, A_n^{\mathbf{L}}(v)) \in \mathbb{Z}_{\geq 0}^n$ and $\mathbf{C}^{\mathbf{L}} = (C_1^{\mathbf{L}}(v), C_2^{\mathbf{L}}(v), \dots, C_n^{\mathbf{L}}(v)) \in \mathbb{Z}_{\geq 0}^n$ are prescribed by setting

$$\begin{aligned} A_c^{\mathbf{L}}(v) &= \Lambda_k^{(c)}(i-1) - \Lambda_{k+1}^{(c)}(i-1) = \mathbf{L}_k^{(c)}(i-1) - \mathbf{L}_{k+1}^{(c)}(i-1) - (\mathbf{L}_k^{(c+1)}(i-1) - \mathbf{L}_{k+1}^{(c+1)}(i-1)); \\ C_c^{\mathbf{L}}(v) &= \Lambda_k^{(c)}(i) - \Lambda_{k+1}^{(c)}(i) = \mathbf{L}_k^{(c)}(i) - \mathbf{L}_{k+1}^{(c)}(i) - (\mathbf{L}_k^{(c+1)}(i) - \mathbf{L}_{k+1}^{(c+1)}(i)), \end{aligned}$$

for each $c \in \llbracket 1, n \rrbracket$ (observe that both are nonnegative since $\Lambda^{(c)}$ is a line ensemble), and the indices $b^{\mathbf{L}}(v), d^{\mathbf{L}}(v) \in \llbracket 0, n \rrbracket$ are prescribed by setting

$$\begin{aligned} b^{\mathbf{L}}(v) &= \max \{ c \in \llbracket 1, n \rrbracket : \mathbf{L}_{k+1}^{(c)}(i-1) - \mathbf{L}_{k+1}^{(c)}(i) = 1 \}; \\ d^{\mathbf{L}}(v) &= \max \{ c \in \llbracket 1, n \rrbracket : \mathbf{L}_k^{(c)}(i-1) - \mathbf{L}_k^{(c)}(i) = 1 \}, \end{aligned}$$

where the maxima are by definition set to 0 if such an index $c \in \llbracket 1, n \rrbracket$ does not exist. This assignment of arrow configurations is consistent and satisfies arrow conservation; therefore, it defines a colored higher spin path ensemble $\mathcal{E}^{\mathbf{L}}$ associated with the simple colored line ensemble \mathbf{L} .

The following lemma indicates that the associations from Definition 4.1 and Definition 4.4 are compatible; we omit its proof, which is a quick verification using the second and third statements of Lemma 4.3.

Lemma 4.5. *If $\mathcal{E}^{\mathbf{L}} = \mathcal{E}_\mu$ for some $(M; \sigma)$ -ascending sequence μ of n -compositions, then \mathbf{L} is associated with μ in the sense of Definition 4.1.*

4.2. Properties of Random Colored Line Ensembles. In this section we discuss some properties of colored line ensembles \mathbf{L}_μ associated with an $(M; \sigma)$ -ascending sequence μ of n -compositions sampled from the measure $\mathbb{P}_{\text{fG}}^\sigma$ (recall Definition 3.3). Let us first assign notation to this law on colored line ensembles.

Definition 4.6. Let $\mathbb{P}_{\text{scL}}^\sigma = \mathbb{P}_{\text{scL}; n; s; \mathbf{x}; \mathbf{y}}^\sigma$ denote the law of a simple colored line ensemble \mathbf{L}_μ associated with a random $(M; \sigma)$ -ascending sequence μ of n -compositions (as in Definition 4.1) sampled from the measure $\mathbb{P}_{\text{fG}; n; s; \mathbf{x}; \mathbf{y}}^\sigma$.

The following result, which is a quick consequence of Corollary 3.8, provides under this setup a matching in law between the top curves of \mathbf{L} (under $\mathbb{P}_{\text{scL}}^\sigma$) and the height functions for a colored stochastic six-vertex model (recall Definition 3.6).

Theorem 4.7. *Sample a simple colored line ensemble \mathbf{L} on $\llbracket 0, M+N \rrbracket$ from the measure $\mathbb{P}_{\text{scL}; n; s; \mathbf{x}; \mathbf{y}}^\sigma$, and sample a random colored six-vertex ensemble \mathcal{E} under $\mathbb{P}_{\text{SV}; \mathbf{x}; \mathbf{y}}^\sigma$. For each $c \in \llbracket 1, n \rrbracket$, define the function $H_c : \llbracket 0, M+N \rrbracket \rightarrow \mathbb{Z}$ by setting*

$$H_c(k) = \mathfrak{h}_{\leq c}^{\leftarrow}(M, k), \quad \text{if } k \in \llbracket 0, N \rrbracket; \quad H_c(k) = \mathfrak{h}_{\geq c}^{\leftarrow}(M+N-k, N), \quad \text{if } k \in \llbracket N, M+N \rrbracket,$$

where $\mathfrak{h}_{\leq c}^{\leftarrow}$ is the height function associated with \mathcal{E} . Then, the joint law of $(L_1^{(1)}, L_1^{(2)}, \dots, L_1^{(n)})$ is the same as that of (H_1, H_2, \dots, H_n) .

Proof. Since $\mathfrak{h}_{\leq c}^{\leftarrow}(i, j) = \ell_{[c, n]} - \mathfrak{h}_{\geq c}^{\rightarrow}(i, j)$ holds for any integer $c \in \llbracket 1, n \rrbracket$ and vertex $(i, j) \in \{(M, 0), (M, 1), \dots, (M, N), (M, N-1), \dots, (0, N)\}$ along the northeast boundary of $\llbracket 0, M \rrbracket \times \llbracket 0, N \rrbracket$, this theorem follows from (4.1) and Corollary 3.8. \square

The next theorem explains the effect of conditioning on some of the curves in \mathbf{L} , if μ is sampled under the $\mathbb{P}_{\text{scL}}^\sigma$ measure; see Figure 16 for a depiction. We will use this as a Gibbs property for the line ensemble \mathbf{L} . In the below, we recall the notion of compatibility for line ensembles from Definition 1.5; the vertex weights $L_{x; s}$ from Definition 2.1; the association of a colored line ensemble with an ascending sequence of n -compositions from Definition 4.1; and the notation from Definition 4.4.

Theorem 4.8. *Sample $\mathbf{L} = \mathbf{L}_\mu$ under $\mathbb{P}_{\text{scL}; n; s; \mathbf{x}; \mathbf{y}}^\sigma$. Fix integers $j > i \geq 0$ and $u, v \in \llbracket 0, M+N \rrbracket$ with $u < v$; set $i_0 = \max\{i, 1\}$; and condition on the curves $L_k^{(c)}(m)$ for all $c \in \llbracket 1, n \rrbracket$ and $(k, m) \in (\mathbb{Z}_{>0} \times \llbracket 0, M+N \rrbracket) \setminus (\llbracket i+1, j \rrbracket \times \llbracket u, v-1 \rrbracket)$. For any simple colored line ensemble \mathbf{l} that is $\llbracket i+1, j \rrbracket \times \llbracket u, v-1 \rrbracket$ -compatible with \mathbf{L} , we have*

$$(4.4) \quad \begin{aligned} \mathbb{P}[\mathbf{L} = \mathbf{l}] &= \mathcal{Z}^{-1} \cdot \prod_{k=i_0}^j \prod_{\substack{m \in \llbracket u, v \rrbracket \\ m \leq N}} L_{x_m; s}(\mathbf{A}^{\mathbf{l}}(-k, m), b^{\mathbf{l}}(-k, m); \mathbf{C}^{\mathbf{l}}(-k, m), d^{\mathbf{l}}(-k, m)) \\ &\times \prod_{k=i_0}^j \prod_{\substack{m \in \llbracket u, v \rrbracket \\ m > N}} L_{y_{m-N}; s}(\mathbf{A}^{\mathbf{l}}(-k, m), b^{\mathbf{l}}(-k, m); \mathbf{C}^{\mathbf{l}}(-k, m), d^{\mathbf{l}}(-k, m)). \end{aligned}$$

Here, the probability on the left side of (4.4) is with respect to the conditional law of \mathbf{L} . Moreover, \mathcal{Z} is a normalizing constant defined so that the sum of the right side of (4.4), over all simple colored line ensembles \mathbf{l} that are $\llbracket i+1, j \rrbracket \times \llbracket u, v-1 \rrbracket$ -compatible with \mathbf{L}_μ , is equal to 1.

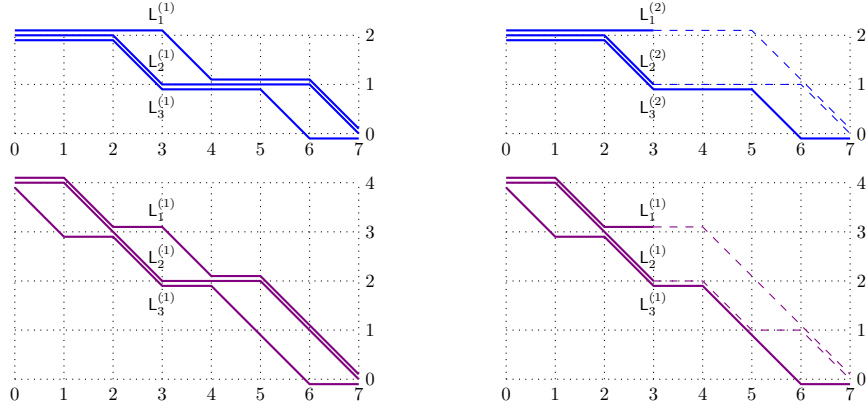


FIGURE 16. To the left is a simple colored line ensemble \mathbf{L} . To the right, we have conditioned on $\mathbf{L}_k^{(c)}(m)$ for $(k, m) \notin \llbracket 1, 2 \rrbracket \times \llbracket 4, 6 \rrbracket$ and resampled the first two curves on $\llbracket 4, 6 \rrbracket$ (shown as dashed).

Proof. Letting $\boldsymbol{\mu}$ be distributed according to $\mathbb{P}_{\text{fG};n;s;\mathbf{x};\mathbf{y}}^\sigma$, (2.7), (2.8), and (3.2) together imply that (4.5)

$$\begin{aligned} \mathbb{P}[\boldsymbol{\mu}] &= \mathcal{Z}_{\mathbf{x};\mathbf{y}}^{-1} \cdot \prod_{k=1}^{\infty} \prod_{m=1}^N \widehat{L}_{x_m;s}(\mathbf{A}_{\mathcal{E}_\mu}(-k, m), b_{\mathcal{E}_\mu}(-k, m); \mathbf{C}_{\mathcal{E}_\mu}(-k, m), d_{\mathcal{E}_\mu}(-k, m)) \\ &\quad \times \prod_{k=1}^{\infty} \prod_{m=N+1}^{M+N} L_{y_{m-N};s}(\mathbf{A}_{\mathcal{E}_\mu}(-k, m), b_{\mathcal{E}_\mu}(-k, m); \mathbf{C}_{\mathcal{E}_\mu}(-k, m), d_{\mathcal{E}_\mu}(-k, m)), \end{aligned}$$

where $(\mathbf{A}_{\mathcal{E}_\mu}(-k, m), b_{\mathcal{E}_\mu}(-k, m); \mathbf{C}_{\mathcal{E}_\mu}(-k, m), d_{\mathcal{E}_\mu}(-k, m))$ denotes the arrow configuration in the colored higher spin path ensemble \mathcal{E}_μ (recall Remark 3.2) at $(-k, m) \in \mathbb{Z}_{\leq 0} \times \llbracket 1, M+N \rrbracket$, and we recall the normalization constant $\mathcal{Z}(\mathbf{x}; \mathbf{y})$ from (3.3).⁹ Next, by Lemma 4.5, each arrow configuration $(\mathbf{A}_{\mathcal{E}_\mu}(-k, m), b_{\mathcal{E}_\mu}(-k, m); \mathbf{C}_{\mathcal{E}_\mu}(-k, m), d_{\mathcal{E}_\mu}(-k, m))$ appearing in (4.5) coincides with $(\mathbf{A}^{\mathbf{L}}(-k, m), b^{\mathbf{L}}(-k, m); \mathbf{C}^{\mathbf{L}}(-k, m), d^{\mathbf{L}}(-k, m))$. Together with (4.5) and the fact that $\widehat{L}_{x;s} = (1 - sx)(x - s)^{-1} \cdot L_{x;s}$ (by Definition 2.1), this yields

$$\begin{aligned} \mathbb{P}[\mathbf{L} = \mathbf{l}] &= \mathcal{Z}_{\mathbf{x};\mathbf{y}}^{-1} \cdot \prod_{k=1}^{\infty} \prod_{m=1}^N \frac{1 - sx_m}{x_m - s} \cdot L_{x_m;s}(\mathbf{A}^{\mathbf{l}}(-k, m), b^{\mathbf{l}}(-k, m); \mathbf{C}^{\mathbf{l}}(-k, m), d^{\mathbf{l}}(-k, m)) \\ (4.6) \quad &\quad \times \prod_{k=1}^{\infty} \prod_{m=N+1}^{M+N} L_{y_{m-N};s}(\mathbf{A}^{\mathbf{l}}(-k, m), b^{\mathbf{l}}(-k, m); \mathbf{C}^{\mathbf{l}}(-k, m), d^{\mathbf{l}}(-k, m)), \end{aligned}$$

where on the left side \mathbf{L} is sampled under the measure $\mathbb{P}_{\text{fG};n;s;\mathbf{x};\mathbf{y}}^\sigma$, without any conditioning yet.

Now, as in the statement of the theorem, we condition on the curves $\mathbf{L}_k^{(c)}(m)$ for $c \in \llbracket 1, n \rrbracket$ and $(k, m) \notin \llbracket i+1, j \rrbracket \times \llbracket u, v-1 \rrbracket$. By Definition 4.4, this amounts to conditioning on the restriction of

⁹Here, to restrict the products on the right side of (4.5) to terms with $k \neq 0$, we implicitly used the facts that the s -parameter in the 0-th column is equal to 0; that $L_{z;0}(\mathbf{A}, b; \mathbf{A}_b^+, 0) = 1$ for any $\mathbf{A} \in \mathbb{Z}_{\geq 0}^n$ and $b \in \llbracket 0, n \rrbracket$ (see (3.11)); and that $d_{\mathcal{E}_\mu}(0, m) = 0$ for all $m \in \llbracket 1, M+N \rrbracket$.

$\mathcal{E}^{\mathbf{L}}$ to the complement of $\llbracket -j, -i \rrbracket \times \llbracket u, v \rrbracket$. Hence, the factors on the right side of (4.6) corresponding to $(k, m) \notin \llbracket i, j \rrbracket \times \llbracket u, v \rrbracket$ are deterministic and can thus be incorporated into the normalization constant, which gives (recalling $i_0 = \max\{i, 1\}$)

$$\begin{aligned} \mathbb{P}[\mathbf{L} = \mathbf{l}] &= \tilde{\mathcal{Z}}^{-1} \cdot \prod_{k=i_0}^j \prod_{\substack{m \in \llbracket u, v \rrbracket \\ m \leq N}} \frac{1 - sx_m}{x_m - s} \cdot L_{x_m; s}(\mathbf{A}^{\mathbf{l}}(-k, m), \mathbf{b}^{\mathbf{l}}(-k, m); \mathbf{C}^{\mathbf{l}}(-k, m), \mathbf{d}^{\mathbf{l}}(-k, m)) \\ &\quad \times \prod_{k=i_0}^j \prod_{\substack{m \in \llbracket u, v \rrbracket \\ m > N}} L_{y_{m-N}; s}(\mathbf{A}^{\mathbf{l}}(-k, m), \mathbf{b}^{\mathbf{l}}(-k, m); \mathbf{C}^{\mathbf{l}}(-k, m), \mathbf{d}^{\mathbf{l}}(-k, m)), \end{aligned}$$

for some normalization constant $\tilde{\mathcal{Z}}$. Similarly incorporating the product $\prod_{m=1}^N (1 - sx_m)(x_m - s)^{-1}$ into the normalization constant gives (4.4). \square

4.3. Color Merging. In this section we describe several *color merging* properties, which enable us to obtain a system with $n - 1$ colors by merging two colors (say 1 and 2) in a corresponding system with n colors. Some of the proofs in this section will only be outlined, since analogous color merging phenomena have been discussed extensively in the literature already; see, for example, [25, Section 2.4], [20, Proposition 4.11], and [5, Sections 2.3 and 5.2]. Throughout this section, we will define several functions that all have the effect of merging colors 1 and 2. They will each be denoted by ϑ , which should not cause confusion since they act on different spaces.

First define $\vartheta : \llbracket 0, n \rrbracket \rightarrow \llbracket 0, n - 1 \rrbracket$ by setting

$$(4.7) \quad \vartheta(0) = 0, \quad \vartheta(1) = 1, \quad \vartheta(2) = 1, \quad \text{and} \quad \vartheta(i) = i - 1, \quad \text{for each } i \in \llbracket 3, n \rrbracket.$$

Also define its action on n -tuples of integers $\vartheta : \mathbb{Z}_{\geq 0}^n \rightarrow \mathbb{Z}_{\geq 0}^{n-1}$ by setting

$$(4.8) \quad \vartheta(\mathbf{I}) = (I_1 + I_2, I_3, \dots, I_n), \quad \text{for any } \mathbf{I} = (I_1, I_2, \dots, I_n) \in \mathbb{Z}_{\geq 0}^n.$$

With this notation, it is quickly verified¹⁰ that the weights from Definition 2.1 satisfy the following color-merging property for $n \geq 2$. Fix integers $\check{b}, \check{d} \in \llbracket 0, n - 1 \rrbracket$ and $(n - 1)$ -tuples $\check{\mathbf{A}}, \check{\mathbf{C}} \in \mathbb{Z}_{\geq 0}^{n-1}$, as well as an integer $b \in \llbracket 0, n \rrbracket$ and an n -tuple $\mathbf{A} \in \mathbb{Z}_{\geq 0}^n$, such that $\vartheta(b) = \check{b}$ and $\vartheta(\mathbf{A}) = \check{\mathbf{A}}$. Then,

$$(4.9) \quad \sum_{\substack{\mathbf{C} \in \mathbb{Z}_{\geq 0}^n \\ \vartheta(\mathbf{C}) = \check{\mathbf{C}}}} \sum_{d \in \llbracket 0, n \rrbracket} L_{x; s}^{(n)}(\mathbf{A}, b; \mathbf{C}, d) = L_{x; s}^{(n-1)}(\check{\mathbf{A}}, \check{b}; \check{\mathbf{C}}, \check{d});$$

the analogous statement also holds for the \widehat{L} -weights. The equality (4.9) indicates that identifying colors 1 and 2 in an n -color L -weight yields an $(n - 1)$ -color one.

The next lemma states that merging colors 1 and 2 in either the n -color f or G yields the same function, but on $n - 1$ colors. In the below, we define the action of ϑ on n -compositions $\vartheta : \text{Comp}_n \rightarrow \text{Comp}_{n-1}$ by for any $\boldsymbol{\mu} = (\mu^{(1)} \mid \mu^{(2)} \mid \dots \mid \mu^{(n)}) \in \text{Comp}_n$, setting

$$(4.10) \quad \vartheta(\boldsymbol{\mu}) = (\mu^{(1)} \cup \mu^{(2)} \mid \mu^{(3)} \mid \dots \mid \mu^{(n)}),$$

where $\mu^{(1)} \cup \mu^{(2)}$ is the signature obtained by taking the disjoint union of $\mu^{(1)}$ and $\mu^{(2)}$, and sorting its parts in non-increasing order. Moreover, given any function $\varsigma : \llbracket 1, N \rrbracket \rightarrow \llbracket 1, n \rrbracket$ further define

¹⁰This also follows from applying fusion (see Section 6) below to [20, Proposition 4.3].

the function $\vartheta(\varsigma) : \llbracket 1, N \rrbracket \rightarrow \llbracket 1, n-1 \rrbracket$ by setting

$$(4.11) \quad \vartheta(\varsigma)(i) = \vartheta(\varsigma(i)), \quad \text{for each } i \in \llbracket 1, N \rrbracket, \text{ and set } \check{\sigma} = \vartheta(\sigma),$$

where we recall $\sigma : \llbracket 1, N \rrbracket \rightarrow \llbracket 1, n \rrbracket$ that was fixed in the beginning of Section 4.

Lemma 4.9. *Fix an integer $k \geq 1$; $(n-1)$ -compositions $\check{\mu}, \check{\nu}, \check{\kappa} \in \text{Comp}_{n-1}$; and an n -composition $\nu \in \text{Comp}_n$, such that $\vartheta(\nu) = \check{\nu}$. We have*

$$\sum_{\substack{\mu \in \text{Comp}_n \\ \vartheta(\mu) = \check{\mu}}} f_{\mu/\nu; s}^{\sigma}(\mathbf{x}) = f_{\check{\mu}/\check{\nu}; s}^{\check{\sigma}}(\mathbf{x}); \quad \sum_{\substack{\kappa \in \text{Comp}_n \\ \vartheta(\kappa) = \check{\kappa}}} G_{\nu/\kappa; s}(\mathbf{y}) = G_{\check{\nu}/\check{\kappa}; s}(\mathbf{y}).$$

Proof (Outline). Recalling the definitions (2.8) of f and G as partition functions (under the \widehat{L} -weights and L -weights, respectively), this follows quickly from inductively applying the color merging (4.9) of vertex weights. See also [20, Proposition 4.11] (which can in fact be seen to directly imply Lemma 4.9 using fusion, defined in Section 6), for a very similar argument; we omit further details. \square

The next lemma describes the effect of merging colors 1 and 2 in a random n -composition sampled from the measure $\mathbb{P}_{\text{fG}; n; s; \mathbf{x}; \mathbf{y}}^{\sigma}$ (recall Definition 3.3). In the following, given a sequence of n -compositions $\boldsymbol{\mu} = (\mu(0), \mu(1), \dots, \mu(M+N))$, we set

$$(4.12) \quad \vartheta(\boldsymbol{\mu}) = \left(\vartheta(\mu(0)), \vartheta(\mu(1)), \dots, \vartheta(\mu(M+N)) \right),$$

which is an $(M; \check{\sigma})$ -ascending sequence of $(n-1)$ -compositions.

Lemma 4.10. *If an $(M; \sigma)$ -ascending sequence of n -compositions $\boldsymbol{\mu}$ is sampled from $\mathbb{P}_{\text{fG}; n; s; \mathbf{x}; \mathbf{y}}^{\sigma}$, then the $(M; \check{\sigma})$ -ascending sequence $\vartheta(\boldsymbol{\mu})$ of $(n-1)$ -compositions has law $\mathbb{P}_{\text{fG}; n-1; s; \mathbf{x}; \mathbf{y}}^{\check{\sigma}}$.*

Proof. Fix an $(M; \check{\sigma})$ -ascending sequence $\check{\boldsymbol{\mu}} = (\check{\mu}(0), \check{\mu}(1), \dots, \check{\mu}(M+N))$ of $(n-1)$ -compositions. For any integers $j \in \llbracket 1, N \rrbracket$ and $i \in \llbracket N+1, M+N \rrbracket$, and n -compositions $\mu(j-1), \mu(i-1) \in \text{Comp}_n$ such that $\vartheta(\mu(j-1)) = \check{\mu}(j-1)$ and $\vartheta(\mu(i-1)) = \check{\mu}(i-1)$, we have by Lemma 4.9 that

$$\begin{aligned} \sum_{\substack{\mu(j) \in \text{Comp}_n \\ \vartheta(\mu(j)) = \check{\mu}(j)}} f_{\mu(j)/\mu(j-1); s}^{\sigma}(x_j) &= f_{\check{\mu}(j)/\check{\mu}(j-1); s}^{\check{\sigma}}(x_j); \\ \sum_{\substack{\mu(i) \in \text{Comp}_n \\ \vartheta(\mu(i)) = \check{\mu}(i)}} G_{\mu(i-1)/\mu(i); s}(y_{i-N}) &= G_{\check{\mu}(i-1)/\check{\mu}(i); s}(y_{i-N}). \end{aligned}$$

Inductively applying these equalities, and using Definition 3.3, it follows that

$$\begin{aligned} \mathbb{P}_{\text{fG}; n; s; \mathbf{x}; \mathbf{y}}^{\sigma}[\vartheta(\boldsymbol{\mu}) = \check{\boldsymbol{\mu}}] &= \mathcal{Z}_{\mathbf{x}; \mathbf{y}}^{-1} \cdot \sum_{\vartheta(\boldsymbol{\mu}) = \check{\boldsymbol{\mu}}} \prod_{j=1}^N f_{\mu(j)/\mu(j-1); s}^{\sigma}(x_j) \prod_{i=N+1}^{M+N} G_{\mu(i-1)/\mu(i); s}(y_{i-N}) \\ &= \mathcal{Z}_{\mathbf{x}; \mathbf{y}}^{-1} \cdot \prod_{j=1}^N f_{\check{\mu}(j)/\check{\mu}(j-1); s}^{\check{\sigma}}(x_j) \prod_{i=N+1}^{M+N} G_{\check{\mu}(i-1)/\check{\mu}(i); s}(y_{i-N}) \\ &= \mathbb{P}_{\text{fG}; n-1; s; \mathbf{x}; \mathbf{y}}^{\check{\sigma}}[\check{\boldsymbol{\mu}}], \end{aligned}$$

which yields the lemma. \square


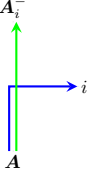
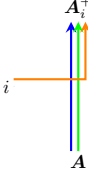
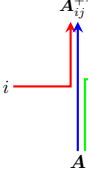

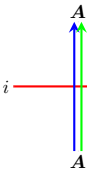
$1 \leq i \leq n$			$1 \leq i < j \leq n$		
					
$(\mathbf{A}, 0; \mathbf{A}, 0)$	$(\mathbf{A}, 0; \mathbf{A}_i^-, i)$	$(\mathbf{A}, i; \mathbf{A}_i^+, 0)$	$(\mathbf{A}, i; \mathbf{A}_{ij}^{+-}, j)$	$(\mathbf{A}, j; \mathbf{A}_{ji}^{+ -}, i)$	$(\mathbf{A}, i; \mathbf{A}, i)$
1	$(1 - q^{A_i})q^{A_{[i+1, n]}}x$	1	$(1 - q^{A_j})q^{A_{[j+1, n]}}x$	0	$q^{A_{[i+1, n]}}x$

 FIGURE 17. The $L_{x;0}$ weights are depicted above.

We conclude this section with the following proposition indicating that the marginal joint law of all line ensembles but the second¹¹ in a colored line ensemble \mathbf{L} sampled under $\mathbb{P}_{\text{scL};n;\mathbf{x};\mathbf{y}}^\sigma$ (recall Definition 4.6) is equal to that of a colored line ensemble (with $n - 1$ colors) sampled under $\mathbb{P}_{\text{scL};n-1;\mathbf{x};\mathbf{y}}^{\check{\sigma}}$ (where we recall $\check{\sigma} = \vartheta(\sigma)$ from (4.11)).

Proposition 4.11. *Sample $\mathbf{L} = (\mathbf{L}^{(1)}, \mathbf{L}^{(2)}, \dots, \mathbf{L}^{(n)})$ under $\mathbb{P}_{\text{scL};n;s;\mathbf{x};\mathbf{y}}^\sigma$. Then the joint law of the colored line ensemble $\check{\mathbf{L}} = (\mathbf{L}^{(1)}, \mathbf{L}^{(3)}, \mathbf{L}^{(4)}, \dots, \mathbf{L}^{(n)})$ (with $n - 1$ colors) is given by $\mathbb{P}_{\text{scL};n-1;s;\mathbf{x};\mathbf{y}}^{\check{\sigma}}$.*

Proof. Sample $\boldsymbol{\mu}$ under $\mathbb{P}_{\text{fG};n;s;\mathbf{x};\mathbf{y}}^\sigma$ (recall Definition 3.3). By Definition 4.6, we may identify \mathbf{L} as the colored line ensemble $\mathbf{L}_\boldsymbol{\mu}$ associated with $\boldsymbol{\mu}$. By Definition 4.1, the $n - 1$ line ensembles $\check{\mathbf{L}} = (\mathbf{L}^{(1)}, \mathbf{L}^{(3)}, \mathbf{L}^{(4)}, \dots, \mathbf{L}^{(n)})$ in $\mathbf{L} = \mathbf{L}_\boldsymbol{\mu}$ constitute the colored line ensemble associated with $\vartheta(\boldsymbol{\mu})$, which has law $\mathbb{P}_{\text{fG};n-1;s;\mathbf{x};\mathbf{y}}^{\check{\sigma}}$ by Lemma 4.10. Hence, again by Definition 4.6, $\check{\mathbf{L}}$ has law $\mathbb{P}_{\text{scL};n-1;s;\mathbf{x};\mathbf{y}}^{\check{\sigma}}$, thereby establishing the proposition. \square

Remark 4.12. Throughout this section, we have merged the colors 1 and 2. It is more generally possible to merge several (disjoint) intervals of colors; see [20, Sections 4.4 and 4.9] and [5, Sections 2.3 and 5.2] for similar setups. This would correspond in Proposition 4.11 to omitting line ensembles $\mathbf{L}^{(i)}$, for $i \in \llbracket 2, n \rrbracket$ arbitrary (depending on the corresponding merged color intervals), in \mathbf{L} .

5. EXAMPLES

In this section we examine the colored line ensembles introduced in Section 4 under two specializations; in both, we take $s = 0$ and refer to Figure 17 for a depiction of the $L_{x;0}$ weights. We investigate the case $n = 1$ in Section 5.1 and the case $q = 0$ in Section 5.2 (where we also prove Theorem 1.6); we also restrict to the *homogeneous* cases of both, when the entries in \mathbf{x} (and in \mathbf{y}) are all equal. Throughout this section, we fix integers $n, M, N \geq 1$; a composition $\boldsymbol{\ell} = (\ell_1, \ell_2, \dots, \ell_n)$ of N ; a function $\sigma : \llbracket 1, N \rrbracket \rightarrow \llbracket 1, n \rrbracket$, such that for each $i \in \llbracket 1, n \rrbracket$ we have $\ell_i = \#\{\sigma^{-1}(i)\}$; and real numbers $x, y \in (0, 1)$ with $y < x$. We also assume that $q \in (0, 1)$ and define the sequences $\mathbf{x} = (x, x, \dots, x)$ and $\mathbf{y} = (y, y, \dots, y)$, where x and y appear with multiplicities N and M , respectively. We also recall the notation from Section 4.1 throughout.

¹¹This could be replaced by the k -th, for any $k \in \llbracket 2, n \rrbracket$, through a similar proof.

5.1. **The Case $n = 1$.** Throughout this section, we set $n = 1$, $s = 0$, and sample $\mathbf{L} = \mathbf{L}^{(1)}$ under the probability measure $\mathbb{P}_{\text{scL};1}^\sigma = \mathbb{P}_{\text{scL};1;0;\mathbf{x};\mathbf{y}}^\sigma$. We will analyze how \mathbf{L} , and in particular its Gibbs property, behaves. Since $n = 1$, we omit the superscripts indexing the color 1 from the notation in what follows, writing $\mathbf{L} = (L_1, L_2, \dots)$. Define for any integers $(k, i) \in \mathbb{Z}_{>0} \times \llbracket 0, M + N \rrbracket$ and line ensemble $\mathbf{l} = (l_1, l_2, \dots)$ on $\llbracket 0, M + N \rrbracket$ the quantity

$$(5.1) \quad \Delta_{k;\mathbf{l}}(i) = l_k(i) - l_{k+1}(i),$$

where by definition $L_0(i) = l_0(i) = \infty$ for each $i \in \llbracket 1, M + N \rrbracket$.

Given this notation, we have the following proposition explaining the Gibbs property (Theorem 4.8) in this setting when we resample one curve (say that i -th one L_i) of \mathbf{L} .

Proposition 5.1. *Adopt the above notation and assumptions. Let $j \geq i \geq 1$ and $u, v \in \llbracket 0, M + N \rrbracket$ be integers with $v \geq u$, and condition on the curves $L_k(m)$ for $(k, m) \notin \llbracket i, j \rrbracket \times \llbracket u, v \rrbracket$; set $u_0 = \max\{u - 1, N\}$ and $v_0 = \min\{v + 1, N\}$. For any simple line ensemble $\mathbf{l} = (l_1, l_2, \dots)$ that is $\{i\} \times \llbracket u, v \rrbracket$ -compatible with \mathbf{L} , we have*

$$(5.2) \quad \mathbb{P}[\mathbf{L} = \mathbf{l}] = \mathcal{Z}^{-1} \cdot \prod_{k=i}^j x^{-l_k(v_0)} y^{l_k(u_0)} \prod_{k=i-1}^j \prod_{m=u}^{v+1} (1 - q^{\Delta_k(m-1)} \cdot \mathbb{1}_{\Delta_k(m-1) - \Delta_k(m)=1}),$$

for some normalization constant $\mathcal{Z} > 0$, where we have abbreviated $\Delta_k = \Delta_{k;\mathbf{l}}$.

Proof. To make use of Theorem 4.8, we must first understand how the quantities on the right side of (4.4) behave. By Definition 4.4 (and the fact that $n = 1$), we have for any vertex $(-k, m) \in \mathbb{Z}_{\leq -1} \times \llbracket 1, M + N \rrbracket$ that

$$(5.3) \quad \begin{aligned} A^{\mathbf{l}}(-k, m) &= l_k(m-1) - l_{k+1}(m-1) = \Delta_k(m-1); & b^{\mathbf{l}}(-k, m) &= l_{k+1}(m-1) - l_{k+1}(m); \\ C^{\mathbf{l}}(-k, m) &= l_k(m) - l_{k+1}(m) = \Delta_k(m); & d^{\mathbf{l}}(-k, m) &= l_k(m-1) - l_k(m), \end{aligned}$$

where we omit the subscript indexing the color 1 (as $n = 1$). Further observe (see Figure 17) that, if $A + b = C + d$, then

$$L_{x;0}(A, b; C, d) = x^d \cdot L_{1;0}(A, b; C, d); \quad L_{1;0}(A, b; C, d) = 1 - q^A \cdot \mathbb{1}_{d-b=1},$$

and (by (5.3) and (5.1)) that

$$d^{\mathbf{l}}(-k, m) - b^{\mathbf{l}}(-k, m) = l_k(m-1) - l_k(m) - (l_{k+1}(m-1) - l_{k+1}(m)) = \Delta_k(m-1) - \Delta_k(m).$$

Inserting these into Theorem 4.8 (with the $(i, j; u, v)$ there equal to $(i-1, j; u, v+1)$ here), yields

$$(5.4) \quad \begin{aligned} \mathbb{P}[\mathbf{L} = \mathbf{l}] &= \mathcal{Z}^{-1} \cdot \prod_{k=i-1}^j \prod_{\substack{m \in \llbracket u, v+1 \rrbracket \\ m \leq N}} x^{l_k(m-1) - l_k(m)} \prod_{\substack{m \in \llbracket u, v+1 \rrbracket \\ m > N}} y^{l_k(m-1) - l_k(m)} \\ &\times \prod_{k=i-1}^j \prod_{m=u}^{v+1} (1 - q^{\Delta_k(m-1)} \cdot \mathbb{1}_{\Delta_k(m-1) - \Delta_k(m)=1}), \end{aligned}$$

for some normalization constant $\mathcal{Z} > 0$.

Next observe since $u_0 = \max\{u - 1, N\}$ and $v_0 = \min\{v + 1, N\}$ that

$$\begin{aligned} \sum_{m=u}^{\min\{v+1, N\}} (l_k(m-1) - l_k(m)) &= (l_k(u-1) - l_k(v_0)) \cdot \mathbb{1}_{u \leq N}; \\ \sum_{m=\max\{N+1, u\}}^{v+1} (l_k(m-1) - l_k(m)) &= (l_k(u_0) - l_k(v+1)) \cdot \mathbb{1}_{v \geq N}. \end{aligned}$$

As we conditioned on $\mathbf{L}_{i-1}(m) = l_{i-1}(m)$ for all m , and on $\mathbf{L}_k(m) = l_k(m)$ and $\mathbf{L}_k(m) = l_k(m)$ for all k and $m \notin \llbracket u, v \rrbracket$, we may incorporate the factors $x^{(l_{i-1}(u-1) - l_{i-1}(v_0)) \cdot \mathbb{1}_{u \leq N}} \cdot y^{(l_{i-1}(u_0) - l_{i-1}(v+1)) \cdot \mathbb{1}_{v \geq N}}$ and $x^{l_k(u-1) \cdot \mathbb{1}_{u \leq N} + l_k(v_0) \cdot \mathbb{1}_{u > N}} \cdot y^{-l_i(v+1) \cdot \mathbb{1}_{v \geq N} - l_i(u_0) \cdot \mathbb{1}_{v < N}}$ for $k \in \llbracket i, j \rrbracket$ appearing in the right side of (5.4) into the normalization constant \mathcal{Z} (where we used the facts that if $u > N$ then $v > N$ and so $v_0 = N \leq u - 1$, and that if $v < N$ then $u < N$ and so $u_0 = N \geq v + 1$). This gives

$$\mathbb{P}[\mathbf{L} = \mathbf{l}] = \mathcal{Z}^{-1} \cdot \prod_{k=i}^j x^{-l_k(v_0)} y^{l_k(u_0)} \prod_{k=i-1}^j \prod_{m=u}^{v+1} (1 - q^{\Delta_k(m-1)} \cdot \mathbb{1}_{\Delta_k(m-1) - \Delta_k(m)=1}),$$

after altering \mathcal{Z} if necessary, which yields the proposition. \square

The Gibbs property described by Proposition 5.1 coincides the Hall–Littlewood Gibbs property introduced in [33, Definition 3.4].¹² Moreover, setting $n = 1$ in Theorem 4.7 yields that the law of \mathbf{L}_1 has the same law as the height function of the (uncolored) stochastic six-vertex model introduced in [46]; this had been shown earlier in [15, Theorem 5.5]. More generally, it can be shown (although we do not do so here) that the $n = 1$ case of \mathbf{L} coincides (up to an affine transformation) with the Hall–Littlewood Gibbsian line ensemble introduced in [33, Section 3.2]. This is to be expected, since taking the $n = 1$ case of our arguments in the preceding sections would essentially yield the content described in [15, Section 5.7] and [33, Proposition 3.9].

Remark 5.2. Observe that (5.2) only depends on x and y through their ratio $x^{-1}y$. Indeed, if $u - 1 \geq N$ or $N \geq v + 1$, then the factor $x^{-l_i(v_0)} y^{l_i(u_0)} = x^{-l_i(v+1)} y^{l_i(u-1)}$ on the right side of (5.2) is fixed by the conditioning and can therefore be incorporated into the normalization constant. Otherwise, $N \in \llbracket u, v \rrbracket$, and so the factor $x^{-l_i(v_0)} y^{l_i(u_0)} = (x^{-1}y)^{l_i(N)}$ only depends on $x^{-1}y$.

5.2. The Case $q = 0$. Throughout this section, we set $q = 0$, $s = 0$, and sample the colored line ensemble $\mathbf{L} = (\mathbf{L}^{(1)}, \mathbf{L}^{(2)}, \dots, \mathbf{L}^{(n)})$ from the measure $\mathbb{P}_{\text{scL}}^\sigma = \mathbb{P}_{\text{scL}; n; 0; \mathbf{x}; \mathbf{y}}^\sigma$. The following proposition explains the Gibbs property (Theorem 4.8) for \mathbf{L} . Below, we restrict to the scenario when $\llbracket u, v \rrbracket$ does not contain N , since the Gibbs property will be simplest to state in this situation (as, analogously to Remark 5.2, it will not depend on x or y).

Proposition 5.3. *Adopt the above notation and assumptions, and let $j \geq i \geq 1$ and $u, v \in \llbracket 0, M + N \rrbracket$ be integers such that $u \leq v$ and $N \notin \llbracket u, v \rrbracket$. Then, the following two statements hold.*

- (1) *For any $(c, k, m) \in \llbracket 1, n \rrbracket \times \mathbb{Z}_{>0} \times \llbracket 1, M + N \rrbracket$ such that $\mathbf{L}_k^{(c+1)}(m) > \mathbf{L}_{k+1}^{(c+1)}(m)$, we almost surely have*

$$(5.5) \quad \mathbf{L}_k^{(c)}(m-1) - \mathbf{L}_k^{(c)}(m) = \mathbf{L}_k^{(c+1)}(m-1) - \mathbf{L}_k^{(c+1)}(m),$$

¹²To properly observe the match, one must read first our line ensemble in reverse (from right to left), and then apply a gauge transformation to its weights that does not affect its Gibbs property (namely, multiply them by $(q; q)_{\Delta_i(m-1)}^{-1} (q; q)_{\Delta_{i-1}(m-1)}^{-1} (q; q)_{\Delta_i(m)} (q; q)_{\Delta_{i-1}(m)}$).

(2) *Condition on the curves $\mathbf{l}_k^{(c)}(m)$ for all $c \in \llbracket 1, n \rrbracket$ and $(k, m) \notin \llbracket i, j \rrbracket \times \llbracket u, v \rrbracket$. Then the law of \mathbf{L} is uniform over all simple colored line ensembles $\mathbf{l} = (\mathbf{l}^{(1)}, \mathbf{l}^{(2)}, \dots, \mathbf{l}^{(n)})$ that are $\llbracket i, j \rrbracket \times \llbracket u, v \rrbracket$ -compatible with \mathbf{L} such that, for any $(c, k, m) \in \llbracket 1, n \rrbracket \times \mathbb{Z}_{>0} \times \llbracket 1, M+N \rrbracket$ with $l_k^{(c+1)}(m) > l_{k+1}^{(c+1)}(m)$, we have*

$$(5.6) \quad l_k^{(c)}(m-1) - l_k^{(c)}(m) = l_k^{(c+1)}(m-1) - l_k^{(c+1)}(m).$$

To prove Proposition 5.3, we require the next lemma that explains why $l_k^{(c+1)}(m) > l_{k+1}^{(c+1)}(m)$ should imply (5.6).

Lemma 5.4. *Let $\mathbf{l} = (\mathbf{l}^{(1)}, \mathbf{l}^{(2)}, \dots, \mathbf{l}^{(n)})$ denote a simple colored line ensemble on $\llbracket 0, M+N \rrbracket$; $\mathcal{E}^{\mathbf{l}}$ denote the associated higher spin path ensemble; and $(\mathbf{A}^{\mathbf{l}}(-k, m), b^{\mathbf{l}}(-k, m); \mathbf{C}^{\mathbf{l}}(-k, m), d^{\mathbf{l}}(-k, m))$ denote the arrow configuration in $\mathcal{E}^{\mathbf{l}}$ at any $(-k, m) \in \mathbb{Z}_{\geq 0} \times \llbracket 1, M+N \rrbracket$. Then, for any $(-k, m) \in \mathbb{Z}_{\geq 0} \times \llbracket 1, M+N \rrbracket$, we have that $L_{1;0}(\mathbf{A}^{\mathbf{l}}(-k, m), b^{\mathbf{l}}(-k, m); \mathbf{C}^{\mathbf{l}}(-k, m), d^{\mathbf{l}}(-k, m)) = 1$ if and only if, for any $c \in \llbracket 1, n \rrbracket$ with $l_k^{(c+1)}(m) > l_{k+1}^{(c+1)}(m)$, (5.6) holds. Otherwise, we have that the weight $L_{1;0}(\mathbf{A}^{\mathbf{l}}(-k, m), b^{\mathbf{l}}(-k, m); \mathbf{C}^{\mathbf{l}}(-k, m), d^{\mathbf{l}}(-k, m)) = 0$.*

Proof. By Definition 4.4, we have for any $c \in \llbracket 1, n \rrbracket$ that

$$(5.7) \quad \begin{aligned} \mathbf{C}_c^{\mathbf{l}}(-k, m) &= l_k^{(c)}(m) - l_{k+1}^{(c)}(m) - (l_k^{(c+1)}(m) - l_{k+1}^{(c+1)}(m)); \\ d^{\mathbf{l}} &= \max \{ d \in \llbracket 1, n \rrbracket : l_k^{(d)}(m-1) - l_k^{(d)}(m) = 1 \}, \end{aligned}$$

with $d^{\mathbf{l}} = 0$ if no such $d \in \llbracket 1, n \rrbracket$ exists. Further observe (see Figure 17) that for $q = 0$, if $\mathbf{A} + \mathbf{e}_b = \mathbf{C} + \mathbf{e}_d$, then

$$L_{1;0}(\mathbf{A}, b; \mathbf{C}, d) = 1 - \mathbb{1}_{d>0} \cdot \mathbb{1}_{C_{[d+1, n]} > 0}.$$

By (5.7), we have for any $d \in \llbracket 1, n \rrbracket$ that

$$\mathbf{C}_{[d+1, n]}^{\mathbf{l}}(-k, m) = l_k^{(d+1)}(m) - l_{k+1}^{(d+1)}(m).$$

Also by (5.7), we have $d^{\mathbf{l}}(-k, m) = d \geq 1$ if and only if $l_k^{(d)}(m-1) - l_k^{(d)}(m) - (l_k^{(d+1)}(m-1) - l_k^{(d+1)}(m)) > 0$, that is, if and only if (5.6) does not hold.

Hence, $L_{1;0}(\mathbf{A}^{\mathbf{l}}(-k, m), b^{\mathbf{l}}(-k, m); \mathbf{C}^{\mathbf{l}}(-k, m), d^{\mathbf{l}}(-k, m)) = 1$ if and only if, for any $c \in \llbracket 1, n \rrbracket$ such that $l_k^{(c+1)}(m) > l_{k+1}^{(c+1)}(m)$, (5.6) holds. Otherwise, this weight is equal to 0. \square

Now we can establish Proposition 5.3.

Proof of Proposition 5.3. Observe (see Figure 17) for any $\mathbf{A}, \mathbf{C} \in \mathbb{Z}_{\geq 0}^n$ and $b, d \in \llbracket 0, n \rrbracket$ with $\mathbf{A} + \mathbf{e}_b = \mathbf{C} + \mathbf{e}_d$ that

$$(5.8) \quad L_{x;0}(\mathbf{A}, b; \mathbf{C}, d) = x^{\mathbb{1}_{d>0}} \cdot L_{1;0}(\mathbf{A}, b; \mathbf{C}, d); \quad L_{1;0}(\mathbf{A}, b; \mathbf{C}, d) = 1 - \mathbb{1}_{d>0} \cdot \mathbb{1}_{C_{[d+1, n]} > 0}.$$

Thus, since \mathbf{L} was sampled according to the measure $\mathbb{P}_{\text{scL}}^{\sigma}$, (2.7), (2.8), (3.2), and Lemma 4.5 together imply that

$$\begin{aligned} \mathbb{P}_{\text{scL}}^{\sigma}[\mathbf{L}] &= Z_{\mathbf{x}; \mathbf{y}}^{-1} \cdot \prod_{k=1}^{\infty} \prod_{m=1}^N \widehat{L}_{x_m;0}(\mathbf{A}^{\mathbf{l}}(-k, m), b^{\mathbf{l}}(-k, m); \mathbf{C}^{\mathbf{l}}(-k, m), d^{\mathbf{l}}(-k, m)) \\ &\quad \times \prod_{k=1}^{\infty} \prod_{m=N+1}^{M+N} L_{y_{m-N};0}(\mathbf{A}^{\mathbf{l}}(-k, m), b^{\mathbf{l}}(-k, m); \mathbf{C}^{\mathbf{l}}(-k, m), d^{\mathbf{l}}(-k, m)), \end{aligned}$$

which by the first statement of (5.8) (and the fact that $x, y \neq 0$) is nonzero if and only if $L_{1;0}(\mathbf{A}^{\mathbf{l}}(-k, m), b^{\mathbf{l}}(-k, m); \mathbf{C}^{\mathbf{l}}(-k, m), d^{\mathbf{l}}(-k, m)) \neq 0$ for all $(-k, m) \in \mathbb{Z}_{\leq 0} \times \llbracket 1, M + N \rrbracket$. By Lemma 5.4, this is true if and only if, for any $(c, k, m) \in \llbracket 1, n \rrbracket \times \mathbb{Z}_{>0} \times \llbracket 1, M + N \rrbracket$ such that $\mathbb{L}_k^{(c+1)}(m) > \mathbb{L}_{k+1}^{(c+1)}(m)$, (5.5) holds. This confirms the first statement of the proposition.

To verify the second, we first apply Theorem 4.8 (with the $(i, j; u, v)$ there equal to $(i-1, j; u, v+1)$ here) and (5.8) to deduce for some normalization constant $\mathcal{Z} > 0$ that

$$(5.9) \quad \mathbb{P}_{\text{scL}}^{\sigma}[\mathbf{L} = \mathbf{l}] = \mathcal{Z}^{-1} \cdot \prod_{k=i-1}^j \prod_{\substack{m \in \llbracket u, v+1 \rrbracket \\ m \leq N}} x^{\mathbb{1}_{d^{\mathbf{l}}(-k, m) > 0}} \cdot L_{1;0}(\mathbf{A}^{\mathbf{l}}(-k, m), b^{\mathbf{l}}(-k, m); \mathbf{C}^{\mathbf{l}}(-k, m), d^{\mathbf{l}}(-k, m)) \\ \times \prod_{k=i-1}^j \prod_{\substack{m \in \llbracket u, v+1 \rrbracket \\ m > N}} y^{\mathbb{1}_{d^{\mathbf{l}}(-k, m) > 0}} \cdot L_{1;0}(\mathbf{A}^{\mathbf{l}}(-k, m), b^{\mathbf{l}}(-k, m); \mathbf{C}^{\mathbf{l}}(-k, m), d^{\mathbf{l}}(-k, m)),$$

where in the probability on the left side of (5.9) we have conditioned on the curves $\mathbb{L}_k^{(c)}(m)$ for $c \in \llbracket 1, n \rrbracket$ and $(k, m) \notin \llbracket i, j \rrbracket \times \llbracket u, v \rrbracket$. Moreover, by Definition 4.4 (with the fact that $\mathbf{l}^{(c)}$ is simple), we have $\mathbb{1}_{d^{\mathbf{l}}(-k, m) > 0} = \mathbb{L}_{k+1}^{(1)}(m-1) - \mathbb{L}_{k+1}^{(1)}(m)$. Hence, setting $u_0 = \max\{u-1, N\}$ and $v_0 = \min\{v+1, N\}$, we have

$$\prod_{\substack{m \in \llbracket u, v+1 \rrbracket \\ m \leq N}} x^{\mathbb{1}_{d^{\mathbf{l}}(-k, m) > 0}} = x^{(\mathbb{L}_k^{(1)}(u-1) - \mathbb{L}_k^{(1)}(v_0)) \cdot \mathbb{1}_{u \leq N}}; \quad \prod_{\substack{m \in \llbracket u, v+1 \rrbracket \\ m > N}} y^{\mathbb{1}_{d^{\mathbf{l}}(-k, m) > 0}} = y^{(\mathbb{L}_k^{(1)}(u_0) - \mathbb{L}_k^{(1)}(v+1)) \cdot \mathbb{1}_{v \geq N}}.$$

Since $u-1, u_0, v_0, v+1 \notin \llbracket u, v \rrbracket$ (as $N \notin \llbracket u, v \rrbracket$), the above factors are fixed by the conditioning. Thus, on the right side of (5.9), we may incorporate them into the normalization constant \mathcal{Z} to obtain (after altering \mathcal{Z} if necessary)

$$\mathbb{P}_{\text{scL}}^{\sigma}[\mathbf{L} = \mathbf{l}] = \mathcal{Z}^{-1} \cdot \prod_{k=i-1}^j \prod_{\substack{m \in \llbracket u, v+1 \rrbracket \\ m \leq N}} L_{1;0}(\mathbf{A}^{\mathbf{l}}(-k, m), b^{\mathbf{l}}(-k, m); \mathbf{C}^{\mathbf{l}}(-k, m), d^{\mathbf{l}}(-k, m)) \\ \times \prod_{k=i-1}^j \prod_{\substack{m \in \llbracket u, v+1 \rrbracket \\ m > N}} L_{1;0}(\mathbf{A}^{\mathbf{l}}(-k, m), b^{\mathbf{l}}(-k, m); \mathbf{C}^{\mathbf{l}}(-k, m), d^{\mathbf{l}}(-k, m)).$$

By Lemma 5.4, the above product is equal to 1 if and only if, for any $(c, k, m) \in \llbracket 1, n \rrbracket \times \mathbb{Z}_{>0} \times \llbracket 1, M + N \rrbracket$ with $\mathbb{L}_k^{(c+1)}(m) > \mathbb{L}_{k+1}^{(c+1)}(m)$, (5.6) holds; otherwise it is equal to 0. This confirms the second part of the proposition. \square

Now we can quickly establish Theorem 1.6.

Proof of Theorem 1.6. The first part of this theorem follows from the $q = 0$ case of Theorem 4.7; the second and third follow from Proposition 5.3. \square

6. FUSION

Until now, we have used colored six-vertex or higher spin path ensembles; they only allowed at most one arrow to occupy any horizontal edge. In this section we remove that restriction using the fusion procedure originally introduced in [62], and describe the counterparts to the statements

from Section 2 and Section 3 when horizontal edges may accommodate more than one arrow. Since such ideas have been used repeatedly throughout the literature, and since many statements in this section are similar to those in Section 2 and Section 3, we will sometimes only outline (or omit) the proofs of the below results. Throughout this section, we fix an integer $n \geq 1$.

6.1. Stochastic Fused Vertex Models. A *colored fused arrow configuration* is a quadruple $(\mathbf{A}, \mathbf{B}; \mathbf{C}, \mathbf{D})$ of elements in $\mathbb{Z}_{\geq 0}^n$. We view this as an assignment of directed up-right colored arrows to a vertex $v \in \mathbb{Z}^2$, in which a (horizontal or vertical) edge can accommodate arbitrarily many arrows. In particular, for each $k \in \llbracket 1, n \rrbracket$, the numbers A_k, B_k, C_k , and D_k denote the numbers of arrows of color k vertically entering, horizontally entering, vertically exiting, and horizontally exiting v , respectively.

As in Section 1.2 and Section 2.2, a *colored fused path ensemble* on a domain $\mathcal{D} \subseteq \mathbb{Z}^2$ is a consistent assignment of a colored fused arrow configuration $(\mathbf{A}(v), \mathbf{B}(v); \mathbf{C}(v), \mathbf{D}(v))$ to each vertex $v \in \mathcal{D}$. Observe that the arrows in a colored fused path ensemble on \mathcal{D} form colored up-right directed paths (that can share horizontal and vertical edges) connecting vertices of \mathcal{D} . Associated with a colored fused path ensemble \mathcal{E} on some domain $\mathcal{D} \subseteq \mathbb{Z}^2$ are height functions $\mathfrak{h}_c^{\rightarrow}, \mathfrak{h}_c^{\leftarrow}, \mathfrak{h}_{\geq c}^{\rightarrow}, \mathfrak{h}_{\geq c}^{\leftarrow} : \mathbb{Z}^2 \rightarrow \mathbb{Z}$, which are defined in the same way as in Section 2.2.

The probability measure on random colored fused path ensembles on $\mathbb{Z}_{>0}^2$ that we next define depends on four sequences of complex parameters $\mathbf{x} = (x_1, x_2, \dots); \mathbf{r} = (r_1, r_2, \dots); \mathbf{y} = (y_1, y_2, \dots);$ and $\mathbf{s} = (s_1, s_2, \dots)$. We view x_j and r_j as associated with the j -th row, so they are called row rapidity and spin parameters, respectively; we view y_i and s_i as associated with the i -th column, so they are called column rapidity and fusion parameters, respectively. The specific forms of these probability measures are expressed through certain weights $U_{x_j/y_i; r_j, s_i}(\mathbf{A}, \mathbf{B}; \mathbf{C}, \mathbf{D})$ associated with each vertex $v = (i, j) \in \mathbb{Z}_{>0}^2$ (analogously to Definition 1.1). We use the following ones, due to [26, Equation (7.10)] (though our notation is closer to [25]¹³), that satisfy the Yang–Baxter equation (see Lemma 6.6 below). In the following, we define the function $\varphi : \mathbb{R}^n \times \mathbb{R}^n \rightarrow \mathbb{R}$ by setting

$$\varphi(\mathbf{X}, \mathbf{Y}) = \sum_{1 \leq i < j \leq n} X_i Y_j, \quad \text{for any } \mathbf{X}, \mathbf{Y} \in \mathbb{R}^n.$$

Definition 6.1 ([25, Equation (C.1.4)]). Fix $r, s, z \in \mathbb{C}$ and $\mathbf{A}, \mathbf{B}, \mathbf{C}, \mathbf{D} \in \mathbb{Z}_{\geq 0}^n$, and let $t = |\mathbf{T}|$ for each index $T \in \{A, B, C, D\}$. Define the vertex weight

$$(6.1) \quad \begin{aligned} & U_{z; r, s}(\mathbf{A}, \mathbf{B}; \mathbf{C}, \mathbf{D}) \\ &= z^{d-b} r^{2(c-a)} s^{2d} q^{\varphi(\mathbf{D}, \mathbf{C})} \frac{(r^2; q)_d}{(r^2; q)_b} \sum_{p=0}^{\min\{b, c\}} (r^{-2}z)^p \frac{(r^{-2}s^2z; q)_{c-p} (r^2z^{-1}; q)_p (z; q)_{b-p}}{(s^2z; q)_{c+d-p}} \\ & \quad \times \mathbb{1}_{\mathbf{A}+\mathbf{B}=\mathbf{C}+\mathbf{D}} \cdot \sum_{\substack{\mathbf{P} < \mathbf{B}, \mathbf{C} \\ |\mathbf{P}|=p}} q^{\varphi(\mathbf{B}-\mathbf{D}-\mathbf{P}, \mathbf{P})} \prod_{i=1}^n \frac{(q; q)_{C_i+D_i-P_i}}{(q; q)_{D_i} (q; q)_{C_i-P_i}} \frac{(q; q)_{B_i}}{(q; q)_{P_i} (q; q)_{B_i-P_i}}, \end{aligned}$$

where the sum is over all $\mathbf{P} = (P_1, \dots, P_n) \in \mathbb{Z}_{\geq 0}^n$ such that $|\mathbf{P}| = p$ and $0 \leq P_i \leq \min\{B_i, C_i\}$ for each $i \in \llbracket 1, n \rrbracket$.

Remark 6.2. As in Remark 1.2, the U -weights from Definition 6.1 are stochastic in the sense that $\sum_{\mathbf{C}, \mathbf{D} \in \mathbb{Z}_{\geq 0}^n} U_{z; r, s}(\mathbf{A}, \mathbf{B}; \mathbf{C}, \mathbf{D}) = 1$, for each $r, s, z \in \mathbb{C}$ and $\mathbf{A}, \mathbf{B} \in \mathbb{Z}_{\geq 0}^n$; see [25, Proposition C.1.2].

¹³The (r, s) in Definition 6.1 are the $(q^{-L/2}, q^{-M/2})$ from [25].

We can now use these U -weights to describe (similarly to Section 1.2) how to sample a random colored fused path ensemble on $\mathbb{Z}_{>0}^2$. We first define probability measures \mathbb{P}_{FV}^n on the set of colored fused ensembles whose vertices are all contained in the triangles $\mathbb{T}_N = \{(x, y) \in \mathbb{Z}_{>0}^2 : x + y \leq N\}$. The initial measure \mathbb{P}_{FV}^0 is supported by the empty ensemble.

For each integer $N \geq 1$, we will define $\mathbb{P}_{\text{FV}}^{N+1}$ from \mathbb{P}_{FV}^N by first using \mathbb{P}_{FV}^N to sample a colored fused path ensemble \mathcal{E}_N on \mathbb{T}_N . This yields arrow configurations for all vertices in the triangle \mathbb{T}_{N-1} . To extend this to a colored six-vertex ensemble on \mathbb{T}_{N+1} , we must prescribe arrow configurations to all vertices on the diagonal $\mathbb{D}_N = \{(x, y) \in \mathbb{Z}_{>0}^2 : x + y = N\}$. Since \mathcal{E}_N and the initial data prescribe the first two coordinates (\mathbf{A}, \mathbf{B}) of the arrow configuration to each vertex in \mathbb{D}_N , it remains to explain how to assign the second two coordinates (\mathbf{C}, \mathbf{D}) of the arrow configuration at any vertex $(i, j) \in \mathbb{D}_N$, given its first two coordinates (\mathbf{A}, \mathbf{B}) . This is done according to the transition probability $\mathbb{P}_{\text{FV}}^N[(\mathbf{C}, \mathbf{D}) | (\mathbf{A}, \mathbf{B})] = U_{y_i/x_j; r_j, s_i}(\mathbf{A}, \mathbf{B}; \mathbf{C}, \mathbf{D})$. We assume that the parameters $(\mathbf{x}; \mathbf{y}; \mathbf{r}; \mathbf{s}; q)$ are chosen so that these probabilities are all nonnegative (see Section 8 below for one example, although there are also numerous other choices of parameters satisfying this property); the stochasticity of the U -weights (Remark 6.2) then ensures that \mathbb{P}_{FV}^N indeed defines a probability measure.

Choosing (\mathbf{C}, \mathbf{D}) according to the above transition probabilities yields a random colored fused path ensemble \mathcal{E}_{N+1} , now defined on \mathbb{T}_{N+1} ; the probability distribution of \mathcal{E}_{N+1} is then denoted by $\mathbb{P}_{\text{FV}}^{N+1}$. Taking the limit as N tends to ∞ yields a probability measure on colored fused path ensembles on the quadrant. We refer to it as the *colored stochastic fused vertex model*; observe that it may also be sampled on any rectangle $\mathcal{D} \subset \mathbb{Z}^2$ in the same way as it was above on the quadrant.

6.2. Yang–Baxter Equation for Fused Weights. In this section we state the Yang–Baxter equation for the U -weights from Definition 6.1, with another family of weights given by the W and \widehat{W} ones below. The latter two weights serve as analogs of the L and \widehat{L} ones from Definition 2.1, respectively; indeed, it is quickly verified from Definition 2.1 and Definition 6.3 below that the (L, \widehat{L}) weights are the $r = q^{-1/2}$ special cases of the (W, \widehat{W}) ones.

Definition 6.3. Adopting the notation of Definition 6.1, define the weight

$$W_{x;r,s}(\mathbf{A}, \mathbf{B}; \mathbf{C}, \mathbf{D}) = (-s)^{-d} \cdot U_{x/s;r,s}(\mathbf{A}, \mathbf{B}; \mathbf{C}, \mathbf{D}),$$

so that

$$(6.2) \quad \begin{aligned} & W_{x;r,s}(\mathbf{A}, \mathbf{B}; \mathbf{C}, \mathbf{D}) \\ &= (-1)^d x^{d-b} r^{2(c-a)} s^b q^{\varphi(\mathbf{D}, \mathbf{C})} \frac{(r^2; q)_d}{(r^2; q)_b} \sum_{p=0}^{\min\{b,c\}} (r^2 s)^{-p} x^p \frac{(r^{-2} s x; q)_{c-p} (r^2 s x^{-1}; q)_p (s^{-1} x; q)_{b-p}}{(s x; q)_{c+d-p}} \\ & \quad \times \mathbb{1}_{\mathbf{A}+\mathbf{B}=\mathbf{C}+\mathbf{D}} \cdot \sum_{\substack{\mathbf{P} \leq \mathbf{B}, \mathbf{C} \\ |\mathbf{P}|=p}} q^{\varphi(\mathbf{B}-\mathbf{D}-\mathbf{P}, \mathbf{P})} \prod_{i=1}^n \frac{(q; q)_{C_i+D_i-P_i}}{(q; q)_{D_i} (q; q)_{C_i-P_i}} \frac{(q; q)_{B_i}}{(q; q)_{P_i} (q; q)_{B_i-P_i}}. \end{aligned}$$

We also set $W_{x;r,0}(\mathbf{A}, \mathbf{B}; \mathbf{C}, \mathbf{D}) = \lim_{s \rightarrow 0} W_{x;r,s}(\mathbf{A}, \mathbf{B}; \mathbf{C}, \mathbf{D})$, where the existence (and an explicit form) of this limit follows from Lemma 6.7 below. Additionally, if there exists an integer $R \geq 1$ for which $r = q^{-R/2}$, then set

$$(6.3) \quad \widehat{W}_{x;r,s}(\mathbf{A}, \mathbf{B}; \mathbf{C}, \mathbf{D}) = W_{x;r,s}(\mathbf{A}, \mathbf{B}; \mathbf{C}, \mathbf{D}) \cdot (-s)^{-R} \frac{(s x; q)_R}{(s^{-1} x; q)_R}.$$

Remark 6.4. Observe for any $r, s, z \in \mathbb{C}$ and $\mathbf{B} \in \mathbb{Z}_{\geq 0}^n$ that

$$U_{z;r,s}(\mathbf{e}_0, \mathbf{B}; \mathbf{e}_0, \mathbf{B}) = s^{2b} \cdot \frac{(z; q)_b}{(s^2 z; q)_b}; \quad W_{z;r,s}(\mathbf{e}_0, \mathbf{B}; \mathbf{e}_0, \mathbf{B}) = (-s)^b \cdot \frac{(s^{-1}z; q)_b}{(sz; q)_b},$$

which quickly follow from the fact that the sums in (6.1) and (6.2) are supported on the term $\mathbf{P} = \mathbf{e}_0$ (as $\mathbf{C} = \mathbf{e}_0$).

Remark 6.5. Let us explain the sense in which the \widehat{W} -weight from Definition 6.3 is analogous to the \widehat{L} one from (2.3). The latter was chosen to be the (unique) normalization of L_x such that $\widehat{L}_x(\mathbf{e}_0, k; \mathbf{e}_0, k) = 1$ for each $k \in \llbracket 1, n \rrbracket$; the arrow configuration $(\mathbf{e}_0, k; \mathbf{e}_0, k)$ could be viewed as “horizontally saturated,” since horizontal edges could accommodate at most one arrow under the L -weights. The analog of this constraint would be to make $\widehat{W}_{z;r,s}$ a normalization of $W_{z;r,s}$ such that $\widehat{W}_{z;r,s} = 1$ at a fused arrow configuration that is “horizontally saturated” in one color. One way to make sense of “horizontal saturation” for fused arrow configurations is to impose a threshold $R \in \mathbb{Z}_{>0}$ for the number of arrows that can occupy a horizontal edge; this is done by setting $r = q^{-R/2}$ (as then the factor of $(r^2; q)_d$ in the W -weight (6.2) is equal to 0 if $d > R$). In this case, the normalization condition would be for

$$(6.4) \quad \widehat{W}_{z;r,s}(\mathbf{e}_0, \mathbf{R}\mathbf{e}_k; \mathbf{e}_0, \mathbf{R}\mathbf{e}_k) = 1, \quad \text{for each } k \in \llbracket 1, n \rrbracket,$$

so that $\widehat{W}_{z;r,s}(\mathbf{A}, \mathbf{B}; \mathbf{C}, \mathbf{D}) = W_{z;r,s}(\mathbf{A}, \mathbf{B}; \mathbf{C}, \mathbf{D}) \cdot W_{z;r,s}(\mathbf{e}_0, \mathbf{R}\mathbf{e}_k; \mathbf{e}_0, \mathbf{R}\mathbf{e}_k)^{-1}$, which by Remark 6.4 yields (6.3).

Let us also briefly mention that another way of imposing “horizontal saturation” would be to have infinitely many arrows of some color $k \in \llbracket 1, n \rrbracket$ travel along rows of the model. One should then track how many arrows of color k leave a row (as well as how many arrows of the other colors enter it), that is, one “complements” the arrow configuration in the color k . This should enable one to remove the restriction that $r = q^{-R/2}$ for some integer $R \geq 1$; similar ideas were also used in [2, Section 3.1.3] and [5, Section 17.7.3]. However, we will not pursue this direction here,¹⁴ and keep ourselves constrained to the case when $r^2 \in q^{\mathbb{Z} < 0}$ whenever using the \widehat{W} -weights.

The following proposition states that the U and W weights (of Definition 6.1 and Remark 6.5) satisfy the Yang-Baxter equation; it is due to [26, Equation (3.20)] (though, as stated below, it appears in [25]¹⁵); it is a fused generalization of Lemma 2.2.

Lemma 6.6 ([25, Theorem C.1.1]). *Fix $x, y, z, r, s, t \in \mathbb{C}$ and $\mathbf{I}_1, \mathbf{J}_1, \mathbf{K}_1, \mathbf{I}_3, \mathbf{J}_3, \mathbf{K}_3 \in \mathbb{Z}_{\geq 0}$. Then,*

$$\begin{aligned} & \sum_{\mathbf{I}_2, \mathbf{J}_2, \mathbf{K}_2 \in \mathbb{Z}_{\geq 0}^n} U_{x/y;r,s}(\mathbf{I}_1, \mathbf{J}_1; \mathbf{I}_2, \mathbf{J}_2) U_{x/z;r,t}(\mathbf{K}_1, \mathbf{J}_2; \mathbf{K}_2, \mathbf{J}_3) U_{y/z;s,t}(\mathbf{K}_2, \mathbf{I}_2; \mathbf{K}_3, \mathbf{I}_3) \\ &= \sum_{\mathbf{I}_2, \mathbf{J}_2, \mathbf{K}_2 \in \mathbb{Z}_{\geq 0}^n} U_{y/z;s,t}(\mathbf{K}_1, \mathbf{I}_1; \mathbf{K}_2, \mathbf{I}_2) U_{x/z;r,t}(\mathbf{K}_2, \mathbf{J}_1; \mathbf{K}_3, \mathbf{J}_2) U_{x/y;r,s}(\mathbf{I}_2, \mathbf{J}_2; \mathbf{I}_3, \mathbf{J}_3). \end{aligned}$$

¹⁴See, however, Appendix A below, which implements a version of this complementation to degenerate the colored stochastic fused vertex model to the log-gamma polymer.

¹⁵In [25, Theorem C.1.1], it was assumed that $r^2, s^2, t^2 \in q^{\mathbb{Z} < 0}$, but this assumption can be removed by using analytic continuation (with the fact that the U -weights are rational in r, s , and t).

Therefore, if there exists an integer $R > 0$ such that $r = q^{-R/2}$, then

$$\begin{aligned} & \sum_{\mathbf{I}_2, \mathbf{J}_2, \mathbf{K}_2 \in \mathbb{Z}_{\geq 0}^n} U_{x/y;r,s}(\mathbf{I}_1, \mathbf{J}_1; \mathbf{I}_2, \mathbf{J}_2) \widehat{W}_{x/z;r,t}(\mathbf{K}_1, \mathbf{J}_2; \mathbf{K}_2, \mathbf{J}_3) W_{y/z;s}(\mathbf{K}_2, \mathbf{I}_2; \mathbf{K}_3, \mathbf{I}_3) \\ &= \sum_{\mathbf{I}_2, \mathbf{J}_2, \mathbf{K}_2 \in \mathbb{Z}_{\geq 0}^n} U_{y/z;s,t}(\mathbf{K}_1, \mathbf{I}_1; \mathbf{K}_2, \mathbf{I}_2) \widehat{W}_{x/z;r,t}(\mathbf{K}_2, \mathbf{J}_1; \mathbf{K}_3, \mathbf{J}_2) W_{x/y;r}(\mathbf{I}_2, \mathbf{J}_2; \mathbf{I}_3, \mathbf{J}_3). \end{aligned}$$

Before proceeding, we record the following results that evaluate the $W_{x;r,0}$ weights.

Lemma 6.7. *Adopting the notation of Definition 6.3, we have*

$$\begin{aligned} W_{z;r,0}(\mathbf{A}, \mathbf{B}; \mathbf{C}, \mathbf{D}) &= (-1)^{b-d} z^d r^{2(c-a)} q^{\varphi(\mathbf{D}, \mathbf{C}) + \binom{b}{2}} \frac{(r^2; q)_d}{(r^2; q)_b} \cdot \mathbb{1}_{\mathbf{A} + \mathbf{B} = \mathbf{C} + \mathbf{D}} \\ &\quad \times \prod_{i=1}^n \left(\sum_{p=0}^{\min\{B_i, C_i\}} (-r^{-2})^p q^{\binom{p+1}{2} - p(B_{[i,n]} + D_{[1, i-1]})} \right. \\ &\quad \left. \times \frac{(q; q)_{C_i + D_i - p}}{(q; q)_{C_i - p} (q; q)_{D_i}} \frac{(q; q)_{B_i}}{(q; q)_{B_i - p} (q; q)_p} \right). \end{aligned}$$

Proof. Throughout this proof, we assume that $\mathbf{A} + \mathbf{B} = \mathbf{C} + \mathbf{D}$, as otherwise $W_{z;r,0}(\mathbf{A}, \mathbf{B}; \mathbf{C}, \mathbf{D}) = 0$ (as $U_{z;r,s}(\mathbf{A}, \mathbf{B}; \mathbf{C}, \mathbf{D}) = 0$ for any $s \in \mathbb{C}$, by Definition 6.1). Inserting the equalities

$$\lim_{s \rightarrow 0} s^{b-p} (s^{-1}z; q)_{b-p} = (-1)^{b-p} q^{\binom{b-p}{2}} z^{b-p}; \quad \lim_{s \rightarrow 0} \frac{(r^{-2}sz; q)_{c-p} (r^2sz^{-1}; q)_p}{(sz; q)_{c+d-p}} = 1,$$

into (6.1), we obtain

$$\begin{aligned} W_{z;r,0}(\mathbf{A}, \mathbf{B}; \mathbf{C}, \mathbf{D}) &= (-1)^{b-d} z^d r^{2(c-a)} q^{\varphi(\mathbf{D}, \mathbf{C})} \frac{(r^2; q)_d}{(r^2; q)_b} \sum_{p=0}^{\min\{b,c\}} (-r^{-2})^p q^{\binom{b-p}{2}} \sum_{\substack{\mathbf{P} \leq \mathbf{B}, \mathbf{C} \\ |\mathbf{P}|=p}} q^{\varphi(\mathbf{B} - \mathbf{D} - \mathbf{P}, \mathbf{P})} \\ &\quad \times \prod_{i=1}^n \frac{(q; q)_{C_i + D_i - P_i}}{(q; q)_{D_i} (q; q)_{C_i - P_i}} \frac{(q; q)_{B_i}}{(q; q)_{P_i} (q; q)_{B_i - P_i}}. \end{aligned}$$

Also since

$$\begin{aligned} \binom{b-p}{2} &= \binom{b}{2} - bp + \binom{p+1}{2}; & \binom{p+1}{2} - \varphi(\mathbf{P}, \mathbf{P}) &= \sum_{i=1}^n \binom{P_i + 1}{2}; \\ \varphi(\mathbf{B}, \mathbf{P}) - bp &= - \sum_{1 \leq i \leq j \leq n} P_i B_j = - \sum_{i=1}^n B_i P_i - \varphi(\mathbf{P}, \mathbf{B}); \end{aligned}$$

and since $\varphi(\mathbf{B} - \mathbf{D} - \mathbf{P}, \mathbf{P}) = \varphi(\mathbf{B}, \mathbf{P}) - \varphi(\mathbf{D}, \mathbf{P}) - \varphi(\mathbf{P}, \mathbf{P})$ (by the bilinearity of φ), we have

$$(6.5) \quad \begin{aligned} & W_{z;r,0}(\mathbf{A}, \mathbf{B}; \mathbf{C}, \mathbf{D}) \\ &= (-1)^{b-d} z^d r^{2(c-a)} q^{\varphi(\mathbf{D}, \mathbf{C}) + \binom{b}{2}} \frac{(r^2; q)_d}{(r^2; q)_b} \prod_{i=1}^n \frac{(q; q)_{B_i}}{(q; q)_{D_i}} \\ &\quad \times \sum_{p=0}^{\min\{b,c\}} (-r^{-2})^p \sum_{\substack{\mathbf{P} < \mathbf{B}, \mathbf{C} \\ |\mathbf{P}|=p}} q^{-\varphi(\mathbf{P}, \mathbf{B}) - \varphi(\mathbf{D}, \mathbf{P})} \prod_{i=1}^n q^{\binom{P_i+1}{2} - B_i P_i} \frac{(q; q)_{C_i + D_i - P_i}}{(q; q)_{C_i - P_i} (q; q)_{P_i} (q; q)_{B_i - P_i}}. \end{aligned}$$

Now observe for any complex number $w \in \mathbb{C}$; n -tuples $\mathbf{X}, \mathbf{Y}, \mathbf{Z} \in \mathbb{Z}^n$; and functions $f_1, f_2, \dots, f_n : \mathbb{Z}_{\geq 0} \rightarrow \mathbb{C}$ we have

$$\sum_{\substack{\mathbf{P} \in \mathbb{Z}_{\geq 0}^n \\ \mathbf{P} \leq \mathbf{Z}}} w^{|\mathbf{P}|} q^{\varphi(\mathbf{P}, \mathbf{X}) + \varphi(\mathbf{Y}, \mathbf{P})} \prod_{i=1}^n f_i(P_i) = \prod_{i=1}^n \left(\sum_{p=0}^{Z_i} q^{p(X_{[i+1,n]} + Y_{[1,i-1]})} w^p f_i(p) \right),$$

by expanding the product on the right side. Applying this in (6.5) with

$$w = -r^{-2}; \quad \mathbf{X} = -\mathbf{B}; \quad \mathbf{Y} = -\mathbf{D}; \quad \mathbf{Z} = \min\{\mathbf{B}, \mathbf{C}\};$$

$$f_i(k) = q^{\binom{k+1}{2} - B_i k} \frac{(q; q)_{C_i + D_i - k}}{(q; q)_{C_i - k} (q; q)_k (q; q)_{B_i - k}},$$

yields the lemma (where $\min\{\mathbf{B}, \mathbf{C}\}$ denotes the entry-wise minimum of \mathbf{B} and \mathbf{C}). \square

Corollary 6.8. *Adopting the notation of Definition 6.3, we have $W_{z;r,0}(\mathbf{A}, \mathbf{B}; \mathbf{A} + \mathbf{B}, \mathbf{e}_0) = 1$.*

Proof. By Lemma 6.7 and the facts that $(q; q)_{B_i} (q; q)_{B_i - p}^{-1} = (-1)^p q^{B_i p - \binom{p}{2}} (q^{-B_i}; q)_p$; that $B_i - B_{[i,n]} = -B_{[i+1,n]}$; and that $\binom{p+1}{2} - \binom{p}{2} = p$, we have

$$(6.6) \quad W_{z;r,0}(\mathbf{A}, \mathbf{B}; \mathbf{A} + \mathbf{B}, \mathbf{e}_0) = (-1)^b r^{2b} q^{\binom{b}{2}} (r^2; q)_b^{-1} \cdot \prod_{i=1}^n \left(\sum_{p=0}^{B_i} (r^{-2} q^{1 - B_{[i+1,n]}})^p \frac{(q^{-B_i}; q)_p}{(q; q)_p} \right).$$

From the q -binomial theorem, we have for each $i \in [1, n]$ that

$$\sum_{p=0}^{B_i} (r^{-2} q^{1 - B_{[i+1,n]}})^p \frac{(q^{-B_i}; q)_p}{(q; q)_p} = (r^{-2} q^{1 - B_{[i,n]}}; q)_{B_i},$$

and hence

$$\begin{aligned} \prod_{i=1}^n \left(\sum_{p=0}^{B_i} (r^{-2} q^{1 - B_{[i+1,n]}})^p \frac{(q^{-B_i}; q)_p}{(q; q)_p} \right) &= \prod_{i=1}^n (r^{-2} q^{1 - B_{[i,n]}}; q)_{B_i} \\ &= (r^{-2}; q^{-1})_b = (-1)^b r^{-2b} q^{-\binom{b}{2}} (r^2; q)_b. \end{aligned}$$

Inserting this into (6.6) yields the corollary. \square

Remark 6.9. An alternative (and perhaps more conceptual) way of proving Corollary 6.8 would be through fusion, using the fact that it holds at $R = 1$ by (3.11); we will not provide further details on that route here.

6.3. Fused Nonsymmetric Functions. In this section we formulate the fused analogs of the functions f and G (from Definition 2.6), as well as some of their properties. We begin with the following definition, which is parallel to Definition 2.3.

Definition 6.10. Fix an integer $N \geq 1$; a complex number $s \in \mathbb{C}$; sequences of complex numbers $\mathbf{r} = (r_1, r_2, \dots, r_N)$ and $\mathbf{x} = (x_1, x_2, \dots, x_N)$; and a colored fused path ensemble \mathcal{E} on $\mathcal{D}_N = \mathbb{Z}_{\leq 0} \times \llbracket 1, N \rrbracket$, whose arrow configuration at any $v \in \mathcal{D}_N$ is denoted by $(\mathbf{A}(v), \mathbf{B}(v); \mathbf{C}(v), \mathbf{D}(v))$. Set

$$\begin{aligned} W_{\mathbf{x}; \mathbf{r}; s}(\mathcal{E}) &= \prod_{k=1}^{\infty} \prod_{j=1}^N W_{x_j; r_j, s}(\mathbf{A}(-k, j), \mathbf{B}(-k, j); \mathbf{C}(-k, j), \mathbf{D}(-k, j)) \\ &\quad \times \prod_{j=1}^N W_{x_j; r_j, 0}(\mathbf{A}(0, j), \mathbf{B}(0, j); \mathbf{C}(0, j), \mathbf{D}(0, j)); \\ \widehat{W}_{\mathbf{x}; \mathbf{r}; s}(\mathcal{E}) &= \prod_{k=1}^{\infty} \prod_{j=1}^N \widehat{W}_{x_j; r_j, s}(\mathbf{A}(-k, j), \mathbf{B}(-k, j); \mathbf{C}(-k, j), \mathbf{D}(-k, j)) \\ &\quad \times \prod_{j=1}^N W_{x_j; r_j, 0}(\mathbf{A}(0, j), \mathbf{B}(0, j); \mathbf{C}(0, j), \mathbf{D}(0, j)), \end{aligned}$$

where in the second equality it is assumed that $r_j^2 \in q^{\mathbb{Z}_{<0}}$, for each $j \in \llbracket 1, N \rrbracket$.

Now we can define the following (non)symmetric functions, in a way parallel to Definition 2.6, but with three differences. First, the vertex models are fused path ensembles, instead of higher spin ones. Second, they have weights the W and \widehat{W} , instead of the L and \widehat{L} . Third, in defining f below, we have multiple arrows entering all rows, instead of only one, with the purpose of fully saturating them (see Figure 18).

Definition 6.11. Fix an integer $N \geq 1$; a sequence of positive integers $\mathbf{R} = (R_1, R_2, \dots, R_N)$; two n -compositions $\mu, \nu \in \text{Comp}_n$; and a function $\sigma : \llbracket 1, N \rrbracket \rightarrow \llbracket 1, n \rrbracket$.

If $\ell(\mu) = \ell(\nu) + \mathbf{R}_{\llbracket 1, N \rrbracket}$, then let $\mathfrak{P}_{\mathbf{F}}(\mu/\nu; \sigma; \mathbf{R})$ denote the set of colored fused path ensembles on $\mathcal{D}_N = \mathbb{Z}_{\leq 0} \times \llbracket 1, N \rrbracket$ with the following boundary data.

- (1) For each $j \in \llbracket 1, N \rrbracket$, R_j arrows of color $\sigma(j)$ horizontally enters \mathcal{D}_N through $(-\infty, j)$.
- (2) For each $k \geq 0$ and $c \in \llbracket 1, n \rrbracket$, $\mathbf{m}_k(\nu^{(c)})$ arrows of color c vertically enter \mathcal{D}_N through $(-k, 1)$.
- (3) For each $k \geq 0$ and $c \in \llbracket 1, n \rrbracket$, $\mathbf{m}_k(\mu^{(c)})$ arrows of color c vertically exit \mathcal{D}_N through $(-k, N)$.

See the left side of Figure 18 for a depiction when $\mu = (7, 2, 0 \mid 5, 5, 4, 1, 1, 0 \mid 5, 2, 2)$; $\nu = (\emptyset \mid 6 \mid 6, 5)$; $(\sigma(1), \sigma(2), \sigma(3), \sigma(4), \sigma(5)) = (1, 3, 2, 1, 2)$; and $\mathbf{R} = (2, 1, 3, 1, 2)$. There, red, green, and blue are colors 1, 2, and 3, respectively.

Similarly, if $\ell(\mu) = \ell(\nu)$, then let $\mathfrak{P}_{\mathbf{G}}(\mu/\nu)$ denote the set of colored fused path ensembles on $\mathcal{D}_N = \mathbb{Z}_{\leq 0} \times \llbracket 1, N \rrbracket$, with the following boundary data.

- (1) For each $j \in \llbracket 1, N \rrbracket$, no arrow horizontally enters or exits \mathcal{D}_N through the j -th row.
- (2) For each $k \geq 0$ and $c \in \llbracket 1, n \rrbracket$, $\mathbf{m}_k(\mu^{(c)})$ arrows of color c vertically enter \mathcal{D}_N through $(-k, 1)$.
- (3) For each $k \geq 0$ and $c \in \llbracket 1, n \rrbracket$, $\mathbf{m}_k(\nu^{(c)})$ arrows of color c vertically exit \mathcal{D}_N through $(-k, N)$.

See the right side of Figure 18 for a depiction when $\mu = (7, 5 \mid 7, 6 \mid 6, 4)$ and $\nu = (5, 2 \mid 5, 1 \mid 3, 2)$.

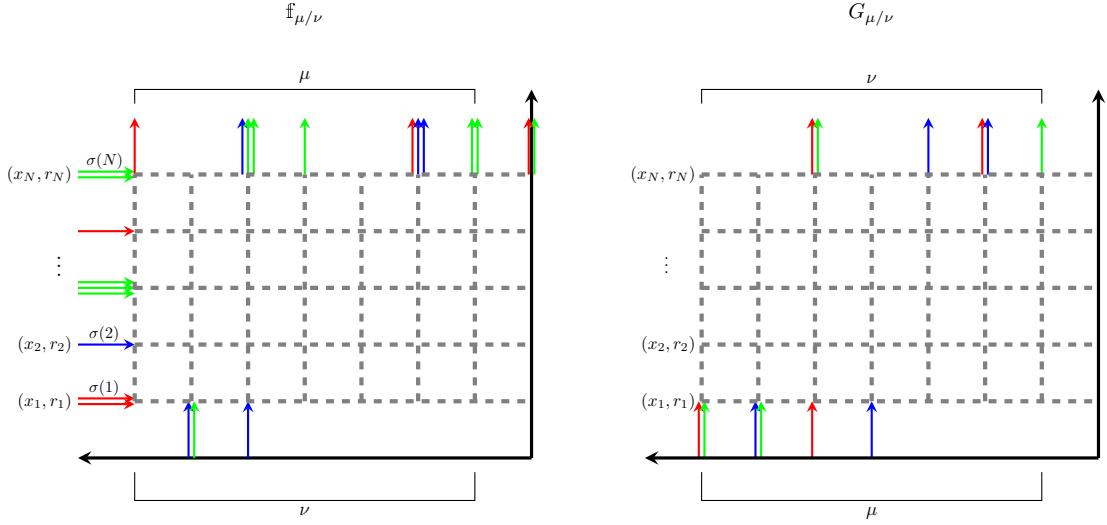


FIGURE 18. Depicted to the left and right are vertex models for $f_{\mu/\nu;s}^\sigma$ and $G_{\mu/\nu;s}$, respectively.

For any complex number $s \in \mathbb{C}$, and sequences of complex numbers $\mathbf{r} = (r_1, r_2, \dots, r_N)$ and $\mathbf{x} = (x_1, x_2, \dots, x_N)$, let

$$(6.7) \quad f_{\mu/\nu;s}^\sigma(\mathbf{x}; \mathbf{r}) = \sum_{\mathfrak{P}_f(\mu/\nu; \sigma; \mathbf{R})} \widehat{W}_{\mathbf{x}; \mathbf{r}; s}(\mathcal{E}); \quad G_{\mu/\nu;s}(\mathbf{x}; \mathbf{r}) = \sum_{\mathfrak{P}_G(\mu/\nu)} W_{\mathbf{x}; \mathbf{r}; s}(\mathcal{E}),$$

where in the first equality it is assumed that $r_j^{-2} = q^{R_j}$ for each $j \in \llbracket 1, N \rrbracket$ (and \mathbf{r} can be arbitrary in the second). If $\nu = \emptyset$ is empty, we write $f_{\mu;s}^\sigma(\mathbf{x}; \mathbf{r}) = f_{\mu/\emptyset;s}^\sigma(\mathbf{x}; \mathbf{r})$ and $G_{\mu;s}(\mathbf{x}; \mathbf{r}) = G_{\mu/0^N;s}(\mathbf{x}; \mathbf{r})$. If $N = 1$, we may write $f_{\mu/\nu;s}^{\sigma(1)}$ in place of $f_{\mu/\nu;s}^\sigma$.

Observe that the quantity $\widehat{W}_{\mathbf{x}; \mathbf{r}; s}(\mathcal{E})$ appearing as the summand in (6.7) defining $f_{\mu/\nu}^\sigma$ is bounded, since all but finitely many vertices in any ensemble $\mathcal{E} \in \mathfrak{P}_f(\mu/\nu; \sigma; \mathbf{R})$ have arrow configurations of the form $(\mathbf{e}_0, R_j \mathbf{e}_{\sigma(j)}; \mathbf{e}_0, R_j \mathbf{e}_{\sigma(j)})$ for some $j \in \llbracket 1, N \rrbracket$, and $\widehat{W}_{x_j; r_j; s}(\mathbf{e}_0, R_j \mathbf{e}_{\sigma(j)}; \mathbf{e}_0, R_j \mathbf{e}_{\sigma(j)}) = 1$ for $r_j = q^{-R_j/2}$, by (6.4). Similarly, $W_{\mathbf{x}; \mathbf{r}; s}(\mathcal{E})$ appearing as the summand in (6.7) defining $G_{\mu/\nu;s}$ is bounded, since all but finitely many vertices in any $\mathcal{E} \in \mathfrak{P}_G(\mu/\nu)$ have arrow configurations of the form $(\mathbf{e}_0, \mathbf{e}_0; \mathbf{e}_0, \mathbf{e}_0)$, and we have $W_{x; r; s}(\mathbf{e}_0, 0; \mathbf{e}_0, 0) = 1$ by Remark 6.4.

Remark 6.12. It may be possible to analytically continue the f functions in the parameters \mathbf{r} (so as to avoid imposing the assumption that each $r_j \in q^{\mathbb{Z} < 0}$), by following the complementation procedure outlined at the end of Remark 6.5. However, we will not pursue this here.

6.4. Properties of f and G . In this section we provide properties of the f and G functions from Definition 6.11. The first is the *fusion* property that relates these to the f and G functions from Definition 2.6, when the parameters of the latter are specialized to unions of geometric progressions. We omit its proof, as very similar statements have appeared repeatedly throughout the literature; see [23, Section 6E], [20, Theorem 6.2], and [5, Proposition 7.2.3] for references in the colored case and [22, Proposition 5.5] in the uncolored one.

Lemma 6.13. *Adopt the notation of Definition 6.11, and assume $r_j = q^{-R_j/2}$ for each $j \in \llbracket 1, N \rrbracket$. Define $\omega : \llbracket 1, R_{\llbracket 1, N \rrbracket} \rrbracket \rightarrow \llbracket 1, n \rrbracket$ by for each $j \in \llbracket 1, R_{\llbracket 1, N \rrbracket} \rrbracket$ setting $\omega(j) = \sigma(j')$, where $j' \in \llbracket 1, N \rrbracket$ is the unique index satisfying $R_{\llbracket 1, j'-1 \rrbracket} + 1 \leq j \leq R_{\llbracket 1, j' \rrbracket}$; also define the $R_{\llbracket 1, N \rrbracket}$ -tuple of complex numbers*

$$\mathbf{z} = (x_1, qx_1, \dots, q^{R_1-1}x_1, x_2, qx_2, \dots, q^{R_2-1}x_2, \dots, x_N, qx_N, \dots, q^{R_N-1}x_N).$$

Then, we have $\mathbb{f}_{\mu/\nu; s}^\sigma(\mathbf{x}; \mathbf{r}) = f_{\mu/\nu; s}^\omega(\mathbf{z})$ and $\mathbb{G}_{\mu/\nu; s}(\mathbf{x}; \mathbf{r}) = G_{\mu/\nu; s}(\mathbf{z})$.

We next provide symmetry properties, branching statements, and Cauchy identities for the \mathbb{f} and \mathbb{G} functions, which are parallel to their counterparts (Lemma 2.7, Lemma 2.8, and Lemma 2.9, respectively) for the f and g functions. They are quick consequences of the latter, together with Lemma 6.13 and analytic continuation.

Lemma 6.14. *Adopt the notation of Definition 6.11, and let $\varsigma : \llbracket 1, M \rrbracket \rightarrow \llbracket 1, M \rrbracket$ denote a permutation. We have $\mathbb{G}_{\mu/\nu; s}(\mathbf{y}; \mathbf{r}) = \mathbb{G}_{\mu/\nu; s}(\varsigma(\mathbf{y}); \varsigma(\mathbf{r}))$, where $\varsigma(\mathbf{y}) = (y_{\varsigma(1)}, y_{\varsigma(2)}, \dots, y_{\varsigma(M)})$ and $\varsigma(\mathbf{r}) = (r_{\varsigma(1)}, r_{\varsigma(2)}, \dots, r_{\varsigma(N)})$.*

Proof. If there exist positive integers (R_1, R_2, \dots, R_N) such that $r_j = q^{-R_j/2}$ for each $j \in \llbracket 1, N \rrbracket$, then this follows from Lemma 6.13 and Lemma 2.7. The fact that the lemma holds for an arbitrary set \mathbf{r} of complex numbers then follows from uniqueness of analytic continuation, as \mathbb{G} is a rational function in \mathbf{r} (since the W -weights from Definition 6.3 are). \square

Lemma 6.15. *Adopting the notation of Definition 6.11; letting $\ell = \ell(\nu)$; and fixing an integer $k \in \llbracket 1, N \rrbracket$, we have*

$$\begin{aligned} \mathbb{f}_{\mu/\nu; s}^\sigma(\mathbf{x}; \mathbf{r}) &= \sum_{\kappa \in \text{Comp}_n(\ell+k)} \mathbb{f}_{\kappa/\nu; s}^{\sigma|_{\llbracket 1, k \rrbracket}}(\mathbf{x}_{\llbracket 1, k \rrbracket}; \mathbf{r}_{\llbracket 1, k \rrbracket}) \mathbb{f}_{\mu/\kappa; s}^{\sigma|_{\llbracket k+1, N \rrbracket}}(\mathbf{x}_{\llbracket k+1, N \rrbracket}; \mathbf{r}_{\llbracket k+1, N \rrbracket}); \\ \mathbb{G}_{\mu/\nu; s}(\mathbf{x}; \mathbf{r}) &= \sum_{\kappa \in \text{Comp}_n(\ell)} \mathbb{G}_{\mu/\kappa; s}(\mathbf{x}_{\llbracket 1, k \rrbracket}; \mathbf{r}_{\llbracket 1, k \rrbracket}) \mathbb{G}_{\kappa/\nu; s}(\mathbf{x}_{\llbracket k+1, N \rrbracket}; \mathbf{r}_{\llbracket k+1, N \rrbracket}). \end{aligned}$$

where in the first equality we assume that $r_j = q^{-R_j/2}$ for each $j \in \llbracket 1, N \rrbracket$ (and \mathbf{r} can be arbitrary in the second). Here, we have defined the variable sets $\mathbf{x}_{\llbracket 1, k \rrbracket} = (x_1, x_2, \dots, x_k)$, $\mathbf{x}_{\llbracket k+1, N \rrbracket} = (x_{k+1}, x_{k+2}, \dots, x_N)$, $\mathbf{r}_{\llbracket 1, k \rrbracket} = (r_1, r_2, \dots, r_k)$, and $\mathbf{r}_{\llbracket k+1, N \rrbracket} = (r_{k+1}, r_{k+2}, \dots, r_N)$. For any interval $I = \llbracket i_0 + 1, i_0 + |I| \rrbracket \subset \llbracket 1, N \rrbracket$, we have also defined the function $\sigma|_I : \llbracket 1, |I| \rrbracket \rightarrow \llbracket 1, n \rrbracket$ by setting $\sigma|_I(i) = \sigma(i + i_0)$ for each $i \in \llbracket 1, |I| \rrbracket$.

Proof. The first equality in the lemma follows from Lemma 2.8 and Lemma 6.13. If $r_j = q^{-R_j/2}$ for each $j \in \llbracket 1, N \rrbracket$, the second follows from the same two statements; for general \mathbf{r} , it then follows from uniqueness of analytic continuation, as \mathbb{G} is rational in \mathbf{r} . \square

Lemma 6.16. *Fix integers $n, M, N \geq 1$; a sequence of positive integers $\mathbf{R} = (R_1, R_2, \dots, R_N)$; sequences of complex variables $\mathbf{r} = (r_1, r_2, \dots, r_N)$, $\mathbf{t} = (t_1, t_2, \dots, t_M)$, $\mathbf{x} = (x_1, x_2, \dots, x_N)$, and $\mathbf{y} = (y_1, y_2, \dots, y_M)$; and a function $\sigma : \llbracket 1, N \rrbracket \rightarrow \llbracket 1, n \rrbracket$. Assume for each $j \in \llbracket 1, N \rrbracket$ that $r_j = q^{-R_j/2}$ and that*

$$(6.8) \quad \max_{\substack{1 \leq i \leq M \\ 1 \leq j \leq N}} \sup_{\substack{(b, b') \in \mathbb{Z}_{\geq 0} \times \llbracket 0, R_j \rrbracket \\ (b, b') \neq (0, R_j)}} \left| (-s)^b \frac{(s^{-1}y_j; q)_b}{(sy_j; q)_b} \cdot (-s)^{b'-R_j} \frac{(s^{-1}x_i; q)_{b'}}{(sx_i; q)_{b'}} \frac{(sx_i; q)_{R_j}}{(s^{-1}x_i; q)_{R_j}} \right| < 1.$$

Then,

$$\sum_{\mu \in \text{Comp}_n(\mathbf{R}_{[1,N]})} \mathfrak{f}_{\mu;s}^\sigma(\mathbf{x}; \mathbf{r}) \mathbb{G}_{\mu;s}(\mathbf{y}; \mathbf{t}) = \prod_{i=1}^M \prod_{j=1}^N \frac{(t_i^2 x_j y_i^{-1}; q)_{\mathbf{R}_j}}{t_i^{2\mathbf{R}_j} (x_j y_i^{-1}; q)_{\mathbf{R}_j}}.$$

Proof (Outline). The proof is analogous to that of Lemma 2.9, so we only briefly outline it. We will use the equality of partition functions depicted in Figure 19 (which is similar to the equality of the partition functions depicted in Figure 7 and Figure 8). On both sides of that figure, \mathbf{R}_j arrows of color $\sigma(j)$ enter horizontally through the $(M+j)$ -th row (from the bottom) for each $j \in [1, N]$, and all arrows exit vertically through the y -axis. The weights on both sides are assigned as follows. In the crosses, we use $U_{x_j/y_i; r_j, t_i}$ at the intersection of the j -th row (from the bottom) and i -th column (from the left). Along the y -axis, we use $W_{x_j; r_j, 0}$ or $W_{y_i; t_i, 0}$, depending on whether the row is marked by (x_j, t_j) or (y_i, s_i) in Figure 19. In $\mathbb{Z}_{<0} \times [1, M+N]$, we use $\widehat{W}_{x_j; r_j, s}$ or $W_{y_i; t_i, s}$, again depending on the marking of the row. The equality of partition functions depicted in Figure 19 is then a consequence of the Yang–Baxter equation Lemma 6.6; denote this partition function by \mathcal{Z} .

The vertex model on the left side of Figure 19 is frozen; it is quickly verified that it has weight

$$(6.9) \quad \mathcal{Z} = 1,$$

using Remark 6.4 (at $b = 0$), (6.4), and Corollary 6.8. To analyze the right side of Figure 19, first observe by (6.8), Remark 6.4, and (6.3) that, for any $(i, j) \in [1, M] \times [1, N]$, we have

$$\sup_{\substack{(b, b') \in \mathbb{Z}_{\geq 0} \times [0, \mathbf{R}_j] \\ (b, b') \neq (0, \mathbf{R}_j)}} \max_{\substack{\mathbf{B}, \mathbf{B}' \in \mathbb{Z}_{\geq 0}^n \\ |\mathbf{B}|=b, |\mathbf{B}'|=b'}} \left| \frac{\widehat{W}_{x_j; r_j, s}(\mathbf{e}_0, \mathbf{B}'; \mathbf{e}_0, \mathbf{B}')}{\widehat{W}_{x_j; r_j, s}(\mathbf{e}_0, \mathbf{R}_j \mathbf{e}_{\sigma(j)}; \mathbf{e}_0, \mathbf{R}_j \mathbf{e}_{\sigma(j)})} \cdot \frac{W_{y_i; t_i, s}(\mathbf{e}_0, \mathbf{B}; \mathbf{e}_0, \mathbf{B})}{W_{y_i; t_i, s}(\mathbf{e}_0, \mathbf{e}_0; \mathbf{e}_0, \mathbf{e}_0)} \right| < 1.$$

Using this bound, one can verify (see, for example, the proof of [5, Proposition 6.2.2] for a very similar argument) that the vertex model on the right side of Figure 19 has nonzero weight only if all but finitely many vertices in rows marked by (y_i, t_i) for some $i \in [1, M]$ have arrow configuration $(\mathbf{e}_0, \mathbf{e}_0; \mathbf{e}_0, \mathbf{e}_0)$. This implies that the cross on the right side of Figure 19 is frozen to have arrow configuration $(\mathbf{e}_0, \mathbf{R}_j \mathbf{e}_{\sigma(j)}; \mathbf{e}_0, \mathbf{R}_j \mathbf{e}_{\sigma(j)})$ at each vertex in its j -th row.

Hence, the weight of the cross is

$$\prod_{i=1}^M \prod_{j=1}^N U_{x_j/y_i; r_j, t_i}(\mathbf{e}_0, \mathbf{R}_j \mathbf{e}_{\sigma(j)}; \mathbf{e}_0, \mathbf{R}_j \mathbf{e}_{\sigma(j)}) = \sum_{i=1}^M \prod_{j=1}^N \frac{t_i^{2\mathbf{R}_j} (x_j y_i^{-1}; q)_{\mathbf{R}_j}}{(t_i^2 x_j y_i^{-1}; q)_{\mathbf{R}_j}}.$$

Moreover, by (6.7), the weight of the part of the right side of Figure 19 on $\mathbb{Z}_{\leq 0} \times [1, M+N]$ is given by $\sum_{\mu \in \text{Comp}_n(\mathbf{R}_{[1,N]})} \mathfrak{f}_{\mu}^\sigma(\mathbf{x}; \mathbf{r}) \mathbb{G}_{\mu}(\mathbf{y}; \mathbf{t})$. Hence,

$$\mathcal{Z} = \prod_{i=1}^M \prod_{j=1}^N \frac{t_i^{2\mathbf{R}_j} (x_j y_i^{-1}; q)_{\mathbf{R}_j}}{(t_i^2 x_j y_i^{-1}; q)_{\mathbf{R}_j}} \cdot \sum_{\mu \in \text{Comp}_n(\mathbf{R}_{[1,N]})} \mathfrak{f}_{\mu}^\sigma(\mathbf{x}; \mathbf{r}) \mathbb{G}_{\mu}(\mathbf{y}; \mathbf{t}).$$

This, together with (6.9), yields the lemma. \square

6.5. Ascending $\mathfrak{f}\mathbb{G}$ Measures. In this section we introduce the fused variants of the probability measures from Definition 3.3. Throughout, we fix integers $M, N \geq 1$; a sequence of positive integers $\mathbf{R} = (\mathbf{R}_1, \mathbf{R}_2, \dots, \mathbf{R}_N)$; a composition $\ell = (\ell_1, \ell_2, \dots, \ell_n)$ of $\mathbf{R}_{[1,N]}$; and a function $\sigma : [1, N] \rightarrow [1, n]$ such that $\ell_i = \sum_{j \in \sigma^{-1}(i)} \mathbf{R}_j$ for each $i \in [1, n]$. We must first introduce the relevant family of n -compositions.

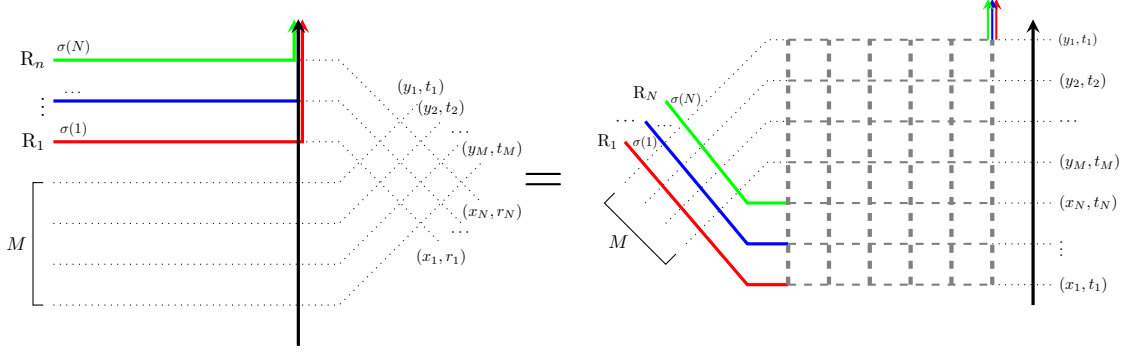


FIGURE 19. Depicted above is the equality of partition functions used in the proof of Lemma 6.16.

Definition 6.17. A sequence $\boldsymbol{\mu} = (\mu(0), \mu(1), \dots, \mu(M+N))$ of n -compositions is called $(M; \sigma; \mathbf{R})$ -ascending if the following hold.

- (1) We have $\mu(0) = (\emptyset \mid \dots \mid \emptyset)$ and $\mu(M+N) = (0^{\ell_1} \mid \dots \mid 0^{\ell_n})$.
- (2) (a) For all $j \in \llbracket 0, N \rrbracket$ and $c \in \llbracket 1, n \rrbracket$, we have $\ell(\mu^{(c)}(j)) = \sum_{k=1}^j R_k \cdot \mathbb{1}_{\sigma(k)=c}$. Thus, $\ell(\mu(j)) = R_{\llbracket 1, j \rrbracket}$.
- (b) For all $i \in \llbracket N, M+N \rrbracket$ and $c \in \llbracket 1, n \rrbracket$, we have $\ell(\mu^{(c)}(i)) = \ell_c$. Thus, $\ell(\mu(i)) = R_{\llbracket 1, N \rrbracket}$.
- (3) For each $(c, k, i) \in \llbracket 1, n \rrbracket \times \mathbb{Z}_{>0} \times \llbracket 1, M+N \rrbracket$, we have

$$(6.10) \quad \mathfrak{Q}_c^\mu(k, i) = \mathfrak{m}_{\leq k-1}(\mu^{(c)}(i)) - \mathfrak{m}_{\leq k-1}(\mu^{(c)}(i-1)) \geq 0.$$

For each $(k, i) \in \mathbb{Z}_{>0} \llbracket 1, M+N \rrbracket$, we set $\mathfrak{Q}^\mu(k, i) = (\mathfrak{Q}_1^\mu(k, i), \mathfrak{Q}_2^\mu(k, i), \dots, \mathfrak{Q}_n^\mu(k, i)) \in \mathbb{Z}_{\geq 0}^n$.

Let us also define the sequence $\mathfrak{Q}(\boldsymbol{\mu}) = (\mathfrak{Q}^\mu(1, 1), \mathfrak{Q}^\mu(1, 2), \dots, \mathfrak{Q}^\mu(1, M+N))$.

Remark 6.18. Given an $(M; \sigma; \mathbf{R})$ -ascending sequence of compositions $\boldsymbol{\mu}$ as in Definition 6.17, we will often view the n -composition $\mu(i)$ as indexing the positions (as in Remark 2.5) of the colored arrows exiting the row $\{y = i\}$, in a vertex model on $\mathbb{Z}_{\leq 0} \times \llbracket 1, M+N \rrbracket$. This yields a colored fused path ensemble on $\mathbb{Z}_{\leq 0} \times \llbracket 1, M+N \rrbracket$, that we will denote by \mathcal{E}_μ . In this way, the c -th entry in $\mathfrak{Q}^\mu(k, i)$ denotes the number of color c arrows in \mathcal{E}_μ along the edge connecting $(-k, i)$ to $(1-k, i)$. Therefore, $\mathfrak{Q}(\boldsymbol{\mu})$ records the colors of the arrows (from bottom to top) along the horizontal edges in \mathcal{E}_μ joining the (-1) -st column to the 0-th one.

The boundary data for this ensemble is described as follows. For each $j \in \llbracket 1, N \rrbracket$, it has R_j arrows of color $\sigma(j)$ horizontally entering the row $\{y = j\}$, and it has no other arrows horizontally entering or exiting any other row of the model. For each $c \in \llbracket 1, n \rrbracket$, it has ℓ_c arrows of color c vertically exiting the y -axis $\{x = 0\}$, and it has no other arrows horizontally entering or exiting any other column of the model. We denote by $\mathfrak{P}_{\text{fG}}(M; \sigma; \mathbf{R})$ the set of colored fused path ensembles on $\mathbb{Z}_{\leq 0} \times \llbracket 1, M+N \rrbracket$ with these boundary conditions, as any $\mathcal{E}_\mu \in \mathfrak{P}_{\text{fG}}(M; \sigma; \mathbf{R})$ can be thought of an ensemble from $\mathfrak{P}_{\text{G}}(\mu/\emptyset)$ that is juxtaposed above one from $\mathfrak{P}_{\text{f}}(\mu/\emptyset; \sigma; \mathbf{R})$ (recall Definition 6.11), for some n -composition $\mu \in \text{Comp}_n(\mathbf{R}_{\llbracket 1, N \rrbracket})$. It is quickly verified that the above procedure is a bijection between $\mathfrak{P}_{\text{fG}}(M; \sigma; \mathbf{R})$ and $(M; \sigma; \mathbf{R})$ -ascending sequences $\boldsymbol{\mu}$ of n -compositions.

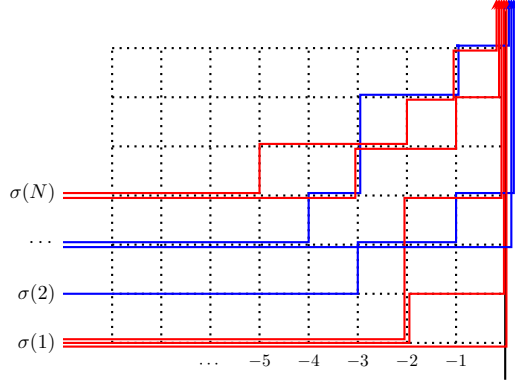


FIGURE 20. Depicted above is the colored fused path ensemble associated with the sequence $\boldsymbol{\mu}$ in the example at the end of Remark 6.18. Here, red and blue are colors 1 and 2, respectively.

See Figure 20 for a depiction, where $(n, M, N) = (2, 3, 4)$, $(R_1, R_2, R_3, R_4) = (3, 1, 2, 2)$, $(\ell_1, \ell_2) = (5, 3)$, $(\sigma(1), \sigma(2), \sigma(3), \sigma(4)) = (1, 2, 2, 1)$, and

$$\begin{aligned} \mu(1) &= (2, 2, 0 \mid \emptyset), & \mu(2) &= (2, 0, 0 \mid 3), & \mu(3) &= (2, 0, 0 \mid 4, 1, 0), \\ \mu(4) &= (5, 3, 0, 0, 0 \mid 3, 0, 0), & \mu(5) &= (2, 1, 0, 0, 0 \mid 3, 0, 0), & \mu(6) &= (1, 0, 0, 0, 0 \mid 1, 0, 0). \end{aligned}$$

Next we define the following probability measure on sequences of ascending compositions.

Definition 6.19. Fix a complex number $s \in \mathbb{C}$ and four sequences $\mathbf{r} = (r_1, r_2, \dots, r_N)$; $\mathbf{t} = (t_1, t_2, \dots, t_M)$; $\mathbf{x} = (x_1, x_2, \dots, x_N)$; and $\mathbf{y} = (y_1, y_2, \dots, y_M)$ of complex numbers, with $r_j = q^{-R_j/2}$ for each $j \in \llbracket 1, n \rrbracket$. Define the probability measure $\mathbb{P}_{\mathbf{fG}}^\sigma = \mathbb{P}_{\mathbf{fG}; n; s; \mathbf{x}; \mathbf{y}; \mathbf{r}; \mathbf{t}}^\sigma$ on $(M; \sigma; \mathbf{R})$ -ascending sequences of n -compositions, by setting

$$(6.11) \quad \mathbb{P}_{\mathbf{fG}}^\sigma[\boldsymbol{\mu}] = \mathcal{Z}_{\mathbf{x}; \mathbf{y}; \mathbf{r}; \mathbf{t}}^{-1} \cdot \prod_{j=1}^N \mathbb{f}_{\mu^{(j)}/\mu^{(j-1)}; s}^{\sigma(j)}(x_j; r_j) \prod_{i=N+1}^{M+N} \mathbb{G}_{\mu^{(i-1)}/\mu^{(i)}; s}(y_{i-N}; t_{i-N}).$$

for each $(M; \sigma; \mathbf{R})$ -ascending sequence $\boldsymbol{\mu} = (\mu(0), \mu(1), \dots, \mu(M+N))$, where

$$(6.12) \quad \mathcal{Z}_{\mathbf{x}; \mathbf{y}; \mathbf{r}; \mathbf{t}} = \prod_{i=1}^M \prod_{j=1}^N \frac{(t_i^2 x_j y_i^{-1}; q)_{R_j}}{t_i^{2R_j} (x_j y_i^{-1}; q)_{R_j}}.$$

Here, we implicitly assume that s , \mathbf{x} , \mathbf{y} , \mathbf{R} , and \mathbf{t} are such that the right side of (6.11) is nonnegative and (6.8) holds. The fact that these probabilities sum to one follows from Lemma 6.20 below.

The proof of the below lemma, given Lemma 6.15 and Lemma 6.16, is entirely analogous to that of Lemma 3.4, given Lemma 2.8 and Lemma 2.9; it is therefore omitted.

Lemma 6.20. *Under the notation and assumptions of Definition 6.19, we have*

$$\sum_{\boldsymbol{\mu}} \prod_{j=1}^N \mathbb{f}_{\mu^{(j)}/\mu^{(j-1)}; s}^{\sigma(j)}(x_j; r_j) \cdot \prod_{i=N+1}^{M+N} \mathbb{G}_{\mu^{(i-1)}/\mu^{(i)}; s}(y_{i-N}; t_{i-N}) = \mathcal{Z}_{\mathbf{x}; \mathbf{y}; \mathbf{r}; \mathbf{t}},$$

where the sum on the left side is over all $(M; \sigma; \mathbf{R})$ -ascending sequences of n -compositions $\boldsymbol{\mu}$.

6.6. Matching Between Colored Stochastic Six-Vertex Models and $\mathbb{P}_{\mathfrak{fG}}^\sigma$. In this section we provide a matching between the law of the $(M + N)$ -tuple $\mathcal{Q}(\boldsymbol{\mu})$ of elements in $\mathbb{Z}_{\geq 0}^n$ (recall Definition 6.17) associated with a sequence of compositions sampled from $\mathbb{P}_{\mathfrak{fG}}^\sigma$ (from Definition 6.19), with a certain random variable associated with the colored fused vertex model (from Section 6.1). We begin by defining the latter, which is analogous to Definition 3.5. Throughout this section, we fix integers $M, N \geq 1$; a complex number $s \in \mathbb{C}$; sequence of positive integers $\mathbf{R} = (R_1, R_2, \dots, R_N)$; sequences of complex numbers $\mathbf{r} = (r_1, r_2, \dots, r_N)$, $\mathbf{t} = (t_1, t_2, \dots, t_M)$, $\mathbf{x} = (x_1, x_2, \dots, x_N)$, and $\mathbf{y} = (y_1, y_2, \dots, y_M)$, satisfying (6.8) and $r_j = q^{-R_j/2}$ for each $j \in \llbracket 1, N \rrbracket$; and a function $\sigma : \llbracket 1, N \rrbracket \rightarrow \llbracket 1, n \rrbracket$.

Definition 6.21. Let \mathcal{E} denote a colored fused path ensemble on the rectangle domain $\mathcal{D}_{M;N} = \llbracket 1, M \rrbracket \times \llbracket 1, N \rrbracket$. For each integer $i \in \llbracket 1, M \rrbracket$, let $\mathbf{C}(i) = \mathbf{C}^\mathcal{E}(i) \in \mathbb{Z}_{\geq 0}^n$ be such that the k -th entry $C_k(i)$ of $\mathbf{C}(i)$ denotes the number of color k arrows in \mathcal{E} vertically exiting $\mathcal{D}_{M;N}$ through (i, N) , for each $k \in \llbracket 1, n \rrbracket$. For each integer $j \in \llbracket 1, N \rrbracket$, let $\mathbf{D}(j) = \mathbf{D}^\mathcal{E}(j) \in \mathbb{Z}_{\geq 0}^n$ be such that the k -th entry $D_k(j)$ of $\mathbf{D}(j)$ denotes the number of color k arrows in \mathcal{E} horizontally exiting $\mathcal{D}_{M;N}$ through (M, j) . Then set $\mathcal{C}(\mathcal{E}) = (\mathbf{C}(1), \mathbf{C}(2), \dots, \mathbf{C}(M)) \in (\mathbb{Z}_{\geq 0}^n)^M$ and $\mathcal{D}(\mathcal{E}) = (\mathbf{D}(1), \mathbf{D}(2), \dots, \mathbf{D}(N)) \in (\mathbb{Z}_{\geq 0}^n)^N$.

We next require notation for the colored stochastic fused vertex model (defined at the end of Section 6.1) with specific boundary data.

Definition 6.22. We say that a colored fused path ensemble on the rectangle domain $\mathcal{D}_{M;N} = \llbracket 1, M \rrbracket \times \llbracket 1, N \rrbracket$ has $(\sigma; \mathbf{R})$ -entrance data if the following holds. For each $j \in \llbracket 1, N \rrbracket$, R_j paths of color $\sigma(j)$ horizontally enters $\mathcal{D}_{M;N}$ from the site $(j, 0)$ on the y -axis, and no path vertically enters $\mathcal{D}_{M;N}$ from any site on the x -axis. Let $\mathbb{P}_{\text{FV}}^\sigma = \mathbb{P}_{\text{FV}; \mathbf{x}; \mathbf{y}; \mathbf{r}; \mathbf{t}}^\sigma$ denote the measure on colored fused path ensembles on $\mathcal{D}_{M;N}$ obtained by running the colored stochastic fused vertex model on $\mathcal{D}_{M;N}$ under $(\sigma; \mathbf{R})$ -boundary data, with weight $U_{y_i/x_j; r_j, t_i}$ (recall Definition 6.1) at any vertex $(i, j) \in \mathcal{D}_{M;N}$.

The following proposition now provides a matching between the $(M + N)$ -tuple $\mathcal{Q}(\boldsymbol{\mu})$ (recall Definition 6.17) sampled under $\mathbb{P}_{\mathfrak{fG}}^\sigma$ of Definition 6.19 and the $(M + N)$ -tuple $\mathcal{D}(\mathcal{E}) \cup \overline{\mathcal{C}}(\mathcal{E})$ sampled under $\mathbb{P}_{\text{FV}}^\sigma$ of Definition 6.22. We omit its proof, which is very similar to that of Proposition 3.7 (with the few necessary modifications already explained in the proof outline of Lemma 6.16).

Proposition 6.23. Let $\mathcal{Q} = (\boldsymbol{\Omega}(1), \boldsymbol{\Omega}(2), \dots, \boldsymbol{\Omega}(M + N))$ denote an $(M + N)$ -tuple of elements in $\mathbb{Z}_{\geq 0}^n$, and define the M -tuple $\mathcal{C} = (\boldsymbol{\Omega}(M + N), \boldsymbol{\Omega}(M + N - 1), \dots, \boldsymbol{\Omega}(N + 1))$ and N -tuple $\mathcal{D} = (\boldsymbol{\Omega}(1), \boldsymbol{\Omega}(2), \dots, \boldsymbol{\Omega}(N))$. Then,

$$(6.13) \quad \mathbb{P}_{\text{FV}}^\sigma \left[\{\mathcal{C}(\mathcal{E}) = \mathcal{C}\} \cap \{\mathcal{D}(\mathcal{E}) = \mathcal{D}\} \right] = \mathbb{P}_{\mathfrak{fG}}^\sigma [\mathcal{Q}(\boldsymbol{\mu}) = \mathcal{Q}].$$

Here, on the left side of (6.13), the colored fused path ensemble \mathcal{E} is sampled under the colored stochastic fused vertex measure $\mathbb{P}_{\text{FV}; \mathbf{x}; \mathbf{y}; \mathbf{r}; \mathbf{t}}^\sigma$. On the right side of (6.13), the $(M; \sigma; \mathbf{R})$ -ascending sequence $\boldsymbol{\mu}$ of colored compositions is sampled under the measure $\mathbb{P}_{\mathfrak{fG}; n; s; \mathbf{x}; \mathbf{y}; \mathbf{r}; \mathbf{t}}^\sigma$.

The following corollary of Proposition 6.23 equates the joint law of the height functions (recall Section 2.2) evaluated along the exit sites of an $M \times N$ rectangle, sampled under the colored stochastic fused vertex model, with the joint law of the number of zero entries in a family $\boldsymbol{\mu}$ of n -compositions, sampled under the $\mathbb{P}_{\mathfrak{fG}}^\sigma$ measure. We omit its proof, which given Proposition 6.23 is entirely analogous to that of Corollary 3.8 given Proposition 3.7.

Corollary 6.24. *The joint law of all the height functions*

$$(6.14) \quad \bigcup_{c=1}^n (\mathfrak{h}_{\geq c}^{\rightarrow}(M, 1), \mathfrak{h}_{\geq c}^{\rightarrow}(M, 2), \dots, \mathfrak{h}_{\geq c}^{\rightarrow}(M, N), \mathfrak{h}_{\geq c}^{\rightarrow}(M-1, N), \dots, \mathfrak{h}_{\geq c}^{\rightarrow}(0, N)),$$

is equal to the joint law of all zero-entry counts

$$(6.15) \quad \bigcup_{c=1}^n (\mathfrak{m}_0^{\geq c}(\mu(1)), \mathfrak{m}_0^{\geq c}(\mu(2)), \dots, \mathfrak{m}_0^{\geq c}(\mu(N)), \mathfrak{m}_0^{\geq c}(\mu(N+1)), \dots, \mathfrak{m}_0^{\geq c}(\mu(M+N))).$$

Here, the height functions in (6.14) are associated with a colored fused path ensemble sampled under $\mathbb{P}_{\mathbb{FV}; \mathbf{x}; \mathbf{y}; \mathbf{r}; \mathbf{t}}^{\sigma}$, and the zero-entry counts in (6.15) are associated with a $(M; \sigma; \mathbf{R})$ -ascending sequence of n -compositions $\boldsymbol{\mu} = (\mu(0), \mu(1), \dots, \mu(M+N))$ sampled under $\mathbb{P}_{\mathbb{FG}; n; \mathbf{s}; \mathbf{x}; \mathbf{y}; \mathbf{r}; \mathbf{t}}^{\sigma}$.

7. COLORED LINE ENSEMBLES FOR FUSED VERTEX MODELS

This section may be viewed as the fused counterpart of Section 4, in which we describe the colored line ensembles associated with fused stochastic vertex models. Unlike in Section 4.1, the line ensembles we obtain will no longer be simple, which is a manifestation of the fact that horizontal edges in the associated stochastic fused vertex model can accommodate more than one arrow. Outside of this difference, the content in this section will closely follow that in Section 4. Throughout this section, we fix integers $n, M, N \geq 1$; a complex number $s \in \mathbb{C}$; a sequence of positive integers $\mathbf{R} = (R_1, R_2, \dots, R_N)$; sequences of complex numbers $\mathbf{r} = (r_1, r_2, \dots, r_N)$, $\mathbf{t} = (t_1, t_2, \dots, t_M)$, $\mathbf{x} = (x_1, x_2, \dots, x_N)$ and $\mathbf{y} = (y_1, y_2, \dots, y_M)$, satisfying (6.8) and $r_j = q^{-R_j/2}$ for each $j \in \llbracket 1, N \rrbracket$; a composition $\boldsymbol{\ell} = (\ell_1, \ell_2, \dots, \ell_n)$ of $R_{\llbracket 1, N \rrbracket}$; and a function $\sigma : \llbracket 1, N \rrbracket \rightarrow \llbracket 1, n \rrbracket$, such that $\ell_i = \sum_{j \in \sigma^{-1}(i)} R_j$ for each $i \in \llbracket 1, n \rrbracket$.

7.1. Fused Colored Line Ensembles and Ascending Sequences. In this section, given an $(M; \sigma; \mathbf{R})$ -ascending sequence $\boldsymbol{\mu}$ of n -compositions, we associate a colored line ensemble (which, unlike in Definition 4.1 and Lemma 4.3, need not be simple). This is done through the following definition (where in the below we recall the notion of a colored line ensemble from Definition 1.4).

Definition 7.1. Let $\boldsymbol{\mu} = (\mu(0), \mu(1), \dots, \mu(M+N))$ denote an $(M; \sigma; \mathbf{R})$ -ascending sequence of n -compositions. The associated colored line ensemble $\mathbb{L} = \mathbb{L}_{\boldsymbol{\mu}} = (\mathbb{L}^{(1)}, \mathbb{L}^{(2)}, \dots, \mathbb{L}^{(n)})$ on $\llbracket 0, M+N \rrbracket$ is defined as follows. For each $c \in \llbracket 1, n \rrbracket$ let $\mathbb{L}^{(c)} = \mathbb{L}_{\boldsymbol{\mu}}^{(c)} = (\mathbb{L}_1^{(c)}, \mathbb{L}_2^{(c)}, \dots)$, where for each $k \geq 1$ the function $\mathbb{L}_k^{(c)} = \mathbb{L}_{k; \boldsymbol{\mu}}^{(c)} : \llbracket 0, M+N \rrbracket \rightarrow \mathbb{Z}$ is prescribed by setting

$$(7.1) \quad \mathbb{L}_k^{(c)}(i) = \ell_{[c, n]} - \mathfrak{m}_{\leq k-1}^{\geq c}(\mu(i)), \quad \text{for each } i \in \llbracket 0, M+N \rrbracket.$$

The fact that this defines a colored line ensemble follows from Lemma 7.2 below. We moreover set the differences $\Lambda^{(c)} = (\Lambda_1^{(c)}, \Lambda_2^{(c)}, \dots)$ of \mathbb{L} by $\Lambda_k^{(c)}(i) = \mathbb{L}_k^{(c)}(i) - \mathbb{L}_k^{(c+1)}(i)$, for each $(c, k, i) \in \llbracket 1, n \rrbracket \times \mathbb{Z}_{>0} \times \llbracket 0, M+N \rrbracket$, where $\mathbb{L}_k^{(n+1)} : \llbracket 0, M+N \rrbracket \rightarrow \mathbb{Z}$ is defined by setting $\mathbb{L}_k^{(n+1)}(i) = 0$ for each $(k, i) \in \mathbb{Z}_{>0} \times \llbracket 0, M+N \rrbracket$.

Lemma 7.2. *Adopting the notation and assumptions of Definition 7.1, $\mathbb{L}_{\boldsymbol{\mu}}$ is a colored line ensemble, which satisfies the following three properties for any $c \in \llbracket 1, n \rrbracket$, $k \in \mathbb{Z}_{>0}$, and $i \in \llbracket 0, M+N \rrbracket$.*

- (1) *We have $\mathbb{L}_1^{(c)}(i) \geq \mathbb{L}_2^{(c)}(i) \geq \dots$ and $\mathbb{L}_k^{(1)}(i) \geq \mathbb{L}_k^{(2)}(i) \geq \dots$.*
- (2) *We have $\Lambda_k^{(c)}(i) - \Lambda_{k+1}^{(c)}(i) = \mathfrak{m}_k(\mu^{(c)}(i))$.*
- (3) *If $i \geq 1$, we have $\Lambda_k^{(c)}(i-1) - \Lambda_k^{(c)}(i) = \Omega_c^{\boldsymbol{\mu}}(k, i)$.*

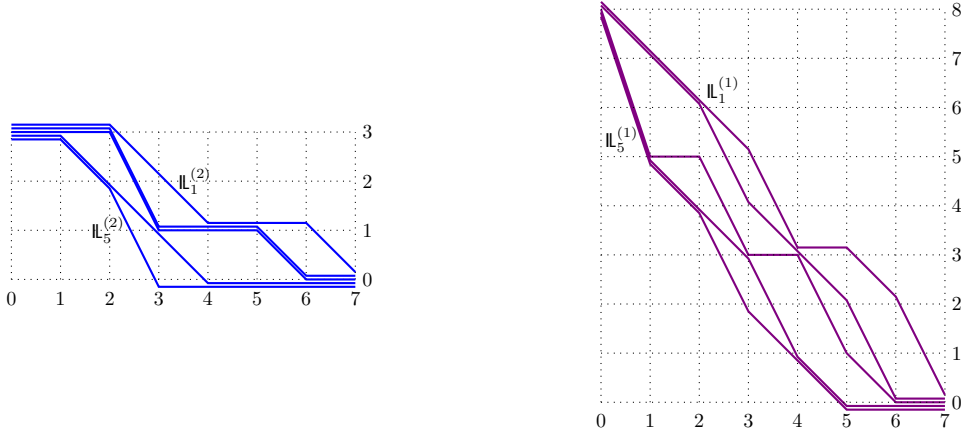


FIGURE 21. Depicted above are the top five lines (of each color) of the colored line ensemble associated with the fused path ensemble in Figure 20.

Proof. The proofs of the first two parts of the lemma are very similar to those of Lemma 4.3 and are therefore omitted. The third follows from the fact that

$$\begin{aligned}
 \Lambda_k^{(c)}(i-1) - \Lambda_k^{(c)}(i) &= (\mathbb{L}_k^{(c)}(i-1) - \mathbb{L}_k^{(c)}(i)) - (\mathbb{L}_k^{(c+1)}(i-1) - \mathbb{L}_k^{(c+1)}(i)) \\
 &= \mathbf{m}_{\leq k-1}^{\geq c}(\mu(i)) - \mathbf{m}_{\leq k-1}^{\geq c}(\mu(i-1)) - \left(\mathbf{m}_{\leq k-1}^{\geq c+1}(\mu(i)) - \mathbf{m}_{\leq k-1}^{\geq c+1}(\mu(i-1)) \right) \\
 &= \mathbf{m}_{\leq k-1}(\mu^{(c)}(i)) - \mathbf{m}_{\leq k-1}(\mu^{(c)}(i-1)) \\
 &= \mathfrak{Q}_{[c,n]}^{\mu}(k,i) - \mathfrak{Q}_{[c+1,n]}^{\mu}(k,i) = \mathfrak{Q}_c^{\mu}(k,i) \geq 0,
 \end{aligned}$$

where in the first statement we used the definition of $\Lambda^{(c)}$ from Definition 7.1; in the second we used (7.1); in the third we used the definition of \mathbf{m} ; and in the fourth we used (6.10). The second and third statements of the lemma together imply that each $\Lambda^{(c)}$ is a line ensemble, and thus \mathbb{L}_{μ} is a colored line ensemble by Definition 1.4. \square

Remark 7.3. As in Remark 6.18, we may interpret μ as associated with a colored fused path ensemble $\mathcal{E}_{\mu} \in \mathfrak{P}_{\mathfrak{fG}}(M; \sigma; \mathbf{R})$ on $\mathbb{Z}_{\leq 0} \times \llbracket 1, M+N \rrbracket$. Then $\mathbb{L}_k^{(c)}(i) = \mathfrak{h}_{\geq c}^{\leftarrow}(-k, i)$, where the height function $\mathfrak{h}_{\geq c}^{\leftarrow}$ is with respect to \mathcal{E}_{μ} ; stated alternatively, $\mathbb{L}_k^{(c)}(i)$ denotes the number of arrows with color at least c that horizontally exit the column $\{x = -k\}$ strictly above the vertex $(-k, i)$. See Figure 21 for a depiction of the colored line ensemble in the example at the end of Remark 6.18 (and shown in Figure 20).

By Lemma 7.2, Definition 7.1 associates a colored line ensemble to a given $(M; \sigma; \mathbf{R})$ -ascending sequence of n -compositions. Since the former are in bijection with colored higher spin path ensembles in $\mathfrak{P}_{\mathfrak{fG}}(M; \sigma; \mathbf{R})$ by Remark 6.18, this associates a colored line ensemble with any element of $\mathfrak{P}_{\mathfrak{fG}}(M; \sigma; \mathbf{R})$. The following definition is towards the reverse direction; it associates a colored fused path ensemble with a colored line ensemble \mathbb{L} .

Definition 7.4. Fix a colored line ensemble $\mathbb{L} = (\mathbb{L}^{(1)}, \mathbb{L}^{(2)}, \dots, \mathbb{L}^{(n)})$, and for each $c \in \llbracket 1, n \rrbracket$ denote $\mathbb{L}^{(c)} = (\mathbb{L}_1^{(c)}, \mathbb{L}_2^{(c)}, \dots)$. For any $v = (-k, i) \in \mathbb{Z}_{\leq 0} \times \llbracket 1, M+N \rrbracket$, define the arrow configuration

$(\mathbf{A}^{\mathbb{L}}(v), \mathbf{B}^{\mathbb{L}}(v); \mathbf{C}^{\mathbb{L}}(v), \mathbf{D}^{\mathbb{L}}(v))$ as follows. For each $c \in \llbracket 1, n \rrbracket$ and set

$$\begin{aligned} A_c^{\mathbb{L}}(v) &= \Lambda_k^{(c)}(i-1) - \Lambda_{k+1}^{(c)}(i-1) = \mathbb{L}_k^{(c)}(i-1) - \mathbb{L}_{k+1}^{(c)}(i-1) - (\mathbb{L}_k^{(c+1)}(i-1) - \mathbb{L}_{k+1}^{(c+1)}(i-1)); \\ B_c^{\mathbb{L}}(v) &= \Lambda_{k+1}^{(c)}(i-1) - \Lambda_{k+1}^{(c)}(i) = \mathbb{L}_{k+1}^{(c)}(i-1) - \mathbb{L}_{k+1}^{(c)}(i) - (\mathbb{L}_{k+1}^{(c+1)}(i-1) - \mathbb{L}_{k+1}^{(c+1)}(i)); \\ C_c^{\mathbb{L}}(v) &= \Lambda_k^{(c)}(i) - \Lambda_{k+1}^{(c)}(i) = \mathbb{L}_k^{(c)}(i) - \mathbb{L}_{k+1}^{(c)}(i) - (\mathbb{L}_k^{(c+1)}(i) - \mathbb{L}_{k+1}^{(c+1)}(i)); \\ D_c^{\mathbb{L}}(v) &= \Lambda_k^{(c)}(i-1) - \Lambda_k^{(c)}(i) = \mathbb{L}_k^{(c)}(i-1) - \mathbb{L}_k^{(c)}(i) - (\mathbb{L}_k^{(c+1)}(i-1) - \mathbb{L}_k^{(c+1)}(i)), \end{aligned}$$

where we observe that all four quantities are nonnegative since $\Lambda^{(c)}$ is a line ensemble. This assignment of arrow configurations is consistent and therefore defines a colored fused path ensemble $\mathcal{E}^{\mathbb{L}}$ associated with the colored line ensemble \mathbb{L} .

The following lemma indicates that the associations from Definition 7.1 and Definition 7.4 are compatible; we omit its proof, which is a quick verification using the second and third properties of Lemma 7.2.

Lemma 7.5. *If $\mathcal{E}^{\mathbb{L}} = \mathcal{E}_{\mu}$ for some $(M; \sigma; \mathbf{R})$ -ascending sequence μ of n -compositions, then \mathbb{L} is associated with μ in the sense of Definition 7.1.*

7.2. Properties of Random Fused Colored Line Ensembles. In this section we discuss some properties of colored line ensembles \mathbb{L}_{μ} associated (recall Definition 7.1) with an $(M; \sigma; \mathbf{R})$ -ascending sequence μ of n -compositions sampled from the measure $\mathbb{P}_{\mathbb{F}\mathbb{G}}^{\sigma}$ (recall Definition 6.19). Let us first give notation to this law on colored line ensembles.

Definition 7.6. Let $\mathbb{P}_{\text{cL}}^{\sigma} = \mathbb{P}_{\text{cL}; n; s; \mathbf{x}; \mathbf{y}; \mathbf{r}; \mathbf{t}}^{\sigma}$ denote the law of a colored line ensemble \mathbb{L}_{μ} associated with a random $(M; \sigma; \mathbf{R})$ -ascending sequence μ of n -compositions (as in Definition 7.1) sampled from the measure $\mathbb{P}_{\mathbb{F}\mathbb{G}; n; s; \mathbf{x}; \mathbf{y}; \mathbf{r}; \mathbf{t}}^{\sigma}$.

The following result, which is a quick consequence of Corollary 6.24, provides under this setup a matching in law between the top curves of \mathbb{L} (under $\mathbb{P}_{\text{cL}}^{\sigma}$) and the height functions for a colored stochastic fused vertex model (recall Definition 6.22).

Theorem 7.7. *Sample a colored line ensemble \mathbb{L} on $\llbracket 0, M+N \rrbracket$ from the measure $\mathbb{P}_{\text{cL}; n; s; \mathbf{x}; \mathbf{y}; \mathbf{r}; \mathbf{t}}^{\sigma}$ and sample a random colored fused path ensemble \mathcal{E} under $\mathbb{P}_{\mathbb{F}\mathbb{V}; \mathbf{x}; \mathbf{y}; \mathbf{r}; \mathbf{t}}^{\sigma}$. For each $c \in \llbracket 1, n \rrbracket$, define the function $H_c : \llbracket 0, M+N \rrbracket \rightarrow \mathbb{Z}$ by setting*

$$H_c(k) = \mathfrak{h}_{\geq c}^{\leftarrow}(M, k), \quad \text{if } k \in \llbracket 0, N \rrbracket; \quad H_c(k) = \mathfrak{h}_{\geq c}^{\leftarrow}(M+N-k, N), \quad \text{if } k \in \llbracket N, M+N \rrbracket,$$

where $\mathfrak{h}_{\geq c}^{\leftarrow}$ is the height function associated with \mathcal{E} . Then, the joint law of $(\mathbb{L}_1^{(1)}, \mathbb{L}_1^{(2)}, \dots, \mathbb{L}_1^{(n)})$ is the same as that of (H_1, H_2, \dots, H_n) .

Proof. Since $\mathfrak{h}_{\geq c}^{\leftarrow}(i, j) = \ell_{[c, n]} - \mathfrak{h}_{\geq c}^{\rightarrow}(i, j)$ holds for any integer $c \in \llbracket 1, n \rrbracket$ and vertex $(i, j) \in \{(M, 0), (M, 1), \dots, (M, N), (M, N-1), \dots, (0, N)\}$ along the northeast boundary of $\llbracket 0, M \rrbracket \times \llbracket 0, N \rrbracket$, this theorem follows from Definition 7.1 and Corollary 6.24. \square

The next theorem explains the effect of conditioning on some of the curves in \mathbb{L} (the Gibbs property), if μ is sampled under the $\mathbb{P}_{\text{cL}}^{\sigma}$ measure, which is given by the following theorem; its proof is omitted, as it is very similar to that of Theorem 4.8. Below, we recall the vertex weights $W_{x; r, s}$ from Definition 6.3; the association of a colored line ensemble with an ascending sequence of n -compositions from Definition 7.1; and the notation from Definition 7.4.

Theorem 7.8. *Sample $\mathbb{L} = \mathbb{L}_\mu$ under $\mathbb{P}_{\text{cL};n;s;\mathbf{x};\mathbf{y};\mathbf{r};\mathbf{t}}^\sigma$. Fix integers $j > i \geq 0$ and $u, v \in \llbracket 0, M+N \rrbracket$ with $u < v$; set $i_0 = \max\{i, 1\}$; and condition on the curves $\mathbb{L}_k^{(c)}(m)$ for all $c \in \llbracket 1, n \rrbracket$ and $(k, m) \in (\mathbb{Z}_{>0} \times \llbracket 0, M+N \rrbracket) \setminus (\llbracket i+1, j \rrbracket \times \llbracket u, v-1 \rrbracket)$. For any colored line ensemble \mathbb{I} that is $\llbracket i+1, j \rrbracket \times \llbracket u, v-1 \rrbracket$ -compatible with \mathbb{L} , we have*

$$(7.2) \quad \mathbb{P}[\mathbb{L} = \mathbb{I}] = \mathcal{Z}^{-1} \cdot \prod_{k=i_0}^j \prod_{\substack{m \in \llbracket u, v \rrbracket \\ m \leq N}} W_{x_m; r_m, s}(\mathbf{A}^l(-k, m), \mathbf{B}^l(-k, m); \mathbf{C}^l(-k, m), \mathbf{D}^l(-k, m)) \\ \times \prod_{k=i_0}^j \prod_{\substack{m \in \llbracket u, v \rrbracket \\ m > N}} W_{y_{m-N}; t_{m-N}, s}(\mathbf{A}^l(-k, m), \mathbf{B}^l(-k, m); \mathbf{C}^l(-k, m), \mathbf{D}^l(-k, m)).$$

Here, the probability on the left side of (7.2) is with respect to the conditional law of \mathbb{L} . Moreover, \mathcal{Z} is a normalizing constant defined so that the sum of the right side of (7.2), over all colored line ensembles \mathbb{I} that are $\llbracket i+1, j \rrbracket \times \llbracket u, v-1 \rrbracket$ -compatible with \mathbb{L}_μ , is equal to 1.

Let us also describe color merging properties for line ensembles sampled according to $\mathbb{P}_{\text{cL}}^\sigma$, which will be parallel to those discussed in Section 4.3. To that end, we have the following proposition generalizing Proposition 4.11, where below we recall the definition of ϑ from (4.10) (as a function on Comp_n), (4.11) (as a functional on the set of functions $\varsigma : \llbracket 1, N \rrbracket \rightarrow \llbracket 1, n \rrbracket$), and (4.12) (as a function on sequences of n -compositions); we also recall that $\check{\sigma} = \vartheta(\sigma)$ from (4.11).

Proposition 7.9. *Sample $\mathbb{L} = (\mathbb{L}^{(1)}, \mathbb{L}^{(2)}, \dots, \mathbb{L}^{(n)})$ under $\mathbb{P}_{\text{cL};n;s;\mathbf{x};\mathbf{y};\mathbf{r};\mathbf{t}}^\sigma$. Then the joint law of the colored line ensemble $\check{\mathbb{L}} = (\mathbb{L}^{(1)}, \mathbb{L}^{(3)}, \mathbb{L}^{(4)}, \dots, \mathbb{L}^{(n)})$ (with $n-1$ colors) is given by $\mathbb{P}_{\text{cL};n-1;s;\mathbf{x};\mathbf{y};\mathbf{r};\mathbf{t}}^{\check{\sigma}}$.*

To establish Proposition 7.9, we require the following lemma that is parallel to Lemma 4.9.

Lemma 7.10. *Fix an integer $k \geq 1$; $(n-1)$ -compositions $\check{\mu}, \check{\nu}, \check{\kappa} \in \text{Comp}_{n-1}$; and n -compositions $\kappa, \mu \in \text{Comp}_n$, such that $\vartheta(\kappa) = \check{\kappa}$ and $\vartheta(\mu) = \check{\mu}$. We have*

$$(7.3) \quad \sum_{\substack{\varsigma: \llbracket 1, N \rrbracket \rightarrow \llbracket 1, n \rrbracket \\ \vartheta(\varsigma) = \check{\sigma}}} \sum_{\substack{\nu \in \text{Comp}_n \\ \vartheta(\nu) = \check{\nu}}} \mathbb{f}_{\mu/\nu; s}^\varsigma(\mathbf{x}; \mathbf{r}) = \mathbb{f}_{\check{\mu}/\check{\nu}; s}^{\check{\sigma}}(\mathbf{x}; \mathbf{r}); \quad \sum_{\substack{\nu \in \text{Comp}_n \\ \vartheta(\nu) = \check{\nu}}} \mathbb{G}_{\nu/\kappa; s}(\mathbf{y}; \mathbf{t}) = \mathbb{G}_{\check{\nu}/\check{\kappa}; s}(\mathbf{y}; \mathbf{t}).$$

Proof. Combining Lemma 4.9 with Lemma 6.13 yields the first statement of (7.3), as well as the second one if $t_i^2 \in q^{\mathbb{Z}_{<0}}$ for each $i \in \llbracket 1, M \rrbracket$. The fact that the second statement in (7.3) holds for arbitrary \mathbf{t} then follows from uniqueness of analytic continuation, as \mathbb{G} is rational in \mathbf{t} (since the W -weights of Definition 6.3 are). \square

The next lemma is parallel to Lemma 4.10. Its proof given Lemma 7.10 is entirely analogous to that of Lemma 4.10 given Lemma 4.9 and is therefore omitted.

Lemma 7.11. *If an $(M; \sigma; \mathbf{R})$ -ascending sequence of n -compositions μ is sampled from $\mathbb{P}_{\mathbf{fG};n;s;\mathbf{x};\mathbf{y}}^\sigma$, then the $(M; \check{\sigma})$ -ascending sequence $\vartheta(\mu)$ of $(n-1)$ -compositions has law $\mathbb{P}_{\mathbf{fG};n-1;s;\mathbf{x};\mathbf{y}}^{\check{\sigma}}$.*

Now we can establish Proposition 7.9.

Proof of Proposition 7.9. Sample μ under $\mathbb{P}_{\mathbf{fG};n;s;\mathbf{x};\mathbf{y};\mathbf{r};\mathbf{t}}^\sigma$ (recall Definition 6.19). By Definition 7.6, we may identify \mathbb{L} as the colored line ensemble \mathbb{L}_μ associated with μ . By Definition 7.1, the $n-1$ line ensembles $\check{\mathbb{L}} = (\mathbb{L}^{(1)}, \mathbb{L}^{(3)}, \dots, \mathbb{L}^{(n)})$ in $\mathbb{L} = \mathbb{L}_\mu$ constitute the colored line ensemble associated with $\vartheta(\mu)$, which has law $\mathbb{P}_{\mathbf{fG};n-1;s;\mathbf{x};\mathbf{y};\mathbf{r};\mathbf{t}}^{\check{\sigma}}$ by Lemma 7.11. Hence, again by Definition 7.6, $\check{\mathbb{L}}$ has law $\mathbb{P}_{\text{cL};n-1;s;\mathbf{x};\mathbf{y};\mathbf{r};\mathbf{t}}^{\check{\sigma}}$, thereby establishing the proposition. \square

$1 \leq i \leq n$			$1 \leq i < j \leq n$		
$(\mathbf{A}, 0; \mathbf{A}, 0)$	$(\mathbf{A}, 0; \mathbf{A}_i^-, i)$	$(\mathbf{A}, i; \mathbf{A}_j^+, 0)$	$(\mathbf{A}, i; \mathbf{A}_{ij}^{+-}, j)$	$(\mathbf{A}, j; \mathbf{A}_{ji}^{-+}, i)$	$(\mathbf{A}, i; \mathbf{A}, i)$
$\frac{1 - s^2 x q^{A_{[1,n]}}}{1 - s^2 x}$	$\frac{s^2 x (q^{A_i} - 1) q^{A_{[i+1,n]}}}{1 - s^2 x}$	$\frac{1 - s^2 q^{A_{[1,n]}}}{1 - s^2 x}$	$\frac{s^2 x (q^{A_j} - 1) q^{A_{[j+1,n]}}}{1 - s^2 x}$	$\frac{s^2 (q^{A_i} - 1) q^{A_{[i+1,n]}}}{1 - s^2 x}$	$\frac{s^2 (q^{A_i} - x) q^{A_{[i+1,n]}}}{1 - s^2 x}$
$\frac{1 + \nu q^{A_{[1,n]}}}{1 + \nu}$	$\frac{\nu (1 - q^{A_i}) q^{A_{[i+1,n]}}}{1 + \nu}$	$\frac{1 + \nu q^{A_{[1,n]}}}{1 + \nu}$	$\frac{\nu (1 - q^{A_j}) q^{A_{[j+1,n]}}}{1 + \nu}$	$\frac{\nu (1 - q^{A_i}) q^{A_{[i+1,n]}}}{1 + \nu}$	$\frac{\nu (1 - q^{A_i}) q^{A_{[i+1,n]}}}{1 + \nu}$

FIGURE 22. Depicted in the second to last row are the weights for the colored stochastic higher spin vertex model, and depicted in the last row are those for the discrete time q -boson model.

Remark 7.12. The above discussion describes the merging of colors 1 and 2. As in Remark 4.12, it is more generally possible to merge several (disjoint) intervals of colors, which would correspond in Proposition 7.9 to omitting line ensembles $\mathbb{L}^{(i)}$, for $i \in \llbracket 2, n \rrbracket$ arbitrary (depending on the corresponding merged color intervals), in \mathbb{L} .

8. LINE ENSEMBLES FOR DISCRETE TIME q -BOSON MODELS

In this section we specialize the results of Section 7 to the discrete time q -boson model, which involves setting each R_j there equal to 1. Throughout this section, we adopt the notation of Section 7 (where here we do not necessarily assume that (6.8) holds), and set $R_j = 1$ for all $j \in \llbracket 1, n \rrbracket$, so that each $r_j = q^{-1/2}$.

8.1. Colored Stochastic Higher Spin Vertex and q -Boson Models. In this section we describe the $R = 1$ case of the stochastic fused vertex models from Section 6.1. Recall that we have set each $R_j = 1$, and thus each $r_j = q^{-1/2}$.

Under this specialization, it is quickly verified that the $U_{z; q^{-1/2}, s}$ -weights (recall Definition 6.1) permit at most one arrow along any horizontal edge, that is, $U_{z; q^{-1/2}, s}(\mathbf{A}, \mathbf{B}; \mathbf{C}, \mathbf{D}) = 0$ unless there exist indices $b, d \in \llbracket 0, n \rrbracket$ such that $\mathbf{B} = \mathbf{e}_b$ and $\mathbf{D} = \mathbf{e}_d$. Therefore, the associated colored stochastic fused vertex model (recall Section 6.1) is called the *colored stochastic higher spin vertex model*; it originally appeared in [63, Appendix A]. For any $\mathbf{A}, \mathbf{C} \in \mathbb{Z}_{\geq 0}^n$ and $b, d \in \llbracket 0, n \rrbracket$, we denote these specialized stochastic weights by

$$U_{z; s}^{\text{hs}}(\mathbf{A}, b; \mathbf{C}, d) = U_{z; q^{-1/2}, s}(\mathbf{A}, \mathbf{e}_b; \mathbf{C}, \mathbf{e}_d).$$

These weights are depicted in the second to last row of Figure 22. We also denote the associated probability measure on path ensembles (recall Definition 6.22) by $\mathbb{P}_{\text{hs}; \mathbf{x}; \mathbf{y}; \mathbf{t}}^\sigma = \mathbb{P}_{\text{hs}; \mathbf{x}; \mathbf{y}; q^{-1/2}; \mathbf{t}}^\sigma$.

Given an M -tuple of positive parameters $\boldsymbol{\nu} = (\nu_1, \nu_2, \dots, \nu_M)$, the (Bernoulli) *discrete time q -boson model* is the special case of the colored stochastic higher spin vertex model when

$$(8.1) \quad x_j y_i^{-1} = 1, \quad \text{and} \quad \nu_i = -t_i^2, \quad \text{for each } (i, j) \in \llbracket 1, M \rrbracket \times \llbracket 1, N \rrbracket.$$

We denote the associated stochastic weights

$$U_\nu^{\text{dqb}}(\mathbf{A}, b; \mathbf{C}, d) = U_{1; \sqrt{-\nu}}^{\text{hs}}(\mathbf{A}, b; \mathbf{C}, d),$$

which satisfy

$$U_\nu^{\text{dqb}}(\mathbf{A}, i; \mathbf{A}_i^+, 0) = \frac{1 + \nu q^{A_{[1, n]}}}{1 + \nu}, \quad \text{and} \quad U_\nu^{\text{dqb}}(\mathbf{A}, i; \mathbf{A}_{ij}^{+-}, j) = \frac{\nu}{1 + \nu} \cdot (1 - q^{A_i}) q^{A_{[i+1, n]}}$$

for any $i, j \in \llbracket 0, n \rrbracket$ and $\mathbf{A} \in \mathbb{Z}_{\geq 0}^n$; see the last row of Figure 22. The colorless ($n = 1$) case of this model was introduced in [17, Definition 1.6]. We denote the associated probability measure by $\mathbb{P}_{\text{dqb}; \nu}^\sigma$ (which is the specialization of $\mathbb{P}_{\text{hs}; \mathbf{x}; \mathbf{t}}^\sigma$ under (8.1)).

Remark 8.1. Fix positive parameters $\boldsymbol{\alpha} = (\alpha_1, \alpha_2, \dots)$. Suppose we consider the discrete time q -boson model, set $\nu_j = \varepsilon \alpha_j$ for each $j \in \llbracket 1, M \rrbracket$, scale N by ε^{-1} , let M tend to ∞ , and let ε tend to 0. This gives rise to a continuous-time Markov process on $\mathbb{Z}_{>0}$, in which a particle of color $c \in \llbracket 1, n \rrbracket$ at site $k \in \mathbb{Z}_{>0}$ jumps to the right according to an exponential clock of rate $\alpha_k q^{A_{[i+1, n]}(k)} (1 - q^{A_i(k)})$, where $A_j(k)$ denotes the number of particles of color j at site k ; see [25, Proposition 12.4.1]. This model is called the *colored q -boson model* or the *colored q -deformed totally asymmetric zero range process* (TAZRP). The colorless ($n = 1$) case of this model was introduced in [80, Equation (2.6)], which under a change of variables is equivalent to the q -TASEP introduced in [16, Definition 3.3.7].

8.2. q -Hahn Weights. We eventually seek to degenerate Theorem 7.8 to the ($R = 1$) colored stochastic higher spin vertex model case. Recall that this result involves the W -weights from (6.2) with an arbitrary choice of the parameter s , which are in general a bit intricate. So, in this section we discuss a specific choice for s that simplifies these weights considerably.¹⁶ This corresponds to setting $s = x$, a special case that has appeared numerous times in the prior literature [14, 24, 63] and is sometimes known as the q -Hahn specialization; it is given as the below lemma.

Lemma 8.2. *Adopting the notation of Definition 6.3, we have for any $s, t \in \mathbb{C}$ that*

$$\begin{aligned} W_{s; t, s}(\mathbf{A}, \mathbf{B}; \mathbf{C}, \mathbf{D}) &= (-st^{-2})^d q^{\varphi(\mathbf{D}, \mathbf{A} - \mathbf{D})} \cdot \frac{(t^{-2}s^2; q)_{a-d} (t^2; q)_d}{(s^2; q)_a} \cdot \prod_{i=1}^n \frac{(q; q)_{A_i}}{(q; q)_{A_i - D_i} (q; q)_{D_i}} \\ &\quad \times \mathbb{1}_{\mathbf{A} + \mathbf{B} = \mathbf{C} + \mathbf{D}} \cdot \mathbb{1}_{\mathbf{A} \geq \mathbf{D}}. \end{aligned}$$

Proof. We assume throughout this proof that $\mathbf{A} + \mathbf{B} = \mathbf{C} + \mathbf{D}$, as otherwise $W_{s; t, s}(\mathbf{A}, \mathbf{B}; \mathbf{C}, \mathbf{D}) = 0$ by Definition 6.3. Due to the factor of $(s^{-1}x; q)_{b-p}$ in (6.2), any nonzero summand on the right side of (6.2) must at $x = s$ satisfy $p = b$. Together with the fact that $\mathbf{P} \leq \mathbf{B}$ in this sum, it follows that the only nonzero summand is given by $\mathbf{P} = \mathbf{B}$; in particular (since $\mathbf{P} \leq \mathbf{C}$), we must have $\mathbf{B} \leq \mathbf{C}$ for $W_{s; t, s}(\mathbf{A}, \mathbf{B}; \mathbf{C}, \mathbf{D})$ to be nonzero. We assume this in what follows, meaning (as $\mathbf{A} + \mathbf{B} = \mathbf{C} + \mathbf{D}$) that $\mathbf{A} \geq \mathbf{D}$. Then, (6.2) yields

$$\begin{aligned} W_{s; t, s}(\mathbf{A}, \mathbf{B}; \mathbf{C}, \mathbf{D}) &= (-1)^d s^d t^{2(c-a)} q^{\varphi(\mathbf{D}, \mathbf{C})} \frac{(t^2; q)_d}{(t^2; q)_b} \cdot t^{-2b} \frac{(t^{-2}s^2; q)_{c-b} (t^2; q)_b}{(s^2; q)_{c+d-b}} \\ &\quad \times q^{-\varphi(\mathbf{D}, \mathbf{B})} \prod_{i=1}^n \frac{(q; q)_{C_i + D_i - B_i}}{(q; q)_{D_i} (q; q)_{C_i - B_i}}. \end{aligned}$$

This, together with the fact that $\mathbf{A} + \mathbf{B} = \mathbf{C} + \mathbf{D}$ (and hence $a + b = c + d$) yields the lemma. \square

¹⁶This is a colored generalization of what was done in [27, Section 7.3], where a similar idea was implemented to match the height function of the uncolored stochastic higher spin vertex model with the length of a partition sampled under the spin Hall-Littlewood / spin Whittaker measure.

Remark 8.3. Observe for any $\mu, \kappa \in \text{Comp}_n$ that, if $y_i = s$ for each $i \in \llbracket 1, n \rrbracket$, then $\mathbb{G}_{\mu/\kappa; s}(\mathbf{y}; \mathbf{t})$ (from Definition 6.11) is nonzero only if $\max \mu - \max \kappa \leq n$. Indeed, if $\max \mu \geq \max \kappa + n + 1$, then any fused path ensemble $\mathcal{E} \in \mathfrak{P}_{\mathbb{G}}(\mu/\kappa)$ must have at least one arrow configuration $(\mathbf{A}, \mathbf{B}; \mathbf{C}, \mathbf{D})$ that does not satisfy $\mathbf{B} \leq \mathbf{C}$ (equivalently, that does not satisfy $\mathbf{D} \geq \mathbf{A}$). Hence, Lemma 8.2 implies that $W_{\mathbf{y}; \mathbf{t}, s}(\mathcal{E}) = 0$ for each $\mathcal{E} \in \mathfrak{P}_{\mathbb{G}}(\mu/\kappa)$, meaning by (6.7) that $\mathbb{G}_{\mu/\kappa; s}(\mathbf{y}; \mathbf{t}) = 0$.

Remark 8.4. By Remark 8.3, if $y_i = s$ for each $i \in \llbracket 1, M \rrbracket$, then the probability measure $P_{\text{hs}; \mathbf{x}; \mathbf{y}; \mathbf{t}}^\sigma$ from Section 8.1 (see also (6.11)) is supported on $(M; \sigma; \mathbf{R})$ -ascending sequences of n -compositions $\boldsymbol{\mu} = (\mu(0), \mu(1), \dots, \mu(M+N))$ satisfying $\max \mu(N) \leq M$. It follows that this measure is supported on only finitely many such sequences $\boldsymbol{\mu}$, and so by analytic continuation (6.11) defines a probability measure for any¹⁷ choice of the parameters \mathbf{x} and \mathbf{t} , even if (6.8) is not satisfied. In particular, the results from Section 6.6 and Section 7 continue to hold when all $y_i = s$, without assuming (6.8).

8.3. Colored Line Ensembles. In this section we establish the following proposition describing a colored line ensemble for the discrete time q -Boson model (from Section 8.1).¹⁸ In the below, we recall the notation from Definition 7.4, and we define the vertex weights (see Lemma 8.2)

$$(8.2) \quad \mathcal{W}_\nu(\mathbf{A}, \mathbf{B}; \mathbf{C}, \mathbf{D}) = q^{\varphi(\mathbf{D}, \mathbf{A}-\mathbf{D})} \nu^{-d}(-\nu; q)_d \cdot \prod_{i=1}^n \frac{(q; q)_{A_i}}{(q; q)_{A_i - D_i} (q; q)_{D_i}} \cdot \mathbb{1}_{\mathbf{A}+\mathbf{B}=\mathbf{C}+\mathbf{D}} \cdot \mathbb{1}_{\mathbf{A} \geq \mathbf{D}},$$

for any $\nu \in \mathbb{C}$ and $\mathbf{A}, \mathbf{B}, \mathbf{C}, \mathbf{D} \in \mathbb{Z}_{\geq 0}^n$, where we have set $d = |\mathbf{D}|$.

Proposition 8.5. *Fix $\boldsymbol{\nu} = (\nu_1, \nu_2, \dots, \nu_M) \in \mathbb{R}_{>0}^M$; sample a colored path ensemble \mathcal{E} on $\llbracket 1, M \rrbracket \times \llbracket 1, N \rrbracket$ according to the discrete time q -boson model $\mathbb{P}_{\text{dq}; \boldsymbol{\nu}}^\sigma$; and for each $c \in \llbracket 1, n \rrbracket$ define $H_c : \llbracket N, M+N \rrbracket \rightarrow \mathbb{Z}$ by setting $H_c(k) = \mathfrak{h}_{\geq c}^{\leftarrow}(M+N-k, N)$ for each $k \in \llbracket N, M+N \rrbracket$, where $\mathfrak{h}_{\geq c}^{\leftarrow}$ is the height function with respect to \mathcal{E} . There exists a random colored line ensemble $\mathbb{L} = (\mathbb{L}^{(1)}, \mathbb{L}^{(2)}, \dots, \mathbb{L}^{(n)})$ on $\llbracket 0, M+N \rrbracket$ satisfying the following properties.*

- (1) *The joint law of the functions $(\mathbb{L}_1^{(1)}|_{\llbracket N, M+N \rrbracket}, \mathbb{L}_1^{(2)}|_{\llbracket N, M+N \rrbracket}, \dots, \mathbb{L}_1^{(n)}|_{\llbracket N, M+N \rrbracket})$ is the same as that of (H_1, H_2, \dots, H_n) .*
- (2) *We almost surely have $\mathbf{A}^{\mathbb{L}}(-k, i) \geq \mathbf{D}^{\mathbb{L}}(-k, i)$ for each $(-k, i) \in \mathbb{Z}_{\leq 0} \times \llbracket N, M+N \rrbracket$.*
- (3) *Fix integers $j > i \geq 0$ and $u, v \in \llbracket N+1, M+N \rrbracket$ with $u < v$; set $i_0 = \max\{i, 1\}$; and condition on the curves $\mathbb{L}_k^{(c)}(m)$ for all $c \in \llbracket 1, n \rrbracket$ and $(k, m) \notin \llbracket i+1, j \rrbracket \times \llbracket u, v-1 \rrbracket$. For any colored line ensemble \mathbb{I} that is $\llbracket i+1, j \rrbracket \times \llbracket u, v-1 \rrbracket$ -compatible with \mathbb{L} , we have*

$$(8.3) \quad \mathbb{P}[\mathbb{L} = \mathbb{I}] = \mathcal{Z}^{-1} \cdot \prod_{k=i_0}^j \prod_{m=u}^v \mathcal{W}_{\nu_{m-N}}(\mathbf{A}^{\mathbb{I}}(-k, m), \mathbf{B}^{\mathbb{I}}(-k, m); \mathbf{C}^{\mathbb{I}}(-k, m), \mathbf{D}^{\mathbb{I}}(-k, m)).$$

Here, the probability on the left side of (8.3) is with respect to the conditional law of \mathbb{L} . Moreover, \mathcal{Z} is a normalizing constant defined so that the sum of the right side of (8.3), over all colored line ensembles \mathbb{I} that are $\llbracket i+1, j \rrbracket \times \llbracket u, v-1 \rrbracket$ -compatible with \mathbb{L} , is equal to 1.

¹⁷It can be verified that the quantity $\prod_{j=1}^N \mathfrak{f}_{\mu(j)/\mu(j-1); s}^{\sigma(j)}(x_j; q^{-1/2}) \cdot \prod_{i=1}^M \prod_{j=1}^N (1 - x_j s^{-1})$ appearing in the $\mathbb{R}_{j=1}$ case of (6.11) is a polynomial in \mathbf{x} whenever $\max \mu(N) \leq M$ (using the fact that $(1 - xs^{-1}) \cdot \widehat{W}_{x; q^{-1/2}, s}$ is a polynomial in x), and so this measure has no singularities in \mathbf{x} .

¹⁸Proposition 8.5 below examines this line ensemble on the interval $\llbracket N, M+N \rrbracket$, which corresponds to the behavior of the discrete time q -boson model along the north boundary of the rectangle $\llbracket 1, M \rrbracket \times \llbracket 1, N \rrbracket$. One can also formulate more general statements about this line ensemble on its full domain $\llbracket 0, M+N \rrbracket$, but we will not do so here.

Proof. Let $s > 0$ be a small real number; set $x_j = s = y_i$ for each $(i, j) \in \llbracket 1, M \rrbracket \times \llbracket 1, N \rrbracket$ (recalling that $r_j = q^{-1/2}$ for each $j \in \llbracket 1, N \rrbracket$); and set $t_i^2 = -\nu_i$ for each $i \in \llbracket 1, M \rrbracket$. Observe from (8.1) that this specialization sends the stochastic fused vertex model to the discrete time q -boson model. Sample a colored line ensemble $\mathbb{L} = (\mathbb{L}^{(1)}, \mathbb{L}^{(2)}, \dots, \mathbb{L}^{(n)})$ from the measure $\mathbb{P}_{\text{cL};n;s;\mathbf{x};\mathbf{y};\mathbf{r};\mathbf{t}}^\sigma$ (recall Definition 7.6); we will show that the proposition holds for the limit¹⁹ of \mathbb{L} , as s tends to 0.

The fact that \mathbb{L} (for any $s \geq 0$) satisfies the first statement of the proposition follows from Theorem 7.7 (and Remark 8.4, so that we need not assume that (6.8) holds). That it satisfies the second (also for any $s \geq 0$) follows from (7.2) (and Remark 8.4), together with the fact by Lemma 8.2 that for $m > N$ and $y_{m-N} = s$ we have

$$W_{y_{m-N};t_{m-N},s}(\mathbf{A}^{\mathbf{l}}(-k, m), \mathbf{B}^{\mathbf{l}}(-k, m); \mathbf{C}^{\mathbf{l}}(-k, m), \mathbf{D}^{\mathbf{l}}(-k, m)) = 0,$$

unless $\mathbf{A}^{\mathbf{l}}(-k, m) \geq \mathbf{D}^{\mathbf{l}}(-k, m)$.

To verify the third, observe by Theorem 7.8 (and Remark 8.4) that, for any $s \geq 0$,

(8.4)

$$\begin{aligned} \mathbb{P}[\mathbb{L} = \mathbf{l}] &= \mathcal{Z}_0^{-1} \cdot \prod_{k=i_0}^j \prod_{m=u}^v s^{|\mathbf{D}^{\mathbf{l}}(-k, m)|} \\ &\times \prod_{k=i_0}^j \prod_{m=u}^v s^{-|\mathbf{D}^{\mathbf{l}}(-k, m)|} \cdot W_{s;t_{m-N};s}(\mathbf{A}^{\mathbf{l}}(-k, m), \mathbf{B}^{\mathbf{l}}(-k, m); \mathbf{C}^{\mathbf{l}}(-k, m), \mathbf{D}^{\mathbf{l}}(-k, m)), \end{aligned}$$

for some normalization constant $\mathcal{Z}_0 > 0$. Next, we have

$$\sum_{m=u}^v |\mathbf{D}^{\mathbf{l}}(-k, m)| = \sum_{m=u}^v (\mathbf{l}_k^{(1)}(m-1) - \mathbf{l}_k^{(1)}(m)) = \mathbf{l}_k^{(1)}(u-1) - \mathbf{l}_k^{(1)}(v) = \mathbb{L}_k^{(1)}(u-1) - \mathbb{L}_k^{(1)}(v),$$

where the first equality holds by Definition 7.4, the second by performing the sum, and the third by the fact that \mathbf{l} is $\llbracket u, v-1 \rrbracket \times \llbracket i+1, j \rrbracket$ -compatible with \mathbb{L} . This quantity is fixed by the conditioning, so the first product on the right side of (8.4) can be incorporated into the normalization constant \mathcal{Z}_0 . This gives

$$\mathbb{P}[\mathbb{L} = \mathbf{l}] = \mathcal{Z}_1^{-1} \cdot \prod_{k=i_0}^j \prod_{m=u}^v s^{-|\mathbf{D}^{\mathbf{l}}(-k, m)|} \cdot W_{s;t_{m-N};s}(\mathbf{A}^{\mathbf{l}}(-k, m), \mathbf{B}^{\mathbf{l}}(-k, m); \mathbf{C}^{\mathbf{l}}(-k, m), \mathbf{D}^{\mathbf{l}}(-k, m)),$$

for some normalization constant $\mathcal{Z}_1 > 0$. Letting s tend to 0, together with the fact by Lemma 8.2 and (8.2) (and as $t_i^2 = -\nu_i$) that

$$\lim_{s \rightarrow 0} s^{-|\mathbf{D}^{\mathbf{l}}|} \cdot W_{s;t_i,s}(\mathbf{A}, \mathbf{B}; \mathbf{C}, \mathbf{D}) = \mathcal{W}_{\nu_i}(\mathbf{A}, \mathbf{B}; \mathbf{C}, \mathbf{D}),$$

yields the third part of the proposition. \square

¹⁹This limit exists since that of $\mathbb{P}_{\text{fG};n;s;\mathbf{x};\mathbf{y};\mathbf{r};\mathbf{t}}^\sigma$ does as s tends to 0, as it can be quickly verified that the products $s^{|\mu(N)|} \cdot \prod_{j=1}^N \mathbb{f}_{\mu(j)/\mu(j-1);s}^{\sigma(j)}(x_j; q^{-1/2})$ and $s^{-|\mu(N)|} \cdot \prod_{i=1}^N \mathbb{G}_{\mu(i-1)/\mu(i);s}(s; t_{i-N})$ appearing in (6.11) remain nonsingular as s tends to 0 (since the weights $s^{\mathbb{1}_{j>0}} \cdot \widehat{W}_{x;q^{-1/2},s}(\mathbf{A}, i; \mathbf{A}_{ij}^{+-}, j)$ and $s^{|\mathbf{D}^{\mathbf{l}}|} \cdot W_{s;t,s}(\mathbf{A}, \mathbf{B}; \mathbf{C}, \mathbf{D})$ do).

APPENDIX A. DEGENERATION TO THE LOG-GAMMA POLYMER

In this section we explain how to recover the log-gamma polymer (introduced in [81]) from the colored stochastic fused vertex model (recall Section 6.1); this involves a complementation procedure (of the type alluded to in Remark 6.5), an analytic continuation, and limit degeneration. We begin by describing the complementation procedure and evaluating the associated complemented weights in Section A.1. We then analyze (limits of) analytic continuations of these weights in Section A.2 and Section A.3, and analyze the behavior of them as q tends to 1 in Section A.4, Section A.5, and Section A.6. We conclude in Section A.7 by explaining convergence of the vertex model with these degenerated weights to the log-gamma polymer (and also describing the reason for choosing this specialization in Remark A.25). In what follows, given a real number $\theta > 0$, we say that X is a $\text{Gamma}(\theta)$ random variable if $\mathbb{P}[x \leq X \leq x + dx] = \Gamma(\theta)^{-1} \cdot x^{\theta-1} e^{-x} dx$ for any $x \in \mathbb{R}$. Throughout this section, $n \geq 1$ is an integer, and we assume that $q \in (0, 1)$.

A.1. Complemented Fused Weights. In this section we implement (a case of) the complementation procedure mentioned in Remark 6.5, which will be necessary to degenerate the fused stochastic vertex model of Section 6.1 to the log-gamma polymer. To that end, we require some additional notation. Let $L \in \mathbb{Z}_{\geq 0}$ be an integer, and let

$$(A.1) \quad \overline{\mathbf{X}} = (X_1, X_2, \dots, X_{n-1}) \in \mathbb{Z}_{\geq 0}^{n-1}, \quad \text{for any } \mathbf{X} \in \mathbb{Z}_{\geq 0}^n, \text{ and set } \bar{x} = \lfloor \overline{\mathbf{X}} \rfloor.$$

For any $\mathbf{B}, \mathbf{D} \in \mathbb{Z}_{\geq 0}^n$ such that $|\mathbf{B}| \leq L$ and $\mathbf{D} \leq L$, we set

$$(A.2) \quad B_n = L - B_n; \quad \mathbf{b} = L - |\mathbf{B}|; \quad D_n = L - D_n; \quad \mathbf{d} = L - |\mathbf{D}|.$$

In this way, we have $\mathbf{B} = (\overline{\mathbf{B}}, L - B_n)$ and $\mathbf{D} = (\overline{\mathbf{D}}, L - D_n)$, so that

$$(A.3) \quad \mathbf{b} = B_n - \bar{b}; \quad \mathbf{d} = D_n - \bar{d}.$$

We will evaluate the weight $U_{z;r,s}(\mathbf{A}, \mathbf{B}; \mathbf{C}, \mathbf{D})$ when $r^2 = q^{-L}$ (which is the reason we imposed the conditions $|\mathbf{B}|, |\mathbf{D}| \leq L$ above), $s^2 = q^{-\mathfrak{M}}$, and $z = q^{\mathfrak{N}-L+1}$ (for some complex numbers $\mathfrak{M}, \mathfrak{N} \in \mathbb{C}$). This weight will happen to be rational in q^L , so let us define it when the integer L is replaced by an arbitrary complex number \mathfrak{L} . In what follows, for any integers $m, k \geq 0$, and complex numbers $z \in \mathbb{C}$, $a_1, a_2, \dots, a_k \in \mathbb{C}$, and $b_1, b_2, \dots, b_k \in \mathbb{C}$, we denote the terminating basic hypergeometric series by

$$(A.4) \quad {}_{k+1}\varphi_k \left(\begin{matrix} q^{-m}; a_1, a_2, \dots, a_k \\ b_1, b_2, \dots, b_k \end{matrix} \middle| q, z \right) = \sum_{i=0}^m z^i \frac{(q^{-m}; q)_i}{(q; q)_i} \cdot \prod_{j=1}^k \frac{(a_j; q)_i}{(b_j; q)_i}.$$

Definition A.1. Let $\mathfrak{L}, \mathfrak{M}, \mathfrak{N} \in \mathbb{C}$ be complex numbers; $B_n, D_n \in \mathbb{Z}_{\geq 0}$ be integers; $\overline{\mathbf{B}}, \overline{\mathbf{D}} \in \mathbb{Z}_{\geq 0}^n$ be $(n-1)$ -tuples, such that $\bar{b} = \lfloor \overline{\mathbf{B}} \rfloor \leq B_n$ and $\bar{d} = \lfloor \overline{\mathbf{D}} \rfloor \leq D_n$; and $\mathbf{A}, \mathbf{C} \in \mathbb{Z}_{\geq 0}^n$ be n -tuples. Setting

$a = |\mathbf{A}|$ and $c = |\mathbf{C}|$; letting $\mathbf{b}, \mathbf{d} \in \mathbb{Z}_{\geq 0}$ be as in (A.3), and recalling (A.1), define the weight

$$\begin{aligned} & \mathcal{U}_{q^{\mathfrak{L}}; q^{\mathfrak{M}}; q^{\mathfrak{N}}}(\mathbf{A}, (\overline{\mathbf{B}}, \mathbf{B}_n); \mathbf{C}, (\overline{\mathbf{D}}, \mathbf{D}_n)) \\ &= (-1)^{C_n} q^{\varphi(\overline{\mathbf{D}}, \overline{\mathbf{C}}) + \binom{C_n+1}{2} + \overline{\mathbf{c}}\mathbf{d} + \mathfrak{L}C_n} \cdot \mathbb{1}_{\overline{\mathbf{A}} + \overline{\mathbf{B}} = \overline{\mathbf{C}} + \overline{\mathbf{D}}} \cdot \mathbb{1}_{\mathbf{b} - a = \mathbf{d} - c} \\ & \times \frac{(q; q)_{\mathbf{b}}}{(q; q)_{\mathbf{d}}} \frac{(q^{\mathfrak{M} - \mathfrak{N} - c}; q)_{\mathbf{d}}}{(q; q)_{C_n}} \frac{(q^{\mathbf{D}_n - C_n - \mathfrak{L}}; q)_{C_n}}{(q^{-\mathfrak{N}}; q)_{\mathbf{b}}} \frac{(q^{-\mathfrak{N}}; q)_{\infty}}{(q^{\mathfrak{L} - \mathfrak{N}}; q)_{\infty}} \frac{(q^{\mathfrak{L} + \mathfrak{M} - \mathfrak{N}}; q)_{\infty}}{(q^{\mathfrak{M} - \mathfrak{N}}; q)_{\infty}} \cdot \prod_{j=1}^{n-1} \frac{(q; q)_{B_j}}{(q; q)_{D_j}} \\ & \times \sum_{\overline{\mathbf{P}} \leq \overline{\mathbf{B}}, \overline{\mathbf{C}}} (-1)^{\overline{\mathbf{P}}} q^{\varphi(\overline{\mathbf{B}} - \overline{\mathbf{D}} - \overline{\mathbf{P}}, \overline{\mathbf{P}})} \frac{(q^{-\mathfrak{N} - 1}; q)_{\overline{\mathbf{P}}} (q^{\mathfrak{M} - \mathfrak{N} + \mathbf{d} - c}; q)_{\overline{\mathbf{P}}}}{(q^{\mathfrak{M} - \mathfrak{N} - c}; q)_{\overline{\mathbf{P}}} (q^{\mathbf{b} - \mathfrak{N}}; q)_{\overline{\mathbf{P}}}} \cdot \prod_{j=1}^{n-1} \frac{(q; q)_{C_j + D_j - P_j}}{(q; q)_{C_j - P_j} (q; q)_{P_j} (q; q)_{B_j - P_j}} \\ & \times q^{\overline{\mathbf{P}}(\mathbf{b} - \mathbf{d} + 1) + \binom{\overline{\mathbf{P}}}{2}} \cdot {}_4\varphi_3 \left(\begin{matrix} q^{-C_n}; q^{\mathbf{B}_n - \mathfrak{L}}, q^{\overline{\mathbf{P}} - \mathfrak{N} - 1}, q^{\mathfrak{M} - \mathfrak{N} + \mathbf{d} - c + \overline{\mathbf{P}}} \\ q^{\mathfrak{M} - \mathfrak{N} - c + \overline{\mathbf{P}}}, q^{\mathbf{b} - \mathfrak{N} + \overline{\mathbf{P}}}, q^{\mathbf{D}_n - C_n - \mathfrak{L}} \end{matrix} \middle| q, q \right). \end{aligned}$$

Remark A.2. The appearance of the ${}_4\varphi_3$ basic hypergeometric series in the \mathcal{U} -weights defined above is a common phenomenon for fused vertex weights in the colorless $n = 1$ case; see, for example, [65, Equation (1.1)] and [39, Theorem 3.15].

The following lemma provides an expression for the U_z -weight at $z = q^{\mathfrak{N} - L + 1}$ in terms of \mathcal{U} .

Lemma A.3. *Fix an integer $L \geq 1$ and complex number $\mathfrak{M}, \mathfrak{N} \in \mathbb{C}$. Let $\mathbf{A}, \mathbf{B}, \mathbf{C}, \mathbf{D} \in \mathbb{Z}_{\geq 0}^n$, let $a = |\mathbf{A}|$ and $c = |\mathbf{C}|$, and adopt the notation in (A.1) and (A.2). For any $\mathfrak{N} \in \mathbb{C}$, we have*

$$U_{q^{\mathfrak{N} - L + 1}; q^{-L/2}, q^{-\mathfrak{M}/2}}(\mathbf{A}, \mathbf{B}; \mathbf{C}, \mathbf{D}) = \mathcal{U}_{q^{\mathfrak{L}}; q^{\mathfrak{M}}; q^{\mathfrak{N}}}(\mathbf{A}, (\overline{\mathbf{B}}, \mathbf{B}_n); \mathbf{C}, (\overline{\mathbf{D}}, \mathbf{D}_n)).$$

Proof. Let us assume throughout this proof that $\mathbf{A} + \mathbf{B} = \mathbf{C} + \mathbf{D}$, or equivalently that $\overline{\mathbf{A}} + \overline{\mathbf{B}} = \overline{\mathbf{C}} + \overline{\mathbf{D}}$ and $\mathbf{b} - a = L - |\mathbf{A}| - |\mathbf{B}| = L - |\mathbf{C}| - |\mathbf{D}| = \mathbf{d} - c$; otherwise, (6.1) implies that $U_{q^{\mathfrak{N} - L + 1}; q^{-L/2}, q^{-\mathfrak{M}/2}}(\mathbf{A}, \mathbf{B}; \mathbf{C}, \mathbf{D}) = 0$, which matches with $\mathcal{U}_{q^{\mathfrak{L}}; q^{\mathfrak{M}}; q^{\mathfrak{N}}}(\mathbf{A}, \mathbf{B}; \mathbf{C}, \mathbf{D})$, by Definition A.1. Next, inserting (A.2) into (6.1) (and using the facts that $a - c = |\mathbf{A}| - |\mathbf{C}| = |\mathbf{D}| - |\mathbf{B}| = \mathbf{b} - \mathbf{d}$ and that $\varphi(\mathbf{B}, \mathbf{X}) = \varphi(\overline{\mathbf{B}}, \mathbf{X})$ and $\varphi(\mathbf{D}, \mathbf{X}) = \varphi(\overline{\mathbf{D}}, \mathbf{X})$ for any $\mathbf{X} \in \mathbb{Z}_{\geq 0}^n$), we obtain

$$\begin{aligned} & (A.5) \\ & U_{q^{\mathfrak{N} - L + 1}; q^{-L/2}, q^{-\mathfrak{M}/2}}(\mathbf{A}, \mathbf{B}; \mathbf{C}, \mathbf{D}) \\ &= q^{(\mathfrak{N} + 1)(\mathbf{b} - \mathbf{d}) - (L - \mathbf{d})\mathfrak{M} + \varphi(\overline{\mathbf{D}}, \mathbf{C})} \frac{(q^{-L}; q)_{L - \mathbf{d}}}{(q^{-L}; q)_{L - \mathbf{b}}} \frac{(q; q)_{L - \mathbf{B}_n}}{(q; q)_{L - \mathbf{D}_n}} \prod_{j=1}^{n-1} \frac{(q; q)_{B_j}}{(q; q)_{D_j}} \\ & \times \sum_{p=0}^{\min\{L - \mathbf{b}, c\}} q^{(\mathfrak{N} + 1)p} \frac{(q^{\mathfrak{N} - \mathfrak{M} + 1}; q)_{c - p}}{(q^{\mathfrak{N} - L - \mathfrak{M} + 1}; q)_{L + c - \mathbf{d} - p}} (q^{-\mathfrak{N} - 1}; q)_p (q^{\mathfrak{N} - L + 1}; q)_{L - \mathbf{b} - p} \\ & \times \sum_{\substack{\mathbf{P} \leq \mathbf{B}, \mathbf{C} \\ |\overline{\mathbf{P}}| = p}} q^{\varphi(\overline{\mathbf{B}} - \overline{\mathbf{D}} - \overline{\mathbf{P}}, \mathbf{P})} \frac{(q; q)_{L + C_n - \mathbf{D}_n - P_n}}{(q; q)_{C_n - P_n} (q; q)_{P_n} (q; q)_{L - \mathbf{B}_n - P_n}} \prod_{j=1}^{n-1} \frac{(q; q)_{C_j + D_j - P_j}}{(q; q)_{C_j - P_j} (q; q)_{P_j} (q; q)_{B_j - P_j}}. \end{aligned}$$

We will next separate the parameter L (as well as p and P_n) from the other ones in the subscripts of the q -Pochhammer symbols. To that end, observe that

$$(A.6) \quad \frac{(q; q)_{L - \mathbf{B}_n}}{(q; q)_{L - \mathbf{D}_n}} \frac{(q^{-L}; q)_{L - \mathbf{d}}}{(q^{-L}; q)_{L - \mathbf{b}}} = (-1)^{\mathbf{b} + \mathbf{B}_n - \mathbf{d} - \mathbf{D}_n} q^{\binom{\mathbf{B}_n}{2} - \binom{\mathbf{D}_n}{2} + L(\mathbf{D}_n - \mathbf{B}_n) + \binom{\mathbf{d} + 1}{2} - \binom{\mathbf{b} + 1}{2}} \frac{(q^{-L}; q)_{\mathbf{D}_n}}{(q^{-L}; q)_{\mathbf{B}_n}} \frac{(q; q)_{\mathbf{b}}}{(q; q)_{\mathbf{d}}},$$

due to the identities

$$\begin{aligned} \frac{(q; q)_{L-B_n}}{(q; q)_{L-D_n}} &= \frac{(q^L; q^{-1})_{D_n}}{(q^L; q^{-1})_{B_n}} = (-1)^{B_n-D_n} q^{\binom{B_n}{2} - \binom{D_n}{2} + L(D_n-B_n)} \frac{(q^{-L}; q)_{D_n}}{(q^{-L}; q)_{B_n}}, \\ \frac{(q^{-L}; q)_{L-d}}{(q^{-L}; q)_{L-b}} &= \frac{(q^{-b}; q)_b}{(q^{-d}; q)_d} = (-1)^{b-d} q^{\binom{d+1}{2} - \binom{b+1}{2}} \frac{(q; q)_b}{(q; q)_d}, \end{aligned}$$

where in the first we used the fact that $(u; q^{-1})_k = (-u)^k q^{-\binom{k}{2}} (u^{-1}; q)_k$ for any $k \in \mathbb{Z}_{\geq 0}$ and $u \in \mathbb{C}$. We further have that

$$(A.7) \quad \begin{aligned} \frac{(q^{\mathfrak{N}-\mathfrak{M}+1}; q)_{c-p}}{(q^{\mathfrak{N}-L-\mathfrak{M}+1}; q)_{L+c-d-p}} (q^{\mathfrak{N}-L+1}; q)_{L-b-p} &= \frac{(q^{\mathfrak{N}-\mathfrak{M}+1}; q)_c}{(q^{\mathfrak{N}-\mathfrak{M}+c}; q^{-1})_p} \frac{(q^{\mathfrak{N}-L+1}; q)_L}{(q^{\mathfrak{N}}; q^{-1})_{b+p}} \frac{(q^{\mathfrak{N}-\mathfrak{M}}; q^{-1})_{d-c-p}}{(q^{\mathfrak{N}-\mathfrak{M}-L+1}; q)_L}, \\ \frac{(q; q)_{L+C_n-D_n-P_n}}{(q; q)_{C_n-P_n} (q; q)_{L-B_n-P_n}} &= \frac{(q^L; q^{-1})_{B_n+P_n} (q^{C_n}; q^{-1})_{P_n}}{(q; q)_{C_n} (q^L; q^{-1})_{D_n-C_n+P_n}}, \end{aligned}$$

due the identities

$$\begin{aligned} (q^{\mathfrak{N}-L+1}; q)_{L-b-p} &= \frac{(q^{\mathfrak{N}-L+1}; q)_L}{(q^{\mathfrak{N}}; q^{-1})_{b+p}}; & (q^{\mathfrak{N}-\mathfrak{M}+1}; q)_{c-p} &= \frac{(q^{\mathfrak{N}-\mathfrak{M}+1}; q)_c}{(q^{\mathfrak{N}-\mathfrak{M}+c}; q^{-1})_p}; \\ (q^{\mathfrak{N}-\mathfrak{M}-L+1}; q)_{L+c-d-p} &= \frac{(q^{\mathfrak{N}-\mathfrak{M}-L+1}; q)_L}{(q^{\mathfrak{N}-\mathfrak{M}}; q^{-1})_{d-c+p}}; & (q; q)_{L-B_n-P_n} &= \frac{(q; q)_L}{(q^L; q^{-1})_{B_n+P_n}}; \\ (q; q)_{L+C_n-D_n-P_n} &= \frac{(q; q)_L}{(q^L; q^{-1})_{D_n-C_n+P_n}}; & (q; q)_{C_n-P_n} &= \frac{(q; q)_{C_n}}{(q^{C_n}; q^{-1})_{P_n}}. \end{aligned}$$

Inserting (A.6) and (A.7) into (A.5), we obtain

$$(A.8) \quad \begin{aligned} &U_{q^{\mathfrak{N}-L+1}, q^{-L/2}, q^{-\mathfrak{M}/2}}(\mathbf{A}, \mathbf{B}; \mathbf{C}, \mathbf{D}) \\ &= (-1)^{b+B_n-d-D_n} q^{(\mathfrak{N}+1)(b-d) - (L-d)\mathfrak{M} + \varphi(\overline{\mathbf{D}}, \mathbf{C})} q^{\binom{B_n}{2} - \binom{D_n}{2} + L(D_n-B_n)} q^{\binom{d+1}{2} - \binom{b+1}{2}} \\ &\quad \times \frac{(q; q)_b}{(q; q)_d} \frac{(q^{\mathfrak{N}-\mathfrak{M}+1}; q)_c}{(q; q)_{C_n}} \frac{(q^{-L}; q)_{D_n}}{(q^{-L}; q)_{B_n}} \frac{(q^{\mathfrak{N}-L+1}; q)_L}{(q^{\mathfrak{N}-\mathfrak{M}-L+1}; q)_L} \prod_{j=1}^{n-1} \frac{(q; q)_{B_j}}{(q; q)_{D_j}} \\ &\quad \times \sum_{p=0}^{\min\{b, c\}} q^{(\mathfrak{N}+1)p} \frac{(q^{-\mathfrak{N}-1}; q)_p (q^{\mathfrak{N}-\mathfrak{M}}; q^{-1})_{d-c+p}}{(q^{\mathfrak{N}-\mathfrak{M}+c}; q^{-1})_p (q^{\mathfrak{N}}; q^{-1})_{b+p}} \\ &\quad \times \sum_{\substack{\mathbf{P} \leq \mathbf{B}, \mathbf{C} \\ |\overline{\mathbf{P}}|=p}} q^{\varphi(\overline{\mathbf{B}}-\overline{\mathbf{D}}-\overline{\mathbf{P}}, \mathbf{P})} \frac{(q^L; q^{-1})_{B_n+P_n} (q^{C_n}; q^{-1})_{P_n}}{(q; q)_{P_n} (q^L; q^{-1})_{D_n-C_n+P_n}} \prod_{j=1}^{n-1} \frac{(q; q)_{C_j+D_j-P_j}}{(q; q)_{C_j-P_j} (q; q)_{P_j} (q; q)_{B_j-P_j}}. \end{aligned}$$

Next observe, as $(u; q)_k = (-u)^k q^{\binom{k}{2}} (q^{1-k} u^{-1}; q)_k$ for any $k \in \mathbb{Z}_{\geq 0}$ and $u \in \mathbb{C}$, that

$$(A.9) \quad \frac{(q^{\mathfrak{N}-L+1}; q)_L}{(q^{\mathfrak{N}-L-\mathfrak{M}+1}; q)_L} = q^{L\mathfrak{M}} \frac{(q^{-\mathfrak{N}}; q)_L}{(q^{\mathfrak{M}-\mathfrak{N}}; q)_L}; \quad (q^{\mathfrak{N}-\mathfrak{M}+1}; q)_c = (-1)^c q^{(\mathfrak{N}-\mathfrak{M})c + \binom{c+1}{2}} (q^{\mathfrak{M}-\mathfrak{N}-c}; q)_c.$$

We further convert the quantities of the form $(u; q^{-1})_k$ on the right side of (A.8) into ones of the form $(u'; q)_k$. To do so, we repeatedly use the identity $(u; q^{-1})_k = (-u)^k q^{-\binom{k}{2}} (u^{-1}; q)_k$ for any

$k \in \mathbb{Z}_{\geq 0}$ and $u \in \mathbb{C}$, which gives

$$(A.10) \quad \frac{(q^{\mathfrak{M}-\mathfrak{M}}; q^{-1})_{d-c+p}}{(q^L; q^{-1})_{D_n-C_n+P_n}} = (-1)^{d-c+p-D_n+C_n-P_n} q^{(\mathfrak{M}-\mathfrak{M})(d-c+p)-L(D_n-C_n+P_n)} q^{\binom{D_n-C_n+P_n}{2}-\binom{d-c+p}{2}} \\ \times \frac{(q^{\mathfrak{M}-\mathfrak{M}}; q)_{d-c+p}}{(q^{-L}; q)_{D_n-C_n+P_n}};$$

and

$$(A.11) \quad \frac{(q^L; q^{-1})_{B_n+P_n}}{(q^{\mathfrak{M}}; q^{-1})_{b+p}} = (-1)^{B_n+P_n-b-p} q^{L(B_n+P_n)-\mathfrak{M}(b+p)} q^{\binom{b+p}{2}-\binom{B_n+P_n}{2}} \frac{(q^{-L}; q)_{B_n+P_n}}{(q^{-\mathfrak{M}}; q)_{b+p}}; \\ \frac{(q^{C_n}; q^{-1})_{P_n}}{(q^{\mathfrak{M}-\mathfrak{M}+c}; q^{-1})_p} = (-1)^{p+P_n} q^{P_n C_n+(\mathfrak{M}-\mathfrak{M}-c)p} q^{\binom{p}{2}-\binom{P_n}{2}} \frac{(q^{-C_n}; q)_{P_n}}{(q^{\mathfrak{M}-\mathfrak{M}-c}; q)_p}.$$

Inserting (A.9), (A.10), and (A.11) into (A.8) gives

$$U_{q^{\mathfrak{M}-L+1}; q^{-L/2}, q^{-\mathfrak{M}/2}}(\mathbf{A}, \mathbf{B}; \mathbf{C}, \mathbf{D}) \\ = (-1)^{b+B_n-d-D_n+c} q^{(\mathfrak{M}+1)(b-d)+d\mathfrak{M}+\varphi(\overline{\mathbf{D}}, \mathbf{C})} q^{\binom{B_n}{2}-\binom{D_n}{2}+L(D_n-B_n)} q^{\binom{d+1}{2}-\binom{b+1}{2}+c(\mathfrak{M}-\mathfrak{M})+\binom{c+1}{2}} \\ \times \frac{(q; q)_b}{(q; q)_d} \frac{(q^{\mathfrak{M}-\mathfrak{M}-c}; q)_c}{(q; q)_{C_n}} \frac{(q^{-L}; q)_{D_n}}{(q^{-L}; q)_{B_n}} \frac{(q^{-\mathfrak{M}}; q)_L}{(q^{\mathfrak{M}-\mathfrak{M}}; q)_L} \prod_{j=1}^{n-1} \frac{(q; q)_{B_j}}{(q; q)_{D_j}} \\ \times \sum_{p=0}^{\min\{L-b, c\}} \sum_{\mathbf{P} \leq \mathbf{B}, \mathbf{C}} (-1)^{d-c+p-D_n-C_n+P_n} q^{(\mathfrak{M}+1)p} q^{(\mathfrak{M}-\mathfrak{M})(d-c+p)-L(D_n-C_n+P_n)} \\ \times q^{\binom{D_n-C_n+P_n}{2}-\binom{d-c+p}{2}} (-1)^{B_n+P_n-b-p} q^{L(B_n+P_n)-\mathfrak{M}(b+p)} q^{\binom{b+p}{2}-\binom{B_n+P_n}{2}} \\ \times \frac{(q^{-\mathfrak{M}-1}; q)_p}{(q^{\mathfrak{M}-\mathfrak{M}-c}; q)_p} \frac{(q^{\mathfrak{M}-\mathfrak{M}}; q)_{d-c+p}}{(q^{-\mathfrak{M}}; q)_{b+p}} (-1)^{p+P_n} q^{P_n C_n+p(\mathfrak{M}-\mathfrak{M}-c)} q^{\binom{p}{2}-\binom{P_n}{2}} q^{\varphi(\overline{\mathbf{B}}-\overline{\mathbf{D}}-\overline{\mathbf{P}}, \mathbf{P})} \\ \times \frac{(q^{-L}; q)_{B_n+P_n} (q^{-C_n}; q)_{P_n}}{(q; q)_{P_n} (q^{-L}; q)_{D_n-C_n+P_n}} \prod_{j=1}^{n-1} \frac{(q; q)_{C_j+D_j-P_j}}{(q; q)_{C_j-P_j} (q; q)_{P_j} (q; q)_{B_j-P_j}}.$$

Before proceeding, we next simplify the powers of -1 and q appearing on the right side. Doing so directly yields

$$\begin{aligned}
& U_{q^{\mathfrak{N}-L+1}; q^{-L/2}, q^{-\mathfrak{N}/2}}(\mathbf{A}, \mathbf{B}; \mathbf{C}, \mathbf{D}) \\
&= (-1)^{C_n} q^{\varphi(\overline{\mathbf{D}}, \mathbf{C})} q^{\mathbb{L}C_n + \binom{B_n}{2} - \binom{D_n}{2}} q^{\binom{d+1}{2} - \binom{b+1}{2} + b-d + \binom{c+1}{2}} \\
&\quad \times \frac{(q; q)_b}{(q; q)_d} \frac{(q^{\mathfrak{N}-\mathfrak{N}-c}; q)_c}{(q; q)_{C_n}} \frac{(q^{-L}; q)_{D_n}}{(q^{-L}; q)_{B_n}} \frac{(q^{-\mathfrak{N}}; q)_L}{(q^{\mathfrak{N}-\mathfrak{N}}; q)_L} \prod_{j=1}^{n-1} \frac{(q; q)_{B_j}}{(q; q)_{D_j}} \\
&\quad \times \sum_{p=0}^{\min\{L-b, c\}} \sum_{\mathbf{P} \leq \mathbf{B}, \mathbf{C}} (-1)^{p+P_n} q^{\binom{D_n - C_n + P_n}{2} + P_n C_n - \binom{P_n}{2} - \binom{d-c+p}{2} + \binom{p}{2} + p - pc} q^{\binom{b+p}{2} - \binom{B_n + P_n}{2}} \\
&\quad \quad \times q^{\varphi(\overline{\mathbf{B}} - \overline{\mathbf{D}} - \overline{\mathbf{P}}, \mathbf{P})} \frac{(q^{-\mathfrak{N}-1}; q)_p (q^{\mathfrak{N}-\mathfrak{N}}; q)_{d-c+p}}{(q^{\mathfrak{N}-\mathfrak{N}-c}; q)_p (q^{-\mathfrak{N}}; q)_{b+p}} \frac{(q^{-L}; q)_{B_n + P_n} (q^{-C_n}; q)_{P_n}}{(q; q)_{P_n} (q^{-L}; q)_{D_n - C_n + P_n}} \\
&\quad \quad \times \prod_{j=1}^{n-1} \frac{(q; q)_{C_j + D_j - P_j}}{(q; q)_{C_j - P_j} (q; q)_{P_j} (q; q)_{B_j - P_j}}.
\end{aligned}$$

Let us continue to simplify the power of q above. Since

$$\begin{aligned}
& \binom{D_n - C_n + P_n}{2} + P_n C_n - \binom{P_n}{2} = \binom{D_n - C_n}{2} + P_n D_n; \\
& \binom{B_n + P_n}{2} = \binom{B_n}{2} + \binom{P_n}{2} + B_n P_n; \\
& \binom{d-c+p}{2} - \binom{p}{2} + pc = \binom{d-c}{2} + pd; \quad \binom{b+p}{2} = \binom{b+1}{2} - b + \binom{p}{2} + bp,
\end{aligned}$$

it follows that

(A.12)

$$\begin{aligned}
& U_{q^{\mathfrak{N}-L+1}; q^{-L/2}, q^{-\mathfrak{N}/2}}(\mathbf{A}, \mathbf{B}; \mathbf{C}, \mathbf{D}) \\
&= (-1)^{C_n} q^{\varphi(\overline{\mathbf{D}}, \mathbf{C})} q^{\binom{D_n - C_n}{2} - \binom{d-c}{2} + \mathbb{L}C_n - \binom{D_n}{2}} q^{\binom{d+1}{2} - d + \binom{c+1}{2}} \\
&\quad \times \frac{(q; q)_b}{(q; q)_d} \frac{(q^{\mathfrak{N}-\mathfrak{N}-c}; q)_c}{(q; q)_{C_n}} \frac{(q^{-L}; q)_{D_n}}{(q^{-L}; q)_{B_n}} \frac{(q^{-\mathfrak{N}}; q)_L}{(q^{\mathfrak{N}-\mathfrak{N}}; q)_L} \prod_{j=1}^{n-1} \frac{(q; q)_{B_j}}{(q; q)_{D_j}} \\
&\quad \times \sum_{p=0}^{\min\{L-b, c\}} \sum_{\mathbf{P} \leq \mathbf{B}, \mathbf{C}} (-1)^{p+P_n} q^{P_n(D_n - B_n) + p(b-d+1) + \binom{p}{2} - \binom{P_n}{2}} \\
&\quad \quad \times q^{\varphi(\overline{\mathbf{B}} - \overline{\mathbf{D}} - \overline{\mathbf{P}}, \mathbf{P})} \frac{(q^{-\mathfrak{N}-1}; q)_p (q^{\mathfrak{N}-\mathfrak{N}}; q)_{d-c+p}}{(q^{\mathfrak{N}-\mathfrak{N}-c}; q)_p (q^{-\mathfrak{N}}; q)_{b+p}} \frac{(q^{-L}; q)_{B_n + P_n} (q^{-C_n}; q)_{P_n}}{(q; q)_{P_n} (q^{-L}; q)_{D_n - C_n + P_n}} \\
&\quad \quad \times \prod_{j=1}^{n-1} \frac{(q; q)_{C_j + D_j - P_j}}{(q; q)_{C_j - P_j} (q; q)_{P_j} (q; q)_{B_j - P_j}}.
\end{aligned}$$

We additionally have by (A.3) and the equality $p = \bar{p} + P_n$ that

$$\begin{aligned} \binom{d+1}{2} - d &= \binom{d}{2}; & \varphi(\bar{\mathbf{B}} - \bar{\mathbf{D}} - \bar{\mathbf{P}}, \mathbf{P}) &= \varphi(\bar{\mathbf{B}} + \bar{\mathbf{D}} - \bar{\mathbf{P}}, \bar{\mathbf{P}}) + (\bar{b} - \bar{d} - \bar{p})P_n; \\ \binom{p}{2} - \binom{P_n}{2} - \bar{p}P_n &= \binom{\bar{p}}{2}; & p(b-d+1) &= \bar{p}(b-d+1) + P_n(b-d) + P_n; \\ P_n(b-d+D_n - B_n + \bar{b} - \bar{d}) &= 0; & \binom{D_n - C_n}{2} - \binom{D_n}{2} &= \binom{C_n + 1}{2} - C_n D_n; \\ \varphi(\bar{\mathbf{D}}, \mathbf{C}) &= \varphi(\bar{\mathbf{D}}, \bar{\mathbf{C}}) + C_n \bar{d}; & \binom{c+1}{2} + \binom{d}{2} - \binom{d-c}{2} &= cd = \bar{c}d + C_n(D_n - \bar{d}). \end{aligned}$$

Together with (A.3) and (A.12), these give

$$\begin{aligned} U_{q^{\mathfrak{M}-L+1}; q^{-L/2}, q^{-\mathfrak{M}/2}}(\mathbf{A}, \mathbf{B}; \mathbf{C}, \mathbf{D}) &= (-1)^{C_n} q^{\varphi(\bar{\mathbf{D}}, \bar{\mathbf{C}}) + \binom{C_n+1}{2} + \bar{c}d + LC_n} \\ &\times \frac{(q; q)_b (q^{\mathfrak{M}-\mathfrak{M}-c}; q)_c (q^{-L}; q)_{D_n} (q^{-\mathfrak{M}}; q)_L}{(q; q)_d (q; q)_{C_n} (q^{-L}; q)_{B_n} (q^{\mathfrak{M}-\mathfrak{M}}; q)_L} \prod_{j=1}^{n-1} \frac{(q; q)_{B_j}}{(q; q)_{D_j}} \\ &\times \sum_{p=0}^{\min\{L-b, c\}} \sum_{\mathbf{P} \leq \mathbf{B}, \mathbf{C}} (-1)^{\bar{p}} q^{\bar{p}(b-d+1) + P_n + \binom{\bar{p}}{2}} q^{\varphi(\bar{\mathbf{B}} - \bar{\mathbf{D}} - \bar{\mathbf{P}}, \bar{\mathbf{P}})} \\ &\times \frac{(q^{\mathfrak{M}-\mathfrak{M}}; q)_{d-c+p} (q^{-L}; q)_{B_n+P_n} (q^{-C_n}; q)_{P_n}}{(q^{\mathfrak{M}-\mathfrak{M}-c}; q)_p (q; q)_{P_n} (q^{-L}; q)_{D_n - C_n + P_n}} \\ &\times \frac{(q^{-\mathfrak{M}-1}; q)_p}{(q^{-\mathfrak{M}}; q)_{b+p}} \prod_{j=1}^{n-1} \frac{(q; q)_{C_j + D_j - P_j}}{(q; q)_{C_j - P_j} (q; q)_{P_j} (q; q)_{B_j - P_j}}. \end{aligned}$$

Next, observe by (A.3) and the equality $p = \bar{p} + P_n$ that

$$\begin{aligned} (q^{\mathfrak{M}-\mathfrak{M}-c}; q)_c (q^{\mathfrak{M}-\mathfrak{M}}; q)_{d-c+p} &= (q^{\mathfrak{M}-\mathfrak{M}-c}; q)_d (q^{\mathfrak{M}-\mathfrak{M}+d-c}; q)_{\bar{p}} (q^{\mathfrak{M}-\mathfrak{M}+d-c+\bar{p}}; q)_{P_n}; \\ (q^{\mathfrak{M}-\mathfrak{M}-c}; q)_p &= (q^{\mathfrak{M}-\mathfrak{M}-c}; q)_{\bar{p}} (q^{\mathfrak{M}-\mathfrak{M}-c+\bar{p}}; q)_{P_n}; & \frac{(q^{-L}; q)_{D_n}}{(q^{-L}; q)_{D_n - C_n + P_n}} &= \frac{(q^{D_n - C_n - L}; q)_{C_n}}{(q^{D_n - C_n - L}; q)_{P_n}}; \\ \frac{(q^{-L}; q)_{B_n + P_n}}{(q^{-L}; q)_{B_n}} &= (q^{B_n - L}; q)_{P_n}; & \frac{(q^{-\mathfrak{M}-1}; q)_p}{(q^{-\mathfrak{M}}; q)_{b+p}} &= \frac{(q^{-\mathfrak{M}-1}; q)_{\bar{p}} (q^{\bar{p}-\mathfrak{M}-1}; q)_{P_n}}{(q^{-\mathfrak{M}}; q)_b (q^{b-\mathfrak{M}}; q)_{\bar{p}} (q^{b-\mathfrak{M}+\bar{p}}; q)_{P_n}}, \end{aligned}$$

from which it follows that

$$\begin{aligned} U_{q^{\mathfrak{M}-L+1}; q^{-L/2}, q^{-\mathfrak{M}/2}}(\mathbf{A}, \mathbf{B}; \mathbf{C}, \mathbf{D}) &= (-1)^{C_n} q^{\varphi(\bar{\mathbf{D}}, \bar{\mathbf{C}}) + \binom{C_n+1}{2} + \bar{c}d + LC_n} \frac{(q; q)_b (q^{\mathfrak{M}-\mathfrak{M}-c}; q)_d (q^{D_n - C_n - L}; q)_{C_n} (q^{-\mathfrak{M}}; q)_L}{(q; q)_d (q; q)_{C_n} (q^{-\mathfrak{M}}; q)_b (q^{\mathfrak{M}-\mathfrak{M}}; q)_L} \prod_{j=1}^{n-1} \frac{(q; q)_{B_j}}{(q; q)_{D_j}} \\ &\times \sum_{\bar{\mathbf{P}} \leq \bar{\mathbf{B}}, \bar{\mathbf{C}}} (-1)^{\bar{p}} q^{\varphi(\bar{\mathbf{B}} - \bar{\mathbf{D}} - \bar{\mathbf{P}}, \bar{\mathbf{P}})} \frac{(q^{-\mathfrak{M}-1}; q)_{\bar{p}} (q^{\mathfrak{M}-\mathfrak{M}+d-c}; q)_{\bar{p}}}{(q^{\mathfrak{M}-\mathfrak{M}-c}; q)_{\bar{p}} (q^{b-\mathfrak{M}}; q)_{\bar{p}}} \prod_{j=1}^{n-1} \frac{(q; q)_{C_j + D_j - P_j}}{(q; q)_{C_j - P_j} (q; q)_{P_j} (q; q)_{B_j - P_j}} \\ &\times q^{\bar{p}(b-d+1) + \binom{\bar{p}}{2}} \sum_{P_n=0}^{C_n} q^{P_n} \frac{(q^{\bar{p}-\mathfrak{M}-1}; q)_{P_n}}{(q^{\mathfrak{M}-\mathfrak{M}-c+\bar{p}}; q)_{P_n}} \frac{(q^{\mathfrak{M}-\mathfrak{M}+d-c+\bar{p}}; q)_{P_n}}{(q^{b-\mathfrak{M}+\bar{p}}; q)_{P_n}} \frac{(q^{B_n - L}; q)_{P_n} (q^{-C_n}; q)_{P_n}}{(q; q)_{P_n} (q^{D_n - C_n - L}; q)_{P_n}}, \end{aligned}$$

where we used the fact that any summands on the right side with $P_n > B_n = L - B_n$ are equal to 0, due to the factor of $(q^{B_n - L}; q)_{P_n}$. This, with $(q^{-\mathfrak{N}}; q)_L = (q^{-\mathfrak{N}}; q)_\infty (q^{L - \mathfrak{N}}; q)_\infty^{-1}$, $(q^{\mathfrak{M} - \mathfrak{N}}; q)_L^{-1} = (q^{L + \mathfrak{M} - \mathfrak{N}}; q)_\infty (q^{\mathfrak{M} - \mathfrak{N}}; q)_\infty^{-1}$, and (A.4), yields the lemma. \square

A.2. Degenerations of the Fused Complemented Weights. We next proceed to take limits of the weights from Definition A.1 that will eventually lead us to the log-gamma polymer. The first is to let $q^{\mathfrak{M}}$ and $q^{\mathfrak{N}}$ tend to infinity, in such a way that (\mathfrak{L}) and $q^{\mathfrak{M} - \mathfrak{N}} = q^{-\mathfrak{L}}\gamma$ (for some constant $\gamma \in \mathbb{C}$) remains fixed.

Lemma A.4. *Adopting the notation of Lemma A.3, we have for any complex number $\gamma \in \mathbb{C}$ that*

$$\begin{aligned}
& \lim_{q^{\mathfrak{M}} \rightarrow \infty} \mathcal{U}_{q^{\mathfrak{L}}; q^{\mathfrak{M}}; q^{\mathfrak{M} + \mathfrak{L}}/\gamma}(\mathbf{A}, (\overline{\mathbf{B}}, \mathbf{B}_n); \mathbf{C}, (\overline{\mathbf{D}}, \mathbf{D}_n)) \\
&= (-1)^{C_n} q^{\varphi(\overline{\mathbf{D}}, \overline{\mathbf{C}}) + \binom{C_n + 1}{2} + \overline{\mathbf{d}} + \mathfrak{L} C_n} \cdot \prod_{j=1}^{n-1} \frac{(q; q)_{B_j}}{(q; q)_{D_j}} \cdot \mathbb{1}_{\overline{\mathbf{A}} + \overline{\mathbf{B}} = \overline{\mathbf{C}} + \overline{\mathbf{D}}} \cdot \mathbb{1}_{\mathbf{b} - \mathbf{a} = \mathbf{d} - \mathbf{c}} \\
&\times \frac{(q; q)_{\mathbf{b}}}{(q; q)_{\mathbf{d} - C_n}} \frac{(q^{-\mathbf{c} - \mathfrak{L}}\gamma; q)_{\mathbf{d}}}{(q; q)_{C_n}} \frac{(q^{B_n - \mathfrak{L}}; q)_{C_n}(\gamma; q)_\infty}{(q^{\mathfrak{L} + \mathbf{c} - C_n - \overline{\mathbf{p}} + 1}\gamma^{-1}; q)_{C_n} (q^{-\mathfrak{L}}\gamma; q)_\infty} \\
&\times \sum_{\overline{\mathbf{P}} \leq \overline{\mathbf{B}}, \overline{\mathbf{C}}} (-1)^{\overline{\mathbf{P}}} q^{\varphi(\overline{\mathbf{B}} - \overline{\mathbf{D}} - \overline{\mathbf{P}}, \overline{\mathbf{P}})} \frac{(q^{\mathbf{d} - \mathbf{c} - \mathfrak{L}}\gamma; q)_{\overline{\mathbf{P}}}}{(q^{-\mathfrak{L} - \mathbf{c}}\gamma; q)_{\overline{\mathbf{P}}}} \prod_{j=1}^{n-1} \frac{(q; q)_{C_j + D_j - P_j}}{(q; q)_{C_j - P_j} (q; q)_{P_j} (q; q)_{B_j - P_j}} \\
&\times q^{\overline{\mathbf{p}}(\mathbf{b} - \mathbf{d} + 1) + \binom{\overline{\mathbf{P}}}{2}} \cdot {}_3\varphi_2 \left(\begin{matrix} q^{-C_n}; q^{-A_n}, q^{\mathfrak{L} - C_n + \mathbf{c} - \overline{\mathbf{p}} + 1}\gamma^{-1} \\ q^{\mathbf{d} - C_n + 1}, q^{\mathfrak{L} - B_n - C_n + 1} \end{matrix} \middle| q, q \right).
\end{aligned} \tag{A.13}$$

Proof. We assume throughout this proof that $\overline{\mathbf{A}} + \overline{\mathbf{B}} = \overline{\mathbf{C}} + \overline{\mathbf{D}}$ and $\mathbf{b} - \mathbf{a} = \mathbf{d} - \mathbf{c}$, for otherwise both sides of (A.13) are equal to 0 by Lemma A.3. Then letting $q^{\mathfrak{N}}$ and $q^{\mathfrak{M}}$ tend to ∞ , while keeping $q^{\mathfrak{M} - \mathfrak{N}} = q^{-\mathfrak{L}}\gamma$ fixed, in Lemma A.3 yields

$$\begin{aligned}
& \lim_{q^{\mathfrak{M}} \rightarrow \infty} \mathcal{U}_{q^{\mathfrak{L}}; q^{\mathfrak{M}}; q^{\mathfrak{M} + \mathfrak{L}}/\gamma}(\mathbf{A}, (\overline{\mathbf{B}}, \mathbf{B}_n); \mathbf{C}, (\overline{\mathbf{D}}, \mathbf{D}_n)) \\
&= (-1)^{C_n} q^{\varphi(\overline{\mathbf{D}}, \overline{\mathbf{C}}) + \binom{C_n + 1}{2} + \overline{\mathbf{d}} + \mathfrak{L} C_n} \frac{(q; q)_{\mathbf{b}}}{(q; q)_{\mathbf{d}}} \frac{(q^{-\mathbf{c} - \mathfrak{L}}\gamma; q)_{\mathbf{d}}}{(q; q)_{C_n}} \frac{(q^{D_n - C_n - \mathfrak{L}}; q)_{C_n}(\gamma; q)_\infty}{(q^{-\mathfrak{L}}\gamma; q)_\infty} \prod_{j=1}^{n-1} \frac{(q; q)_{B_j}}{(q; q)_{D_j}} \\
&\times \sum_{\overline{\mathbf{P}} \leq \overline{\mathbf{B}}, \overline{\mathbf{C}}} (-1)^{\overline{\mathbf{P}}} q^{\varphi(\overline{\mathbf{B}} - \overline{\mathbf{D}} - \overline{\mathbf{P}}, \overline{\mathbf{P}})} \frac{(q^{\mathbf{d} - \mathbf{c} - \mathfrak{L}}\gamma; q)_{\overline{\mathbf{P}}}}{(q^{-\mathfrak{L} - \mathbf{c}}\gamma; q)_{\overline{\mathbf{P}}}} \prod_{j=1}^{n-1} \frac{(q; q)_{C_j + D_j - P_j}}{(q; q)_{C_j - P_j} (q; q)_{P_j} (q; q)_{B_j - P_j}} \\
&\times q^{\overline{\mathbf{p}}(\mathbf{b} - \mathbf{d} + 1) + \binom{\overline{\mathbf{P}}}{2}} \cdot {}_3\varphi_2 \left(\begin{matrix} q^{-C_n}; q^{B_n - \mathfrak{L}}, q^{\mathbf{d} - \mathbf{c} + \overline{\mathbf{p}} - \mathfrak{L}}\gamma \\ q^{\overline{\mathbf{p}} - \mathfrak{L} - \mathbf{c}}\gamma, q^{D_n - C_n - \mathfrak{L}} \end{matrix} \middle| q, q \right).
\end{aligned} \tag{A.14}$$

Next recall from the Sears identity [45, Equation (3.2.9)] that, for any integer $m \geq 0$ and complex numbers $A, B, C, D, E, F \in \mathbb{C}$ with $q^{1-m}ABC = DEF$, we have

$${}_4\varphi_3 \left(\begin{matrix} q^{-m}; A, B, C \\ D, E, F \end{matrix} \middle| q, q \right) = \frac{(B; q)_m \left(\frac{DE}{AB}; q \right)_m \left(\frac{DE}{BC}; q \right)_m}{(D; q)_m (E; q)_m \left(\frac{DE}{ABC}; q \right)_m} \cdot {}_4\varphi_3 \left(\begin{matrix} q^{-m}; \frac{D}{B}, \frac{E}{B}, \frac{DE}{ABC} \\ \frac{DE}{AB}, \frac{DE}{BC}, q^{1-m}B^{-1} \end{matrix} \middle| q, q \right).$$

Letting A and E tend to 0 in such a way that $\frac{A}{E} = q^{m-1} \frac{DF}{BC}$ remains fixed, we deduce (under no restrictions on $B, C, D, F \in \mathbb{C}$) that

$${}_3\varphi_2 \left(\begin{matrix} q^{-m}; B, C \\ D, F \end{matrix} \middle| q, q \right) = \frac{(B; q)_m (q^{1-m}CF^{-1}; q)_m}{(D; q)_m (q^{1-m}F^{-1}; q)_m} \cdot {}_3\varphi_2 \left(\begin{matrix} q^{-m}; \frac{D}{B}, q^{1-m}F^{-1} \\ q^{1-m}CF^{-1}, q^{1-m}B^{-1} \end{matrix} \middle| q, q \right).$$

Taking $m = C_n$ and $(B, C; D, F) = (q^{B_n - \mathfrak{L}}, q^{d-c+\bar{p}-\mathfrak{L}}\gamma; q^{D_n - C_n - \mathfrak{L}}, q^{\bar{p}-\mathfrak{L}-c}\gamma)$ (and using the fact that $B_n - A_n = D_n - C_n$, by (A.3) and the equalities $b - a = d - c$ and $\bar{A} + \bar{B} = \bar{C} + \bar{D}$), we obtain

$${}_{3\varphi_2} \left(\begin{matrix} q^{-C_n}; q^{B_n - \mathfrak{L}}, q^{d-c+\bar{p}-\mathfrak{L}}\gamma \\ q^{\bar{p}-\mathfrak{L}-c}\gamma, q^{D_n - C_n - \mathfrak{L}} \end{matrix} \middle| q, q \right) = \frac{(q^{B_n - \mathfrak{L}}; q)_{C_n} (q^{d-C_n+1}; q)_{C_n}}{(q^{D_n - C_n - \mathfrak{L}}; q)_{C_n} (q^{\mathfrak{L}+c-C_n-\bar{p}+1}\gamma^{-1}; q)_{C_n}} \\ \times {}_{3\varphi_2} \left(\begin{matrix} q^{-C_n}; q^{-A_n}, q^{\mathfrak{L}-C_n+c-\bar{p}+1}\gamma^{-1} \\ q^{d-C_n+1}, q^{\mathfrak{L}-C_n-B_n+1} \end{matrix} \middle| q, q \right).$$

Inserting this into (A.14), and using the fact that $(q^{d-C_n+1}; q)_{C_n} (q; q)_d^{-1} = (q; q)_{d-C_n}^{-1}$, gives the lemma. \square

We next take the further limit in Lemma A.4 as $q^{\mathfrak{L}}$ tends to ∞ . The below definition provides this limit; see the lemma that follows.

Definition A.5. Adopting the notation of Definition A.1, define for any $\gamma \in \mathbb{C}$ the q -discrete polymer weight $\mathcal{U}_\gamma^{\text{qp};n}(\mathbf{A}, (\bar{\mathbf{B}}, B_n); \mathbf{C}, (\bar{\mathbf{D}}, D_n)) = \mathcal{U}_\gamma^{\text{qp}}(\mathbf{A}, (\bar{\mathbf{B}}, B_n); \mathbf{C}, (\bar{\mathbf{D}}, D_n))$ by

$$(A.15) \\ \mathcal{U}_\gamma^{\text{qp}}(\mathbf{A}, (\bar{\mathbf{B}}, B_n); \mathbf{C}, (\bar{\mathbf{D}}, D_n)) \\ = q^{\varphi(\bar{\mathbf{D}}, \bar{\mathbf{C}}) + \bar{c}(B_n - A_n - \bar{d})}(\gamma; q)_\infty \frac{(q; q)_b}{(q; q)_{B_n - A_n - \bar{d}}} \cdot \mathbb{1}_{\bar{A} + \bar{B} = \bar{C} + \bar{D}} \cdot \mathbb{1}_{b-a=d-c} \cdot \prod_{j=1}^{n-1} \frac{(q; q)_{C_j + D_j}}{(q; q)_{C_j} (q; q)_{D_j}} \\ \times \sum_{k=0}^{C_n} \frac{\gamma^{C_n - k}}{(q; q)_{C_n - k}} \frac{(q^{A_n - k + 1}; q)_k}{(q; q)_k (q^{B_n - A_n - \bar{d} + 1}; q)_k} q^{k(B_n - A_n + \bar{c} + k)} \\ \times \sum_{\bar{P} \leq \bar{B}, \bar{C}} q^{\bar{P}(A_n - k + 1) + \varphi(\bar{P}, \bar{\mathbf{D}} - \bar{\mathbf{B}})} \prod_{j=1}^{n-1} \frac{(q^{-B_j}; q)_{P_j} (q^{-C_j}; q)_{P_j}}{(q; q)_{P_j} (q^{-C_j - D_j}; q)_{P_j}}.$$

Remark A.6. If $n = 1$, then the \mathcal{U}^{qp} weights from Definition A.5 coincide with those of the geometric q -PushTASEP introduced in [68, Section 6.3], which degenerates to the log-gamma polymer [68, Theorem 8.7]. This is the reason behind the term, “ q -discrete polymer weight” in Definition A.5.

Lemma A.7. *Under the notation of Lemma A.4, we have*

$$\lim_{q^{\mathfrak{L}} \rightarrow \infty} \left(\lim_{q^{\text{gr}} \rightarrow \infty} \mathcal{U}_{q^{\mathfrak{L}}; q^{\text{gr}}; q^{\text{gr}+\mathfrak{L}}/\gamma}(\mathbf{A}, (\bar{\mathbf{B}}, B_n); \mathbf{C}, (\bar{\mathbf{D}}, D_n)) \right) = \mathcal{U}_\gamma^{\text{qp}}(\mathbf{A}, (\bar{\mathbf{B}}, B_n); \mathbf{C}, (\bar{\mathbf{D}}, D_n)).$$

Proof. Throughout this proof, we assume that $\bar{A} + \bar{B} = \bar{C} + \bar{D}$ and $b - a = d - c$, for otherwise the lemma holds by Lemma A.4 and Definition A.5. Since $\lim_{a \rightarrow \infty} a^{-k} (ab; q)_k = (-b)^k q^{\binom{k}{2}}$ for any $b \in \mathbb{C}$ and $k \in \mathbb{Z}_{\geq 0}$, we have

$$\lim_{q^{\mathfrak{L}} \rightarrow \infty} (-1)^{C_n} q^{\mathfrak{L}C_n + \binom{C_n+1}{2}} (q^{\mathfrak{L}+c-C_n-\bar{p}+1}\gamma^{-1}; q)_{C_n}^{-1} = q^{C_n(C_n-c+\bar{p})}\gamma^{C_n}; \\ \lim_{q^{\mathfrak{L}} \rightarrow \infty} {}_{3\varphi_2} \left(\begin{matrix} q^{-C_n}; q^{-A_n}, q^{\mathfrak{L}-C_n+c-\bar{p}+1}\gamma^{-1} \\ q^{d-C_n+1}, q^{\mathfrak{L}-B_n-C_n+1} \end{matrix} \middle| q, q \right) = {}_{2\varphi_1} \left(\begin{matrix} q^{-C_n}; q^{-A_n} \\ q^{d-C_n+1} \end{matrix} \middle| q, q^{B_n+c-\bar{p}+1}\gamma^{-1} \right),$$

where in the second statement we used (A.4). Inserting these (with the fact that $C_n - c = -\bar{c}$), into the limit as q^ε tends to ∞ of (A.4), we find

$$\begin{aligned}
& \lim_{q^\varepsilon \rightarrow \infty} \left(\lim_{q^{\mathfrak{m}} \rightarrow \infty} \mathcal{U}_{q^\varepsilon; q^{\mathfrak{m}}; q^{\mathfrak{m}+\varepsilon}/\gamma}(\mathbf{A}, (\bar{\mathbf{B}}, \mathbf{B}_n); \mathbf{C}, (\bar{\mathbf{D}}, \mathbf{D}_n)) \right) \\
&= q^{\varphi(\bar{\mathbf{D}}, \bar{\mathbf{C}}) + \bar{c}(d - C_n)} \gamma^{C_n} \frac{(q; q)_b}{(q; q)_{d - C_n} (q; q)_{C_n}} (\gamma; q)_\infty \cdot \prod_{j=1}^{n-1} \frac{(q; q)_{B_j}}{(q; q)_{D_j}} \\
&\times \sum_{\bar{\mathbf{P}} \leq \bar{\mathbf{B}}, \bar{\mathbf{C}}} (-1)^{\bar{p}} q^{\varphi(\bar{\mathbf{B}} - \bar{\mathbf{D}} - \bar{\mathbf{P}}, \bar{\mathbf{P}})} \cdot \prod_{j=1}^{n-1} \frac{(q; q)_{C_j + D_j - P_j}}{(q; q)_{C_j - P_j} (q; q)_{P_j} (q; q)_{B_j - P_j}} \\
&\times q^{\bar{p}(b - d + 1) + \binom{\bar{p}}{2}} q^{\bar{p}C_n} \cdot {}_2\varphi_1 \left(\begin{matrix} q^{-C_n}, q^{-A_n} \\ q^{d - C_n + 1} \end{matrix} \middle| q, q^{\mathbf{B}_n + c - \bar{p} + 1} \gamma^{-1} \right).
\end{aligned} \tag{A.16}$$

Next we separate the P_j subscripts in the q -Pochhammer symbols on the right side of (A.16) from the other ones. To that end, observe since $(q; q)_{m-k} = (-1)^k q^{\binom{k}{2} - mk} (q; q)_m (q^{-m}; q)_k^{-1}$ that we have

$$\frac{(q; q)_{C_j + D_j - P_j}}{(q; q)_{C_j - P_j} (q; q)_{B_j - P_j}} = (-1)^{P_j} q^{P_j(B_j - D_j) - \binom{P_j}{2}} \frac{(q; q)_{C_j + D_j}}{(q; q)_{C_j} (q; q)_{B_j}} \frac{(q^{-C_j}; q)_{P_j} (q^{-B_j}; q)_{P_j}}{(q^{-C_j - D_j}; q)_{P_j}}. \tag{A.17}$$

We also have

$$\begin{aligned}
& \varphi(\bar{\mathbf{B}} - \bar{\mathbf{D}} - \bar{\mathbf{P}}, \bar{\mathbf{P}}) + \bar{p}(b - d + C_n + 1) + \binom{\bar{p}}{2} + \sum_{j=1}^{n-1} \left(P_j(B_j - D_j) - \binom{P_j}{2} \right) \\
&= \bar{p}(A_n + 1) + \varphi(\bar{\mathbf{P}}, \bar{\mathbf{D}} - \bar{\mathbf{B}}),
\end{aligned} \tag{A.18}$$

since

$$\begin{aligned}
\binom{\bar{p}}{2} &= \varphi(\bar{\mathbf{P}}, \bar{\mathbf{P}}) + \sum_{j=1}^{n-1} \binom{P_j}{2}; & \varphi(\bar{\mathbf{B}} - \bar{\mathbf{D}}, \bar{\mathbf{P}}) + \bar{p}(\bar{d} - \bar{b}) + \sum_{j=1}^{n-1} P_j(B_j - D_j) &= \varphi(\bar{\mathbf{P}}, \bar{\mathbf{D}} - \bar{\mathbf{B}}); \\
\bar{p}(\bar{b} - \bar{d}) + \bar{p}(b - d) + \bar{p}C_n &= \bar{p}(B_n - D_n) + \bar{p}C_n = \bar{p}A_n.
\end{aligned}$$

Inserting (A.17) and (A.18) into (A.16) yields

$$\begin{aligned}
& \lim_{q^\varepsilon \rightarrow \infty} \left(\lim_{q^{\mathfrak{m}} \rightarrow \infty} \mathcal{U}_{q^\varepsilon; q^{\mathfrak{m}}; q^{\mathfrak{m}+\varepsilon}/\gamma}(\mathbf{A}, (\bar{\mathbf{B}}, \mathbf{B}_n); \mathbf{C}, (\bar{\mathbf{D}}, \mathbf{D}_n)) \right) \\
&= q^{\varphi(\bar{\mathbf{D}}, \bar{\mathbf{C}}) + \bar{c}(d - C_n)} \gamma^{C_n} \frac{(q; q)_b}{(q; q)_{d - C_n} (q; q)_{C_n}} (\gamma; q)_\infty \cdot \prod_{j=1}^{n-1} \frac{(q; q)_{C_j + D_j}}{(q; q)_{C_j} (q; q)_{D_j}} \\
&\times \sum_{\bar{\mathbf{P}} \leq \bar{\mathbf{B}}, \bar{\mathbf{C}}} q^{\bar{p}(A_n + 1) + \varphi(\bar{\mathbf{P}}, \bar{\mathbf{D}} - \bar{\mathbf{B}})} \cdot \prod_{j=1}^{n-1} \frac{(q^{-C_j}; q)_{P_j} (q^{-B_j}; q)_{P_j}}{(q^{-C_j - D_j}; q)_{P_j} (q; q)_{P_j}} \\
&\times {}_2\varphi_1 \left(\begin{matrix} q^{-C_n}, q^{-A_n} \\ q^{d - C_n + 1} \end{matrix} \middle| q, q^{\mathbf{B}_n + c - \bar{p} + 1} \gamma^{-1} \right).
\end{aligned}$$

Thus, using (A.4) to write the ${}_2\varphi_1$ basic hypergeometric series as a sum, we obtain

$$\begin{aligned} & \lim_{q^{\mathfrak{L}} \rightarrow \infty} \left(\lim_{q^{\mathfrak{M}} \rightarrow \infty} \mathcal{U}_{q^{\mathfrak{L}}, q^{\mathfrak{M}}; q^{\mathfrak{M}+\mathfrak{L}}/\gamma}(\mathbf{A}, (\overline{\mathbf{B}}, \mathbf{B}_n); \mathbf{C}, (\overline{\mathbf{D}}, \mathbf{D}_n)) \right) \\ &= q^{\varphi(\overline{\mathbf{D}}, \overline{\mathbf{C}}) + \overline{c}(\mathbf{d} - C_n)}(\gamma; q)_{\infty} \frac{(q; q)_{\mathbf{b}}}{(q; q)_{\mathbf{d} - C_n}} \prod_{j=1}^{n-1} \frac{(q; q)_{C_j + D_j}}{(q; q)_{C_j} (q; q)_{D_j}} \\ & \quad \times \sum_{k=0}^{C_n} \frac{\gamma^{C_n - k}}{(q; q)_{C_n}} \frac{(q^{-C_n}; q)_k (q^{-A_n}; q)_k}{(q; q)_k (q^{\mathbf{d} - C_n + 1}; q)_k} q^{k(\mathbf{B}_n + c + 1)} \\ & \quad \times \sum_{\overline{\mathbf{P}} \leq \overline{\mathbf{B}}, \overline{\mathbf{C}}} q^{\overline{p}(\mathbf{A}_n - k + 1) + \varphi(\overline{\mathbf{P}}, \overline{\mathbf{D}} - \overline{\mathbf{B}})} \prod_{j=1}^{n-1} \frac{(q^{-B_j}; q)_{P_j} (q^{-C_j}; q)_{P_j}}{(q; q)_{P_j} (q^{-C_j - D_j}; q)_{P_j}}. \end{aligned}$$

Together with the facts that

$$(q^{-C_n}; q)_k (q; q)_{C_n}^{-1} = (-1)^k q^{\binom{k}{2} - C_n k} (q; q)_{C_n - k}^{-1}; \quad (q^{-A_n}; q)_k = (-1)^k q^{\binom{k}{2} - A_n k} (q^{A_n - k + 1}; q)_k,$$

that $c - C_n = \overline{c}$, and that $\mathbf{d} - C_n = \mathbf{D}_n - \overline{\mathbf{d}} - C_n = \mathbf{B}_n - A_n - \overline{\mathbf{d}}$, this yields the lemma. \square

Remark A.8. By Remark 6.2, Lemma A.3, Lemma A.4, Lemma A.7, and uniqueness of analytic continuation (with the fact that the \mathcal{U}^{qp} weights are rational in $q^{\mathfrak{L}}$, to extend from $\mathfrak{L} \in \mathbb{Z}_{\geq 0}$ to $\mathfrak{L} \in \mathbb{C}$) the \mathcal{U}^{qp} weights are stochastic, in the sense that for any $\mathbf{A} \in \mathbb{Z}_{\geq 0}^n$ and $(\overline{\mathbf{B}}, \mathbf{B}_n) \in \mathbb{Z}_{\geq 0}^{n-1} \times \mathbb{Z}_{\geq 0}$, we have $\sum \mathcal{U}_{\gamma}(\mathbf{A}, (\overline{\mathbf{B}}, \mathbf{B}_n); \mathbf{C}, (\overline{\mathbf{D}}, \mathbf{D}_n)) = 1$, where we sum over all $\mathbf{C} \in \mathbb{Z}_{\geq 0}^n$ and $(\overline{\mathbf{D}}, \mathbf{D}_n) \in \mathbb{Z}_{\geq 0}^{n-1} \times \mathbb{Z}_{\geq 0}$.

A.3. An Additional Degenerated Weight. In this section we provide an additional degeneration of the complemented $U_{z;r,s}$ -weight, which will eventually serve as boundary weights for the polymer model. We begin with the following lemma from [20] providing a specialization of the $U_{z;r,s}$ -weights from Definition 6.1.

Lemma A.9 ([20, Lemma 6.8]). *For any integer $L \geq 1$ and n -tuples $\mathbf{A}, \mathbf{C}, \mathbf{D} \in \mathbb{Z}_{\geq 0}^n$, we have*

$$\lim_{s \rightarrow 0} U_{z/s^2; q^{-L/2}, s}(\mathbf{A}, \mathbf{L}e_n; \mathbf{C}, \mathbf{D}) = \frac{(zq^L)^{|\mathbf{D}|} (q^{-L}; q)_{|\mathbf{D}|}}{(z; q)_L (q; q)_{|\mathbf{D}|}} \cdot \mathbb{1}_{\mathbf{A} + \mathbf{L} \cdot \mathbf{e}_n = \mathbf{C} + \mathbf{D}} \cdot \mathbb{1}_{\mathbf{D} = |\mathbf{D}| \cdot \mathbf{e}_n}.$$

We will next implement the complementation procedure explained in Section A.1 on the weights specialized as in Lemma A.9. The below definition provides the eventual form they will take, which is shown in the corollary following it.

Definition A.10. For any complex numbers $z, \mathfrak{L} \in \mathbb{C}$ and integer $k \geq 0$, define the q -discrete boundary weight

$$\mathcal{U}_{z; q^{\mathfrak{L}}}^{\mathbf{b}; n}(k) = \mathcal{U}_{z; q^{\mathfrak{L}}}^{\mathbf{b}}(k) = z^{-k} \frac{(z^{-1}; q)_{\infty} (q^{-\mathfrak{L}}; q)_k}{(q^{-\mathfrak{L}} z^{-1}; q)_{\infty} (q; q)_k}.$$

We further set

$$\mathcal{U}_z^{\mathbf{b}; n}(k) = \mathcal{U}_z^{\mathbf{b}}(k) = \mathcal{U}_{z; \infty}^{\mathbf{b}}(k) = z^{-k} \frac{(z^{-1}; q)_k}{(q; q)_k}.$$

Observe that both the $\mathcal{U}_{z; q^{\mathfrak{L}}}^{\mathbf{b}}$ -weights and the $\mathcal{U}_z^{\mathbf{b}}$ -weights are stochastic, by the q -binomial theorem.

Corollary A.11. *Adopt the notation of Lemma A.9, and set $\mathbf{D}_n = \mathbf{L} - |\mathbf{D}|$. We have*

$$(A.19) \quad \lim_{s \rightarrow 0} U_{z/s^2; q^{-L/2}, s}(\mathbf{A}, \mathbf{L}e_n; \mathbf{C}, \mathbf{D}) = \mathcal{U}_{z/q^L}^{\mathbf{b}}(\mathbf{D}_n) \cdot \mathbb{1}_{\mathbf{A} + \mathbf{D}_n \cdot \mathbf{e}_n = \mathbf{C}} \cdot \mathbb{1}_{\mathbf{D} = (\mathbf{L} - \mathbf{D}_n) \cdot \mathbf{e}_n}.$$

Proof. We may assume throughout this proof that $\mathbf{A} + \mathbf{L}e_n = \mathbf{C} + \mathbf{D}$ and that $\mathbf{D} = |\mathbf{D}|e_n = (\mathbf{L} - \mathbf{D}_n)e_n$, for otherwise both sides of (A.19) are equal to 0 (by Lemma A.9). Then, combining the equalities

$$(zq^L)^{|\mathbf{D}|} = (zq^L)^{\mathbf{L}-\mathbf{D}_n}; \quad (z; q)_L = (-z)^L q^{\binom{L}{2}} (q^{1-L}z^{-1}; q)_L;$$

$$(q^{-L}; q)_{\mathbf{L}-\mathbf{D}_n} = (-1)^{\mathbf{L}-\mathbf{D}_n} q^{\binom{\mathbf{D}_n+1}{2} - \binom{\mathbf{L}+1}{2}} \frac{(q; q)_L}{(q; q)_{\mathbf{D}_n}}; \quad (q; q)_{\mathbf{L}-\mathbf{D}_n} = (-1)^{\mathbf{D}_n} q^{\binom{\mathbf{D}_n}{2} - \mathbf{L}\mathbf{D}_n} \frac{(q; q)_L}{(q^{-L}; q)_{\mathbf{D}_n}},$$

with Corollary A.11, we deduce

$$\lim_{s \rightarrow 0} U_{z/s^2; q^{-L/2}, s}(\mathbf{A}, \mathbf{L}e_n; \mathbf{C}, \mathbf{D}) = \frac{(zq^L)^{\mathbf{L}-\mathbf{D}_n} (q^{-L}; q)_{\mathbf{L}-\mathbf{D}_n}}{(z; q)_L (q; q)_{\mathbf{L}-\mathbf{D}_n}} = \frac{(qz^{-1})^{\mathbf{D}_n} (q^{-L}; q)_{\mathbf{D}_n}}{(q^{1-L}z^{-1}; q)_L (q; q)_{\mathbf{D}_n}}.$$

This, with Definition A.10, yields the corollary. \square

A.4. The $q \rightarrow 1$ Limit. In this section we analyze the limit as q tends to 1 of the q -discrete polymer weights \mathcal{U}^{qp} from Definition A.5 (and their boundary counterparts \mathcal{U}^{b} from Definition A.10). Throughout this section, we fix a real number $\theta > 0$ and n -tuples of nonnegative real numbers $(\mathbf{a}_1, \mathbf{a}_2, \dots, \mathbf{a}_n)$ and $(\mathbf{b}_1, \mathbf{b}_2, \dots, \mathbf{b}_n)$. Moreover, $\varepsilon \in (0, 1)$ will be a parameter that we view as tending to 0. If for some functions f and g of ε we have $\lim_{\varepsilon \rightarrow 0} |f(\varepsilon) - g(\varepsilon)| = 0$, then we write $f \sim g$. We further let $\mathbf{B}_n = \mathbf{B}_n^\varepsilon \in \mathbb{Z}_{\geq 0}$ be an integer, $\overline{\mathbf{B}} = \overline{\mathbf{B}}^\varepsilon \in \mathbb{Z}_{\geq 0}^{n-1}$ be an $(n-1)$ -tuple, and $\mathbf{A} = \mathbf{A}^\varepsilon \in \mathbb{Z}_{\geq 0}^n$ be an n -tuple (all dependent on ε); throughout this section, we assume that

$$(A.20) \quad \varepsilon A_n - \log \varepsilon^{-1} \sim \mathbf{a}_n; \quad \varepsilon A_j \sim \mathbf{a}_j; \quad \varepsilon \mathbf{B}_n - \log \varepsilon^{-1} = \mathbf{b}_n; \quad \varepsilon B_j \sim \mathbf{b}_j,$$

for each $j \in \llbracket 1, n-1 \rrbracket$. Also define $q = q_\varepsilon \in (0, 1)$ and $\gamma = \gamma_{\varepsilon, \theta} \in (0, 1)$ by setting

$$(A.21) \quad q_\varepsilon = e^{-\varepsilon}; \quad \gamma = q^\theta.$$

Recalling from Remark A.8 that the \mathcal{U}^{qp} weights are stochastic, the following proposition describes the limiting law of the n -tuple \mathbf{C} sampled²⁰ according to $\mathcal{U}_\gamma^{\text{qp}}(\mathbf{A}, \mathbf{B}; \mathbf{C}, \mathbf{D})$ as ε tends to 0; it indicates that this law can be expressed through a single Gamma(θ) random variable \mathfrak{Y} .

Proposition A.12. *Let $q = q_\varepsilon \in (0, 1)$ and $\gamma = \gamma_{\varepsilon, \theta} \in (0, 1)$ be as in (A.21); also let $\mathbf{B}_n \in \mathbb{Z}_{\geq 0}$, $\overline{\mathbf{B}} \in \mathbb{Z}_{\geq 0}^{n-1}$, and $\mathbf{A} \in \mathbb{Z}_{\geq 0}^n$ be as in (A.20). Sample $(\mathbf{C}, (\overline{\mathbf{D}}, \mathbf{D}_n)) \in \mathbb{Z}_{\geq 0}^n \times \mathbb{Z}_{\geq 0}^{n-1} \times \mathbb{Z}_{\geq 0}$ with probability $\mathcal{U}_\gamma^{\text{qp}}(\mathbf{A}, (\overline{\mathbf{B}}, \mathbf{B}_n); \mathbf{C}, (\overline{\mathbf{D}}, \mathbf{D}_n))$, and denote*

$$\mathbf{c}_n = \varepsilon C_n - \log \varepsilon^{-1}, \quad \text{and} \quad \mathbf{c}_j = \varepsilon C_j, \quad \text{for each } j \in \llbracket 1, n-1 \rrbracket.$$

The joint law of $(\mathbf{c}_{[j, n]})_{j \in \llbracket 1, n \rrbracket}$ converges to that of $(\log(e^{\mathbf{a}_{[j, n]} - \mathbf{b}_n + \mathbf{b}_{[j, n-1]}} + 1) - \log \mathfrak{Y})_{j \in \llbracket 1, n \rrbracket}$ as ε tends to 0, where $\mathfrak{Y} \in \mathbb{R}_{> 0}$ is a Gamma(θ) random variable.

Remark A.13. Denoting $(\mathfrak{d}_1, \mathfrak{d}_2, \dots, \mathfrak{d}_n) = (\varepsilon D_1, \varepsilon D_2, \dots, \varepsilon D_{n-1}, \varepsilon D_n - \log \varepsilon^{-1})$ in Proposition A.12, the joint limiting law of $(\mathfrak{d}_{[j, n]})_{j \in \llbracket 1, n \rrbracket}$ is determined by that of $(\mathbf{c}_{[j, n]})_{j \in \llbracket 1, n \rrbracket}$ by arrow conservation.

To establish Proposition A.12, we will express the right side of (A.15) as a convolution of the following two functions, which we will then analyze separately.

²⁰We do not verify here that the $\mathcal{U}_\gamma^{\text{qp}}$ -weights are all nonnegative for fixed $q \in (0, 1)$. However, it can quickly be deduced from the proof of Lemma A.18 below that the sum of the absolute values of all negative $\mathcal{U}_\gamma^{\text{qp}}$ -weights tends to 0, as ε tends to 0. Together with the stochasticity of the \mathcal{U}^{qp} weights, this implies that one can view \mathcal{U}^{qp} as prescribing a probability measure, as ε tends to 0.

Definition A.14. Define the function $\Phi_\varepsilon : \mathbb{Z}_{\geq 0} \rightarrow \mathbb{R}$ by setting, for any integer $\ell \geq 0$,

$$(A.22) \quad \Phi_\varepsilon(\ell) = (\gamma; q)_\infty \cdot \frac{\gamma^\ell}{(q; q)_\ell}.$$

Also define the function $\Psi_\varepsilon : \mathbb{Z}_{\geq 0} \times \mathbb{Z}_{\geq 0}^{n-1}$ by setting, for any integer $k \geq 0$ and $(n-1)$ -tuple $\overline{\mathcal{C}} \in \mathbb{Z}_{\geq 0}^{n-1}$,

$$(A.23) \quad \begin{aligned} \Psi_\varepsilon(k; \overline{\mathcal{C}}) &= q^{\varphi(\overline{\mathcal{D}}, \overline{\mathcal{C}}) + \tau(\mathbb{B}_n - A_n - \overline{d})} \frac{(q; q)_b}{(q; q)_{\mathbb{B}_n - A_n - \overline{d}}} \cdot \prod_{j=1}^{n-1} \frac{(q; q)_{C_j + D_j}}{(q; q)_{C_j} (q; q)_{D_j}} \cdot q^{k(\mathbb{B}_n - A_n + \overline{c} + k)} \\ &\times \frac{(q^{A_n - k + 1}; q)_k}{(q; q)_k (q^{\mathbb{B}_n - A_n - \overline{d} + 1}; q)_k} \sum_{\overline{\mathcal{P}} \leq \overline{\mathcal{B}}, \overline{\mathcal{C}}} q^{\overline{p}(A_n - k + 1) + \varphi(\overline{\mathcal{P}}, \overline{\mathcal{D}} - \overline{\mathcal{B}})} \prod_{j=1}^{n-1} \frac{(q^{-B_j}; q)_{P_j} (q^{-C_j}; q)_{P_j}}{(q; q)_{P_j} (q^{-C_j - D_j}; q)_{P_j}}, \end{aligned}$$

where $\overline{\mathcal{D}} = \overline{\mathcal{A}} + \overline{\mathcal{B}} - \overline{\mathcal{C}}$.

Remark A.15. By Definition A.5, we have

$$(A.24) \quad \mathcal{U}_\gamma^{\text{qp}}(\mathbf{A}, (\overline{\mathcal{B}}, \mathbb{B}_n); \mathbf{C}, (\overline{\mathcal{D}}, \mathbb{D}_n)) = \sum_{k=0}^{C_n} \Phi_\varepsilon(C_n - k) \cdot \Psi_\varepsilon(k; \overline{\mathcal{C}}).$$

Hence, to sample \mathbf{C} as in Proposition A.12, we may first independently sample ℓ and $(k; \overline{\mathcal{C}})$ under the density functions Φ_ε and Ψ_ε (the fact that these give stochastic weights is due to Lemma A.16 below), respectively, and then set $\mathbf{C} = (\overline{\mathcal{C}}, k + \ell)$.

Lemma A.16. *We have*

$$(A.25) \quad \sum_{\ell=0}^{\infty} \Phi_\varepsilon(\ell) = 1; \quad \sum_{\substack{k \geq 0 \\ \overline{\mathcal{C}} \in \mathbb{Z}_{\geq 0}^{n-1}}} \Psi_\varepsilon(k; \overline{\mathcal{C}}) = 1.$$

Proof. The first statement in (A.25) holds by the q -binomial theorem. The second holds since

$$\sum_{\substack{k \geq 0 \\ \overline{\mathcal{C}} \in \mathbb{Z}_{\geq 0}^{n-1}}} \Psi_\varepsilon(k; \overline{\mathcal{C}}) = \sum_{\substack{k, \ell \geq 0 \\ \overline{\mathcal{C}} \in \mathbb{Z}_{\geq 0}^{n-1}}} \Phi_\varepsilon(\ell) \cdot \Psi_\varepsilon(k; \overline{\mathcal{C}}) = \sum_{\substack{C_n \geq 0 \\ \overline{\mathcal{C}} \in \mathbb{Z}_{\geq 0}^{n-1} \\ \mathbf{D} \in \mathbb{Z}_{\geq 0}^n}} \mathcal{U}_\gamma^{\text{qp}}(\mathbf{A}, (\mathbb{B}_n, \overline{\mathcal{B}}); (\overline{\mathcal{C}}, C_n), (\mathbb{D}_n, \overline{\mathcal{D}})) = 1,$$

where in the first equality we used the first statement of (A.25); in the second we used (A.24); and in the third we used the stochasticity of \mathcal{U}^{qp} (from Remark A.8). \square

We next have the following two lemmas that describe the probability measures arising as the limit when ε tends to 0 of those with distribution functions Φ_ε and Ψ_ε . The first shows that the former (as well as the \mathcal{U}_z^b weights from Definition A.10) gives rise to the Gamma(θ) random variable from Proposition A.12; it is due to [40]. The second shows that the latter is given by the delta distribution at a specific pair of real number and $(n-1)$ -tuple; we outline its proof (which is similar to previous results, such as [68, Lemma 8.17] and [20, Proposition 6.19]) in Section A.5 below.

Lemma A.17 ([40, Lemma 2.1]). *The following two statements hold.*

- (1) *Sample $\ell_\varepsilon \in \mathbb{Z}_{\geq 0}$ according to the distribution $\mathbb{P}[\ell_\varepsilon = \ell] = \Phi_\varepsilon(\ell)$. Then, $\varepsilon^{-1} \cdot e^{-\varepsilon \ell_\varepsilon}$ converges in distribution to a Gamma(θ) random variable, as ε tends to 0.*

(2) Sample $\ell_\varepsilon \in \mathbb{Z}_{\geq 0}$ according to the distribution $\mathbb{P}[\ell_\varepsilon = \ell] = \mathcal{U}_{1/\gamma}^b(\ell)$. Then, $\varepsilon^{-1} \cdot e^{-\varepsilon \ell_\varepsilon}$ converges in distribution to a $\text{Gamma}(\theta)$ random variable, as ε tends to 0.

Lemma A.18. Sample an $(n-1)$ -tuple and integer $(\overline{\mathbf{C}}; k) \in \mathbb{Z}_{\geq 0}^{n-1} \times \mathbb{Z}_{\geq 0}$ with probability $\Psi_\varepsilon(\overline{\mathbf{C}}; k)$; denote $\mathbf{c} = (\mathbf{c}_1, \mathbf{c}_2, \dots, \mathbf{c}_{n-1}) = \varepsilon \cdot \overline{\mathbf{C}} \in \mathbb{R}_{\geq 0}^{n-1}$ and $\mathfrak{k} = \varepsilon k \in \mathbb{R}$. As ε tends to 0, we have that

$$(A.26) \quad e^{\mathfrak{k} + \mathbf{c}_{[j, n-1]}} \text{ converges in probability to the constant } e^{\mathfrak{a}_{[j, n]} - \mathfrak{b}_n + \mathfrak{b}_{[j, n-1]}} + 1, \quad \text{for each } j \in \llbracket 1, n \rrbracket.$$

Now we can quickly establish Proposition A.12.

Proof of Proposition A.12. This follows from Remark A.15, Lemma A.17, and Lemma A.18. \square

A.5. Proof Outline of Lemma A.18. In this section we outline the proof of Lemma A.18.

Proof of Lemma A.18 (Outline). First, it is quickly verified that the contribution to the second sum in (A.25) coming from $k \geq (2\varepsilon^{-1}) \log \varepsilon^{-1}$ becomes negligible as ε tends to 0, due to the factor of $q^{k(k+\mathfrak{B}_n - A_n + \overline{\mathfrak{c}})}$ on the right side of (A.23) (namely, the fact that the exponent of q is quadratic in k). We may therefore restrict our attention to when $k \leq (2\varepsilon)^{-1} \log \varepsilon^{-1}$, in which case it can be confirmed that

$$(A.27) \quad \lim_{\varepsilon \rightarrow 0} \sum_{\overline{\mathbf{P}} \leq \overline{\mathbf{B}}, \overline{\mathbf{C}}} q^{\overline{p}(A_n - k + 1) + \varphi(\overline{\mathbf{P}}, \overline{\mathbf{D}} - \overline{\mathbf{B}})} \prod_{j=1}^{n-1} \frac{(q^{-B_j}; q)_{P_j} (q^{-C_j}; q)_{P_j}}{(q; q)_{P_j} (q^{-C_j - D_j}; q)_{P_j}} = 1.$$

Indeed, for sufficiently small ε , we have $q^{\overline{p}(A_n - k + 1)} \leq \varepsilon^{\overline{p}/3}$ (recalling (A.20), (A.21), and the fact that $k \leq (2\varepsilon)^{-1} \log \varepsilon^{-1}$), while the remaining factors in (A.27) grow at most exponentially in \overline{p} (with a uniformly bounded base). Therefore the sum on the left side of (A.27) is asymptotically supported on the term $\overline{\mathbf{P}} = \mathbf{e}_0$, for which $p = 0$, which gives (A.27).

The remaining factors on the right side of (A.23) are nonnegative, since $q \in (0, 1)$. Let us analyze how their k -dependent parts

$$(A.28) \quad F_\varepsilon(k; \overline{\mathbf{C}}) = q^{k(k+\mathfrak{B}_n - A_n + \overline{\mathfrak{c}})} \frac{(q^{A_n - k + 1}; q)_k}{(q; q)_k (q^{\mathfrak{B}_n - A_n - \overline{\mathfrak{d}} + 1}; q)_k},$$

behave as ε tends to 0. Observe for any real numbers $y, z \in \mathbb{R}$ (with $y \geq 0$) that

$$(A.29) \quad \varepsilon \cdot \log(q^{z/\varepsilon}; q)_{\lfloor y/\varepsilon \rfloor} = \varepsilon \sum_{j=0}^{\lfloor y/\varepsilon \rfloor} \log(1 - q^{z/\varepsilon + j}) = \varepsilon \sum_{x \in [0, y] \cap \varepsilon \cdot \mathbb{Z}} \log(1 - e^{-x-z}) \sim \int_0^y \log(1 - e^{-x-z}) dx,$$

as ε tends to 0. Applying this in (A.28), and setting $\mathfrak{k} = \varepsilon k$ and $\overline{\mathbf{c}} = (\mathbf{c}_1, \mathbf{c}_2, \dots, \mathbf{c}_{n-1}) = \varepsilon \cdot \overline{\mathbf{C}}$, we obtain

$$(A.30) \quad \varepsilon \cdot \log F_\varepsilon(k; \overline{\mathbf{C}}) \sim \mathfrak{k}(\mathfrak{a}_n - \mathfrak{b}_n - \mathfrak{k} - \mathbf{c}_{[1, n-1]}) - \int_0^{\mathfrak{k}} \log(1 - e^{-x}) dx$$

$$(A.31) \quad - \int_0^{\mathfrak{k}} \log(1 - e^{\mathfrak{a}_{[1, n]} + \mathfrak{b}_{[1, n-1]} - \mathfrak{b}_n - \mathbf{c}_{[1, n-1]} - x}) dx,$$

where we used the facts that $\bar{d} = \bar{a} + \bar{b} - \bar{c}$ and that $\varepsilon \cdot \log(q^{A_n - k + 1}; q)_k \sim 0$ (as εA_n grows faster than any constant as ε tends to 0, by (A.20)). Denoting the right side of (A.30) by $G(\mathfrak{k})$, we find

$$\begin{aligned} G'(\mathfrak{k}) &= \mathfrak{a}_n - \mathfrak{b}_n - \mathfrak{c}_{[1, n-1]} - 2\mathfrak{k} - \log(1 - e^{-\mathfrak{k}}) - \log(1 - e^{\mathfrak{a}_{[1, n]} + \mathfrak{b}_{[1, n-1]} - \mathfrak{b}_n - \mathfrak{c}_{[1, n-1]} - \mathfrak{k}}); \\ G''(\mathfrak{k}) &= -2 - \frac{e^{-\mathfrak{k}}}{1 - e^{-\mathfrak{k}}} - \frac{e^{\mathfrak{a}_{[1, n]} + \mathfrak{b}_{[1, n-1]} - \mathfrak{b}_n - \mathfrak{c}_{[1, n-1]} - \mathfrak{k}}}{1 - e^{\mathfrak{a}_{[1, n]} + \mathfrak{b}_{[1, n-1]} - \mathfrak{b}_n - \mathfrak{c}_{[1, n-1]} - \mathfrak{k}}} \leq -2 < 0. \end{aligned}$$

Due to the negativity of G'' , we deduce that G is maximized at the solution \mathfrak{k} to the equation $G'(\mathfrak{k}) = 0$, or equivalently to the unique nonnegative solution of

$$(A.32) \quad (e^{\mathfrak{k}} - 1)(e^{\mathfrak{k}} - e^{\mathfrak{a}_{[1, n]} - \mathfrak{b}_n + \mathfrak{b}_{[1, n-1]} - \mathfrak{c}_{[1, n-1]}}) = e^{\mathfrak{a}_n - \mathfrak{b}_n - \mathfrak{c}_{[1, n-1]}}.$$

Hence, as ε tends to 0, the function $F_\varepsilon(k; \overline{\mathbf{C}})$, and thus $\Psi_\varepsilon(k; \overline{\mathbf{C}})$ is maximized when $\varepsilon k = \mathfrak{k}$. By the strict concavity of G , these functions decay exponentially in $\varepsilon^{-1/2} \cdot |\varepsilon k - \mathfrak{k}|$. Hence, sampling $(k; \overline{\mathbf{C}})$ under Ψ , we find that (A.32) must hold as ε tends to 0.

We next analyze the terms in $\Psi_\varepsilon(k; \overline{\mathbf{C}})$ that asymptotically depend on a given C_i . Denoting

$$R = \mathbf{B}_n - A_n - \bar{a} - \bar{b} + k,$$

this quantity is given by (using (A.27) with the fact that $\overline{\mathbf{D}} = \overline{\mathbf{A}} + \overline{\mathbf{B}} - \overline{\mathbf{C}}$)

$$F_{\varepsilon; i}(k; \overline{\mathbf{C}}) = q^{\varphi(\overline{\mathbf{A}} + \overline{\mathbf{B}} - \overline{\mathbf{C}}, \overline{\mathbf{C}}) + \tau(R + \tau)} \frac{1}{(q; q)_{R + \tau}} \frac{1}{(q; q)_{C_i} (q; q)_{A_j + B_j - C_i}}.$$

Using (A.29), and setting

$$(A.33) \quad \mathfrak{r} = \mathfrak{b}_n - \mathfrak{a}_{[1, n]} - \mathfrak{b}_{[1, n-1]} + \mathfrak{k} \sim \varepsilon R; \quad \mathfrak{p}_j = \mathfrak{a}_j + \mathfrak{b}_j,$$

for each $j \in \llbracket 1, n-1 \rrbracket$, it follows that

$$(A.34) \quad \begin{aligned} \varepsilon \cdot \log F_{\varepsilon; i}(k; \overline{\mathbf{C}}) &\sim \sum_{1 \leq j < h \leq n-1} \mathfrak{c}_j \mathfrak{c}_h - \sum_{j=1}^{n-1} \mathfrak{p}_{[1, j-1]} \mathfrak{c}_j - \mathfrak{c}_{[1, n-1]} \mathfrak{r} - \mathfrak{c}_{[1, n-1]}^2 - \int_0^{\mathfrak{r} + \mathfrak{c}_{[1, n-1]}} \log(1 - e^{-x}) dx \\ &\quad - \int_0^{\mathfrak{c}_i} \log(1 - e^{-x}) dx - \int_0^{\mathfrak{p}_i - \mathfrak{c}_i} \log(1 - e^{-x}) dx. \end{aligned}$$

Denoting the right side of (A.34) (as a function in \mathfrak{c}_i) by $G_i(\mathfrak{c}_i)$, we find that

$$\begin{aligned} G'_i(\mathfrak{c}_i) &= \sum_{j \neq i} \mathfrak{c}_j + \mathfrak{p}_{[1, i-1]} - \mathfrak{r} - 2\mathfrak{c}_{[1, n-1]} - \log(1 - e^{-\mathfrak{c}_i}) - \log(1 - e^{-\mathfrak{r} - \mathfrak{c}_{[1, n-1]}}) + \log(1 - e^{\mathfrak{c}_i - \mathfrak{p}_i}) \\ &= \log(1 - e^{\mathfrak{c}_i - \mathfrak{p}_i}) - \mathfrak{p}_{[1, i-1]} - \log(e^{\mathfrak{c}_i} - 1) - \log(e^{\mathfrak{r} + \mathfrak{c}_{[1, n-1]}} - 1), \end{aligned}$$

and hence

$$G''_i(\mathfrak{c}_i) = -\frac{e^{\mathfrak{c}_i - \mathfrak{p}_i}}{1 - e^{\mathfrak{c}_i - \mathfrak{p}_i}} - \frac{e^{\mathfrak{c}_i}}{e^{\mathfrak{c}_i} - 1} - \frac{e^{\mathfrak{r} + \mathfrak{c}_{[1, n-1]}}}{e^{\mathfrak{r} + \mathfrak{c}_{[1, n-1]}} - 1} < -2.$$

Due to this negativity of G''_i , we deduce that G_i is maximized at the solution \mathfrak{c}_i to the equation $G'_i(\mathfrak{c}_i) = 0$, or equivalently the solution of

$$\frac{\mathfrak{e}^{\mathfrak{p}_i} - \mathfrak{e}^{\mathfrak{c}_i}}{\mathfrak{e}^{\mathfrak{c}_i} - 1} = \mathfrak{e}^{\mathfrak{p}_{[1, i]}} \cdot (e^{\mathfrak{r} + \mathfrak{c}_{[1, n-1]}} - 1).$$

Setting

$$(A.35) \quad \eta = \frac{(e^{\mathfrak{r}+\mathfrak{c}_{[1,n-1]}} - 1)e^{\mathfrak{p}_{[1,n-1]}}}{(e^{\mathfrak{r}+\mathfrak{c}_{[1,n-1]}} - 1)e^{\mathfrak{p}_{[1,n-1]}} + 1}, \quad \text{so that} \quad \frac{1-\eta}{\eta} = e^{-\mathfrak{p}_{[1,n-1]}}(e^{\mathfrak{r}+\mathfrak{c}_{[1,n-1]}} - 1)^{-1},$$

it follows that \mathfrak{c}_i solves

$$(A.36) \quad \frac{e^{\mathfrak{c}_i} - 1}{e^{\mathfrak{p}_i} - e^{\mathfrak{c}_i}} = e^{\mathfrak{p}_{[i+1,n-1]}} \cdot \frac{1-\eta}{\eta}, \quad \text{or equivalently} \quad e^{\mathfrak{c}_i} = \frac{\eta + e^{\mathfrak{p}_{[i,n-1]}}(1-\eta)}{\eta + e^{\mathfrak{p}_{[i+1,n-1]}}(1-\eta)}.$$

Hence, as ε tends to 0, the function $F_{\varepsilon;i}(k; \overline{\mathcal{C}})$, and thus $\Psi_\varepsilon(k; \overline{\mathcal{C}})$, is maximized when $\varepsilon C_i = \mathfrak{c}_i$ solves the equation (A.36). By the strict concavity of G_i , these functions decay exponentially in $\varepsilon^{-1/2} \cdot |\varepsilon C_i - \mathfrak{c}_i|$. Hence, sampling $(k; \overline{\mathcal{C}})$ under Ψ , we find that (A.36) must hold for all $i \in \llbracket 1, n-1 \rrbracket$, as ε tends to 0; recall that (A.32) also must hold.

Let us now solve these equations. Fixing some $j \in \llbracket 1, n-1 \rrbracket$, and taking the product in (A.36) over all $i \in \llbracket j, n-1 \rrbracket$, we find that

$$(A.37) \quad e^{\mathfrak{c}_{[j,n-1]}} = \eta + e^{\mathfrak{p}_{[j,n-1]}}(1-\eta), \quad \text{for all } j \in \llbracket 1, n-1 \rrbracket.$$

At $j = 1$, (A.37) gives (using (A.35) and (A.33))

$$(A.38) \quad e^{\mathfrak{c}_{[1,n-1]}} = \frac{e^{\mathfrak{r}+\mathfrak{c}_{[1,n-1]}} + \mathfrak{p}_{[1,n-1]}}{(e^{\mathfrak{r}+\mathfrak{c}_{[1,n-1]}} - 1)e^{\mathfrak{p}_{[1,n-1]}} + 1}, \quad \text{so} \quad e^{\mathfrak{b}_n - \mathfrak{a}_n + \mathfrak{k}} = e^{\mathfrak{r} + \mathfrak{p}_{[1,n-1]}} = \frac{e^{\mathfrak{p}_{[1,n-1]}} - 1}{e^{\mathfrak{c}_{[1,n-1]}} - 1}.$$

Inserting this into (A.32) yields

$$\left(\frac{e^{\mathfrak{a}_n - \mathfrak{b}_n} (e^{\mathfrak{p}_{[1,n-1]}} - 1)}{e^{\mathfrak{c}_{[1,n-1]}} - 1} - 1 \right) \cdot e^{\mathfrak{a}_n - \mathfrak{b}_n} \left(\frac{e^{\mathfrak{p}_{[1,n-1]}} - 1}{e^{\mathfrak{c}_{[1,n-1]}} - 1} - e^{\mathfrak{p}_{[1,n-1]}} - \mathfrak{c}_{[1,n-1]} \right) = e^{\mathfrak{a}_n - \mathfrak{b}_n - \mathfrak{c}_{[1,n-1]}},$$

and thus

$$e^{\mathfrak{a}_n - \mathfrak{b}_n} (e^{\mathfrak{p}_{[1,n-1]}} - 1) (e^{\mathfrak{p}_{[1,n-1]}} - \mathfrak{c}_{[1,n-1]} - 1) = (1 - e^{-\mathfrak{c}_{[1,n-1]}}) (e^{\mathfrak{p}_{[1,n-1]}} - 1).$$

Hence,

$$(A.39) \quad e^{\mathfrak{c}_{[1,n-1]}} = \frac{e^{\mathfrak{a}_n - \mathfrak{b}_n + \mathfrak{p}_{[1,n-1]}} + 1}{e^{\mathfrak{a}_n - \mathfrak{b}_n} + 1}, \quad \text{so} \quad q^{\mathfrak{k}} = e^{\mathfrak{a}_n - \mathfrak{b}_n} + 1.$$

where in the last equality we applied (A.38). Together with (A.33), it follows that

$$e^{\mathfrak{r} + \mathfrak{c}_{[1,n-1]}} = e^{\mathfrak{b}_n - \mathfrak{a}_n - \mathfrak{p}_{[1,n-1]} + \mathfrak{k} + \mathfrak{c}_{[1,n-1]}} = e^{\mathfrak{b}_n - \mathfrak{a}_n - \mathfrak{p}_{[1,n-1]}} + 1,$$

and hence (A.35) implies

$$\eta = \frac{e^{\mathfrak{b}_n - \mathfrak{a}_n}}{e^{\mathfrak{b}_n - \mathfrak{a}_n} + 1}, \quad \text{so} \quad e^{\mathfrak{c}_{[j,n-1]}} = \frac{e^{\mathfrak{a}_n - \mathfrak{b}_n + \mathfrak{p}_{[j,n-1]}} + 1}{e^{\mathfrak{a}_n - \mathfrak{b}_n} + 1}, \quad \text{for any } j \in \llbracket 1, n-1 \rrbracket,$$

where in the last equality we used (A.37). This, together with (A.39) yields (A.26). \square

A.6. The $q \rightarrow 1$ Limiting Weights in Transitional Rows. Recall that in Section A.4 we analyzed the limits of the $\mathcal{U}_\gamma^{\text{qp}}$ weight (from Definition A.5), under the conditions (A.20) of its arguments. While (A.20) may hold in several rows of our eventual fused vertex model converging to the log-gamma polymer, it will not hold in all of them. In particular, there will be some rows in which $A_n = 0$, such as the lowest one in which an arrow of color n enters the system. Such rows may be viewed as “transitional” regions where the “dominant color” changes from $n-1$ to n , in the sense that vertices output about $\varepsilon^{-1} \log \varepsilon^{-1}$ vertical arrows of color $n-1$ in the previous row, but they output about $\varepsilon^{-1} \log \varepsilon^{-1}$ vertical arrows of color n in this one.

In this section we analyze the limit as q tends to 1 of the $\mathcal{U}_\gamma^{\text{qp}}$ weight, under this regime $A_n = 0$. Throughout this section, we fix a real number $\theta > 0$ and nonnegative real numbers $(\mathbf{a}_1, \mathbf{a}_2, \dots, \mathbf{a}_{n-1})$ and $(\mathbf{b}_1, \mathbf{b}_2, \dots, \mathbf{b}_n)$. Moreover, let $\varepsilon \in (0, 1)$ be a real number; set $q = q_\varepsilon$ and $\gamma = \gamma_{\varepsilon, \theta}$ as in (A.21); let $\mathbf{B}_n = \mathbf{B}_n^\varepsilon \in \mathbb{Z}_{\geq 0}$ be an integer; and let $\overline{\mathbf{A}} = \overline{\mathbf{A}}^\varepsilon$ and $\overline{\mathbf{B}} = \overline{\mathbf{B}}^\varepsilon \in \mathbb{Z}_{\geq 0}^{n-1}$ be $(n-1)$ -tuples of integers such that for some (uniformly bounded) integer $\beta \geq 1$ we have

$$(A.40) \quad \begin{aligned} \varepsilon A_j &\sim \mathbf{a}_j, \quad \text{and} \quad \varepsilon B_j \sim \mathbf{b}_j, \quad \text{for each } j \in \llbracket 1, n-2 \rrbracket; \\ \varepsilon A_{n-1} - \log \varepsilon^{-1} &\sim \mathbf{a}_{n-1}; \quad A_n = 0; \quad \varepsilon B_{n-1} - (\beta-1) \log \varepsilon^{-1} \sim \mathbf{b}_{n-1}; \quad \varepsilon \mathbf{B}_n - \beta \log \varepsilon^{-1} \sim \mathbf{b}_n. \end{aligned}$$

The following lemma describes the limiting law of the n -tuple \mathbf{C} sampled according to the stochastic weight $\mathcal{U}_\gamma^{\text{qp}}$ (from Definition A.5), as ε tends to 0.

Lemma A.19. *Let $q = q_\varepsilon \in (0, 1)$ and $\gamma = \gamma_{\varepsilon, \theta} \in (0, 1)$ be as in (A.21); also let $\mathbf{B}_n \in \mathbb{Z}_{\geq 0}$, $\overline{\mathbf{B}} \in \mathbb{Z}_{\geq 0}^{n-1}$, and $\mathbf{A} \in \mathbb{Z}_{\geq 0}^n$ be as in (A.40). Sample $(\mathbf{C}, (\overline{\mathbf{D}}, \mathbf{D}_n)) \in \mathbb{Z}_{\geq 0}^n \times \mathbb{Z}_{\geq 0}^{n-1} \times \mathbb{Z}_{\geq 0}$ with probability $\mathcal{U}_\gamma^{\text{qp}}(\mathbf{A}, (\overline{\mathbf{B}}, \mathbf{B}_n); \mathbf{C}, (\overline{\mathbf{D}}, \mathbf{D}_n))$, and denote*

$$\mathbf{c}_n = \varepsilon C_n - \log \varepsilon^{-1}, \quad \text{and} \quad \mathbf{c}_j = \varepsilon C_j, \quad \text{for each } j \in \llbracket 1, n-1 \rrbracket.$$

The the joint law of $(\mathbf{c}_{[j,n]})_{j \in \llbracket 1, n \rrbracket}$ converges to that of $(\log(e^{\mathbf{a}_{[j,n-1]} - \mathbf{b}_n + \mathbf{b}_{[j,n-1]}} + 1) - \log \mathfrak{Y})_{j \in \llbracket 1, n-1 \rrbracket}$ as ε tends to 0, where $\mathfrak{Y} \in \mathbb{R}_{>0}$ is a $\text{Gamma}(\theta)$ random variable.

Remark A.20. Set $(\mathbf{d}_1, \mathbf{d}_2, \dots, \mathbf{d}_n) = (\varepsilon D_1, \varepsilon D_2, \dots, \varepsilon D_{n-2}, \varepsilon D_{n-1} - \beta \log \varepsilon^{-1}, \varepsilon D_n - (\beta+1) \log \varepsilon^{-1})$ in Lemma A.19. Then, the joint limiting law of $(\mathbf{d}_{[j,n]})_{j \in \llbracket 1, n \rrbracket}$ is determined by that of $(\mathbf{c}_{[j,n]})_{j \in \llbracket 1, n \rrbracket}$ by arrow conservation.

Remark A.21. Observe in Lemma A.19 that the limiting law of $(\mathbf{c}_{[j,n]})_{j \in \llbracket 1, n \rrbracket}$ is independent of β , which will be useful in the proof of Theorem A.23 below.

Proof of Lemma A.19 (Outline). The proof of this lemma is similar to that of Proposition A.12, and so we only briefly outline it. Recalling the notation from Definition A.14, Remark A.15 indicates that, to sample \mathbf{C} , we may first sample ℓ and $(k; \overline{\mathbf{C}})$ under the density functions Φ_ε and Ψ_ε , respectively, and then set $\mathbf{C} = (\overline{\mathbf{C}}; k + \ell)$. By Lemma A.17, the law of $\varepsilon^{-1} \cdot e^{-\varepsilon \ell}$ converges to a $\text{Gamma}(\theta)$ random variable \mathfrak{Y} , as ε tends to 0. Hence, it suffices to show that $\varepsilon C_{[j,n-1]}$ converges to $\log(e^{\mathbf{a}_{[j,n-1]} - \mathbf{b}_n + \mathbf{b}_{[j,n-1]}} + 1)$ as ε tends to 0, if $\overline{\mathbf{C}} = (C_1, C_2, \dots, C_{n-1}) \in \mathbb{Z}_{\geq 0}^{n-1}$ is sampled according to Ψ_ε .

By the factor of $(q^{A_n - k + 1}; q)_k$ on the right side of (A.23), and the fact that $A_n = 0$, we must have $k = 0$ almost surely under Ψ_ε . Then, recalling (A.3) and the fact that $\overline{\mathbf{D}} = \overline{\mathbf{A}} + \overline{\mathbf{B}} - \overline{\mathbf{C}}$ in (A.23), it follows that

$$(A.41) \quad \begin{aligned} \Psi_\varepsilon(0; \overline{\mathbf{C}}) &= q^{\varphi(\overline{\mathbf{A}} + \overline{\mathbf{B}} - \overline{\mathbf{C}}, \overline{\mathbf{C}}) + \bar{c}(\mathbf{B}_n - \bar{a} - \bar{b} + \bar{c})} \frac{(q; q)_{\mathbf{B}_n - \bar{b}}}{(q; q)_{\mathbf{B}_n - \bar{a} - \bar{b} + \bar{c}}} \cdot \prod_{j=1}^{n-1} \frac{(q; q)_{A_j + B_j}}{(q; q)_{C_j} (q; q)_{A_j + B_j - C_j}} \\ &\times \sum_{\overline{\mathbf{P}} \leq \overline{\mathbf{B}}, \overline{\mathbf{C}}} q^{\bar{p} + \varphi(\overline{\mathbf{P}}, \overline{\mathbf{D}} - \overline{\mathbf{B}})} \prod_{j=1}^{n-1} \frac{(q^{-B_j}; q)_{P_j} (q^{-C_j}; q)_{P_j}}{(q; q)_{P_j} (q^{-A_j - B_j}; q)_{P_j}}. \end{aligned}$$

We first restrict to the case when $\bar{c} = \mathcal{O}(\varepsilon^{-1})$, by showing that otherwise $|\Psi_\varepsilon(0; \overline{\mathbf{C}})|$ would decay faster than $e^{-\varepsilon \bar{c}^2/3}$ and therefore become negligible. Indeed, since $C_j \leq A_j + B_j = \mathcal{O}(\varepsilon^{-1})$ for $j \in \llbracket 1, n-2 \rrbracket$ by (A.40), it suffices to verify that $|\Psi_\varepsilon(0; \overline{\mathbf{C}})| \leq e^{\mathcal{O}(C_{n-1}) - \varepsilon C_{n-1}^2/2}$ if εC_{n-1}

is sufficiently large. To that end, first observe since $\varepsilon(\mathbf{B}_n - \bar{a} - \bar{b}) = \mathcal{O}(1)$ by (A.40), we have $q^{\bar{c}(\mathbf{B}_n - \bar{a} - \bar{b} + \bar{c})} \leq q^{\bar{c}^2 - \mathcal{O}(C_{n-1}/\varepsilon)} \leq e^{\mathcal{O}(C_{n-1}) - \varepsilon C_{n-1}^2}$. Moreover (since $|(q^{-B_j}; q)_{P_j}| < |(q^{-A_j - B_j}; q)_{P_j}|$), the remaining terms on the right side of (A.41) decay at most exponentially in ε^{-1} , except for the term $(q^{-C_{n-1}}; q)_{P_{n-1}}(q; q)_{P_{n-1}}^{-1}$, which is at most $e^{\mathcal{O}(C_{n-1}) - \varepsilon C_{n-1}^2/2}$. Therefore, $|\Psi_\varepsilon(0; \bar{\mathbf{C}})| \leq e^{\mathcal{O}(C_{n-1}) - \varepsilon C_{n-1}^2/2}$, which verifies the above-mentioned decay.

Thus we may assume $\bar{c} = \mathcal{O}(\varepsilon^{-1})$, so $\varepsilon(D_{n-1} - B_{n-1}) = \varepsilon(A_{n-1} - C_{n-1}) = \log \varepsilon^{-1} - \mathcal{O}(1)$. Due to factor of $q^{\varphi(\bar{\mathbf{P}}, \bar{\mathbf{D}} - \bar{\mathbf{B}})}$ in the sum on the right side of (A.41) (and the fact that the remaining terms in the sum grow at most exponentially in $|\bar{\mathbf{P}}|$), one can verify that this sum is asymptotically supported on the $\mathbf{P} \in \mathbb{Z}_{>0}^{n-1}$ satisfying $P_j = 0$ for $j \in \llbracket 1, n-2 \rrbracket$. Moreover, due to the fact that $|(q^{-B_{n-1}}; q)_{P_{n-1}}(q^{-C_{n-1}}; q)_{P_{n-1}}^{-1}(q; q)_{P_{n-1}}^{-1}(q^{-A_{n-1} - B_{n-1}}; q)_{P_{n-1}}^{-1}|$ decays as $q^{P_{n-1}(A_{n-1} - C_{n-1})}$, the asymptotic support of this sum also requires $P_{n-1} = 0$, and hence $\mathbf{P} = \mathbf{e}_0$. Thus, to understand the behavior of $(k; \bar{\mathbf{C}}) = (0; \bar{\mathbf{C}})$ sampled from the density function Ψ_ε , it suffices to understand the limiting behavior as ε tends to 0 of

$$\tilde{\Psi}_\varepsilon(0; \bar{\mathbf{C}}) = q^{\varphi(\bar{\mathbf{A}} + \bar{\mathbf{B}} - \bar{\mathbf{C}}, \bar{\mathbf{C}}) + \bar{c}(\mathbf{B}_n - \bar{a} - \bar{b} + \bar{c})} \frac{(q; q)_{\mathbf{B}_n - \bar{b}}}{(q; q)_{\mathbf{B}_n - \bar{a} - \bar{b} + \bar{c}}} \cdot \prod_{j=1}^{n-1} \frac{(q; q)_{A_j + B_j}}{(q; q)_{C_j} (q; q)_{A_j + B_j - C_j}}.$$

As in the proof of Lemma A.18, the $\bar{\mathbf{C}}$ that contribute to $\tilde{\Psi}_\varepsilon$ will asymptotically be supported on a single value of $\bar{\mathbf{c}} = (\mathbf{c}_1, \mathbf{c}_2, \dots, \mathbf{c}_{n-1}) = \varepsilon \cdot \bar{\mathbf{C}}$. To understand which value, we take the logarithm of the part of $\tilde{\Psi}_\varepsilon$ that depends on $\bar{\mathbf{C}}$, and multiply by ε to obtain (using (A.29) and the facts that $\varepsilon(A_{n-1} + B_{n-1} - C_{n-1}) \geq \log \varepsilon^{-1} - \mathcal{O}(1)$) the function

$$\begin{aligned} G_\varepsilon(\bar{\mathbf{c}}) &= \mathbf{c}_{[1, n-1]} \cdot (\mathbf{p}_{[1, n-1]} - \mathbf{b}_n - \mathbf{c}_{[1, n-1]}) - \sum_{j=1}^{n-1} \mathbf{p}_{[1, j-1]} \mathbf{c}_j - \sum_{j=1}^{n-1} \int_0^{\mathbf{c}_j} \log(1 - e^{-x}) dx \\ &\quad + \sum_{1 \leq j < h \leq n-1} \mathbf{c}_j \mathbf{c}_h - \int_0^{\mathbf{b}_n - \mathbf{p}_{[1, n-1]} + \mathbf{c}_{[1, n-1]}} \log(1 - e^{-x}) dx - \sum_{j=1}^{n-2} \int_0^{\mathbf{p}_j - \mathbf{c}_j} \log(1 - e^{-x}) dx, \end{aligned}$$

where we have denoted $\mathbf{p}_j = \mathbf{a}_j + \mathbf{b}_j$ for each $j \in \llbracket 1, n-1 \rrbracket$. The $\bar{\mathbf{C}}$ that contributes to $\tilde{\Psi}_\varepsilon$ is then obtained at the maximum of G_ε , which is the solution of $\partial_{\mathbf{c}_i} G_\varepsilon(\bar{\mathbf{c}}) = 0$ for each $i \in \llbracket 1, n-1 \rrbracket$. These equations are given by

$$\begin{aligned} \log(e^{\mathbf{p}^i} - e^{\mathbf{c}^i}) - \log(e^{\mathbf{c}^i} - 1) - \mathbf{p}_{[1, i]} - \log(e^{\mathbf{b}_n + \mathbf{c}_{[1, n-1]} - \mathbf{p}_{[1, n-1]}} - 1) &= 0, \quad \text{for } i \in \llbracket 1, n-2 \rrbracket; \\ -\log(e^{\mathbf{c}^{n-1}} - 1) - \log(e^{\mathbf{c}_{[1, n-1]} + \mathbf{b}_n - \mathbf{p}_{[1, n-1]}} - 1) - \mathbf{p}_{[1, n-2]} &= 0. \end{aligned}$$

Denoting

$$(A.42) \quad \eta = \frac{e^{\mathbf{b}_n + \mathbf{c}_{[1, n-1]} - \mathbf{p}_{[1, n-1]}}}{e^{\mathbf{b}_n + \mathbf{c}_{[1, n-1]} - \mathbf{p}_{[1, n-1]}} - 1}, \quad \text{so that} \quad \frac{1}{\eta - 1} = e^{\mathbf{b}_n + \mathbf{c}_{[1, n-1]} - \mathbf{p}_{[1, n-1]}} - 1,$$

it follows that

$$e^{\mathbf{c}^j} = e^{\mathbf{p}^j} \cdot \frac{e^{\mathbf{p}_{[1, j-1]}} + \eta - 1}{e^{\mathbf{p}_{[1, j]}} + \eta - 1}, \quad \text{for each } j \in \llbracket 1, n-2 \rrbracket; \quad e^{\mathbf{c}^{n-1}} = e^{-\mathbf{p}_{[1, n-2]}} (\eta - 1 + e^{\mathbf{p}_{[1, n-2]}}).$$

Thus, for each $j \in \llbracket 1, n-1 \rrbracket$, we have

$$e^{\mathbf{c}^{[j, n-1]}} = e^{-\mathbf{p}_{[1, j-1]}} \cdot (e^{\mathbf{p}_{[1, j-1]}} + \eta - 1),$$

which taken at $j = 1$ implies that $\eta = e^{c_{[1,n-1]}}$. Together with (A.42), this yields $\eta = e^{c_{[1,n-1]}} = e^{\mathfrak{P}_{[1,n-1]}^{-b_n} + 1}$, and therefore

$$(A.43) \quad e^{c_{[j,n-1]}} = e^{\mathfrak{P}_{[j,n-1]}^{-b_n} + 1}.$$

Hence, if we sample $\overline{\mathbf{C}}$ according to Ψ_ε and set $\overline{\mathbf{c}} = (c_1, c_2, \dots, c_{n-1}) = \varepsilon \cdot \overline{\mathbf{C}}$, then (A.43) holds. As mentioned previously, this (with Remark A.15 and Lemma A.17) implies the lemma. \square

A.7. Convergence to the Log-Gamma Polymer. In this section we show convergence of a stochastic vertex model with weights $\mathcal{U}_\gamma^{\text{qp}}$ and $\mathcal{U}_{1/\gamma}^{\text{b}}$ (from Definition A.5 and Definition A.10) to the log-gamma polymer. We begin by defining the latter; throughout this section, we fix positive real parameters $\boldsymbol{\theta} = (\theta_1, \theta_2, \dots)$ and $\boldsymbol{\theta}' = (\theta'_1, \theta'_2, \dots)$.

For each vertex $(i, j) \in \mathbb{Z}_{>0}^2$, let \mathfrak{Y}_{ij} denote a $\text{Gamma}(\theta_i + \theta'_j)$ random variable, with all (\mathfrak{Y}_{ij}) mutually independent over $(i, j) \in \mathbb{Z}_{>0}^2$. For any vertices $u, v \in \mathbb{Z}_{>0}^2$ such that $v - u \in \mathbb{Z}_{\geq 0}^2$, a directed path $\mathcal{P} = (w_0, w_1, \dots, w_k) \in \mathbb{Z}_{>0}^2$ from u to v is a sequence of vertices starting at $w_0 = u$, ending at $w_k = v$, and satisfying $w_i - w_{i-1} \in \{(1, 0), (0, 1)\}$ for each $i \in \llbracket 1, k \rrbracket$. The *polymer weight* of such a directed path is defined to be

$$(A.44) \quad \mathfrak{Z}(\mathcal{P}) = \prod_{(i,j) \in \mathcal{P}} \mathfrak{Y}_{ij}^{-1},$$

and the *point-to-point partition function* from u to v is defined to be

$$(A.45) \quad \mathfrak{Z}(u \rightarrow v) = \sum_{\mathcal{P}} \mathfrak{Z}(\mathcal{P}),$$

where the sum is over all directed paths $\mathcal{P} \subset \mathbb{Z}_{>0}^2$ from u to v .

Now let us describe the stochastic vertex model that converges to the log-gamma polymer. To that end, let $\varepsilon \in (0, 1)$ denote a real number, and set

$$q = q_\varepsilon = e^{-\varepsilon}, \quad \text{and} \quad \gamma_{ij} = q^{\theta_i + \theta'_j}, \quad \text{for each } (i, j) \in \mathbb{Z}_{>0}^2.$$

Fix (possibly infinite) integers $K_1, K_2, \dots \geq 1$. At any vertex $(i, j) \in \mathbb{Z}_{>0}^2$, we will sample a random colored (complemented) arrow configuration $(\mathbf{A}(i, j), (\overline{\mathbf{B}}(i, j), \mathbf{B}_m(i, j)); \mathbf{C}(i, j), (\overline{\mathbf{D}}(i, j), \mathbf{D}_m(i, j)))$, where $\mathbf{B}_m(i, j), \mathbf{D}_m(i, j) \in \mathbb{Z}_{\geq 0}$; $\overline{\mathbf{B}}(i, j), \overline{\mathbf{D}}(i, j) \in \mathbb{Z}_{\geq 0}^{m-1}$; and $\mathbf{A}(i, j), \mathbf{C}(i, j) \in \mathbb{Z}_{\geq 0}^m$. Here, $m = m(j) \geq 1$ is the (unique) positive integer such that $K_{\llbracket 1, m-1 \rrbracket} + 1 \leq j \leq K_{\llbracket 1, m \rrbracket}$. These arrow configurations will be consistent, in the sense that $\mathbf{A}(i, j+1) = \mathbf{C}(i, j)$ and $(\overline{\mathbf{B}}(i+1, j), \mathbf{B}_m(i+1, j)) = (\overline{\mathbf{D}}(i, j), \mathbf{D}_m(i, j))$ for each $(i, j) \in \mathbb{Z}_{>0}^2$ (where if $j = K_{\llbracket 1, m \rrbracket}$, the m -tuple $\mathbf{C}(i, j)$ is interpreted as an $(m+1)$ -tuple by setting its $(m+1)$ -th entry to 0).

We will sample these arrow configurations recursively on triangles of the form $\mathbb{T}_N = \{(x, y) \in \mathbb{Z}_{>0}^2 : x+y \leq N\}$. Given some integer $N \geq 1$, suppose that arrow configurations have been assigned to all vertices in \mathbb{T}_{N-1} ; we will explain how to sample them on \mathbb{T}_N . Fix a vertex on the diagonal $(i, j) \in \mathbb{D}_N = \mathbb{T}_N \setminus \mathbb{T}_{N-1}$. First, set $\mathbf{A}(N-1, 1) = \mathbf{e}_0$, $\overline{\mathbf{B}}(1, N-1) = \mathbf{e}_0$, and $\mathbf{B}_{m(N-1)}(1, N-1) = 0$. Then, if $i = 1$ set $\overline{\mathbf{D}}(1, j) = \mathbf{e}_0$, and inductively define $\mathbf{C}(1, j) = \mathbf{A}(1, j) + \mathbf{D}_{m(j)}(1, j) \cdot \mathbf{e}_{m(j)}$, where $\mathbf{D}_m(1, j)$ is sampled according to the probability (recalling Definition A.10)

$$(A.46) \quad \mathbb{P}[\mathbf{D}_m(1, j) = k] = \mathcal{U}_{1/\gamma_{1,j}}^{\text{b};m}(k)$$

If $i > 1$, then the inputs $\mathbf{A}(i, j) = \mathbf{C}(i, j-1)$ and $(\overline{\mathbf{B}}(i, j), \mathbf{B}_m(i, j)) = (\overline{\mathbf{D}}(i-1, j), \mathbf{D}_m(i-1, j))$ at (i, j) have already been assigned (as they arise from arrow configurations at vertices

in \mathbb{T}_{N-1}). Sample its outputs $(\mathbf{C}(i, j), (\overline{\mathbf{D}}(i, j), \mathbf{D}_m(i, j)))$ according to the probability (recalling Definition A.5)

$$\begin{aligned} & \mathbb{P} \left[\left(\mathbf{C}(i, j), (\overline{\mathbf{D}}(i, j), \mathbf{D}_m(i, j)) \right) \middle| \left(\mathbf{A}(i, j), (\overline{\mathbf{B}}(i, j), \mathbf{B}_m(i, j)) \right) \right] \\ &= \mathcal{U}_{\gamma_{ij}}^{\mathbf{b}; m} \left(\mathbf{A}(i, j), (\overline{\mathbf{B}}(i, j), \mathbf{B}_m(i, j)); \mathbf{C}(i, j), (\overline{\mathbf{D}}(i, j), \mathbf{D}_m(i, j)) \right). \end{aligned}$$

This assigns a random arrow configuration to each vertex in \mathbb{T}_N ; letting N tend to ∞ yields a random ensemble of arrow configurations on the quadrant $\mathbb{Z}_{>0}^2$.

Observe in this way that, by (A.46), arrows of color n begin to enter the system through its $(\mathbf{K}_{[1, n-1]} + 1)$ -st row. As in Section A.6, we will sometimes refer to such rows as *transitional* (as they will be where the most frequent color transitions from $n - 1$ to n). Moreover, due to the forms (from Definition A.5) of the weights \mathcal{U}^{ap} , arrow conservation in the ensemble sampled above appears slightly different from that in the colored fused path ensembles introduced in Section 6.1. Here, it depends on the vertex $(i, j) \in \mathbb{Z}_{>0}^2$, and in particular on the index²¹ $m(j)$ associated with its row; it is given by

$$(A.47) \quad \overline{\mathbf{A}}(i, j) + \overline{\mathbf{B}}(i, j) = \overline{\mathbf{C}}(i, j) + \overline{\mathbf{D}}(i, j); \quad \mathbf{B}_{m(j)}(i, j) - \mathbf{A}_{m(j)}(i, j) = \mathbf{D}_{m(j)}(i, j) - \mathbf{C}_{m(i, j)}(i, j).$$

Still, we will explain how the above ensemble arises from the colored stochastic fused vertex model (from Section 6.1) in Remark A.24 below.

To state convergence of this model to the log-gamma polymer, we need to prescribe an associated height function. Given an integer $c \geq 1$, define the color (at least) c height functions $\mathfrak{h}_c^{\rightarrow}, \mathfrak{h}_{\geq c}^{\rightarrow} : \mathbb{Z}_{\geq 0}^2 \rightarrow \mathbb{Z}$ by for any $(i, j) \in \mathbb{Z}_{\geq 0}^2$ setting (where we let $X_c = 0$ for any $\mathbf{X} \in \mathbb{Z}^n$ and $c > n$)

$$(A.48) \quad \mathfrak{h}_c^{\rightarrow}(i, j) = - \sum_{k=1}^j \mathbb{1}_{c=m(k)} \cdot \mathbf{D}_{m(k)}(1, k) - \sum_{k=2}^i \mathbf{C}_c(k, j); \quad \mathfrak{h}_{\geq c}^{\rightarrow}(i, j) = \sum_{c'=c}^{\infty} \mathfrak{h}_{c'}(i, j).$$

Remark A.22. The height functions are defined above by summing (negative) entries of arrow configurations along the specific up-right path from $(1, 1)$ to (i, j) that first proceeds north to $(1, j)$ and then east to (i, j) . Using arrow conservation (A.47), one obtains the same result by replacing this by any up-right path. For instance, by instead considering the path that first proceeds east to $(i, 1)$ and then north to (i, j) , we also have

$$\mathfrak{h}_c^{\rightarrow}(i, j) = \sum_{k=1}^j \mathbb{1}_{c < m(k)} \cdot \mathbf{D}_c(i, k) - \sum_{k=1}^j \mathbb{1}_{c=m(k)} \cdot \mathbf{D}_{m(k)}(i, k) - \sum_{k=2}^i \mathbb{1}_{c \leq m(i)} \cdot \mathbf{C}_c(k, 1).$$

Given this notation, we have the following theorem. It indicates the convergence, as ε tends to 0, of the height functions for the above vertex model to the point-to-point polymer partition functions of the log-gamma polymer. Observe in this result that the colors are lost in the polymer degeneration, and they instead track one endpoint of the polymer.

Theorem A.23. *Under the above setup, the random variables $\mathfrak{X}_c^\varepsilon(i, j) = \varepsilon^{i+j} \cdot e^{-\varepsilon \mathfrak{h}_{\geq c}^{\rightarrow}(i, j)}$ converge to the log-gamma polymer partition functions $\mathfrak{Z}((1, \mathbf{K}_{[1, c-1]} + 1) \rightarrow (i, j))$, as ε tends to 0, jointly over all (c, i, j) in compact subsets of $\mathbb{Z}_{>0} \times \mathbb{Z}_{>0} \times \mathbb{Z}_{>0}$.*

²¹This is related to the fact that we are implicitly ‘‘complementing’’ the arrows of color $m(j)$ on the j -th row.

Proof. For each $(i, j) \in \mathbb{Z}_{>0}^2$, let $\mathfrak{Y}_{ij} = \mathfrak{Y}_{i,j}$ denote a $\text{Gamma}(\theta_i + \theta'_j)$ random variable, with all (\mathfrak{Y}_{ij}) mutually independent over $(i, j) \in \mathbb{Z}_{>0}^2$. Further set $\mathfrak{Z}_c(i, j) = \mathfrak{Z}((1, K_{[1,c-1]} + 1) \rightarrow (i, j))$ for each $c \in \mathbb{Z}_{>0}$ and $(i, j) \in \mathbb{Z}_{>0}^2$. Then, it follows from (A.44) and (A.45) that for $c > 0$ the $\mathfrak{Z}_c(i, j)$ are determined by the recursive relations

$$(A.49) \quad \begin{aligned} \mathfrak{Z}_c(i, j) &= \mathfrak{Y}_{ij}^{-1} \cdot (\mathfrak{Z}_c(i-1, j) + \mathfrak{Z}_c(i, j-1)), \quad \text{for } (i, j) \in \mathbb{Z}_{>1} \times \mathbb{Z}_{>K_{[1,c-1]}+1}; \\ \mathfrak{Z}_c(1, j) &= \mathfrak{Y}_{1j}^{-1} \cdot \mathfrak{Z}_c(1, j-1), \quad \text{for } j \geq K_{[1,c-1]} + 1; \\ \mathfrak{Z}_c(i, K_{[1,c-1]} + 1) &= \mathfrak{Y}_{i, K_{[1,c-1]}+1}^{-1} \cdot \mathfrak{Z}_c(i-1, K_{[1,c-1]} + 1), \quad \text{for } i \geq 2; \\ \mathfrak{Z}_c(1, K_{[1,c-1]} + 1) &= \mathfrak{Y}_{1, K_{[1,c-1]}+1}^{-1}. \end{aligned}$$

It therefore suffices to show that $\mathfrak{X}_c^\varepsilon(i, j)$ satisfies the same recursion, as ε tends to 0.

To that end let us analyze the behavior, as ε tends to 0, of the dynamics for the arrow configurations $(\mathbf{A}(i, j), (\overline{\mathbf{B}}(i, j), \mathbf{B}_{m(j)}(i, j)); \mathbf{C}(i, j), (\overline{\mathbf{D}}(i, j), \mathbf{D}_{m(j)}(i, j)))$. First observe from (A.46) and the second part of Lemma A.17 that for each $j \geq 1$ we have $B_c(1, j) = D_c(1, j) = 0$ for $c \neq m(j)$, and $\mathbf{B}_{m(j)}(1, j) = 0$ and $\mathbf{D}_{m(j)}(1, j) = \varepsilon^{-1} \log \varepsilon^{-1} + \mathcal{O}(\varepsilon^{-1})$; more specifically, we have

$$(A.50) \quad \varepsilon \cdot e^{\varepsilon \mathbf{D}_{m(j)}(1, j)} \quad \text{converges in distribution to} \quad \mathfrak{Y}_{1j}^{-1}, \quad \text{as } \varepsilon \text{ tends to } 0.$$

We will next understand the behavior of these arrow configurations for $(i, j) \in \mathbb{Z}_{>1} \times \mathbb{Z}_{>0}$. We will see that their behavior depends on whether j is a transitional row, that is, if $j = K_{[1, m(j)-1]} + 1$. In particular, we will show the following by induction on the lexicographic pair (j, i) ; here, we abbreviate $m = m(j)$, and $(\mathfrak{z}_1(i, j), \mathfrak{z}_2(i, j), \dots, \mathfrak{z}_m(i, j))$ are some real numbers that are bounded by a random number independent of ε , for each index $\mathfrak{z} \in \{\mathbf{a}, \mathbf{b}, \mathbf{c}, \mathbf{d}\}$. If $j = K_{[1, m-1]} + 1$ indexes a transitional row, then we will show

$$(A.51) \quad \begin{aligned} A_{m-1}(i, j) &= \varepsilon^{-1} \log \varepsilon^{-1} + \varepsilon^{-1} \mathbf{a}_{m-1}(i, j); & B_{m-1}(i, j) &= (i-2) \cdot \varepsilon^{-1} \log \varepsilon^{-1} + \varepsilon^{-1} \mathbf{b}_{m-1}(i, j); \\ C_{m-1}(i, j) &= \varepsilon^{-1} \mathbf{c}_{m-1}(i, j); & D_{m-1}(i, j) &= (i-1) \cdot \varepsilon^{-1} \log \varepsilon^{-1} + \varepsilon^{-1} \mathbf{d}_{m-1}(i, j); \\ A_m(i, j) &= 0; & \mathbf{B}_m(i, j) &= (i-1) \cdot \varepsilon^{-1} \log \varepsilon^{-1} + \varepsilon^{-1} \mathbf{b}_m(i, j); \\ C_m &= \varepsilon^{-1} \log \varepsilon^{-1} + \varepsilon^{-1} \mathbf{c}_m(i, j); & \mathbf{D}_m(i, j) &= i \cdot \varepsilon^{-1} \log \varepsilon^{-1} + \varepsilon^{-1} \mathbf{d}_m(i, j). \end{aligned}$$

In this way, the transitional row ‘‘absorbs’’ most color $m-1$ arrows from the previous row, and also ‘‘emits’’ arrows of color m ; due to the arrow conservation (A.47), this leads to an accumulation of arrows of both colors $m-1$ and m in this row. If instead $j > K_{[1, m-1]} + 1$ does not index a transitional row, then we will show

$$(A.52) \quad \begin{aligned} Z_{m-1}(i, j) &= \varepsilon^{-1} \mathfrak{z}_{m-1}(i, j), & \text{if } Z \in \{A, B, C, D\}; \\ Z_m(i, j) &= \varepsilon^{-1} \log \varepsilon^{-1} + \varepsilon^{-1} \mathfrak{z}_m(i, j), & \text{if } Z \in \{A, C\}; \\ Z_m(i, j) &= \varepsilon^{-1} \log \varepsilon^{-1} + \varepsilon^{-1} \mathfrak{z}_m(i, j), & \text{if } Z \in \{B, D\}. \end{aligned}$$

In both cases for j , we will also show for any index $Z \in \{A, B, C, D\}$ that

$$(A.53) \quad Z_c(i, j) = \varepsilon^{-1} \mathfrak{z}_c(i, j), \quad \text{if } c \leq m-2.$$

Let us first verify that (A.51) and (A.53) both hold if $j = K_{[1, m-1]} + 1$ indexes a transitional row. To that end, observe by the inductive hypothesis (and the previous discussion on the first column, if $i = 2$) that these statements for the entrance data $A_k(i, j)$, $B_k(i, j)$, and $\mathbf{B}_k(i, j)$ hold. The fact that it also holds for the exit data $C_k(i, j)$, $D_k(i, j)$, and $\mathbf{D}_m(i, j)$ then follows from (the $\beta = i-1$ case of) Lemma A.19, together with Remark A.21 and arrow conservation (A.47) (recall Remark A.20).

We next verify that (A.52) and (A.53) hold if $j > K_{[1,m-1]} + 1$ does not index a transitional row. In this case, again the inductive hypothesis (together with the previous discussion on the first column, if $i = 2$, and (A.51) if $j = K_{[1,m-1]} + 2$ indexes a row directly above a transitional one) verifies these statements for the entrance data $A_k(i, j)$ and $B_k(i, j)$. The fact that it also holds for the exit data $C_k(i, j)$, $D_k(i, j)$, and $D_m(i, j)$ then follows from Proposition A.12, together with arrow conservation (A.47). This verifies (A.51), (A.52), and (A.53); by Proposition A.12 and Lemma A.19, it also shows that

$$(A.54) \quad e^{\mathbf{c}_{[k,m]}(i,j)} \quad \text{converges in distribution to} \quad \mathfrak{Y}_{ij}^{-1} \cdot (e^{\mathbf{a}_{[k,m]}(i,j) - \mathbf{b}_m(i,j) + \mathbf{b}_{[k,m]}(i,j)} + 1),$$

as ε tends to 0 (where we have set $\mathbf{a}_n(i, j) = 0$ if $j = K_{[1,m-1]} + 1$ indexes a transitional row, due to the fact that $A_m = 0$ in (A.51)).

Now let us analyze the height function for this model. First observe for any $(i, j) \in \mathbb{Z}_{>1} \times \mathbb{Z}_{>0}$ and $c \in \llbracket 1, m-1 \rrbracket$, where $m = m(j)$, that the definition (A.48) of the height function, consistency of the ensemble, arrow conservation (A.47), and Remark A.22 together imply that

$$(A.55) \quad \begin{aligned} \mathfrak{h}_c^\rightarrow(i, j-1) &= \mathfrak{h}_c^\rightarrow(i-1, j-1) - A_c(i, j); & \mathfrak{h}_c^\rightarrow(i-1, j) &= \mathfrak{h}_c^\rightarrow(i-1, j-1) + B_c(i, j); \\ \mathfrak{h}_c^\rightarrow(i, j) &= \mathfrak{h}_c^\rightarrow(i-1, j) - C_c(i, j), \end{aligned}$$

and that

$$(A.56) \quad \begin{aligned} \mathfrak{h}_m^\rightarrow(i, j-1) &= \mathfrak{h}_m^\rightarrow(i-1, j-1) - A_m(i, j); & \mathfrak{h}_m^\rightarrow(i-1, j) &= \mathfrak{h}_m(i-1, j-1) - \mathbf{B}_m(i, j); \\ \mathfrak{h}_m^\rightarrow(i, j) &= \mathfrak{h}_m^\rightarrow(i-1, j) - C_m(i, j). \end{aligned}$$

Hence, for any integer $c \geq 1$, we have

$$(A.57) \quad \mathfrak{h}_{\geq c}^\rightarrow(i-1, j) = \mathfrak{h}_{\geq c}^\rightarrow(i, j-1) + A_{[c,m]}(i, j) + B_{[c,m-1]}(i, j) - \mathbf{B}_m(i, j).$$

Thus, setting $\mathfrak{X}_c^0(i, j) = \lim_{\varepsilon \rightarrow 0} \mathfrak{X}_c^\varepsilon(i, j)$, we have if $i > 1$ and $j > K_{[1,c-1]} + 1$ that

$$(A.58) \quad \begin{aligned} \mathfrak{X}_c^0(i, j) &= \lim_{\varepsilon \rightarrow 0} \varepsilon^{i+j} e^{-\varepsilon \mathfrak{h}_{\geq c}^\rightarrow(i, j)} \\ &= \lim_{\varepsilon \rightarrow 0} \varepsilon^{i+j} e^{-\varepsilon \mathfrak{h}_{\geq c}^\rightarrow(i-1, j)} \cdot e^{\varepsilon C_{[c,m]}(i, j)} \\ &= \lim_{\varepsilon \rightarrow 0} \varepsilon^{i+j-1} e^{-\varepsilon \mathfrak{h}_{\geq c}^\rightarrow(i-1, j)} \cdot e^{\mathbf{c}_{[c,m]}(i, j)} \\ &= \lim_{\varepsilon \rightarrow 0} \varepsilon^{i+j-1} e^{-\varepsilon \mathfrak{h}_{[c,m]}^\rightarrow(i-1, j)} \cdot (e^{\mathbf{a}_{[j,m]}(i, j) + \mathbf{b}_{[j,m-1]}(i, j) - \mathbf{b}_m(i, j)} + 1) \cdot \mathfrak{Y}_{ij}^{-1} \\ &= \lim_{\varepsilon \rightarrow 0} \varepsilon^{i+j-1} e^{-\varepsilon \mathfrak{h}_{\geq c}^\rightarrow(i-1, j)} \cdot (e^{\varepsilon A_{[c,m]}(i, j) + \varepsilon B_{[c,m-1]}(i, j) - \varepsilon \mathbf{B}_m(i, j)} + 1) \cdot \mathfrak{Y}_{ij}^{-1} \\ &= \lim_{\varepsilon \rightarrow 0} \varepsilon^{i+j-1} (e^{-\varepsilon \mathfrak{h}_{\geq c}^\rightarrow(i, j-1)} + e^{-\varepsilon \mathfrak{h}_{\geq c}^\rightarrow(i-1, j)}) \cdot \mathfrak{Y}_{ij}^{-1} = \mathfrak{Y}_{ij}^{-1} \cdot (\mathfrak{X}_c^0(i, j-1) + \mathfrak{X}_c^0(i-1, j)), \end{aligned}$$

where the first equality follows from the definition of $\mathfrak{X}_c^\varepsilon(i, j) = \varepsilon^{i+j} \cdot e^{-\varepsilon \mathfrak{h}_{\geq c}^\rightarrow(i, j)}$; the second from the third statements in (A.55) and (A.56); the third from the definition of \mathbf{c}_k in terms of C_k from (A.51), (A.52), and (A.53); the fourth from (A.54); the fifth from the definitions of \mathbf{a}_k and \mathbf{b}_k in terms of A_k and B_k , respectively, from (A.51), (A.52), and (A.53); the sixth from (A.57); and the seventh again from the definition of $\mathfrak{X}_c^\varepsilon(i, j)$. If instead $i > 1$ and $j = K_{[1,c-1]} + 1$ (meaning that

$c = m$ and j indexes a transitionary row), then following (A.58) we obtain

$$\begin{aligned} \mathfrak{X}_c^0(i, j) &= \lim_{\varepsilon \rightarrow 0} \varepsilon^{i+j-1} e^{-\varepsilon \mathfrak{h}_{\geq c}^{\rightarrow}(i-1, j)} \cdot (e^{\mathfrak{a}_{[j, m]}(i, j) + \mathfrak{b}_{[j, m-1]}(i, j) - \mathfrak{b}_m(i, j)} + 1) \cdot \mathfrak{Y}_{ij}^{-1} \\ &= \lim_{\varepsilon \rightarrow 0} \varepsilon^{i+j-1} e^{-\varepsilon \mathfrak{h}_{\geq c}^{\rightarrow}(i-1, j)} \cdot (\varepsilon e^{\varepsilon A_{[c, m]}(i, j) + \varepsilon B_{[c, m-1]}(i, j) - \varepsilon B_m(i, j)} + 1) \cdot \mathfrak{Y}_{ij}^{-1} \\ &= \lim_{\varepsilon \rightarrow 0} \varepsilon^{i+j-1} e^{-\varepsilon \mathfrak{h}_{\geq c}^{\rightarrow}(i-1, j)} \cdot \mathfrak{Y}_{ij}^{-1} = \mathfrak{Y}_{ij}^{-1} \cdot \mathfrak{X}_c^0(i-1, j), \end{aligned}$$

where the second statement follows from (A.51); similarly, it is quickly verified that $\mathfrak{X}_c^0(1, j) = \mathfrak{Y}_{1j}^{-1} \cdot \mathfrak{X}_c^0(1, j-1)$ for $j > K_{[1, c-1]} + 1$ and $\mathfrak{X}_c^0(1, K_{[1, c-1]} + 1) = \mathfrak{Y}_{1, K_{[1, c-1]}}^{-1}$, using (A.50). These, with (A.58) confirm that \mathfrak{X}_c^0 satisfies the same recursion (A.49) determining the $\mathfrak{Z}_c(i, j)$. It follows that $\mathfrak{X}_c^0(i, j) = \mathfrak{Z}_c(i, j)$, which establishes the theorem. \square

Remark A.24. Let us explain how the random ensemble described in this section arises as a specialization of the colored stochastic fused vertex model introduced in Section 6.1. To that end, let $\mathfrak{M} \in \mathbb{R}$ be a real number and $L \geq 1$ be an integer (that we will analytically continue in). The parameters (x_j, r_j) associated with the j -th row of the model, and those (y_i, s_i) associated with the i -th column, will be given by

$$(x_j, r_j) = (q^{1-\theta'_j}, q^{-L/2}), \quad \text{for each } j \geq 1; \quad (y_i, s_i) = (q^{\theta_i - \mathfrak{M}}, q^{-\mathfrak{M}/2}), \quad \text{for each } i \geq 1.$$

Consider a colored stochastic fused vertex model on $\mathbb{Z}_{>0}^2$ with these parameters, and with L arrows of color $m(j)$ entering through row²² j , for each $j \geq 1$. Let $(\mathbf{A}(i, j), \mathbf{B}(i, j); \mathbf{C}(i, j), \mathbf{D}(i, j))$ denote the colored fused arrow configuration in this model at any vertex $(i, j) \in \mathbb{Z}_{>0}^2$. We next “complement” arrows of color $m(j)$ in the j -th row, by setting $\mathbf{B}(i, j) = (\overline{\mathbf{B}}(i, j), L - \mathbf{B}_{m(j)}(i, j))$ and $\mathbf{D}(i, j) = (\overline{\mathbf{D}}(i, j), L - \mathbf{D}_{m(j)}(i, j))$ for each $i \geq 1$. We then track the complemented arrow configuration $(\mathbf{A}(i, j), (\overline{\mathbf{B}}(i, j), \mathbf{B}_{m(j)}(i, j)); \mathbf{C}(i, j), (\overline{\mathbf{D}}(i, j), \mathbf{D}_{m(j)}(i, j)))$ over $(i, j) \in \mathbb{Z}_{>0}^2$.

Now analytically continue in L , replacing it with a real number $\mathfrak{L} \geq 0$. Let \mathfrak{M} tend to ∞ , and then let \mathfrak{L} tend to ∞ . Since $x_j y_i^{-1} = q^{1-\theta_i - \theta'_j + \mathfrak{M}} = q^{\mathfrak{M}+1} \gamma_{ij}^{-1}$, Lemma A.3, Lemma A.4, and Lemma A.7 (with the $q^{\mathfrak{M}}$ in the first two equal to $q^{\mathfrak{M}+L} \gamma_{ij}^{-1}$ here, so that $x_j y_i^{-1} = q^{\mathfrak{M}-L+1}$) implies that this procedure yields at $(i, j) \in \mathbb{Z}_{>0}^2$ the $\mathcal{U}_\gamma^{\text{qp}; m(j)}$ -weights from Lemma A.7. Since $x_j (y_i s_i^2)^{-1} = q \gamma_{ij}^{-1}$, it also at any vertex $(1, j)$ (in the first column) yields the $\mathcal{U}_{1/\gamma_{1j}}^{b; m(j)}$ -weights from Definition A.10. Hence, this gives rise to the vertex model described above Theorem A.23.

Remark A.25. Let us briefly (and informally) explain the reason behind our parameter choices when degenerating the colored fused stochastic vertex model to the log-gamma polymer in Remark A.24. In the uncolored case $n = 1$, [27, Proposition 7.26] describes how to specialize the $U_q(\widehat{\mathfrak{sl}}_2)$ stochastic fused vertex model to the q -Hahn PushTASEP introduced in [37]. However, the arrows in that vertex model are reversed relative to here; they are directed up-left instead of up-right [27, Figure 19]. To remedy this, one must complement those arrow configurations by tracking how many arrows its horizontal edges are from being saturated (as in (A.2)); this directs its paths up-right (and also imposes a change in the spectral parameters involved in the vertex weights). The vertex weights obtained in this way precisely coincide with the $n = 1$ case of the complemented ones provided in Definition A.1 (and Lemma A.3). The subsequent limits taken in Appendix A.2 correspond to degenerating the q -Hahn PushTASEP to the q -PushTASEP; those taken in Appendix A.4 correspond to degenerating the latter to the log-gamma polymer (as described in [68]).

²²Since $m = m(j)$ is defined so that $j \in \llbracket K_{[1, m-1]} + 1, K_{[1, m]} \rrbracket$, this means that there are K_1, K_2, \dots rows inputting arrows of colors $1, 2, \dots$ into the model, respectively.

In the colored case $n > 1$, the setup is similar, though it admits a few differences. The main one is that we only complement arrows of the largest color when defining the complemented weights in Section A.1 (a choice that is essentially forced by the step type boundary conditions we consider). This leads to a seemingly new presence of “transitionary rows,” where the largest color in the model changes, and the limiting behavior of the weights in these rows must be addressed in Appendix A.4.

APPENDIX B. EFFECTIVE CONVERGENCE OF THE SIX-VERTEX MODEL TO ASEP

In Section 4 we described colored line ensembles for the stochastic six-vertex model. It was shown in [18, 1] that under a certain limit degeneration that the latter, with weights (b_1, b_2) as depicted in Figure 23, converges to the asymmetric simple exclusion process (ASEP), with left jump rate L and right jump rate R . This degeneration takes $(b_1, b_2) = (\varepsilon L, \varepsilon R)$, scales the vertical coordinate by ε^{-1} , lets ε tend to 0, and observes the vertically exiting arrows along the main diagonal of \mathbb{Z}^2 ; this in particular makes time (the vertical coordinate) continuous and space (the horizontal coordinate) infinite. A similar limit can be taken on the associated colored line ensemble, and most of its relevant properties would be preserved, including its height function match Theorem 4.7 (in this case, to the colored ASEP) and its Gibbs property Theorem 4.8. However, the domain of this colored line ensemble would be infinite, and therefore its boundary conditions would be lost.

When analyzing line ensembles, it is at times (including in the forthcoming work [6]) useful to keep these boundary conditions intact. Thus, to understand the colored ASEP, it can be helpful not to directly study its line ensemble by letting ε tend to 0 in the colored stochastic six-vertex one, but instead to analyze the latter at $\varepsilon > 0$ (where its boundary conditions are present) and then let ε tend to 0 afterwards. This can require effective convergence rates of the stochastic six-vertex model to the ASEP, which were not proven in [1].

In this section we provide such a convergence result. We state it in Section B.2 after introducing the colored ASEP in Section B.1; its proof is then given in Section B.3 and Section B.4. Throughout this section, we fix real numbers²³ $R, L \geq 0$. The constants below might implicitly depend on R and L , even when not stated explicitly.

B.1. Properties of the Colored ASEP. The *colored ASEP* is a continuous time Markov process that can be described as follows. Particles are initially, at time 0, placed on \mathbb{Z} in such a way that exactly one particle occupies any site. Assigned to each particle is a color, which is a nonnegative integer label that informally measures the “priority” of the particle (those of a larger color are viewed as having higher priority than those of a smaller one). Denote the color of the particle at site $x \in \mathbb{Z}$ and time $t \in \mathbb{R}_{\geq 0}$ by $\eta_t(x) \in \mathbb{Z}_{\geq 0}$; further denote the full state of the process at time t by $\boldsymbol{\eta}_t = (\eta_t(x))_{x \in \mathbb{Z}}$.

Associated with each site $x \in \mathbb{Z}$ are two independent exponential clocks, a “left” one of rate L and a “right” one of rate R . If the left clock of x rings at some time $s \in \mathbb{R}_{> 0}$, then the particle at site x switches places with the one at site $x - 1$ if $\eta_{s^-}(x) > \eta_{s^-}(x - 1)$ (and does nothing otherwise). Similarly, if the right clock of x rings at time s , then the particle at site x switches places with the one at site $x + 1$ if $\eta_{s^-}(x) > \eta_{s^-}(x + 1)$ (and does nothing otherwise).

We next recall from [52, 53] a graphical representation for the colored ASEP. For any $x \in \mathbb{Z}$, let $\mathbf{S}(x) = (\mathbf{S}_1(x), \mathbf{S}_2(x), \dots)$ and $\mathbf{T}(x) = (\mathbf{T}_1(x), \mathbf{T}_2(x), \dots)$ denote the ringing times (in increasing order) for the left and right clocks associated with site x , respectively. For each integer $i \geq 1$, draw a directed arrow on $\mathbb{Z} \times \mathbb{R}_{\geq 0}$ from $(x, \mathbf{S}_i(x))$ to $(x - 1, \mathbf{S}_i(x))$ and from $(x, \mathbf{T}_i(x))$ to $(x + 1, \mathbf{T}_i(x))$. The union of these arrows from a directed graph \mathcal{G} , which we call the ASEP time graph; its horizontal

²³The ASEP usually imposes the asymmetry condition $R \neq L$, but we will not require that here.

and vertical directions index space and time, respectively. Given \mathcal{G} , the dynamics of the colored ASEP are defined by having each particle remain at its site x until it reaches a time t at which there is an arrow in \mathcal{G} connecting (x, t) to some (y, t) (for $y \in \{x-1, x+1\}$). At this time t , the particle at site x switches locations with the one at site y if either $\eta_{t^-}(x) > \eta_{t^-}(y)$ and the edge is directed from (x, t) to (y, t) , or if $\eta_{t^-}(x) < \eta_{t^-}(y)$ and the edge is directed from (y, t) to (x, t) ; otherwise, the particle at x stays in place.

Before proceeding, let us record the following lemma, which is sometimes known as a finite speed of discrepancy bound. It states that, if two colored ASEPs initially agree on a (sufficiently long) interval, then with high probability their dynamics can be coupled so as to agree on a shorter interval, up until a given time.

Lemma B.1. *There exists a constant $C > 1$ such that the following holds. Let $T \geq 0$ and $K > 1$ be real numbers; $U \leq V$ be integers; and $\xi = (\xi_t(x))$ and $\eta = (\eta_t(x))$ denote two colored ASEPs whose initial data satisfy $\xi_0(x) = \eta_0(x)$ for each $x \in \llbracket U - CKT, V + CKT \rrbracket$. Then it is possible to couple ξ and η such that, with probability at least $1 - Ce^{-K(T+1)}$, we have $\xi_t(x) = \eta_t(x)$ for each $(x, t) \in \llbracket U, V \rrbracket \times [0, T]$.*

Proof. Let $C > 1$ be a constant to be fixed later. Couple ξ and η under the same time graph \mathcal{G} . Then $\xi_{t_0}(x_0) \neq \eta_{t_0}(x_0)$ holds for some $(x_0, t_0) \in \llbracket U, V \rrbracket \times [0, T]$ only if there exists some $(x_1, t_1) \in (\mathbb{Z} \setminus \llbracket U - CKT, V + CKT \rrbracket) \times [0, T]$, such that a particle at site x_1 at time t_1 could (for some trajectories of the remaining particles) enter the interval $\llbracket U, V \rrbracket$ sometime during $[0, T]$ under \mathcal{G} ; this is contained in the union of two events. The first is that there exists a sequence of times $0 \leq r_1 \leq r_2 \leq \dots \leq r_{\lfloor CKT \rfloor} \leq T$ for which there exists an arrow in \mathcal{G} connecting $(U - \lfloor CKT \rfloor + i - 1, r_i)$ and $(U - \lfloor CKT \rfloor + i, r_i)$ for each $i \in \llbracket 1, CKT \rrbracket$; the second is that there exists a sequence of times $0 \leq r'_1 \leq r'_2 \leq \dots \leq r'_{\lfloor CKT \rfloor} \leq T$ for which there exists an arrow in \mathcal{G} connecting $(V + \lfloor CKT \rfloor - i + 1, r'_i)$ and $(V + \lfloor CKT \rfloor - i, r'_i)$ for each $i \in \llbracket 1, CKT \rrbracket$.

Now recall that the set of times at which arrows in \mathcal{G} enter or exit a given column $\{x\} \times \mathbb{R}_{\geq 0}$ has the same law as that of the ringing times of an exponential clock of rate $R + L$. Hence, the probability of each of the above events is bounded by the probability that a sum of T exponential random variables with parameter $R + L$ is at least CKT . A Chernoff bound implies that the latter is at most $Ce^{-K(T+1)}$ if C is sufficiently large, establishing the lemma. \square

B.2. Properties of the Colored Stochastic Six-Vortex Model. In this section we state the effective convergence of the stochastic six-vertex model to the colored ASEP, and also provide several properties of the former. Let $b_1, b_2 \in [0, 1]$ denote real numbers; set $q = b_1 b_2^{-1}$; consider the colored stochastic six-vertex model (as defined in Section 1.2) on the quadrant $\mathbb{Z}_{>0}^2$, with spectral parameter $z_{i,j} = (1 - b_2)(1 - b_1)^{-1}$ at each $(i, j) \in \mathbb{Z}_{>0}^2$; and assume that the largest color in this system is at most some integer $n \geq 0$. See Figure 23 for the stochastic weights of this model. For any integer $(x, y) \in \mathbb{Z}_{>0}^2$, let $\eta_y(x) \in \llbracket 0, n \rrbracket$ denote the color of the arrow vertically exiting (x, y) in this model; also let $\boldsymbol{\eta}_y = (\eta_y(x))_{x>0}$ denote the full state of the process at vertical coordinate y .

Next we state the effective²⁴ convergence result; it will be proven in Section B.3 below. In what follows, given a function $\varpi : \mathbb{Z} \rightarrow \llbracket 0, n \rrbracket$, we say that the colored stochastic six-vertex model $\boldsymbol{\eta}$ on the quadrant $\mathbb{Z}_{>0}^2$ has boundary data ϖ if the below holds. For each integer $x \leq 0$, an arrow of color $\varpi(x)$ horizontally enters the quadrant through $(0, 1 - x)$ and, for each integer $x > 0$, an arrow of color $\varpi(x)$ vertically enters the quadrant through $(x, 0)$. We say that the boundary data for this model matches the initial condition for a colored ASEP $\xi = (\xi_t(x))$ if $\varpi = \xi_0$.

²⁴We made no effort to optimize the exponent $\varepsilon^{1/8}$ in the probability in Proposition B.2.

$i \in \llbracket 0, n \rrbracket$	$0 \leq i < j \leq n$				
$(i, i; i, i)$	$(j, i; j, i)$	$(i, j; i, j)$	$(j, i; i, j)$	$(i, j; j, i)$	
1	b_1	b_2	$1 - b_1$	$1 - b_2$	

FIGURE 23. The weights for the colored stochastic six-vertex model in Section B.2 are depicted above.

Proposition B.2. *There exists a constant $C > 1$ such that the following holds. Let $\varepsilon \in (0, 1)$ and $T \geq 0$ be real numbers; let $U \leq V$ be integers; let $\mathcal{T} \subset [0, T]$ denote a finite set of real numbers; and let $\xi = (\xi_t(x))$ denote a colored ASEP with at most n colors. Further let $\eta = (\eta_y(x))$ denote a colored stochastic six-vertex model on $\mathbb{Z}_{>0}^2$ with parameters $(b_1, b_2) = (\varepsilon L, \varepsilon R)$, whose boundary data matches the initial data of ξ . It is possible to couple ξ and η so that, with probability at least $1 - C(V - U + 1)(T + 1)^2 |\mathcal{T}| \varepsilon^{1/8}$, we have*

$$(B.1) \quad \xi_t(x) = \eta_{\lfloor t/\varepsilon \rfloor}(x + \lfloor t\varepsilon^{-1} \rfloor), \quad \text{for each } (x, t) \in \llbracket U, V \rrbracket \times \mathcal{T} \text{ with } x + \lfloor t\varepsilon^{-1} \rfloor > 0.$$

To prove Proposition B.2, it will be useful to introduce notation for the randomness defining the colored stochastic six-vertex model (this discussion also appears in a slightly different, though equivalent, form in [3, Section 2.3] and [64, Section 2.2]). To that end, for any vertex $(x, y) \in \mathbb{Z}_{\geq 0}$, we associate Bernoulli random variables $\chi_{x,y}, \psi_{x,y} \in \{0, 1\}$ with $\mathbb{P}[\chi_{x,y} = 1] = b_1$ and $\mathbb{P}[\psi_{x,y} = 1] = b_2$. Given all of these random variables, the dynamics of the colored stochastic six-vertex model are defined as follows. Fix a vertex $(x, y) \in \mathbb{Z}_{>0}^2$, and suppose that colored six-vertex arrow configurations have been assigned to each $(x', y') \in \mathbb{Z}_{>0}^2$ with $x' + y' < x + y$; this fixes the colors $a = a(x, y)$ and $b = b(x, y)$ of the arrows vertically and horizontally entering (x, y) , respectively. Then define the colors $c = c(x, y)$ and $d = d(x, y)$ of the arrows vertically and horizontally exiting (x, y) , respectively, according to the below procedure.

- (1) If $a = b$, then set $c = d = a = b$.
- (2) If $a > b$, then set $(c, d) = (a, b)$ if $\chi_{x,y} = 1$ and $(c, d) = (b, a)$ if $\chi_{x,y} = 0$.
- (3) If $a < b$, then set $(c, d) = (a, b)$ if $\psi_{x,y} = 1$ and $(c, d) = (b, a)$ if $\psi_{x,y} = 0$.

This provides a way of sampling the colored stochastic six-vertex model defined above. In what follows, for any $x \in \mathbb{Z}$, define the increasing integer sequences $\mathfrak{s}(x) = (\mathfrak{s}_1(x), \mathfrak{s}_2(x), \dots)$ and $\mathfrak{t}(x) = (t_1(x), t_2(x), \dots)$, such that $\mathfrak{s} \in \mathfrak{s}(x)$ if and only if $\chi_{x+\mathfrak{s}-1, \mathfrak{s}} > 0$, and $\mathfrak{t} \in \mathfrak{t}(x)$ if and only if $\psi_{x+\mathfrak{t}, \mathfrak{t}} > 0$ (here, the offsets $x + \mathfrak{s}$ and $x + \mathfrak{t}$ are introduced to match with (B.1)). Observe that the $(\mathfrak{s}(x))$ and $(\mathfrak{t}(x))$ (over all $x \in \mathbb{Z}$) together determine all $(\chi_{x,y}, \psi_{x,y})_{x,y > 0}$.

Before proceeding, we record the following lemma that provides a finite speed of discrepancy bound for the colored stochastic six-vertex model (and is analogous to Lemma B.1).

Lemma B.3. *There exists a constant $C > 1$ such that the following holds. Let $T \geq 0$, $K > 1$, and $\varepsilon \in (0, 1)$ be real numbers; set $(b_1, b_2) = (\varepsilon L, \varepsilon R)$; and let $U \leq V$ be integers. Further let $\xi_y = (\xi_y(x))_{x > 0}$ and $\eta_y = (\eta_y(x))_{x > 0}$ denote two colored stochastic six-vertex models with parameters (b_1, b_2) and boundary data $\varpi^\xi : \mathbb{Z} \rightarrow \llbracket 0, n \rrbracket$ and $\varpi^\eta : \mathbb{Z} \rightarrow \llbracket 0, n \rrbracket$, respectively. Assume that*

$\varpi^\xi(x) = \varpi^\eta(x)$ for each $x \in \llbracket U - CKT, V + CKT \rrbracket$. Then it is possible to couple ξ and η such that, with probability at least $1 - Ce^{-K(T+1)}$, we have $\xi_y(x) = \eta_y(x)$ for each $(x, y) \in \mathbb{Z}_{>0} \times \llbracket 1, T\varepsilon^{-1} \rrbracket$ satisfying $U \leq x - y \leq V$.

Proof. Couple ξ and η under the same processes $(\mathfrak{s}(x))$ and $(\mathfrak{t}(x))$, and define the strip

$$\mathcal{R} = \{(x, y) \in \mathbb{Z}_{>0} \times \llbracket 1, T\varepsilon^{-1} \rrbracket : U \leq x - y \leq V\}.$$

Then $\xi_{y_0}(x_0) \neq \eta_{y_0}(x_0)$ holds for some $(x_0, y_0) \in \mathcal{R}$ only if there exists some (x_1, y_1) on the x -axis or y -axis with $x_1 - y_1 \notin \llbracket U - CKT, V + CKT \rrbracket$, such that a colored path entering the quadrant through (x_1, y_1) could (for some trajectories of the remaining colored paths) enter \mathcal{R} under the above randomness $(\mathfrak{s}(x))$ and $(\mathfrak{t}(x))$. This is contained in the event on which there exists an integer $k \geq 0$; a sequence of integers w_0, w_1, \dots, w_k with $|w_i - w_{i-1}| = 1$ for each $i \in \llbracket 1, k \rrbracket$; and a sequence of positive integers $0 \leq \mathfrak{r}_0 \leq \mathfrak{r}_1 \leq \dots \leq \mathfrak{r}_k \leq T\varepsilon^{-1}$ such that $\mathfrak{r}_i \in \mathfrak{s}(w_i) \cup \mathfrak{t}(w_i)$ for each $i \in \llbracket 1, k \rrbracket$, and one of the following two possibilities holds. The first is that $w_0 \leq U - CKT \leq U \leq w_k$; the second is that $w_0 \geq V + CKT \geq V \geq w_k$.

Now, observe that the differences between consecutive entries of any $\mathfrak{s}(x) \cup \mathfrak{t}(x)$ are distributed as independent geometric random variables with parameter $1 - (1 - \varepsilon L)(1 - \varepsilon R) \leq \varepsilon(L + R)$. Hence, the probability of each of the above possibilities is bounded by the probability that a sum of $\lfloor T\varepsilon^{-1} \rfloor$ geometric random variables with parameter $\varepsilon(L + R)$ is at least CKT . A Chernoff bound implies that the latter is at most $Ce^{-K(T+1)}$ if C is sufficiently large, establishing the lemma. \square

B.3. Proof of Proposition B.2. In this section we establish Proposition B.2. Its proof will use the below lemma, which is shown in Section B.4 below. It indicates that the processes $\mathbf{S}(x)$ and $\mathbf{T}(x)$ from Section B.1 can be coupled to nearly coincide (after scaling) with the $\mathfrak{s}(x)$ and $\mathfrak{t}(x)$ from Section B.2, on a long interval, with high probability. In what follows, we recall the notation from those sections, associating the parameters $(L; R)$ with the $(\mathbf{S}; \mathbf{T})$ processes and $(\varepsilon L; \varepsilon R)$ with the $(\mathfrak{s}; \mathfrak{t})$ ones.

Lemma B.4. *There exists a coupling between $(\mathbf{S}(x); \mathbf{T}(x))_{x \in \mathbb{Z}}$ and $(\mathfrak{s}(x); \mathfrak{t}(x))_{x \in \mathbb{Z}}$, and a constant $C > 1$ such that, for any real numbers $U_0 \leq V_0$, $\varepsilon \in (0, 1)$, and $T \geq 0$, the following statements all hold with probability at least $1 - C(V_0 - U_0 + 1)(T + 1)\varepsilon^{1/4}$.*

- (1) *For any index pair $(R, \mathfrak{r}) \in \{(\mathbf{S}, \mathfrak{s}), (\mathbf{T}, \mathfrak{t})\}$ and each pair $(i, x) \in \mathbb{Z}_{\geq 1} \times \llbracket U_0, V_0 \rrbracket$ such that $R_i(x) \leq T$ or $\mathfrak{r}_i(x) \leq T\varepsilon^{-1}$, we have $\varepsilon \mathfrak{r}_i(x) \leq R_i(x) \leq \varepsilon \mathfrak{r}_i(x) + \varepsilon^{1/2} < T$.*
- (2) *For distinct triples $(R, i, x), (R', i', x') \in \{\mathbf{S}, \mathbf{T}\} \times \mathbb{Z}_{\geq 1} \times \llbracket U_0, V_0 \rrbracket$ such that $R_i(x), R'_{i'}(x') < T$, we have $|R_i(x) - R'_{i'}(x')| > 2\varepsilon^{1/2}$.*

Proof of Proposition B.2. We will assume for notational convenience that the set of times $\mathcal{T} = \{T\}$ (from which the proof of the proposition for general \mathcal{T} quickly follows by a union bound). Set $K = \lceil \varepsilon^{-1/8} \rceil$, and let $C_0 > 1$ denote the maximum of the constants C from Lemma B.1, Lemma B.3, and Lemma B.4.

We first use the finite speed of discrepancy bounds (Lemma B.1 and Lemma B.3) to “cut off” the initial data for ξ and η . To that end, let $\xi' = (\xi'_t(x))$ denote a colored ASEP with initial data $\xi'_0(x) = \xi_0(x) \cdot \mathbb{1}_{x \in \llbracket U - C_0KT, V + C_0KT \rrbracket}$, and let $\eta' = (\eta'_y(x))$ denote a colored stochastic six-vertex model with parameters $(b_1, b_2) = (\varepsilon L, \varepsilon R)$, whose boundary data matches the initial data of ξ' . By Lemma B.1 and Lemma B.3, we may couple ξ and ξ' , and also η and η' , so that with probability at least $1 - 2C_0e^{-K} \geq 1 - 16C_0\varepsilon$ we have $\xi_t(x) = \xi'_t(x)$ for each $(x, t) \in \llbracket U, V \rrbracket \times [0, T]$, and $\eta_y(x) = \eta'_y(x)$ for each $(x, y) \in \mathbb{Z}_{>0} \times \llbracket 1, T\varepsilon^{-1} \rrbracket$ with $U \leq x - y \leq V$. Hence, we may replace ξ and η by ξ' and η' , respectively, so we will assume in what follows that $\xi = \xi'$ and $\eta = \eta'$.

Next define the process $\zeta = (\zeta_y(x))$ from η by setting $\zeta_y(x) = \eta_y(x+y)$ (see (B.1)) for each $(x, y) \in \mathbb{Z}_{>0}^2$. Recall from Section B.1 and Section B.2 that ξ and ζ are determined from the processes $(\mathbf{S}(x); \mathbf{T}(x))_{x \in \mathbb{Z}}$ and $(\mathfrak{s}(x); \mathfrak{t}(x))_{x \in \mathbb{Z}}$, respectively; it will be useful to restrict these processes to a bounded subset of $x \in \mathbb{Z}$. To that end, recall for any $x \in \mathbb{Z}$ that $\mathbf{S}(x) \cup \mathbf{T}(x)$ is given by the ringing times of an exponential clock of rate $L+R$. Hence, the trajectory of the rightmost particle of nonzero color in ξ is stochastically dominated by a random walk starting at $V + C_0KT$, that jumps one space to the right whenever an exponential clock of rate $L+R$ rings. Therefore, a Chernoff bound implies (after increasing C_0 if necessary) that this particle remains left of $V + 2C_0KT$ with probability at least $1 - C_0e^{-K} \geq 1 - 8C_0\varepsilon$. Similarly, the leftmost particle of nonzero color in ξ remains right of $U - 2C_0KT$ with probability at least $1 - 8C_0\varepsilon$.

We may apply analogous reasoning to ζ . In particular, for any $x \in \mathbb{Z}$, the differences of the entries in $\mathfrak{s}(x) \cup \mathfrak{t}(x)$ are given by mutually independent geometric random variables of parameter $1 - (1 - \varepsilon L)(1 - \varepsilon R) \leq \varepsilon(L+R)$. Hence, recalling the diagonal shifts in the definitions of \mathfrak{s} and \mathfrak{t} from Section B.2, the trajectory of the rightmost path (of nonzero color) in ζ is stochastically dominated by a random walk starting at $V + C_0KT$ that jumps to the right according to a geometric random variable of parameter $\varepsilon(L+R)$. Therefore, a Chernoff bound implies (after increasing C_0 if necessary) that this path remains to the left of $V + 2C_0KT$ with probability at least $1 - C_0e^{-K} \geq 1 - 8C_0\varepsilon$. Similarly, the leftmost path of nonzero color in ζ remains right of $U - 2C_0KT$ with probability at least $1 - 8C_0\varepsilon$. Together, these facts yield $\mathbb{P}[\mathcal{E}] \geq 1 - 32C_0\varepsilon$, where $\mathcal{E} = \mathcal{E}_1 \cap \mathcal{E}_2$ and we have denoted the events

$$\begin{aligned} \mathcal{E}_1 &= \{\xi_t(x) = 0, \quad \text{for all } x \notin \llbracket U - 2C_0KT, V + 2C_0KT \rrbracket \text{ and } t \in [0, T]\}; \\ \mathcal{E}_2 &= \{\zeta_y(x) = 0, \quad \text{for all } (x, y) \in \llbracket U - 2C_0KT, V + 2C_0KT \rrbracket \times \llbracket 0, T\varepsilon^{-1} \rrbracket \text{ with } x + y > 0\}. \end{aligned}$$

Now, Lemma B.4 gives a coupling between $(\mathbf{S}(x); \mathbf{T}(x))$ and $(\mathfrak{s}(x); \mathfrak{t}(x))$ such that the following holds on an event \mathcal{F} with $\mathbb{P}[\mathcal{F}] \geq 1 - C_0(V - U + 4C_0KT + 1)(T + 1)\varepsilon^{1/4}$. First, for any index pair $(\mathbf{R}, \mathfrak{r}) \in \{(\mathbf{S}, \mathfrak{s}), (\mathbf{T}, \mathfrak{t})\}$ and each pair $(i, x) \in \mathbb{Z}_{\geq 1} \times \llbracket U - 2C_0KT, V + 2C_0KT \rrbracket$ with $\mathbf{R}_i(x) \leq T$, we have

$$(B.2) \quad \varepsilon \mathfrak{r}_i(x) \leq \mathbf{R}_i(x) \leq \varepsilon \mathfrak{r}_i(x) + \varepsilon^{1/2} < T.$$

Second, for any distinct triples $(\mathbf{R}, i, x), (\mathbf{R}', i', x') \in \{\mathbf{S}, \mathbf{T}\} \times \mathbb{Z}_{\geq 1} \times \llbracket U - 2C_0KT, V + 2C_0KT \rrbracket$ with $\mathbf{R}_i(x), \mathbf{R}'_{i'}(x') \leq T$, we have

$$(B.3) \quad |\mathbf{R}_i(x) - \mathbf{R}'_{i'}(x')| > 2\varepsilon^{1/2}.$$

We claim on $\mathcal{E} \cap \mathcal{F}$ that the ASEP and stochastic six-vertex configurations coincide, namely,

$$(B.4) \quad \xi_T(x) = \zeta_{\lfloor T/\varepsilon \rfloor}(x), \quad \text{for each } x \in \mathbb{Z} \text{ with } x + \lfloor T\varepsilon^{-1} \rfloor > 0.$$

To verify this, first observe on \mathcal{E} that $(\zeta_t)_{t \leq T}$ and $(\xi_y)_{y \leq T/\varepsilon}$ only depend on $(\mathbf{S}(x), \mathbf{T}(x))$ and $(\mathfrak{s}(x), \mathfrak{t}(x))$ for $x \in \llbracket U - 2C_0KT, V + 2C_0KT \rrbracket$, respectively. Let $\mathbf{R}_1 < \mathbf{R}_2 < \dots < \mathbf{R}_m$ and $\mathfrak{r}_1 < \mathfrak{r}_2 < \dots < \mathfrak{r}_{m'}$ be such that

$$\begin{aligned} [0, T] \cap \bigcup_{x=\lceil U-2C_0KT \rceil}^{\lfloor V-2C_0KT \rfloor} (\mathbf{S}(x) \cup \mathbf{T}(x)) &= \{\mathbf{R}_1, \mathbf{R}_2, \dots, \mathbf{R}_m\}; \\ [1, T\varepsilon^{-1}] \cap \bigcup_{x=\lceil U-2C_0KT \rceil}^{\lfloor V-2C_0KT \rfloor} (\mathfrak{s}(x) \cup \mathfrak{t}(x)) &= \{\mathfrak{r}_1, \mathfrak{r}_2, \dots, \mathfrak{r}_{m'}\}. \end{aligned}$$

For each $i \in \llbracket 1, m \rrbracket$, let $w_i \in \llbracket U - 2C_0KT, V + 2C_0KT \rrbracket$ be such that $\mathbf{R}_i \in \mathbf{S}(w_i) \cup \mathbf{T}(w_i)$. Then, by (B.2) and (B.3), we have that $m' = m$ and for each $i \in \llbracket 1, m \rrbracket$ that $\mathbf{r}_i \in \mathbf{s}(w_i) \cup \mathbf{t}(w_i)$ and

$$(B.5) \quad \mathbf{R}_1 - \varepsilon^{1/2} \leq \mathbf{r}_1 \leq \mathbf{R}_1 < \mathbf{R}_2 - \varepsilon^{1/2} \leq \mathbf{r}_2 \leq \mathbf{R}_2 < \dots \leq \mathbf{R}_m - \varepsilon^{1/2} \leq \mathbf{r}_m \leq \mathbf{R}_m < T - \varepsilon^{1/2}.$$

Now, observe if $y \notin \{\mathbf{r}_1, \mathbf{r}_2, \dots, \mathbf{r}_m\}$ then $\eta_{y+1}(x+1) = \eta_y(x)$ holds for all $x \in \mathbb{Z}$, as all paths in $\boldsymbol{\eta}$ proceed one step horizontally and one step vertically; thus, $\zeta_{y+1} = \zeta_y$. Similarly, if $t \notin \{\mathbf{R}_1, \mathbf{R}_2, \dots, \mathbf{R}_m\}$ then $\xi_t = \xi_{t-}$. Hence, to show (B.4), it suffices to show for each $(i, x) \in \llbracket 1, m \rrbracket \times \mathbb{Z}$ that $\xi_{\mathbf{R}_i}(x) = \zeta_{\lfloor \mathbf{R}_i / \varepsilon \rfloor}(x)$.

We do this by induction on $i \in \llbracket 0, m \rrbracket$, where we set $\mathbf{R}_0 = 0$. It holds at $i = 0$, since the boundary data of $\boldsymbol{\eta}$ matches that of $\boldsymbol{\xi}$. Hence, let us assume it holds for all $i \leq m_0 - 1$ for some integer $m_0 \in \llbracket 1, m \rrbracket$ and verify it holds for $i = m_0$. By (B.5) and the inductive hypothesis (with the above discussion that $\zeta_{y+1} = \zeta_y$ if $y \notin \{\mathbf{r}_1, \mathbf{r}_2, \dots, \mathbf{r}_m\}$ and $\xi_t = \xi_{t-}$ if $t \notin \{\mathbf{R}_1, \mathbf{R}_2, \dots, \mathbf{R}_m\}$), we have $\xi_{\mathbf{R}_{m_0}^-}(x) = \xi_{\mathbf{R}_{m_0-1}}(x) = \zeta_{\lfloor \mathbf{R}_{m_0-1} / \varepsilon \rfloor}(x) = \zeta_{\lfloor \mathbf{R}_{m_0} / \varepsilon - 1 \rfloor}(x)$ for each $x \in \mathbb{Z}$. Next, if $\mathbf{r}_{m_0} \in \mathbf{s}(w_{m_0})$, then it follows from the discussion in Section B.2 that $\eta_{\mathbf{r}_{m_0}}(w_{m_0} + \mathbf{r}_{m_0} - 1) = \eta_{\mathbf{r}_{m_0-1}}(w_{m_0} + \mathbf{r}_{m_0} - 1)$, as then the path of color $\eta_{\mathbf{r}_{m_0-1}}(w_{m_0} + \mathbf{r}_{m_0} - 1)$ entering $(w_{m_0} + \mathbf{r}_{m_0} - 1, \mathbf{r}_{m_0})$ proceeds one step vertically and no steps horizontally; thus,

$$(B.6) \quad \zeta_{\lfloor \mathbf{R}_{m_0-1} / \varepsilon \rfloor}(w_{m_0}) = \zeta_{\mathbf{r}_{m_0-1}}(w_{m_0}) = \zeta_{\mathbf{r}_{m_0}}(w_{m_0} - 1) = \zeta_{\lfloor \mathbf{R}_{m_0} / \varepsilon \rfloor}(w_{m_0} - 1),$$

where in the first and last equality we again used (B.5). By (B.5) and (B.3), we then also have $\mathbf{R}_{m_0} \in \mathbf{S}(w_{m_0})$, and so $\zeta_{\lfloor \mathbf{R}_{m_0-1} / \varepsilon \rfloor}(w_{m_0}) = \xi_{\mathbf{R}_{m_0-1}}(w_{m_0}) = \xi_{\mathbf{R}_{m_0}^-}(w_{m_0}) = \xi_{\mathbf{R}_{m_0}}(w_{m_0} - 1)$. This coincides with (B.6); the proof that $\zeta_{\lfloor \mathbf{R}_{m_0} / \varepsilon \rfloor}(x) = \xi_{\mathbf{R}_{m_0}}(x)$ for all other $x \in \mathbb{Z}$ is entirely analogous. This verifies the statement at $i = m_0$ in this case.

If instead $\mathbf{r}_{m_0} \in \mathbf{t}(w_{m_0})$, then $\eta_{\mathbf{r}_{m_0}}(w_{m_0} + \mathbf{r}_{m_0} + 1) = \eta_{\mathbf{r}_{m_0-1}}(w_{m_0} + \mathbf{r}_{m_0} - 1)$, as then the path of color $\eta_{\mathbf{r}_{m_0-1}}(w_{m_0} + \mathbf{r}_{m_0} - 1)$ at $(w_{m_0} + \mathbf{r}_{m_0} - 1, \mathbf{r}_{m_0} - 1)$ proceeds two steps horizontally and one step vertically. So,

$$(B.7) \quad \zeta_{\lfloor \mathbf{R}_{m_0-1} / \varepsilon \rfloor}(w_{m_0}) = \zeta_{\mathbf{r}_{m_0-1}}(w_{m_0}) = \zeta_{\mathbf{r}_{m_0}}(w_{m_0}) = \zeta_{\lfloor \mathbf{R}_{m_0} / \varepsilon \rfloor}(w_{m_0} + 1).$$

By (B.5) and (B.3), we then also have $\mathbf{R}_{m_0} \in \mathbf{T}(w_{m_0})$. Hence, $\zeta_{\lfloor \mathbf{R}_{m_0-1} / \varepsilon \rfloor}(w_{m_0}) = \xi_{\mathbf{R}_{m_0-1}}(w_{m_0}) = \xi_{\mathbf{R}_{m_0}^-}(w_{m_0}) = \xi_{\mathbf{R}_{m_0}}(w_{m_0} + 1)$. This again coincides with (B.7), and the proof that $\zeta_{\lfloor \mathbf{R}_{m_0} / \varepsilon \rfloor}(x) = \xi_{\mathbf{R}_{m_0}}(x)$ for all other $x \in \mathbb{Z}$ is entirely analogous. This confirms (B.4).

Thus, (B.1) holds on $\mathcal{E} \cap \mathcal{F}$. Together with the fact that

$$\begin{aligned} \mathbb{P}[\mathcal{E} \cap \mathcal{F}] &\geq 1 - 32C_0\varepsilon - C_0(V - U + 4C_0KT + 1)(T + 1)\varepsilon^{1/4} \\ &\geq 1 - 40C_0^2(V - U + 1)(T + 1)^2K\varepsilon^{1/4} \geq 1 - 80C_0^2(V - U + 1)(T + 1)^2\varepsilon^{1/8}, \end{aligned}$$

this establishes the proposition. \square

B.4. Proof of Lemma B.4. In this section we establish Lemma B.4 as a quick consequence of the two lemmas below.

Lemma B.5. *For any real number $A > 0$, there exists a constant $C = C(A) > 1$ such that, if $\mathbf{R} = (r_1, r_2, \dots)$ denotes the ringing times in increasing order for an exponential clock with parameter A , then the following two statements hold.*

- (1) *For any real numbers $T \geq 0$ and $K \geq 1$, we have $\mathbb{P}[r_{\lfloor CK(T+1) \rfloor} \geq T] \geq 1 - Ce^{-K(T+1)}$.*
- (2) *For any real numbers $0 < \delta \leq 1 \leq B$, we have $\mathbb{P}[\min_{1 \leq i \leq B}(r_{i+1} - r_i) \geq \delta] \geq 1 - AB\delta$.*

Proof. First observe that the event on which $r_{\lfloor CK(T+1) \rfloor} \geq T$ is that on which the sum of $\lfloor CK(T+1) \rfloor$ independent exponential random variables is at least T . By a Chernoff bound, this is at least

$1 - Ce^{-K(T+1)}$ if $C = C(A) > 1$ is sufficiently large, which verifies the first statement of the lemma. Further observe for any integer $i \geq 1$ that, since $r_{i+1} - r_i$ is an exponential random variable of parameter A , we have $\mathbb{P}[r_{i+1} - r_i \leq \delta] = 1 - e^{-A\delta} \leq A\delta$. This, together with a union bound over $i \in \llbracket 1, B \rrbracket$, implies the second statement of the lemma. \square

Lemma B.6. *Let $A > 0$ and $\delta \in (0, 1)$ be real numbers; let $\mathbf{g} \in \mathbb{Z}_{\geq 0}$ denote a geometric random variable with $\mathbb{P}[\mathbf{g} = k] = A\delta(1 - A\delta)^k$ for each $k \in \mathbb{Z}_{\geq 0}$; and let $\mathbf{e} \in \mathbb{R}_{\geq 0}$ denote an exponential random variable with $\mathbb{P}[\mathbf{e} > x] = e^{-Ax}$ for each $x \in \mathbb{R}_{\geq 0}$. It is possible to couple \mathbf{e} and \mathbf{g} such that*

$$\mathbb{P}[\mathbf{g} = \lfloor \delta^{-1}\mathbf{e} \rfloor] \geq 1 - 12A\delta.$$

Proof. We may assume that $\delta < (2A)^{-1}$, for otherwise $1 - 12A\delta < 0$. It suffices to show that

$$(B.8) \quad e^{-A^2S\delta^2} \cdot \mathbb{P}[S\delta \leq \mathbf{e} < (S+1)\delta] \leq \mathbb{P}[\mathbf{g} = S] \leq (1 + 2A\delta) \cdot \mathbb{P}[S\delta \leq \mathbf{e} < (S+1)\delta],$$

for any integer $S \geq 0$, or equivalently that

$$(B.9) \quad e^{-A^2S\delta^2} \leq \frac{A\delta(1 - A\delta)^S}{e^{-AS\delta}(1 - e^{-A\delta})} \leq 1 + 2A\delta.$$

Indeed, given (B.8), it would follow that

$$\begin{aligned} \sum_{S=0}^{\infty} \left| \mathbb{P}[S\delta \leq \mathbf{e} < (S+1)\delta] - \mathbb{P}[\mathbf{g} = S] \right| &\leq 2 \sum_{S=0}^{\infty} (1 - e^{-A^2S\delta^2} + A\delta) \cdot e^{-AS\delta}(1 - e^{-A\delta}) \\ &\leq 2A^2\delta^2 \sum_{S=0}^{\infty} (AS\delta + 1)e^{-AS\delta} \\ &\leq \frac{2A^2\delta^2}{1 - e^{-A\delta}} + \frac{2A^3\delta^3}{(1 - e^{-A\delta})^2} \leq 12A\delta, \end{aligned}$$

where in the first equality we used the explicit probability distribution for \mathbf{e} ; in the second we used the facts that $1 - e^{-A^2S\delta^2} \leq A^2S\delta^2$ and that $1 - e^{-A\delta} \leq A\delta$; in the third we bounded the sums $\sum_{i=0}^{\infty} r^i = (1 - r)^{-1}$ and $\sum_{i=0}^{\infty} ir^i = r(1 - r)^{-2} \leq (1 - r)^{-2}$ at $r = e^{-A\delta} \in (0, 1)$; and in the fourth we bounded $1 - e^{-A\delta} \geq A\delta/2$ (as $\delta < (2A)^{-1}$). This implies that it is possible to couple \mathbf{e} and \mathbf{g} so that $\mathbf{g} \leq \delta^{-1}\mathbf{e} < \mathbf{g} + 1$, or equivalently that $\mathbf{g} = \lfloor \delta^{-1}\mathbf{e} \rfloor$, with probability at least $1 - 12A\delta$.

It therefore remains to confirm (B.9). To that end, since $1 - e^{-A\delta} \leq A\delta$ and $1 - e^{-A\delta} \geq A\delta(1 - A\delta) \geq A\delta(1 + 2A\delta)^{-1}$ (the latter as $\delta < (2A)^{-1}$), observe that

$$(B.10) \quad 1 \leq \frac{A\delta}{1 - e^{-A\delta}} \leq 1 + 2A\delta.$$

We also have since $\log(1 - x) \leq -x$ for each $x \geq 0$, since $\log(1 - x) \geq -x(1 + x)$ for $x \in (0, 1/2)$, and since $\delta < (2A)^{-1}$ that

$$(B.11) \quad e^{-A^2S\delta^2} \leq e^{AS\delta}(1 - A\delta)^S \leq 1.$$

Combining (B.10) and (B.11) yields (B.9) and thus the lemma. \square

Proof of Lemma B.4. Let C_0 denote the constant C from Lemma B.5; we will assume throughout this proof that $\varepsilon < C_0^{-4}(T+1)^{-4}$, for otherwise $1 - C(V_0 - U_0 + 1)(T+1)\varepsilon^{1/4} \leq 0$ for any $C > C_0$. Let us first bound the cardinalities of $\mathbf{S}(x) \cap [0, T]$ and $\mathbf{T}(x) \cap [0, T]$, with high probability. To that end, observe by the first part of Lemma B.5 (with $A \in \{L, R\}$ and $K = C_0^{-1}(T+1)^{-1}\varepsilon^{-1/4} \geq 1$) that there exist constants $c > 0$ and $C_1 > 1$ such that $\mathbb{P}[\mathbf{S}_{\lfloor \varepsilon^{-1/4} \rfloor}(x) \geq T] \geq 1 - c^{-1}e^{-c\varepsilon^{-1/4}} \geq 1 - C_1\varepsilon$,

and similarly $\mathbb{P}[\mathbb{T}_{\lfloor \varepsilon^{-1/4} \rfloor}(x) \geq T] \geq 1 - C_1\varepsilon$, both hold for any $x \in \mathbb{Z}$. Together with a union bound, it follows that $\mathbb{P}[\mathcal{A}_1] \geq 1 - 2C_1\varepsilon(V_0 - U_0 + 1)$, where

$$(B.12) \quad \mathcal{A}_1 = \bigcap_{x=\lceil U_0 \rceil}^{\lfloor V_0 \rfloor} \left\{ \#\{\mathbf{S}(x) \cap [0, T]\} \leq \varepsilon^{-1/4} \right\} \cap \left\{ \#\{\mathbf{T}(x) \cap [0, T]\} \leq \varepsilon^{-1/4} \right\}.$$

We may therefore restrict to the event \mathcal{A}_1 in what follows.

On \mathcal{A}_1 , there are at most $\varepsilon^{-1/4}$ entries in any $\mathbf{S}(x) \cap [0, T]$ or $\mathbf{T}(x) \cap [0, T]$; their differences are exponential random variables with parameters L and R , respectively. Moreover, the differences between consecutive entries of any $\mathfrak{s}(x)$ and $\mathfrak{t}(x)$ are geometric random variables of parameters $b_1 = 1 - \varepsilon L$ and $b_2 = 1 - \varepsilon R$, respectively. Hence, fixing an integer $x \in \llbracket U, V \rrbracket$ and an index $(R, \mathfrak{r}) \in \{(\mathbf{S}, \mathfrak{s}), (\mathbf{T}, \mathfrak{t})\}$, and applying Lemma B.6 to the at most $\varepsilon^{-1/4}$ differences in $\mathbf{R}(x)$, it follows that we may couple $\mathbf{R}(x) \cap [0, T] = (\mathbf{R}_1(x), \mathbf{R}_2(x), \dots, \mathbf{R}_m(x))$ with $\mathfrak{r}(x) \cap \llbracket 1, T\varepsilon^{-1} \rrbracket = (\mathfrak{r}_1(x), \mathfrak{r}_2(x), \dots, \mathfrak{r}_{m'}(x))$ so that with probability $1 - 12(R + L)\varepsilon^{3/4}$ we have $m \leq m'$ and $\varepsilon\mathfrak{r}_i(x) \leq \mathbf{R}_i(x) \leq \varepsilon(\mathfrak{r}_i(x) + \varepsilon^{-1/4}) \leq \varepsilon\mathfrak{r}_i(x) + \varepsilon^{1/2}$, for each $i \in \llbracket 1, m \rrbracket$. After increasing C_0 if necessary, we further have that $\varepsilon\mathfrak{r}_{m'}(x) < T - \varepsilon^{1/2}$ with probability at least $1 - C_0\varepsilon^{1/2}$ (since the probability that $\mathfrak{r}_{m'}(x)$ lies in any fixed interval at size $\varepsilon^{-1/2} + 1$ is at most $(R + L)\varepsilon \cdot (\varepsilon^{-1/2} + 1) = 2(R + L)\varepsilon^{1/2}$), and so $m = m'$ and $\varepsilon\mathfrak{r}_i(x) \leq \mathbf{R}_i(x) \leq \varepsilon\mathfrak{r}_i(x) + \varepsilon^{1/2} < T$ for all $i \in \llbracket 1, m \rrbracket$. Applying a union bound over $x \in \llbracket U_0, V_0 \rrbracket$ gives the first statement of the lemma.

To establish the second, observe that the law of $\bigcup_{x=\lceil U_0 \rceil}^{\lfloor V_0 \rfloor} (\mathbf{S}(x) \cup \mathbf{T}(x))$ coincides with that of the ringing times of an exponential clock of rate $(R + L) \cdot (\lfloor V_0 \rfloor - \lceil U_0 \rceil + 1) \leq (V_0 - U_0 + 1)(R + L)$. Hence the second part of Lemma B.5 implies, for any real number $B \geq 1$, that with probability at least $1 - 2(V_0 - U_0 + 1)(R + L)B\varepsilon^{1/2}$ we have $|\mathbf{R}_i(x) - \mathbf{R}'_{i'}(x')| > 2\varepsilon^{1/2}$, for any distinct triples $(R, i, x), (R', i', x') \in \{\mathbf{S}, \mathbf{T}\} \times \llbracket 1, B \rrbracket \times \llbracket U_0, V_0 \rrbracket$. Applying this at $B = \varepsilon^{-1/4}$, using our restriction to \mathcal{A}_1 , and applying a union bound then yields the second part of the lemma. \square

REFERENCES

- [1] A. Aggarwal. Convergence of the stochastic six-vertex model to the ASEP: stochastic six-vertex model and ASEP. *Math. Phys. Anal. Geom.*, 20(2):Paper No. 3, 20, 2017.
- [2] A. Aggarwal. Current fluctuations of the stationary ASEP and six-vertex model. *Duke Math. J.*, 167(2):269–384, 2018.
- [3] A. Aggarwal. Limit shapes and local statistics for the stochastic six-vertex model. *Comm. Math. Phys.*, 376(1):681–746, 2020.
- [4] A. Aggarwal, A. Borodin, and A. Bufetov. Stochasticization of solutions to the Yang-Baxter equation. *Ann. Henri Poincaré*, 20(8):2495–2554, 2019.
- [5] A. Aggarwal, A. Borodin, and M. Wheeler. Colored fermionic vertex models and symmetric functions. *Comm. Amer. Math. Soc.*, 3:400–630, 2023.
- [6] A. Aggarwal, I. Corwin, and M. Hegde. Scaling limit of the colored ASEP and stochastic six-vertex model. Preprint, arXiv:2403.01341.
- [7] A. Aggarwal and J. Huang. Strong characterization for the Airy line ensemble. Preprint, arXiv:2308.11908.
- [8] A. Aggarwal, M. Nicoletti, and L. Petrov. Colored interacting particle systems on the ring: Stationary measures from Yang–Baxter equation. Preprint, arXiv:2309.11865.
- [9] G. Barraquand, A. Borodin, I. Corwin, and M. Wheeler. Stochastic six-vertex model in a half-quadrant and half-line open asymmetric simple exclusion process. *Duke Math. J.*, 167(13):2457–2529, 2018.
- [10] G. Barraquand, I. Corwin, and S. Das. KPZ exponents for the half-space log-gamma polymer. Preprint, arXiv:2310.10019.
- [11] G. Barraquand, I. Corwin, and E. Dimitrov. Spatial tightness at the edge of Gibbsian line ensembles. *Comm. Math. Phys.*, 397(3):1309–1386, 2023.
- [12] Y. Baryshnikov. GUEs and queues. *Probab. Theory Related Fields*, 119(2):256–274, 2001.

- [13] V. V. Bazhanov. Trigonometric solutions of triangle equations and classical Lie algebras. *Phys. Lett. B*, 159(4-6):321–324, 1985.
- [14] A. Borodin. On a family of symmetric rational functions. *Adv. Math.*, 306:973–1018, 2017.
- [15] A. Borodin, A. Bufetov, and M. Wheeler. Between the stochastic six vertex model and Hall-Littlewood processes. Preprint, arXiv:1611.09486.
- [16] A. Borodin and I. Corwin. Macdonald processes. *Probab. Theory Related Fields*, 158(1-2):225–400, 2014.
- [17] A. Borodin and I. Corwin. Discrete time q -TASEPs. *Int. Math. Res. Not. IMRN*, (2):499–537, 2015.
- [18] A. Borodin, I. Corwin, and V. Gorin. Stochastic six-vertex model. *Duke Math. J.*, 165(3):563–624, 2016.
- [19] A. Borodin and P. L. Ferrari. Anisotropic growth of random surfaces in $2 + 1$ dimensions. *Comm. Math. Phys.*, 325(2):603–684, 2014.
- [20] A. Borodin, V. Gorin, and M. Wheeler. Shift-invariance for vertex models and polymers. *Proc. Lond. Math. Soc. (3)*, 124(2):182–299, 2022.
- [21] A. Borodin and L. Petrov. Nearest neighbor Markov dynamics on Macdonald processes. *Adv. Math.*, 300:71–155, 2016.
- [22] A. Borodin and L. Petrov. Higher spin six vertex model and symmetric rational functions. *Selecta Math. (N.S.)*, 24(2):751–874, 2018.
- [23] A. Borodin and M. Wheeler. Observables of coloured stochastic vertex models and their polymer limits. *Probab. Math. Phys.*, 1(1):205–265, 2020.
- [24] A. Borodin and M. Wheeler. Spin q -Whittaker polynomials. *Adv. Math.*, 376:Paper No. 107449, 50, 2021.
- [25] A. Borodin and M. Wheeler. Colored stochastic vertex models and their spectral theory. *Astérisque*, (437):ix+225, 2022.
- [26] G. Bosnjak and V. V. Mangazeev. Construction of R -matrices for symmetric tensor representations related to $U_q(\mathfrak{sl}_n)$. *J. Phys. A*, 49(49):495204, 19, 2016.
- [27] A. Bufetov, M. Mucciconi, and L. Petrov. Yang-Baxter random fields and stochastic vertex models. *Adv. Math.*, 388:Paper No. 107865, 94, 2021.
- [28] A. Bufetov and L. Petrov. Yang-Baxter field for spin Hall-Littlewood symmetric functions. *Forum Math. Sigma*, 7:Paper No. e39, 70, 2019.
- [29] O. Busani, T. Seppäläinen, and E. Sorensen. Scaling limit of multi-type invariant measures via the directed landscape. Preprint, arXiv:2310.09824.
- [30] O. Busani, T. Seppäläinen, and E. Sorensen. The stationary horizon and semi-infinite geodesics in the directed landscape. Preprint, arXiv:2203.13242.
- [31] L. Cantini. Algebraic Bethe ansatz for the two species ASEP with different hopping rates. *J. Phys. A*, 41(9):095001, 16, 2008.
- [32] Z. Chen, J. de Gier, I. Hiki, T. Sasamoto, and M. Usui. Limiting current distribution for a two species asymmetric exclusion process. *Comm. Math. Phys.*, 395(1):59–142, 2022.
- [33] I. Corwin and E. Dimitrov. Transversal fluctuations of the ASEP, stochastic six vertex model, and Hall-Littlewood Gibbsian line ensembles. *Comm. Math. Phys.*, 363(2):435–501, 2018.
- [34] I. Corwin, P. Ghosal, and A. Hammond. KPZ equation correlations in time. *Ann. Probab.*, 49(2):832–876, 2021.
- [35] I. Corwin and A. Hammond. Brownian Gibbs property for Airy line ensembles. *Invent. Math.*, 195(2):441–508, 2014.
- [36] I. Corwin and A. Hammond. KPZ line ensemble. *Probab. Theory Related Fields*, 166(1-2):67–185, 2016.
- [37] I. Corwin, K. Matveev, and L. Petrov. The q -Hahn PushTASEP. *Int. Math. Res. Not. IMRN*, (3):2210–2249, 2021.
- [38] I. Corwin, N. O’Connell, T. Seppäläinen, and N. Zygouras. Tropical combinatorics and Whittaker functions. *Duke Math. J.*, 163(3):513–563, 2014.
- [39] I. Corwin and L. Petrov. Stochastic higher spin vertex models on the line. *Comm. Math. Phys.*, 343(2):651–700, 2016.
- [40] I. Corwin, T. Seppäläinen, and H. Shen. The strict-weak lattice polymer. *J. Stat. Phys.*, 160(4):1027–1053, 2015.
- [41] D. Dauvergne, J. Ortmann, and B. Virág. The directed landscape. *Acta Math.*, 229(2):201–285, 2022.
- [42] N. Elkies, G. Kuperberg, M. Larsen, and J. Propp. Alternating-sign matrices and domino tilings. II. *J. Algebraic Combin.*, 1(3):219–234, 1992.
- [43] S. Ganguly, M. Hedge, and L. Zhang. Brownian bridge limit of path measures in the upper tail of KPZ models. Preprint, arXiv:2311.12009.
- [44] S. Ganguly and M. Hegde. Sharp upper tail estimates and limit shapes for the KPZ equation via the tangent method. Preprint, arXiv:2208.08922.

- [45] G. Gasper and M. Rahman. *Basic hypergeometric series*, volume 96 of *Encyclopedia of Mathematics and its Applications*. Cambridge University Press, Cambridge, second edition, 2004. With a foreword by Richard Askey.
- [46] L.-H. Gwa and H. Spohn. Six-vertex model, roughened surfaces, and an asymmetric spin Hamiltonian. *Phys. Rev. Lett.*, 68(6):725–728, 1992.
- [47] J. Haglund, S. Mason, and J. Remmel. Properties of the nonsymmetric Robinson-Schensted-Knuth algorithm. *J. Algebraic Combin.*, 38(2):285–327, 2013.
- [48] A. Hammond. Modulus of continuity of polymer weight profiles in Brownian last passage percolation. *Ann. Probab.*, 47(6):3911–3962, 2019.
- [49] A. Hammond. A patchwork quilt sewn from Brownian fabric: regularity of polymer weight profiles in Brownian last passage percolation. *Forum Math. Pi*, 7:e2, 69, 2019.
- [50] A. Hammond. Exponents governing the rarity of disjoint polymers in Brownian last passage percolation. *Proc. Lond. Math. Soc. (3)*, 120(3):370–433, 2020.
- [51] A. Hammond. Brownian regularity for the Airy line ensemble, and multi-polymer watermelons in Brownian last passage percolation. *Mem. Amer. Math. Soc.*, 277(1363):v+133, 2022.
- [52] T. E. Harris. Nearest-neighbor Markov interaction processes on multidimensional lattices. *Adv. Math.*, 9:66–89, 1972.
- [53] T. E. Harris. Additive set-valued Markov processes and graphical methods. *Ann. Probability*, 6(3):355–378, 1978.
- [54] J. He. Boundary current fluctuations for the half space ASEP and six vertex model. Preprint, arXiv:2303.16335.
- [55] J. He. Shift invariance of half space integrable models. Preprint, arXiv:2205.13029.
- [56] M. Jimbo. Quantum R matrix for the generalized Toda system. *Comm. Math. Phys.*, 102(4):537–547, 1986.
- [57] W. Jockusch, J. Propp, and P. Shor. Random domino tilings and the arctic circle theorem. Preprint, arXiv:9801068, 1998.
- [58] K. Johansson. Discrete polynuclear growth and determinantal processes. *Comm. Math. Phys.*, 242(1-2):277–329, 2003.
- [59] S. G. G. Johnston and N. O’Connell. Scaling limits for non-intersecting polymers and Whittaker measures. *J. Stat. Phys.*, 179(2):354–407, 2020.
- [60] M. Kardar, G. Parisi, and Y.-C. Zhang. Dynamic scaling of growing interfaces. *Phys. Rev. Lett.*, 56(9):889, 1986.
- [61] A. N. Kirillov. Introduction to tropical combinatorics. In *Physics and combinatorics, 2000 (Nagoya)*, pages 82–150. World Sci. Publ., River Edge, NJ, 2001.
- [62] P. P. Kulish, N. Y. Reshetikhin, and E. K. Sklyanin. Yang-Baxter equations and representation theory. I. *Lett. Math. Phys.*, 5(5):393–403, 1981.
- [63] A. Kuniba, V. V. Mangazeev, S. Maruyama, and M. Okado. Stochastic R matrix for $U_q(A_n^{(1)})$. *Nuclear Phys. B*, 913:248–277, 2016.
- [64] Y. Lin. Classification of stationary distributions for the stochastic vertex models. *Electron. J. Probab.*, 28:Paper No. 1, 2023.
- [65] V. V. Mangazeev. On the Yang-Baxter equation for the six-vertex model. *Nuclear Phys. B*, 882:70–96, 2014.
- [66] S. Mason. A decomposition of Schur functions and an analogue of the Robinson-Schensted-Knuth algorithm. *Sém. Lothar. Combin.*, 57:Art. B57e, 24, 2006/08.
- [67] K. Matetski, J. Quastel, and D. Remenik. The KPZ fixed point. *Acta Math.*, 227(1):115–203, 2021.
- [68] K. Matveev and L. Petrov. q -randomized Robinson-Schensted-Knuth correspondences and random polymers. *Ann. Inst. Henri Poincaré D*, 4(1):1–123, 2017.
- [69] M. Mucciconi and L. Petrov. Spin q -Whittaker polynomials and deformed quantum Toda. *Comm. Math. Phys.*, 389(3):1331–1416, 2022.
- [70] M. Nica. Intermediate disorder limits for multi-layer semi-discrete directed polymers. *Electron. J. Probab.*, 26:Paper No. 62, 50, 2021.
- [71] M. Noumi and Y. Yamada. Tropical Robinson-Schensted-Knuth correspondence and birational Weyl group actions. In *Representation theory of algebraic groups and quantum groups*, volume 40 of *Adv. Stud. Pure Math.*, pages 371–442. Math. Soc. Japan, Tokyo, 2004.
- [72] N. O’Connell. A path-transformation for random walks and the Robinson-Schensted correspondence. *Trans. Amer. Math. Soc.*, 355(9):3669–3697, 2003.
- [73] N. O’Connell. Directed polymers and the quantum Toda lattice. *Ann. Probab.*, 40(2):437–458, 2012.
- [74] N. O’Connell and J. Warren. A multi-layer extension of the stochastic heat equation. *Comm. Math. Phys.*, 341(1):1–33, 2016.
- [75] N. O’Connell and M. Yor. Brownian analogues of Burke’s theorem. *Stochastic Process. Appl.*, 96(2):285–304, 2001.

- [76] A. Okounkov and N. Reshetikhin. Correlation function of Schur process with application to local geometry of a random 3-dimensional Young diagram. *J. Amer. Math. Soc.*, 16(3):581–603, 2003.
- [77] M. Prähofer and H. Spohn. Scale invariance of the PNG droplet and the Airy process. volume 108, pages 1071–1106. 2002. Dedicated to David Ruelle and Yasha Sinai on the occasion of their 65th birthdays.
- [78] J. Quastel and S. Sarkar. Convergence of exclusion processes and the KPZ equation to the KPZ fixed point. *J. Amer. Math. Soc.*, 36(1):251–289, 2023.
- [79] H. Rost. Non-equilibrium behaviour of a many particle process: Density profile and local equilibria. *Z. Wahrsch. Verw. Gebiete*, 58(1):41–53, 1981.
- [80] T. Sasamoto and M. Wadati. Exact results for one-dimensional totally asymmetric diffusion models. *J. Phys. A*, 31(28):6057–6071, 1998.
- [81] T. Seppäläinen. Scaling for a one-dimensional directed polymer with boundary conditions. *Ann. Probab.*, 40(1):19–73, 2012.
- [82] J. Warren. Dyson’s Brownian motions, intertwining and interlacing. *Electron. J. Probab.*, 12:no. 19, 573–590, 2007.
- [83] X. Wu. Brownian regularity for the KPZ line ensemble. Preprint, arXiv:2106.08052.
- [84] X. Wu. The KPZ equation and the directed landscape. Preprint, arXiv:2301.00547.
- [85] X. Wu. Tightness of discrete Gibbsian line ensembles with exponential interaction Hamiltonians. *Ann. Inst. Henri Poincaré Probab. Stat.*, 59(4):2106–2150, 2023.
- [86] Z. Yang. Stationary measures for higher spin vertex models on a strip. arXiv:2309.04897.